

**GROUND RESPONSE SPECTRA AT SURFACE FOR MAYAGÜEZ
CONSIDERING IN-SITU SOIL DYNAMIC PROPERTIES**

By

ELVIN J. PÉREZ MARCIAL

A thesis submitted in partial fulfillment of
the requirements for the degree of

MASTER IN SCIENCE

CIVIL ENGINEERING

UNIVERSITY OF PUERTO RICO
MAYAGÜEZ CAMPUS

2005

Approved by:

José A. Martínez Cruzado, Ph.D.
Member Graduate Committee

Date

Miguel A. Pando, Ph.D.
Member Graduate Committee

Date

Luis E. Suárez Colche, Ph.D.
President Graduate Committee

Date

Jose R. Arroyo, Ph.D.
Representative of the Graduate School

Date

Ismael Pagán Trinidad, M.S.
Department Chairperson

Date

ABSTRACT

One dimensional ground response analyses was performed at fifteen sites in Mayagüez Puerto Rico to study their seismic response for the development of response spectra at the surface. Field experiments using the Spectral Analysis of Surface Waves (SASW) method were carried out in nine sites for the development of shear wave velocity profiles. To others six sites, the shear wave velocity profiles were constructed by correlating the shear wave velocity and N values from the Standard Penetration Tests obtained from previous studies. The fifteen sites were classified according to the UBC-97 based on the average shear wave velocity (V_{s30}) obtained for each soil profile. The results were compared with a simplified procedure for estimating V_{s30} from SASW data proposed by Brown (2000).

Using the SASW data and complementing it with available geotechnical information, equivalent linear analyses were performed by using the computer program SHAKE2000. The ground motions considered were four artificial accelerograms compatible with the UBC-97 design response spectrum for seismic zone 3 in rock. A real acceleration record from the El Salvador earthquake of October 10, 1986 was also considered. For each site, the soil profile fundamental period, peak acceleration, and ground response spectrum at the surface are reported. The UBC-97 design response spectra were compared with the response spectra at the surface obtained in this thesis for each soil profile classification. The sites located in the Añasco Valley and part of the downtown area resulted in relatively higher spectral accelerations than the recommended in the UBC-97 for its soil type. Research needs are identified and suggestions for future works are also presented.

RESUMEN

Análisis de respuesta de suelos unidimensional fueron realizados en 15 lugares en Mayagüez Puerto Rico, para estudiar su respuesta sísmica para el desarrollo de espectros de respuesta en la superficie. Utilizando el método de Análisis Espectral de Ondas Superficiales (SASW), se realizaron pruebas de campo en nueve lugares para el desarrollo de perfiles de ondas de corte (V_s). Los perfiles de V_s para los otros seis lugares fueron obtenidos mediante la correlación de la velocidad de onda de corte con los valores de N de ensayos de penetración estándar obtenidos de estudios previos. Los 15 lugares fueron clasificados de acuerdo al UBC-97 basados en la velocidad de onda de corte promedio (V_{s30}). Los resultados fueron comparados con los obtenidos con el método simplificado para estimar el V_{s30} propuesto por Brown (2000) utilizando información obtenida con el método de SASW.

Usando la información de SASW y complementándola con información geotécnica disponible, se realizaron análisis lineales equivalentes utilizando el programa de computadora SHAKE2000. Los registros de aceleración considerados fueron cuatro registros artificiales compatibles con el espectro de diseño del UBC-97 para zona sísmica 3 en roca. Un registro real del terremoto del El Salvador del 10 de octubre de 1986 fue también considerado. Para cada lugar se obtuvo el periodo fundamental del perfil del suelo, aceleración máxima y espectros de respuesta en la superficie. Los espectros de diseño del UBC-97 fueron comparados con los espectros de respuesta en la superficie obtenidos en esta tesis para cada clasificación de suelo. Los lugares localizados en el Valle de Añasco y parte del centro del pueblo resultaron en aceleraciones espectrales relativamente mayores que los recomendados por el UBC-97 para su tipo de suelo. Recomendaciones para futuras investigaciones son también presentadas.

*Dedicated to my love,
Cibel M. Hilerio*

ACKNOWLEDGMENTS

I would like to express my sincere thanks to my advisor, Dr. Luis Suárez for his guidance and support since my undergraduate studies at the UPR-Mayagüez. To Dr. Miguel Pando, for his enthusiasm and suggestions in this thesis and for his support with the experimental field tests. To Dr. José Martínez Cruzado for his valuable comments and remarks throughout this project. Also, the comments by Dr. José R. Arroyo were helpful.

Special thanks to the Puerto Rico Strong Motion Program for their financial support. Also the financial contribution from the USGS through the program of Dr. Miguel Pando is greatly appreciated.

To my friends Wilmel Varela, Carmen Lugo, Fabián Consuegra, Orlando Cundumi, and Omayra Santos for their unconditional help in this thesis. To Dr. James Bay from Utah State University who contribute with the field tests and with the theoretical aspects of the SASW method. The support of the UPR-Mayagüez personnel, Liz, Elvis, Ivan, and Jaffet is also recognized.

And to my family, especially to Cibela Hilerio, for her endless love and encouragement over the years.

TABLE OF CONTENT

CHAPTER 1	1
Introduction.....	1
1.1 Problem Statement	1
1.2 Research Objectives.....	2
1.3 Methodology	3
1.3.1 Field Work Phase – Spectral Analysis of Surface Waves	3
1.3.2 Numerical phase – Ground Response Analyses	3
1.4 Thesis Organizations.....	4
CHAPTER 2	5
Seismic Hazard in Mayagüez from Previous Studies.....	5
2.1 Introduction.....	5
2.2 Previous Seismic Studies	8
2.3 Liquefaction Study.....	10
CHAPTER 3	11
Shear Wave Velocity Profiles for Mayagüez Sites.....	11
3.1 Introduction.....	11
3.2 The Spectral Analysis of Surface Waves (SASW).....	11
3.2.1 Field set up and procedure	12
3.2.2 Phase Angles Curves.....	13
3.2.3 Experimental dispersion curve.....	15
3.2.4 Theoretical Dispersion Curves.....	17
3.2.5 SASW field test locations	18
3.3 SASW Results Summary	20
CHAPTER 4	36
Simplified Vs30 Estimation Method with SASW Data.....	36
4.1 Introduction.....	36
4.2 The Vs30 Simplify Method	37
4.3 Vs30 for Mayagüez sites based on the Brown et al. procedure	38
CHAPTER 5	41
One Dimensional Ground Response Analysis.....	41
5.1 Introduction.....	41

5.2	One-dimensional ground response analysis.....	41
5.3	Dynamic soil properties	43
5.4	Soil simplified profiles.....	56
5.4.1	Group A soil profiles	56
5.4.2	Group B soil profiles.....	60
5.4.3	Group C soil profiles.....	64
5.5	Ground Motions	66
5.5.1	Artificial ground motions.....	66
5.5.2	El Salvador earthquake	67
5.6	Ground response analysis results.....	75
5.6.1	Group A	75
5.6.2	Group B.....	83
5.6.3	Group C.....	92
CHAPTER 6		98
Conclusions and recommendations.....		98
6.1	Introduction.....	98
6.2	Soil Dynamic Properties at Various Sites in Mayagüez.....	99
6.3	Ground Response Spectra for Mayagüez sites.....	100
6.4	Suggestions for Future Works	108
REFERENCES		109
APPENDIX A.....		111
EXPERIMENTAL VERSUS THEORETICAL DISPERSION CURVES FROM SASW TESTS IN MAYAGUEZ.....		111
APPENDIX B.....		116
DETAILED RESULTS OF ONE-DIMENSIONAL GROUND RESPONSE ANALYSES FROM THE ARTIFICIAL GROUND MOTIONS.....		116
APPENDIX C		120
RESPONSE SPECTRA AT SURFACE IN MAYAGUEZ SITES.....		120
FROM LINEAR ANALYSIS.....		120

LIST OF FIGURES

Figure 2.1: Shear wave velocity profile from SASW tests and seismic refraction for the UPR-Athletic Field site (After Muract, 2004).	7
Figure 2.2: Shear wave velocity profile from SASW tests and bore-hole method for the new UPR-Biology Building site (After Muract, 2004).	8
Figure 2.3: Seismic zones around Puerto Rico. (From Martinez, Irizarry, and Portela, 2001)	9
Figure 3.1: SASW field set up.	12
Figure 3.2: Weight drop system constructed at UPR-Mayagüez CE Department.....	13
Figure 3.3: Comparison of phase angle from field data and after the masking process.	15
Figure 3.4: Moving average concept for the calculation of the average experimental dispersion curve (From Joh, 1996)	16
Figure 3.5: Average experimental dispersion curve for the 341HWY site obtained with the moving average concept.	17
Figure 3.6: SASW sites locations in the Mayagüez municipality (map from www.linktopr.com).	19
Figure 3.7: Phase spectrum from field data for the Abonos site for the 30 meters spacing.	21
Figure 3.8: Unwrapped phase spectrum for the Abonos site obtained by the interactive masking process.	21
Figure 3.9: Average experimental dispersion curve for the Abonos site.....	21
Figure 3.10: Experimental versus theoretical dispersion curve for the Abonos site.	22
Figure 3.11: Shear wave velocity profile for the Abonos site.	22
Figure 3.12: Shear wave velocity profile for the 341HWY site.	24
Figure 3.13: Shear wave velocity profile for the Maní site.	25
Figure 3.14: Shear wave velocity profile for the Maní Park site.....	26
Figure 3.15: Shear wave velocity profile for the Seco Park site.....	27
Figure 3.16: Shear wave velocity profile for the Isidoro García site.....	29
Figure 3.17: Shear wave velocity profile for the Ramírez de Arellano site.	30
Figure 3.18: Shear wave velocity profile for the Sultanita site.....	31
Figure 3.19: Shear wave velocity profile for the Civil site.....	33
Figure 3.20: Shear wave velocity profile for the sites near the Mayagüez coast.....	33
Figure 3.21: Shear wave velocity profile for the sites in the Añasco Valley.....	34
Figure 3.22: Shear wave velocity profile for the sites in the Mayagüez west area.....	34

Figure 4.1: Linear regression of V_{s30} versus V_{r40} (after Brown et al. 2000).	38
Figure 4.2: Dispersion curve in the wavelength domain for the Abonos site.	39
Figure 5.1: Flowchart for the equivalent linear ground response analysis.	44
Figure 5.2: Shear modulus reduction curves for sand proposed by Seed and Idriss (1970).	45
Figure 5.3: Damping ratio reduction curves for sand proposed by Seed and Idriss (1970).	45
Figure 5.4: Shear modulus reduction curve for clay proposed by Seed and Sun (1989).	46
Figure 5.5: Damping ratio reduction curves for clay proposed by Seed and Idriss (1970).	46
Figure 5.6: Shear modulus reduction curves for gravel and rock.	48
Figure 5.7: Damping ratio reduction curves for gravel and rock.	48
Figure 5.8: The six additional sites location in Mayagüez.	49
Figure 5.9: Correlation between N values from SPT with shear wave velocity proposed by Imai and Yoshimura (1970) (reproduced from NAVFAC, 1997).	50
Figure 5.10: (a) Soil materials, (b) shear wave velocities, and (c) N values for the Abonos site.	57
Figure 5.11: (a) Soil materials, (b) shear wave velocities, and (c) N values for the Maní site.	58
Figure 5.12: (a) Soil materials, (b) shear wave velocities, and (c) N values for the Biología site.	58
Figure 5.13: (a) Soil materials, (b) shear wave velocities, and (a) N values for the Viaducto site.	59
Figure 5.14: (a) Soil materials, (b) shear wave velocities, and (c) N values for the Civil site.	59
Figure 5.15: (a) Soil materials and (b) shear wave velocity profile for the 341HWY site.	61
Figure 5.16: (a) Soil materials and (b) shear wave velocity profile for the Maní Park site.	61
Figure 5.17: (a) Soil materials and (b) shear wave velocity profile for the Seco Park site.	62
Figure 5.18: (a) Soil materials and (b) shear wave velocity profile for Isidoro García site.	62
Figure 5.19: (a) Soil materials and (b) shear wave velocity profile for the Ramirez de Arellano site.	63
Figure 5.20: (a) Soil materials and (b) shear wave velocity profile for the Sultanita site.	63
Figure 5.21: (a) Soil materials, (b) shear wave velocities, and (c) N values for the El Bosque site.	64
Figure 5.22: (a) Soil materials, (b) shear wave velocity, and (c) N values for the El Castillo site profile.	65
Figure 5.23: (a) Soil materials, (b) shear wave velocity, and (c) N values for the India site.	65
Figure 5.24: (a) Soil materials, (b) shear wave velocity, and (c) N values for the Marina site.	66

Figure 5.25: Response spectra of artificial accelerograms and UBC 97 design spectrum for rock in zone 3.	68
Figure 5.26: (a) Time history and (b) Fourier amplitude spectrum for ground motion 1	69
Figure 5.27: (a) Time history and (b) Fourier amplitude spectrum for ground motion 2	70
Figure 5.28: (a) Time history and (b) Fourier amplitude spectrum for ground motion 3	71
Figure 5.29: (a) Time history and (b) Fourier amplitude spectrum for ground motion 4	72
Figure 5.30: El Salvador earthquake response spectrum and the UBC 97 design spectrum for rock in zone 4.	73
Figure 5.31: (a) Time history and (b) Fourier amplitude spectrum for El Salvador Earthquake.	74
Figure 5.32: Response spectrum at surface of the Abonos site from non linear	78
Figure 5.33: Response spectrum at surface of the Maní site from non linear analysis and UBC 97 design spectrum.	79
Figure 5.34: Ground response spectrum at surface of the Biología site from non linear analysis and UBC 97 design spectrum.....	80
Figure 5.35: Response spectrum at surface and of the Viaducto site from non linear analysis and UBC 97 design spectrum.	81
Figure 5.36: Response spectrum at surface and of the Civil site from non linear analysis UBC 97 design spectrum.	82
Figure 5.37: Response spectrum at surface of the 341HWY site from non linear analysis and UBC 97 design spectrum.	86
Figure 5.38: Response spectrum at surface of the Maní Park site from non linear analysis and UBC 97 design spectrum.	87
Figure 5.39: Response spectrum at surface of the Seco Park site from non linear analysis and UBC 97 design spectrum.	88
Figure 5.40: Response spectrum at surface of the Isidoro García site from non linear analysis and UBC 97 design spectrum.	89
Figure 5.41: Response spectrum at surface of the Ramírez de Arellano site from non linear analysis and UBC 97 design spectrum.....	90
Figure 5.42: Response spectrum at surface of the Sultanita site from non linear analysis and UBC 97 design spectrum.	91
Figure 5.43: Response spectrum at surface of the El Bosque site from non linear analysis and UBC 97 design spectrum.	94

Figure 5.44: Response spectrum at surface for the El Castillo site from non linear analysis and UBC 97 design spectrum.	95
Figure 5.45: Response spectrum at surface of the India site from non linear analysis and UBC 97 design spectrum.	96
Figure 5.46: Response spectrum at surface of the Marina site from non linear analysis and UBC 97 design spectrum.	97
Figure 6.1: Average ground response spectra for the artificial ground motions for the sites in group A and 5% damping ratio.	101
Figure 6.2: Average ground response spectra for the artificial ground motions for the sites in group B and 5% damping ratio.	102
Figure 6.3: Average ground response spectra for the artificial ground motions for the sites in group C and 5% damping ratio.	102
Figure 6.4: Ground response spectra for the El Salvador earthquake record for the sites in group A and 5% damping ratio.	103
Figure 6.5: Ground response spectra for the El Salvador earthquake record for the sites in group B and 5% damping ratio.	103
Figure 6.6: Ground response spectra for the El Salvador earthquake record for the sites in group C and 5% damping ratio.	104
Figure 6.7: Average ground response spectra for the sites classified as soil profile type S_C and the UBC design response spectrum for seismic zone 3.	105
Figure 6.8: Average ground response spectra for the sites classified as soil profile type S_D and the UBC design response spectrum for seismic zone 3.	105
Figure 6.9: Average ground response spectra for the site classified as soil profile type S_E and the UBC design response spectrum for seismic zone 3.	106
Figure 6.10: Average ground response spectra for the sites classified as soil profile type S_C and the UBC design response spectrum for seismic zone 4.	106
Figure 6.11: Average ground response spectra for the sites classified as soil profile type S_D and the UBC design response spectrum for seismic zone 4.	107
Figure 6.12: Average ground response spectra for the site classified as soil profile type S_E and the UBC design response spectrum for seismic zone 4.	107
Figure A.1: Experimental versus theoretical dispersion curves for the Abonos site.	111
Figure A.2: Experimental versus theoretical dispersion curves for the 341HWY site.	112
Figure A.3: Experimental versus theoretical dispersion curves for the Maní site.	112

Figure A.4: Experimental versus theoretical dispersion curves for the the Maní Park site.....	113
Figure A.5: Experimental versus theoretical dispersion curves for the Seco Park site.	113
Figure A.6: Experimental versus theoretical dispersion curves for the Isidoro García site.	114
Figure A.7: Experimental versus theoretical dispersion curves for the Ramírez de Arellano site.	114
Figure A.8: Experimental versus theoretical dispersion curves for the Sultanita site.	115
Figure A.9: Experimental versus theoretical dispersion curves for the Civil site.	115
Figure C.1: Average ground response spectrum at surface from linear analysis for the Abonos Site and UBC 97 design spectrum.	121
Figure C.2: Ground response spectrum at surface from linear analysis for the El Salvador earthquake for the Abonos site and UBC 97 design spectrum.	121
Figure C.3: Average ground response spectrum at surface from linear analysis for the Maní site and UBC 97 design spectrum.	122
Figure C.4: Ground response spectrum at surface from linear analysis for the El Salvador earthquake for the Maní site and UBC 97 design spectrum.	122
Figure C.5: Average ground response spectrum at surface from linear analysis for the Biología site and UBC 97 design spectrum.	123
Figure C.6: Ground response spectrum at surface from linear analysis for the El Salvador earthquake for the Biología site and UBC 97 design spectrum.	123
Figure C.7: Average ground response spectrum at surface from linear analysis for the Viaducto site and UBC 97 design spectrum.	124
Figure C.8: Ground response spectrum at surface from linear analysis for the El Salvador earthquake for the Viaducto site and UBC 97 design spectrum.	124
Figure C.9: Average ground response spectrum at surface from linear analysis for the Civil site and UBC 97 design spectrum.	125
Figure C.10: Ground response spectrum at surface from linear analysis for the El Salvador earthquake for the Civil site and UBC 97 design spectrum.	125
Figure C.11: Average ground response spectrum at surface site from linear analysis for the 341HWY and UBC 97 design spectrum.	126
Figure C.12: Ground response spectrum at surface from linear analysis for the El Salvador earthquake for the 341HWY site and UBC 97 design spectrum.	126
Figure C.13: Average ground response spectrum at surface from linear analysis for the Maní Park site and UBC 97 design spectrum.	127

Figure C.14: Ground response spectrum at surface from linear analysis for the El Salvador earthquake for the Maní Park site and UBC 97 design spectrum.	127
Figure C.15: Average ground response spectrum at surface from linear analysis for the Seco Park site and UBC 97 design spectrum.	128
Figure C.16: Ground response spectrum at surface from linear analysis for the El Salvador earthquake for the Seco Park site and UBC 97 design spectrum.	128
Figure C.17: Average ground response spectrum at surface from linear analysis for the Isidoro García site and UBC 97 design spectrum.	129
Figure C.18: Ground response spectrum at surface from linear analysis for the El Salvador earthquake for the Isidoro García site and UBC 97 design spectrum.	129
Figure C.19: Average ground response spectrum at surface from linear analysis for the Ramírez de Arellano site and UBC 97 design spectrum.	130
Figure C.20: Ground response spectrum at surface from linear analysis for the El Salvador earthquake for the Ramírez de Arellano site and UBC 97 design spectrum.	130
Figure C.21: Average ground response spectrum at surface from linear analysis for the Sultanita site and UBC 97 design spectrum.	131
Figure C.22: Ground response spectrum at surface from linear analysis for the El Salvador earthquake for the Sultanita site and UBC 97 design spectrum.	131
Figure C.23: Average ground response spectrum at surface from linear analysis for the El Bosque site and UBC 97 design spectrum.	132
Figure C.24: Ground response spectrum at surface from linear analysis for the El Salvador earthquake for the El Bosque site and UBC 97 design spectrum.	132
Figure C.25: Average ground response spectrum at surface and UBC 97 design spectrum for El Castillo Site from linear analysis.	133
Figure C.26: Ground response spectrum at surface from linear analysis for the El Salvador earthquake for the El Castillo site and UBC 97 design spectrum.	133
Figure C.27: Average ground response spectrum at surface from linear analysis for the India Site and UBC 97 design spectrum.	134
Figure C.28: Ground response spectrum at surface from linear analysis for the El Salvador earthquake for the India site and UBC 97 design spectrum.	134
Figure C.29: Average ground response spectrum at surface from linear analysis for the Marina Site and UBC 97 design spectrum.	135

Figure C.30: Ground response spectrum at surface from linear analysis for the El Salvador earthquake for the India site and UBC 97 design spectrum..... 135

LIST OF TABLES

Table 2.1: Characteristics of the seismic zones. (From Martinez, Irizarry, and Portela, 2001).	9
Table 3.1: SASW test sites and their coordinates.	19
Table 3.2: Layers thickness and shear wave velocities for the Abonos Site.	23
Table 3.3: Layers thicknesses and shear wave velocities for the 341HWY site.	23
Table 3.4: Layers thicknesses and shear wave velocities for the Maní site.	25
Table 3.5: Layers thicknesses and shear wave velocities for the Maní Park site.	27
Table 3.6: Layers thicknesses and shear wave velocities for the Seco Park site.	28
Table 3.7: Layers thicknesses and shear wave velocities for the Isidoro García site.	29
Table 3.8: Layers thicknesses and shear wave velocities for the Ramírez de Arellano site.	30
Table 3.9: Layers thicknesses and shear wave velocities for the Sultanita site.	32
Table 3.10: Layers thicknesses and shear wave velocities for the Civil site.	32
Table 3.11: Summary of results from the SASW tests.	35
Table 4.1: Average shear wave velocity V_{s30} from the UBC-97 formula and the Simplified Procedure.	39
Table 4.2: UBC-97 soil profile types.	40
Table 5.1: Groups created and sites designation for the ground response analysis.	47
Table 5.2: Typical ranges of compression velocity, density, and Poisson ratio characteristics for different soil materials (from USACE, 1995).	49
Table 5.3: Dynamic soil properties assigned to group A.	51
Table 5.4: Dynamic soil properties assigned to group B.	52
Table 5.5: Dynamic soil properties assigned to group C.	54
Table 5.6: Characteristics of the artificial ground motions.	68
Table 5.7: Characteristics of the El Salvador earthquake.	73
Table 5.8: Summary of average results for Group A sites subjected to artificial ground motions.	76
Table 5.9: Summary of results for Group A sites subjected to the El Salvador earthquake record.	77
Table 5.10: Summary of average results for Group B subjected to artificial ground motions.	84
Table 5.11: Summary of results for Group B sites subjected to the El Salvador earthquake record.	85

Table 5.12: Summary of average results for Group C sites subjected to artificial ground motions.	93
Table 5.13: Summary of results for Group C sites subjected to the El Salvador earthquake record.	93
Table 6.1: Summary of average shear wave velocities and soil periods for the sites in Mayagüez.	100
Table B.1: Artificial ground motions results for Group A.	117
Table B.2: Artificial ground motions results for Group B.	118
Table B.3: Artificial ground motions results for Group C.	119

CHAPTER 1

Introduction

1.1 Problem Statement

The island of Puerto Rico, located in the Caribbean, is surrounded by tectonic plates capable to cause strong ground motions as have been demonstrated in the past. The tectonic plates that affect Puerto Rico are the North American Plate and The Caribbean Plate. To the north of Puerto Rico is found the fault known as The Puerto Rico Trench and to the west the fault known as The Mona Canyon. There are some faults inside the island but their extent and location are still under investigation.

Historic records indicate that the island of Puerto Rico has experienced several large magnitude earthquakes. The most recent earthquake reported to have caused great damage to Puerto Rico was in October 11, 1918. The magnitude for this earthquake was estimated to be 7.3 in the moment magnitude scale. Reid and Taber (1919) reported that at least 116 people lost their lives and the properties damages were quantified in approximately 4 millions dollars of that time. The epicenter for the 1918 earthquake was estimated to be approximately 40 km to the northwest of Puerto Rico. The city of Mayagüez, located in the west part of Puerto Rico with a population of about 17,000 at that time, was one of the cities most damaged (Reid and Taber, 1919). The modified Rossi-Forel intensity was estimated between VIII and IX. These intensities were attributed to the fact that the most populated areas in Mayagüez were concentrated on alluvial soils (Reid and Taber, 1919).

The current population of Mayagüez is estimated to be 98,434 (Census 2000). About 53.3% of this city is located in alluvial deposits. It is well documented in the literature that the seismic waves that reach alluvial soils are very likely to be amplified. Dynamic properties of soils in the Mayagüez region have not been quantified nor have amplification studies been carried out to estimate surface ground motion that incorporate local site effects. This research hopes to help fill this gap through the determination of dynamic soils properties (mainly shear wave velocity profiles) and through the evaluation of seismic amplifications in different areas of Mayagüez where Vs profiles are obtained.

The seismic hazard for the city of Mayagüez is recognized by the scientific and engineering community. It was mentioned that many studies have demonstrated that alluvial

soils, like the soil deposits found in Mayagüez, can amplify seismic waves and this may result in other associated problems such as liquefaction (Llavona, 2004).

This thesis presents the results of field experiments using the Spectral Analysis of Surface Waves (SASW) method that have been carried out at several locations within the city of Mayagüez, Puerto Rico. Using the SASW data and complementing it with available geotechnical information (e.g. Llavona, 2004), seismic amplification evaluations were performed considering the local soil conditions at different locations in Mayagüez. These analyses will help to assess the seismic hazard for this area and to determine the necessary preventive measures to mitigate the damages during a likely future earthquake.

1.2 Research Objectives

The main objective of this research project is to determine ground response spectra at the surface for the city of Mayagüez considering in-situ dynamic soil properties. More specific objectives related to the main objective are:

1. Determine shear wave velocity profiles at nine locations in Mayagüez using the Spectral Analysis of Surface Wave method.
2. Develop the shear wave velocity profile for six more sites where relatively deep (depth greater than 60 ft) geotechnical exploration are available in a database for Mayagüez based in correlations of the shear wave velocity and the Standard Penetration Test N values. A total of fifteen sites were studied in which the average shear wave velocity (V_{s30}) was calculated and the sites were classified according to the UBC-97.
3. Perform ground response analyses using the computer program SHAKE2000 for the fifteen sites and obtain the sites fundamental period and peak acceleration at the surface.
4. Develop ground response spectra at the surface considering in-situ soil properties for different soil types.
5. Use a simplified procedure proposed by Brown et al. (2001) to calculate the average shear wave velocity in the upper 30 meters depth by using the SASW field data, and investigate its applicability for Mayagüez soil profile.
6. Identify research needs for future research projects and provide recommendations based on the results found in the study.

1.3 Methodology

The methodology used in this research project can be divided in two steps. Step one consists in the field work to determine the dynamic soil properties at different locations within the city of Mayagüez and the second step deals with the ground response analyses to develop ground response spectra at the surface for these locations. A summary of each step is presented below. More details of the procedures, equipments, and theories on each step are given in the following chapters.

1.3.1 Field Work Phase - Spectral Analysis of Surface Waves

1. A review of the literature of the previous seismic studies in the city of Mayagüez will be carried out and those areas where more information is needed will be identified.
2. The areas of Mayagüez where there is not enough information from geotechnical explorations or from seismic studies will be identified in a quadrangle of the city.
3. By using the equipment for the SASW test developed in the Civil Engineering Department of the UPR-Mayagüez, a field test program will be planned for nine sites in Mayagüez.
4. Spectral Analysis of Surface Waves tests will be performed at each site and shear wave velocity profiles and their UBC-97 site classification will be determined.
5. A simplify procedure for the calculation of the average shear wave velocity in the upper 100 ft (30 meters) depth proposed by Brown et al. (2000) well be investigated.

1.3.2 Numerical phase – Ground Response Analyses

1. A database of geotechnical explorations in the Civil Engineering Department of the UPR-Mayagüez well be revised and those sites with boring logs with depth greater than 60 ft will be added to the previous nine sites.
2. Develop shear wave velocity profiles for the new sites by correlating the standard penetration test N value with the shear wave velocity using the curves proposed by Imai and Yoshimura (1970).
3. A total of fifteen soil and shear wave velocity profiles models well be developed for ground response analyses using the computer program SHAKE2000.
4. Four synthetic ground motions compatible with the UBC-97 design response spectrum in rock for seismic zone 3 well be developed by using the wavelet transform methodology proposed by Montejo (2004). A fifth real earthquake record from El Salvador in October 10, 1986 well also be considered.

5. The soil damping ratio and shear modulus reduction curves will be assigned for each soil material in the profile.
6. An equivalent linear one-dimensional ground response analyses will be performed to the fifteen sites by using the computer program SHAKE2000.
7. The soil fundamental period, peak acceleration, and ground response spectrum at the surface will be determined for each site.

1.4 Thesis Organizations

A literature review related to the seismicity of Mayagüez and the SASW methodology is included in Chapter 2. Chapter 3 presents a summary of the SASW field experiments carried out for this project. This chapter also provides a brief overview of the SASW method, including the test procedure and equipment description.

Chapter 4 presents a comparison of the average shear wave velocity measured in the upper 100 ft (30 meters) and the values obtained using a simplified method based on the procedure proposed by Brown et al. (2000). The ground response analyses results are described in Chapter 5. In this chapter the equivalent linear method is briefly described and the resulting ground response spectra at the surface for each site are presented. Chapter 6 presents conclusions and recommendations for future research.

CHAPTER 2

Seismic Hazard in Mayagüez from Previous Studies

2.1 Introduction

The seismic hazard in Puerto Rico is a subject of concern for the Island's scientific and engineering community and for those involved with the public safety for natural. The Puerto Rico Seismic Network (PRSN) and the Puerto Rico Strong Motion Program (PRSMP) of the University of Puerto Rico at Mayagüez (UPR-Mayagüez) have monitored the seismic activity of the region for several years. In the year 2002 the PRSN registered at least 967 seismic events and in 1998 an earthquake with magnitude of 5.6 in Richter scale was registered by the PRSN (www.rmsismo.uprm.edu).

The Mayagüez region in the western part of the Island has become an area of interest for researchers involved with seismic hazard assessment. As an example, the United State Geological Survey (USGS) in conjunction with the PRSN performed a series of seismic refraction studies at different locations in Puerto Rico for a site characterization study between the 2004 and 2005. Also, local geotechnical engineering companies had performed geophysical studies in Puerto Rico as mentioned in Muract (2004) by Jaca & Sierra and others. In the following sections the works carried out by Macari (1994), Martinez, Irizarry and Portela (2001), Llavona (2004), and Muract (2004) are summarized.

Previous Geophysical Studies

Macari (1994) performed a series of Spectral Analysis of Surface Waves (SASW) and Piezocone Penetration studies in the western area of Puerto Rico. At eight sites located from the south of Mayagüez to the Añasco Valley and the town of Rincón in the north, Macari obtained the shear wave velocity and shear strength characteristics. Macari cited a work by Moya and McCann in which they reported that the beach, alluvium, and colluviums deposits are characteristic of the area. Therefore, it is expected that these loose soils material will amplify the seismic waves traveling from the bedrock.

From the SASW tests, Macari concluded that the Añasco Valley is composed of deep soil deposits with a relatively low shear wave velocity. Shear wave values starting at 300 ft/sec at the surface and increasing with depth to almost 700 ft/sec in the upper 50 ft were reported. The total depth of the soil deposit is unknown, but it is believed that it extends in excess of 100 ft.

In downtown Mayagüez, three more sites were tested by Macari. These are the Athletic Field at the UPR-Mayagüez, the India Brewery in front of the UPR-Mayagüez, and a site near the Darlington building adjacent to the PR-2 highway. These sites exhibit the same pattern of shear wave velocity profile. A stiff layer was found at the surface followed by alternating layers of stiff and soft materials. The next site tested by Macari was the Guanajibo site located adjacent to the Mayagüez Bay and the Guanajibo River. In this site it was found that the shear wave velocity increases quickly with depth reaching values of 2000 ft/sec to 3000 ft/sec at 30 ft depth. These shear wave velocities values are associated with soft rock and sandstone. A similar situation was found in the Rincón Valley where stiff deposits associated to soft rock and sandstone was encountered at a depth of 20 ft.

The depths of the shear wave velocity profiles obtained by Macari vary from 30ft to 60ft. The SASW inversion analysis was performed by considering only one mode of wave propagation. Researchers have shown that considering one mode is not enough for the data interpretation where a stiff layer is followed by soft soil layers, as it was found in some of the sites tested (Stokoe et al., 1989).

In order to acquire more information about the soil deposits in Mayagüez and other cities of Puerto Rico, Muract (2004) implemented the Spectral Analysis of Surface Wave (SASW) method for shear wave velocity estimations. In his thesis, Muract implemented a multimode analysis of surface waves combined with various filtering methods. To perform the inversion process, i.e. to obtain the soil profiles, Muract proposed a combination of a neural network method and an optimization algorithm. Muract wrote a computer program in Matlab to retrieve field data to construct the experimental dispersion curve and to perform the inversion analysis considering multi modes of wave propagation.

Two sites were tested by Muract and presented in his thesis. The first site was the Athletic Field at the UPR-Mayagüez and the other one was the new Biology Building of the UPR-Mayagüez. Figure 2.1 shows the shear wave velocity profile for the Athletic Field obtained by Muract. An average shear wave velocity in the upper 100 ft (30 meters) depth of 2081.75 ft/sec. (634.52 m/sec) was calculated and the site was classified as soil type Sc in the UBC-97 classification. To validate the proposed procedure, the shear wave velocity profile was compared with seismic refraction data obtained in that site as shown in Figure 2.1.

The second site tested by Muract was in the new Biology Building at UPR-Mayagüez. Figure 2.2 shows the shear wave velocity profile obtained by the SASW test and its comparison with data obtained from a down-hole test conducted at the same site. From the SASW test, the

average shear wave velocity in the upper 100 ft depth was calculated to be 1875.82 ft/sec. (571.75 m/sec) and the site was classified as soil type Sc. The shear wave velocity profile obtained by Muract for this site was used in this thesis for the ground response analysis.

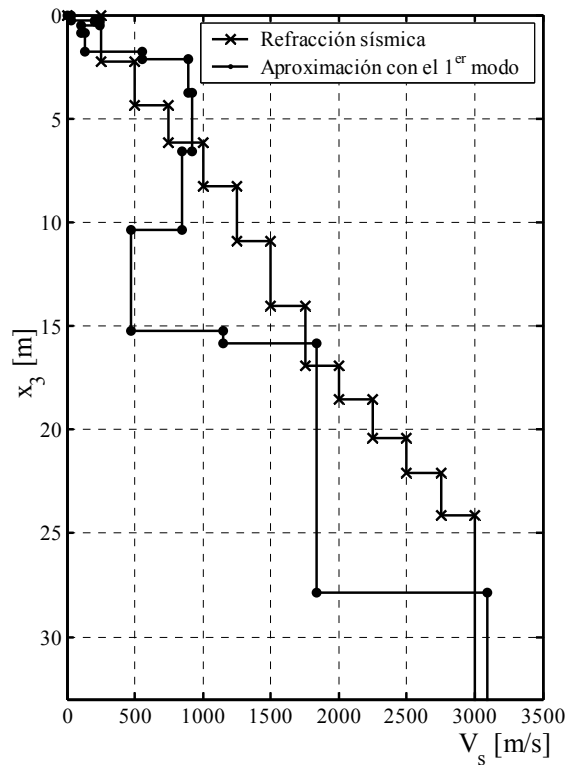


Figure 2.1: Shear wave velocity profile from SASW tests and seismic refraction for the UPR-Athletic Field site (After Muract, 2004).

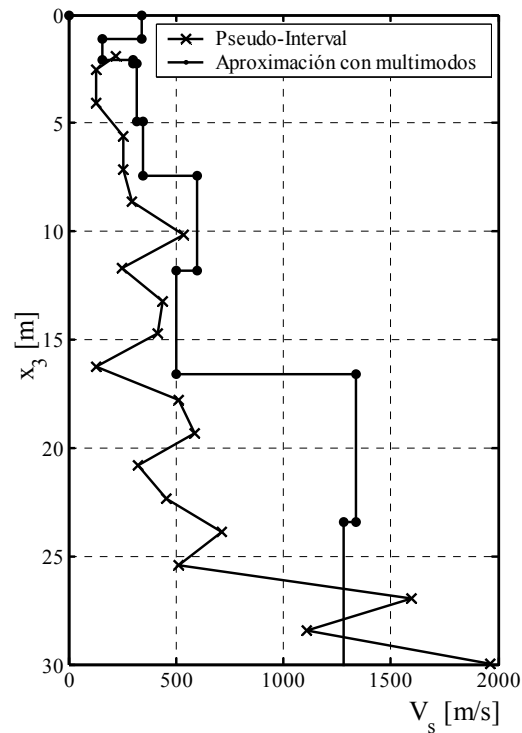


Figure 2.2: Shear wave velocity profile from SASW tests and bore-hole method for the new UPR-Biology Building site (After Muract, 2004).

2.2 Previous Seismic Studies

A very important consideration when performing seismic studies is the ground motion to be used for the analyses. The peak ground acceleration, frequency content, and effective duration are some of these important characteristics of the earthquake accelerogram. In an effort to develop elastic response spectra in rock for the cities of San Juan, Ponce, and Mayagüez, Martinez, Irizarry, and Portela (2001) studied acceleration time histories recorded worldwide. To select the proper records, the authors studied the most active seismic faults in Puerto Rico. Figure 2.3 shows the seismic zone established for their study. Table 2.1 displays their most relevant characteristics. They reported that the maximum magnitude expected for the seismic faults in the ocean is 7.5 except for The P.R. Trench fault which can produce an earthquake with a magnitude of 8.0. The maximum magnitude expected for the faults inside the Island is 6.5.

More than 15,000 ground motions were reviewed from a database compiled by the National Oceanic and Atmospheric Administration (NOAA). From these ground motions they selected those that satisfy the following conditions: (1) the record must be obtained in the open field, (2) they must be recorded in rock, (3) only the horizontal components were considered, (4) the record must be corrected, (5) the record must be obtained inside the range of epicenter

distance established for the corresponding seismic zone, (6) the magnitude must be greater than 5.0, and (7) the focal depth cannot be deeper than that established for the corresponding seismic zone.

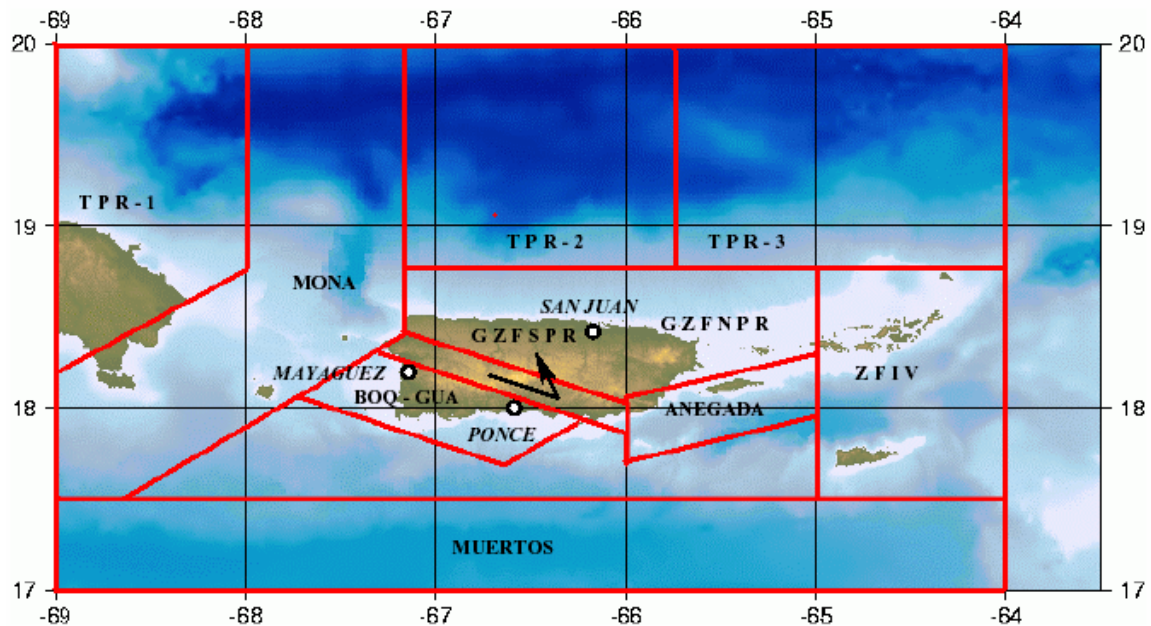


Figure 2.3: Seismic zones around Puerto Rico. (From Martinez, Irizarry, and Portela, 2001)

Table 2.1: Characteristics of the seismic zones. (From Martinez, Irizarry, and Portela, 2001).

Seismic Fault Zone	Maximum Magnitude	Maximum Depth (km)	Minimal Epicenter Distance (km)			Maximum Epicenter Distance (km)		
			San Juan	Ponce	Mayagüez	San Juan	Ponce	Mayagüez
TPR-1	8.0	150	202	167	107	353	339	283
TPR-2	8.0	150	32	81	59	207	243	253
TPR-3	8.0	150	50	122	160	285	357	392
Mona	7.5	200	400	20	20	137	93	136
GZFNPR	6.5	40	64	0	0	179	124	100
GZFSPR	6.5	40	46	64	123	135	175	232
ANEGADA	7.5	30	109	41	19	380	331	296
BOQ-GLIA	6.5	40	107	56	78	349	302	363
MUERTOS	7.5	50	0	20	21	128	193	239
ZFIV	7.5	50	118	170	227	252	291	145

For the Mayagüez area, Martínez et al. found that the response spectrum from two records from the El Salvador earthquake of October 10, 1986, dominates for all the range of periods. These were the records from the National Geographical Institute and from the

Geotechnical Investigation Center. The elastic response spectrum developed for the city of Mayagüez compares well with the design spectrum recommended in the UBC-97 for seismic zone 4 in rock. Comparisons with other studies such as that performed by Dames and Moore (Dames and Moore, 1999) are cited in the report. They found that the design spectrum developed also correlates with that proposed by Dames and Moore for a return period of 2,475 years. It is mentioned that Dames and More recommended for the city of Mayagüez a rock peak acceleration of 0.37g and 0.66g for a return period of 475 years and 2,475 years, respectively, both for rock sites.

2.3 Liquefaction Study

The liquefaction potential is another hazard that needs to be considered in a seismic event. Llavona (2004) performed a study of the liquefaction hazard in Mayagüez for the Puerto Rico Insurance Commission Office. In his study he developed a soil classification map for Mayagüez based on the UBC-97. Also a contour map with liquefaction indexes was presented. Llavona used a database of geotechnical exploration information gathered from many sources by the Civil Engineering Department of the UPR-Mayagüez. From the boring logs, the soil materials, the standard penetration test N values, and the water table were obtained for each site among others parameters. The classification was based on N values obtained from the standard penetration test because the shear wave velocities profiles were not available for most of the sites selected.

The liquefaction hazard analysis was performed by following the recommendations presented by Youd et al. (2001). The report by Youd et al. is based on the simplified procedure for evaluation liquefaction resistance of soils developed by H. B. Seed and I. M. Idriss (1971). In order to use this procedure, the peak ground accelerations at the surface induced by an earthquake must be estimated. To obtain these values, Llavona used the seismic coefficients C_a recommended in the UBC-97 for site classification. From the analyses, a liquefaction factor of safety was determined for each site.

Llavona found that beginning at the northwest part of Mayagüez, following through the coast and ending in the city limits in the southwest part of Mayagüez, the soil profile is classified as SF. In the Llavona study most of the central and east part of Mayagüez was classified as soil profile SD with some areas in the downtown area specified as SE.

CHAPTER 3

Shear Wave Velocity Profiles for Mayagüez Sites

3.1 Introduction

In order to perform site specific ground response analyses and to develop ground response spectra for the city of Mayagüez, it is important to estimate the dynamic soil properties at various locations within the city. Some of these properties are the body wave velocities, shear moduli, and damping ratios for each layer of the soil profiles. The procedures to measure or estimate these properties can be classified as field methods and laboratory methods. In general the field methods are preferred over the laboratory methods because the former do not need to extract samples of the subsoil thus avoiding sample disturbance. Moreover, the information obtained is representative of a larger volume than those from small samples.

For this research project, the Spectral Analysis of Surface Waves (SASW) was chosen to acquire the soil profiles information needed for the development of ground response spectra for Mayagüez that account for site soil properties. A series of SASW field tests were conducted in nine (9) locations within the city of Mayagüez boundaries. The information obtained was used for the ground response analyses to estimate the seismic amplification at the surface, as it is discussed in Chapter 5. The following sections present a brief explanation of the SASW method followed by the results obtained for the Mayagüez sites.

3.2 The Spectral Analysis of Surface Waves (SASW)

The SASW method is an extension of an older test known as the Steady-State Surface Wave method. In this latter method the wavelength of a Rayleigh wave for a specific frequency was determined by applying a source of steady-state vibration at the surface. Then, the phase velocity was calculated by multiplying the frequency by the wavelength. This method requires moving the location of the sensors in the surface to find the wavelength in which the motions recorded by the two sensors are in phase. The process had to be repeated for various frequencies to obtain a curve of phase velocity versus frequency called the dispersion curve.

The modern procedure known as Spectral Analysis of Surface Wave has some similarities with the older method. Some differences are that a steady-state vibrator is not required and others type of sources can be used. Examples of the sources used are impact loads such as those produced by a sledge hammer or a weight drop. These impulsive loads generate a

spectrum of waves with different frequencies thus making the tests less time consuming than the steady-state method. A schematic of the field set up for the SASW test is shown in Figure 3.1.

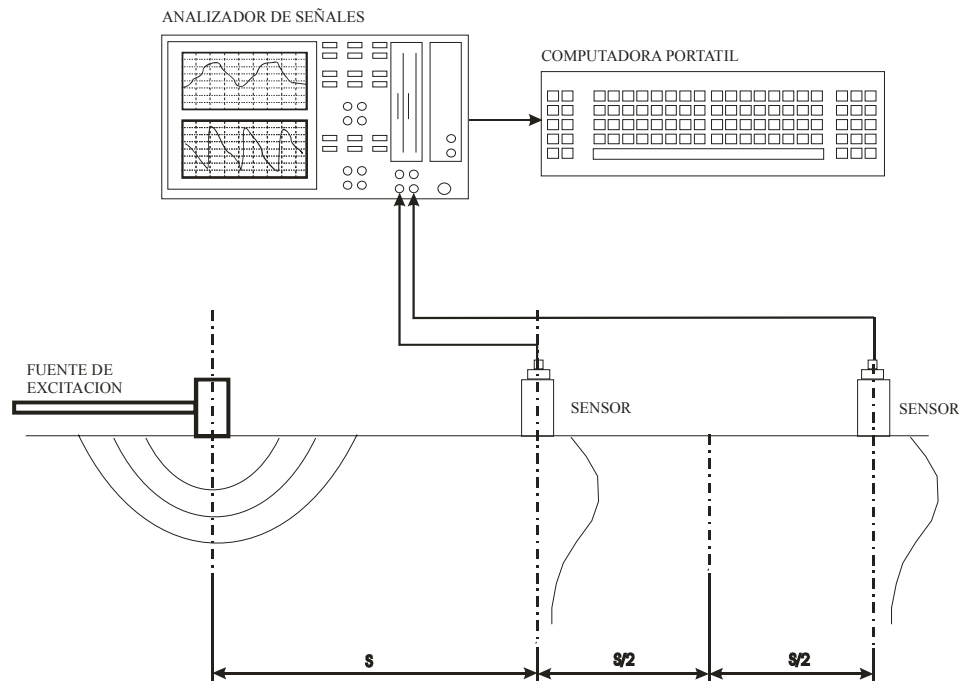


Figure 3.1: SASW field set up.

3.2.1 Field set up and procedure

The SASW test consists of measuring the vertical acceleration or velocity at two points on the surface of a site after a source load is applied. In this project, geophones of the type Mark Products –L4 sensors of 1 Hz and a weight drop estimated in 1200 pounds were used. Figure 3.2 shows the weight drop system constructed at the Civil Engineering (CE) Department of the UPR-Mayagüez. This apparatus was designed and constructed by J. Muract (2004) with the help of technicians from the UPR-Mayagüez CE Department.

For the field tests the sensors were placed at 6.56ft (2m), 13.12ft (4m), 24.60ft (7.5m), 49.21ft (15m), 98.43ft (30m), and 147.64ft (45m) from the source and between them. For the spacing of 6.56ft and 13.12ft, a sledge hammer of 20 pounds was used. The weight was dropped 5 times from a heights ranging between 3ft and 9ft and the signal was averaged for each spacing. The signals were processed using the signal processor HP 35670A in which the cross-power spectrum and coherence for each spacing was saved. This data was used for the development of

the experimental dispersion curve for estimating the shear wave velocity profile. The calculations were performed with a program written in Matlab by Muract (2004) with the modifications explained in the next sections.



Figure 3.2: Weight drop system constructed at UPR-Mayagüez CE Department.

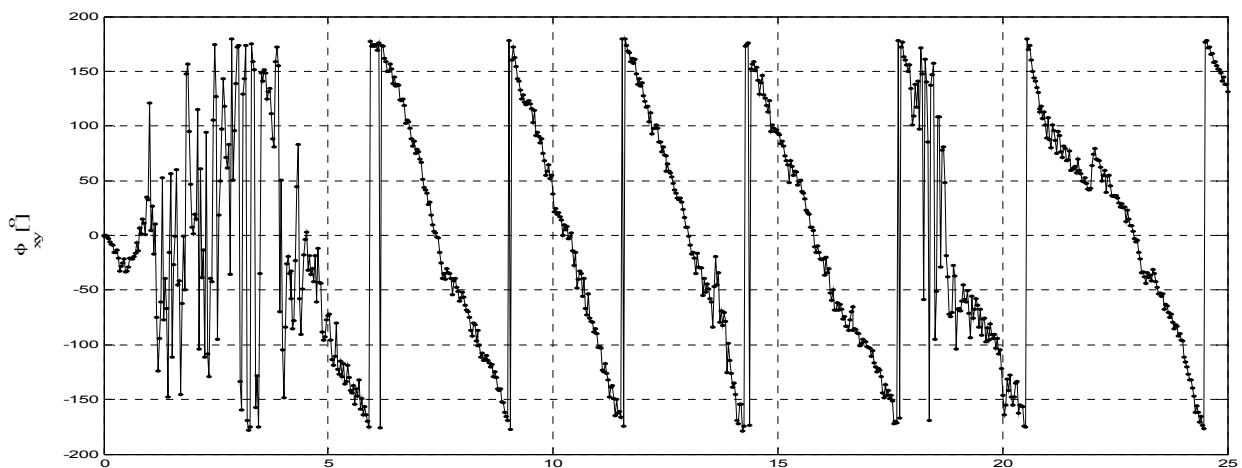
3.2.2 Phase Angles Curves

For the development of the experimental dispersion curves the first step is to calculate the unwrapped phase angle from the cross-power spectrum obtained in the field. The original phase angle $\phi(\omega)$ is calculated with equation 3.1 where S_{12} is the cross power spectrum.

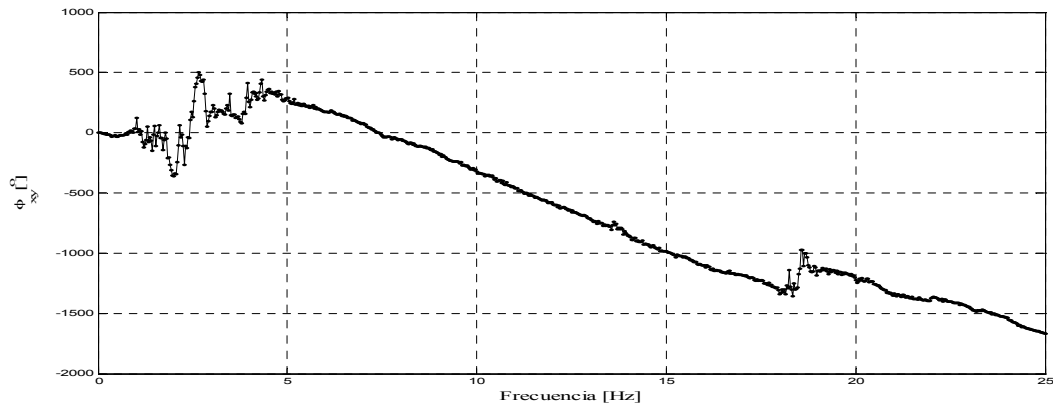
$$\phi(\omega) = \arctan \left[\frac{\text{Im}[S_{12}(\omega)]}{\text{Re}[S_{12}(\omega)]} \right] \quad (3.1)$$

where $\text{Im}[S_{12}]$ and $\text{Re}[S_{12}]$ are respectively the imaginary and real parts of S_{12} . The curve obtained by plotting the phase angle versus frequency is called the phase spectrum. Figure 3.3(a) shows a typical phase spectrum. In this curve the phase angle varies between -180° and

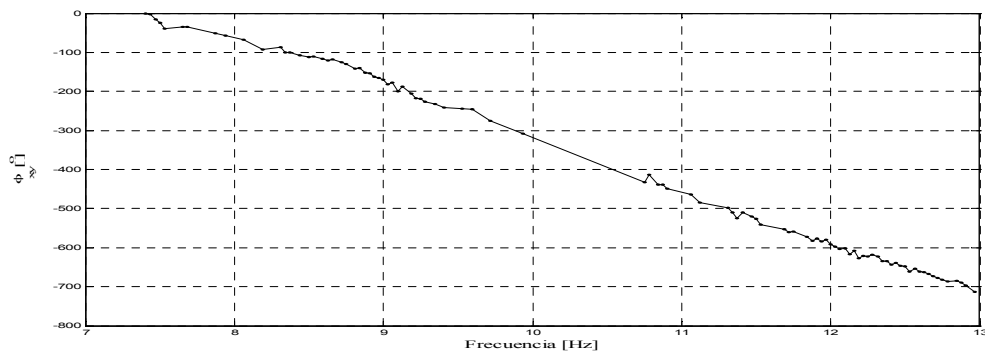
+180°. However, to apply the method one needs the so-called unwrapped angle that increases from 0° up to a maximum value. Figure 3.3(b) displays a typical unwrapped phase angle curve. The original phase angle needs some corrections to eliminate the random variations shown in Figures 3.3(a) and (b) below 5 Hz. Therefore, the code written by Muract (2004) was modified to permit editing the phase spectrum in a process called interactive masking. The methodology implemented for the interpretation of the phase spectrum was proposed by Joh (1996). The interactive masking consists of masking or eliminating the frequency ranges of poor quality. As described by Joh, the poor quality data is considered those regions of significant undulating phase angles, backward saw-toothed pattern, and messy phase angles. Also the near field region defined by the wavelengths less than 2 or 3 times the distance from the source to the first sensor and the wavelengths shorter than four times the diameter of the receiver must be eliminated. The coherence function is also used for editing the phase spectrum eliminating those ranges of low coherence. Figure 3.3 shows a comparison of an unwrapped phase angle without the masking process with an edited one for the Abonos site at a spacing of 100 ft.



a) Phase angle from field data.



b) Unwrapped phase angle without masking.



c) Masked unwrapped phase angle

Figure 3.3: Comparison of phase angle from field data and after the masking process.

3.2.3 Experimental dispersion curve

After editing the field data using the phase spectrum, the second step is to determine the experimental dispersion curve. The dispersion curve is a plot of the Rayleigh wave velocity versus frequency or wavelength. As shown in equation 3.2, the dispersion curve is calculated for each spacing by using the unwrapped phase angle. In equation 3.2 f is the frequency, D is the spacing between sensors and source, and $\phi(f)$ is the unwrapped phase angle for each frequency.

$$V_R(f) = \frac{2\pi fD}{(\phi(f))_{unwrapped}} \quad (3.2)$$

By combining the dispersion curves for each spacing, an average experimental dispersion curve is obtained. A method for averaging the dispersion curves presented by Joh was

implemented in this thesis by modifying to the original computer code written by Muract (2004). The methodology is based on the moving average concept in which, for a group of n data points, a polynomial best-fit calculation is carried out. The average value obtained is assigned to the midpoint of each segment. For the next segment overlapped to the previous one, the average value is calculated again. Figure 3.4 shows the concept of the moving average. For more details the reader is referred to Joh (1996). An example of an average experimental dispersion curve for the 341HWY site is presented in Figure 3.5.

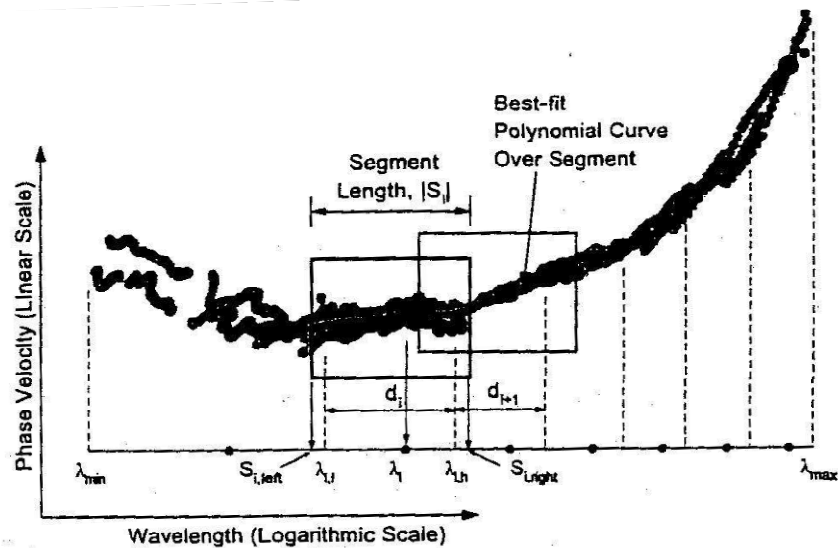


Figure 3.4: Moving average concept for the calculation of the average experimental dispersion curve (From Joh, 1996)

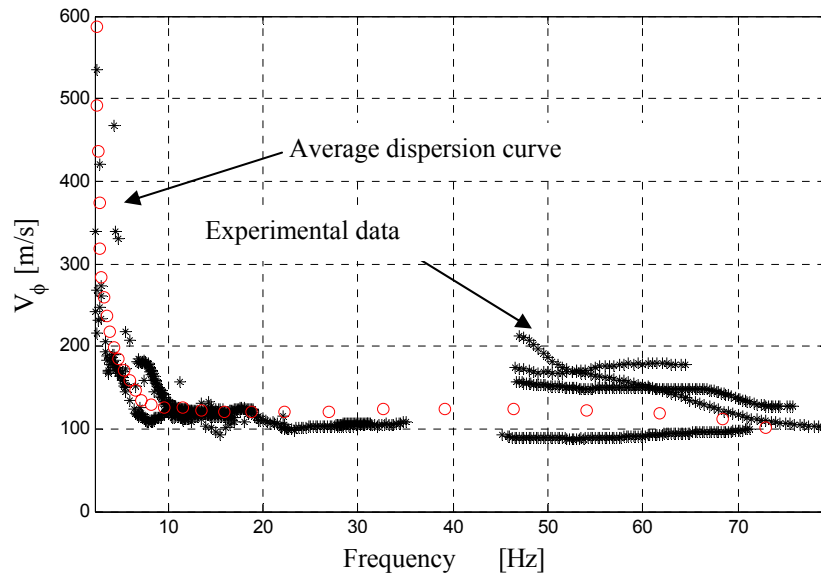


Figure 3.5: Average experimental dispersion curve for the 341HWY site obtained with the moving average concept.

3.2.4 Theoretical Dispersion Curves

The third step in the SASW data interpretation consists of the development of a theoretical dispersion curve for an assumed soil profile for the site. This theoretical curve is then compared with the experimental dispersion curve. The soil profile parameters are then changed until an acceptable error between these curves is attained. The values of the parameters at the last step define the soil profile for the site. The parameters of the layers required for the calculation of the theoretical dispersion curves are the thickness, shear wave velocity, mass density, and Poisson's ratio. This process can be performed by an iterative forward modeling or by inversion modeling. The iterative forward modeling consist of directly changing the parameters, usually the thicknesses of the layers or their shear wave velocities, until an acceptable match between the theoretical and experimental dispersion curve is obtained. The process of inversion modeling consists of the automation of the forward modeling by an optimization technique.

The program written by Muract (2004) was used for the inversion modeling. Muract combined two optimization techniques for minimizing the error between the theoretical and experimental dispersion curves. A first approximation of the soil profile is obtained by the use of neural networks. This first approximation is then entered into the Down-Hill Simplex method to minimize the final error. Muract (2004), show that the use of the Down-Hill Simplex method alone can result in a wrong soil profile because the method cannot distinguish between a local or

global minimum of the function being minimized. Therefore, the neural networks helped to enter a first approximation to the Down-Hill Simplex method that is closed to the global minimum.

The numerical simulation in the inversion modeling of the SASW method consists of the solution of an axisymmetric wave propagation problem by applying a harmonic load on the surface of the soil. The theories of wave propagation and the development of the equations for the SASW numerical simulation is well documented in Muract (2004), Zomorodia (1995), and Nazarian (1993), among others. The development of the governing equations for the SASW simulation is based on the dynamic stiffness matrix approach where the forces applied in the layers are related to their displacements. The stiffness matrix is a function of the frequency and wave number and the solution is performed in the frequency-wave number domain (Zomorodian, 1995). The solution can be found by considering only the fundamental mode of wave propagation, but several researchers had shown that this assumption is not reasonable in soil deposits with considerable stiffness differences between layers or when the stiffness decrease with depth. When these conditions arise, it is recommended to consider other modes of wave propagation. The dispersion curve obtained by using multiple modes will lead to a better match with the experimental dispersion curve.

3.2.5 SASW field test locations

This study is focused in the Mayagüez area. The site selection criteria were based on choosing sites where there was not sufficient geotechnical information for a ground response analysis and other seismic studies. Figure 3.6 displays sites tested on a map of Mayagüez. Table 3.1 lists the sites and their coordinates. The Abonos and 341HWY sites are located on a very deep alluvial soil. The sites Maní Park, Maní, Seco Park, Isidoro García, and Ramírez de Arellano are located along the coast of Mayagüez. Sultanita and Civil are located in residual soil near the hills that border Mayagüez to the east.

Table 3.1: SASW test sites and their coordinates.

Site	Coordinates
Abonos	18° 16' 01N / 67° 09' 44W
341HWY	18° 15' 50N / 67° 10' 35W
Maní	18° 13.79N / 67° 10.33W
Maní Park	18° 14.81N / 67° 10.46W
Seco Park	18° 12.76N / 67° 09.57W
Isidoro García	18° 11' 24N / 67° 09' 14W
Ramírez de Arellano	18° 11.34N / 67° 09.59W
Sultanita	18° 12.81N / 67° 08.65W
Civil	18° 12.81N / 67° 08.39W

Figure 3.6: SASW sites locations in the Mayagüez municipality (map from www.linktopr.com).

3.3 SASW Results Summary

This section presents the results obtained for each site by the Spectral Analysis of Surface Wave tests performed in Mayagüez. The results consist of the shear wave velocity profiles and the soil classification based on the Uniform Building Code 1997 Edition (UBC-97).

Abonos site

The Abonos site is located in the Añasco Valley at the side of the PR-2 highway. The test was performed in a flat surface ground in front of the Abonos Super A factory. Investigation reports mention that these alluvial deposits may extend to depth in excess of 100 ft (Macari 1994). Figure 3.7 shows the phase spectrum obtained from the cross-power spectrum for the 100 ft spacing. After implementing the masking process for editing the phase spectrum defined with field data, the unwrapped phase spectrum shown in Figure 3.8 is obtained. With the masked phase spectrum for each spacing, the average experimental dispersion curve was obtained with the moving average technique described before. Figure 3.9 shows the average experimental dispersion curve for the Abonos site. The inverse modeling considering multiple modes was then performed with the methodology proposed by Muract (2004). The process was performed until a shear wave velocity profile whose theoretical dispersion curve match the experimental dispersion curve was found. The match between the experimental and theoretical dispersion curve is shown in Figure 3.10. The resulting shear wave velocity profile is shown in Figure 3.11.

As it was expected from previous studies in the Añasco Valley, relatively low shear wave velocities were found. A compacted fill material estimated in 2.5 meters thick was found at the surface. Below this fill, relative loose material was found with wave velocities increasing with depth from 150 m/sec to 328 m/sec. The average shear wave velocity in the upper 30 meters depth was 196.9 m/sec and the site classifies as soil type Sd according to the UBC-97. Table 3.2 lists the thicknesses and shear wave velocities of the layers for this site.

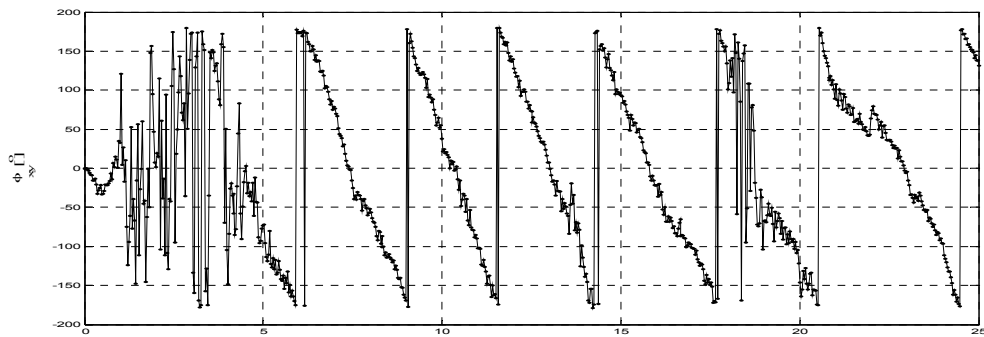


Figure 3.7: Phase spectrum from field data for the Abonos site for the 30 meters spacing.

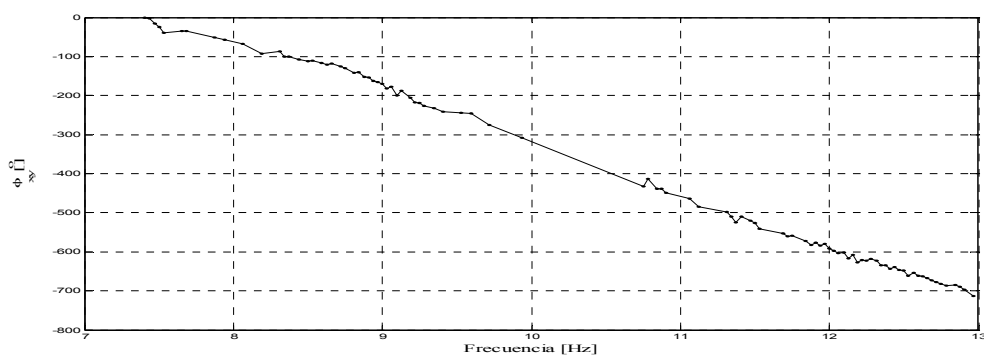


Figure 3.8: Unwrapped phase spectrum for the Abonos site obtained by the interactive masking process.

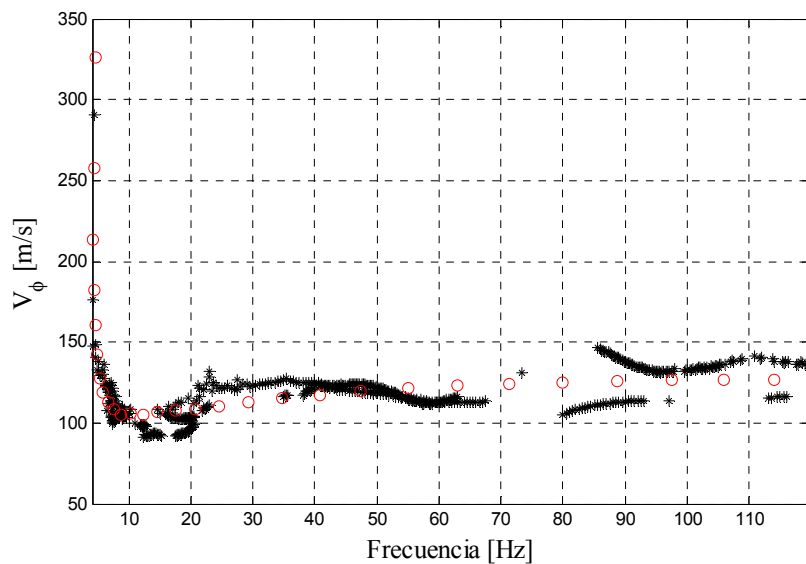


Figure 3.9: Average experimental dispersion curve for the Abonos site.

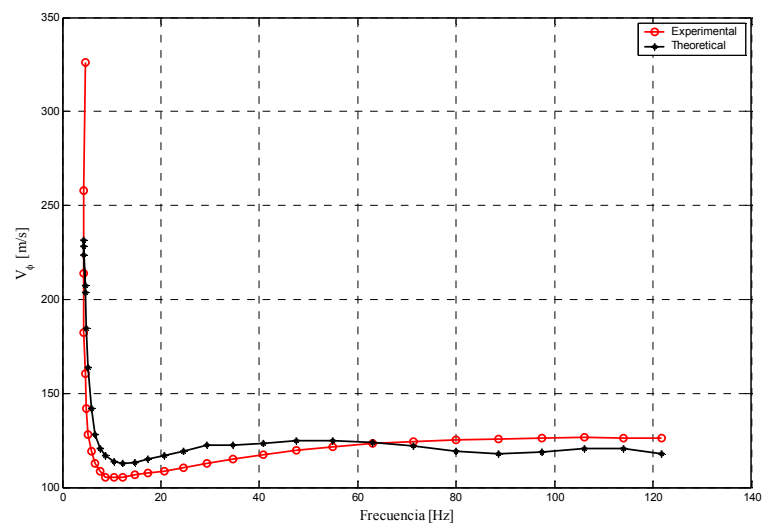


Figure 3.10: Experimental versus theoretical dispersion curve for the Abonos site.

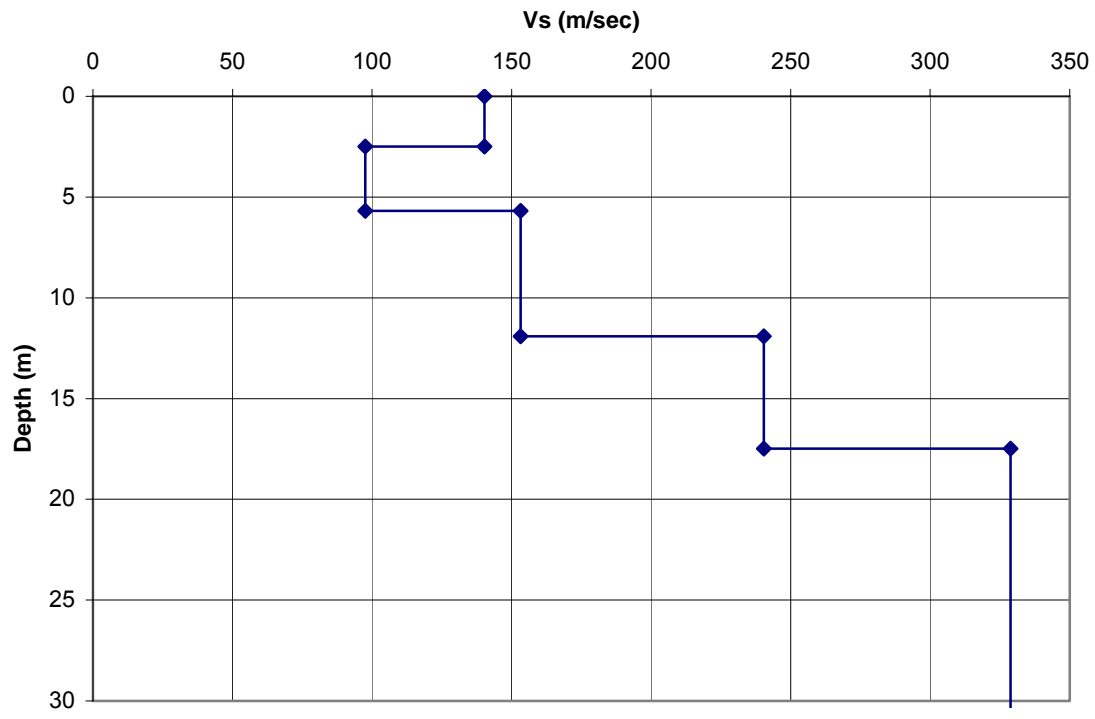


Figure 3.11: Shear wave velocity profile for the Abonos site.

Table 3.2: Layers thickness and shear wave velocities for the Abonos Site.

Velocity Profile	
H [m]	Vs [m/sec]
2.49	140.32
3.19	97.60
6.23	153.26
5.57	240.42
∞	328.81

341HWY Site

The 341HWY site is located to the west of the Abonos site in the Añasco Valley next to highway PR341. A similar geological conditions were expected for this site. The same procedure described for the Abonos site was performed. Figure 3.12 displays the resulting shear wave velocity profile. A stiffer layer was found at a depth of 15 meters compared with the Abonos site. The average shear wave velocity in the upper 30 meters depth was 203.1 m/sec. and thus its UBC-97 classification is Sd. Table 3.3 lists the thicknesses and shear wave velocities of the layers that make up the soil profile for this site.

Table 3.3: Layers thicknesses and shear wave velocities for the 341HWY site.

Velocity Profile	
H [m]	Vs [m/sec]
7.90	122.90
0.10	177.00
7.30	227.70
5.70	366.80
4.70	231.20
12.40	290.90
7.4	904.80
∞	1670.30

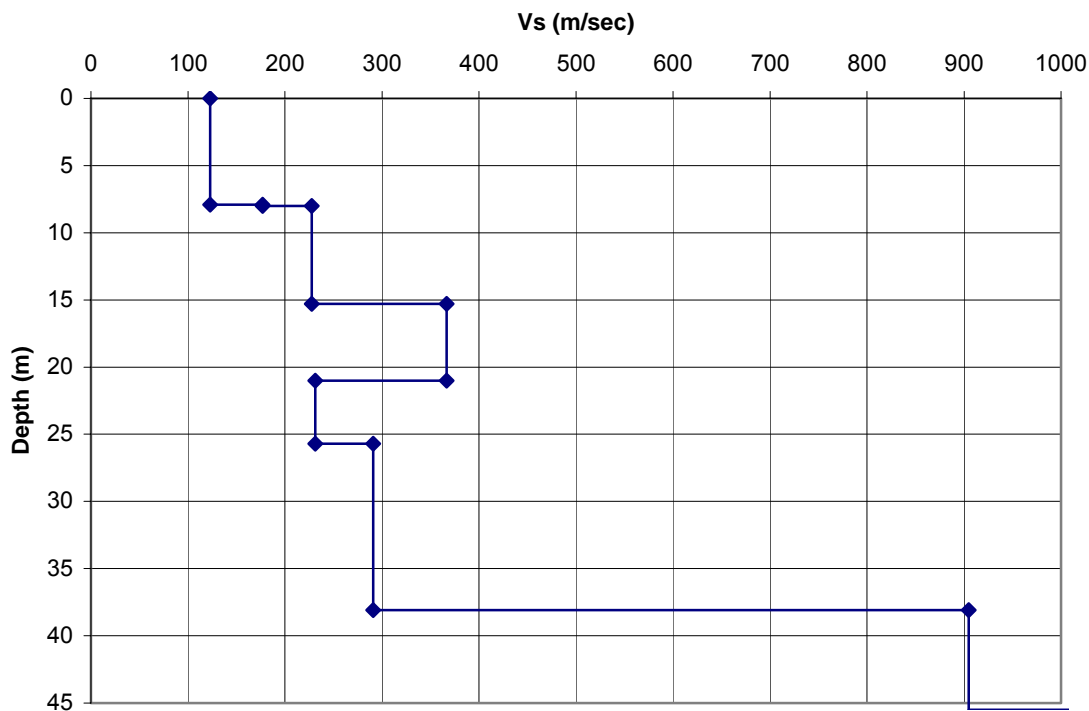


Figure 3.12: Shear wave velocity profile for the 341HWY site.

Maní Site

After completing the 341HWY site, the tests were moved to the coast of Mayagüez. The first coastal site is called El Maní located in the PR-341 highway in the neighborhood of Mayagüez known El Maní. The site consisted of a flat surface ground at the side of the beach. As it is evident in the shear wave velocity profile shown in Figure 3.13, a very high velocity material was found at a depth of 10 meters. This is inferred to be weathered rock, but it does not necessarily represent a geological condition typical of the coast of Mayagüez but rather a particular feature of this site. The layers thickness and shear wave velocity values of the Maní site are listed in Table 3.4. This site was classified as Sc with an average shear wave velocity in the upper 30 meters depth of 503.43 m/sec.

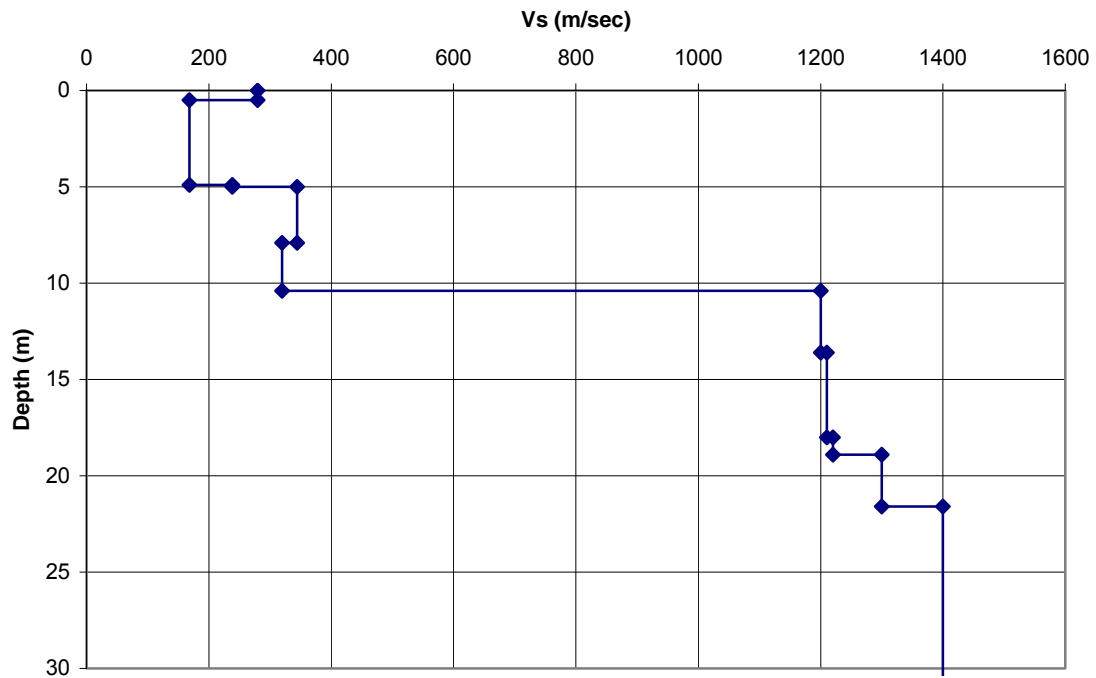


Figure 3.13: Shear wave velocity profile for the Maní site.

Table 3.4: Layers thicknesses and shear wave velocities for the Maní site.

Velocity Profile	
H [m]	Vs [m/sec]
0.50	279.60
4.30	168.50
0.20	238.10
2.90	344.50
2.50	320.00
3.20	1200.00
4.40	1210.00
1.00	1220.00
2.70	1300.00
∞	1400.00

Maní Park Site

The Maní Park site was the second test location near the coast of Mayagüez in the PR-341 highway. The Maní Park (Parque del Maní) is a baseball park located in the end of highway PR341 to the north. A low shear wave velocity was found at this site, as shown in Figure 3.14. The thicknesses of each layer along with the corresponding shear wave velocity are listed in Table 3.5. Velocities from 235 m/sec. at the surface increase with depth to 778 m/sec. at 30 meters depth. This site was classified as Sd with an average shear wave velocity of 274.74 m/sec.

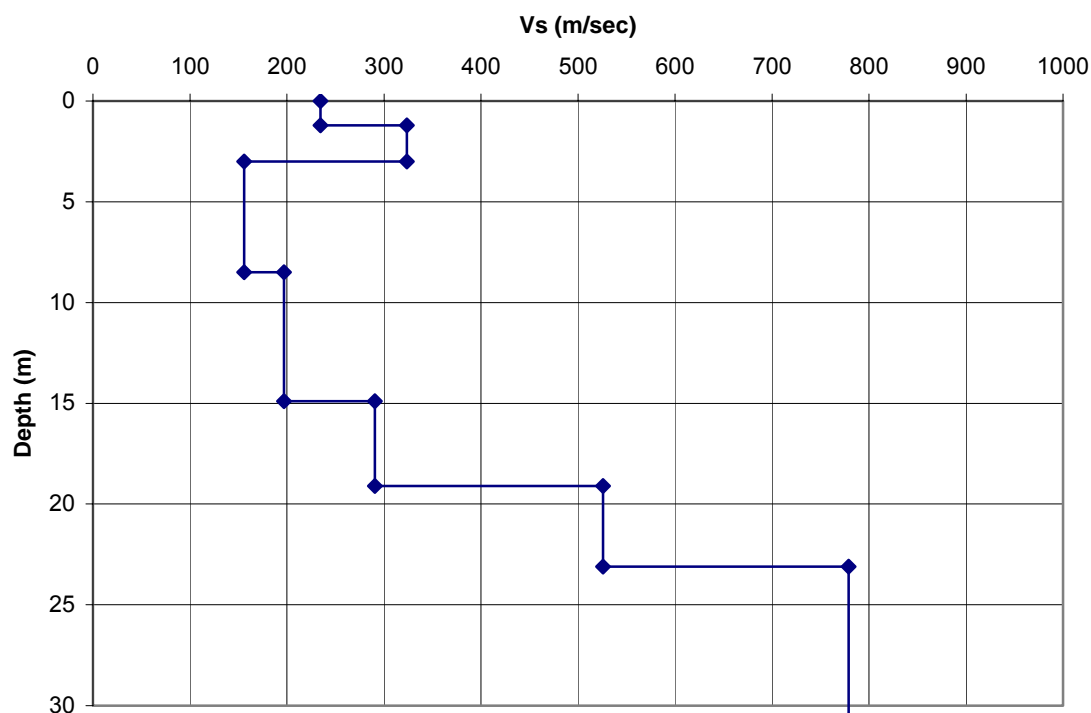


Figure 3.14: Shear wave velocity profile for the Maní Park site.

Seco Park Site

A pattern of shear wave velocity profile similar to the Maní Park site was found in the Seco Park site. The Seco Park site is a baseball park located in the coast of Mayagüez to the south of the Maní Park site in PR-62 highway in the neighborhood known as El Seco. A shear wave velocity around 200 m/sec at the surface drops to 150 m/sec around a depth of 10 meters in a similar way as in the Maní Park site. After a depth of 15 meters depth, the shear wave velocity increases with depth to reach 458 m/sec at 30 meters. The average shear wave velocity calculated using the information in the upper 30 meters of the deposit is 243.72 m/sec. Thus this soil profile

classifies as type Sd per the UBC-97. Figure 3.15 shows the shear wave velocity as a function of depth for the Seco Park site whereas Table 3.6 displays this information in tabular form.

Table 3.5: Layers thicknesses and shear wave velocities for the Maní Park site.

Velocity Profile	
H [m]	Vs [m/sec]
1.20	234.70
1.90	323.40
5.50	155.80
6.40	197.00
4.20	290.50
4.00	525.90
8.20	778.90
∞	1172.70

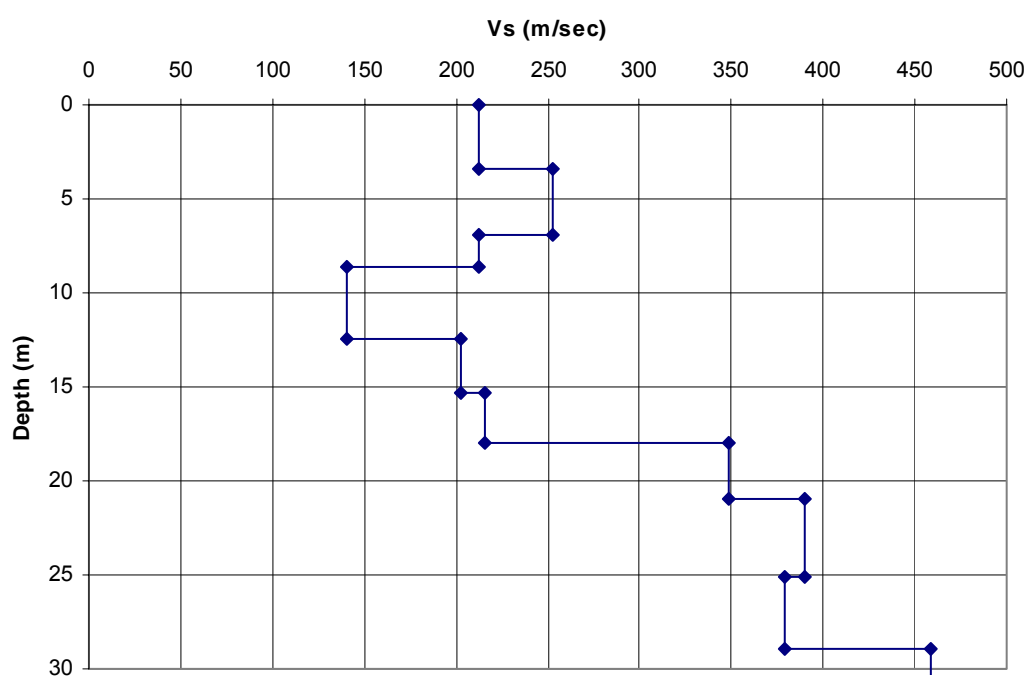


Figure 3.15: Shear wave velocity profile for the Seco Park site.

Table 3.6: Layers thicknesses and shear wave velocities for the Seco Park site.

Velocity Profile	
H [m]	Vs [m/sec]
3.44	212.90
3.49	253.18
1.73	212.57
3.79	140.72
2.86	202.31
2.63	216.12
3.05	349.04
4.09	389.80
3.88	379.45
3.41	458.58
∞	417.09

Isidoro García site

The Isidoro García site is located to the south of the Mayagüez downtown near the coast of Mayagüez at the side of the PR-102 highway. The field consisted of a flat ground surface outside the Isidoro Garcia Baseball Park. Based on the previous results obtained at the coast, low shear wave velocity were expected for this site. There is a low shear wave velocity of 140 m/sec up to a depth of 13.5 meters. The velocity increases to 430 m/sec until a depth of 30 meters. The average shear wave velocity calculated for this site was 211.5 m/sec and the soil profile type is corresponding Sd. The shear wave velocity profile is shown in Figure 3.16. Table 3.7 lists the layers thickness and the shear wave velocities values for the Isidoro García site.

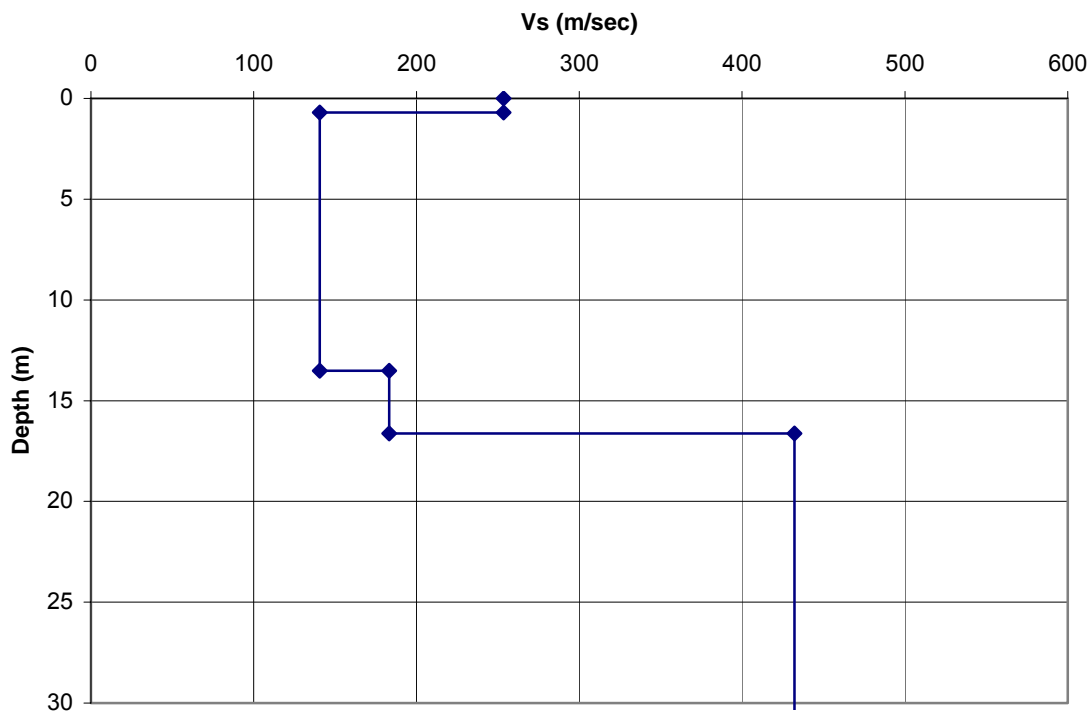


Figure 3.16: Shear wave velocity profile for the Isidoro García site.

Table 3.7: Layers thicknesses and shear wave velocities for the Isidoro García site.

Velocity Profile	
H [m]	Vs [m/sec]
0.69	253.45
12.81	140.60
3.11	183.22
∞	432.06

Ramírez de Arellano site

Figure 3.17 shows the shear wave velocity profile for the Ramírez de Arellano site. This site is located at the south of the city of Mayagüez. The field is between the Ramírez de Arellano residential buildings and the PR-102 at the side of the beach in a flat surface ground. As in the previous site near the coast, a low shear wave velocity was found which varies from 188 m/sec to 452 m/sec up to a depth of 30 meters. The average shear wave velocity up to 30 meters is equal

to 244 m/sec. Thus, this profile classifies as type Sd according to the UBC 97. Table 3.8 lists the thickness of each layer and its shear wave velocity.

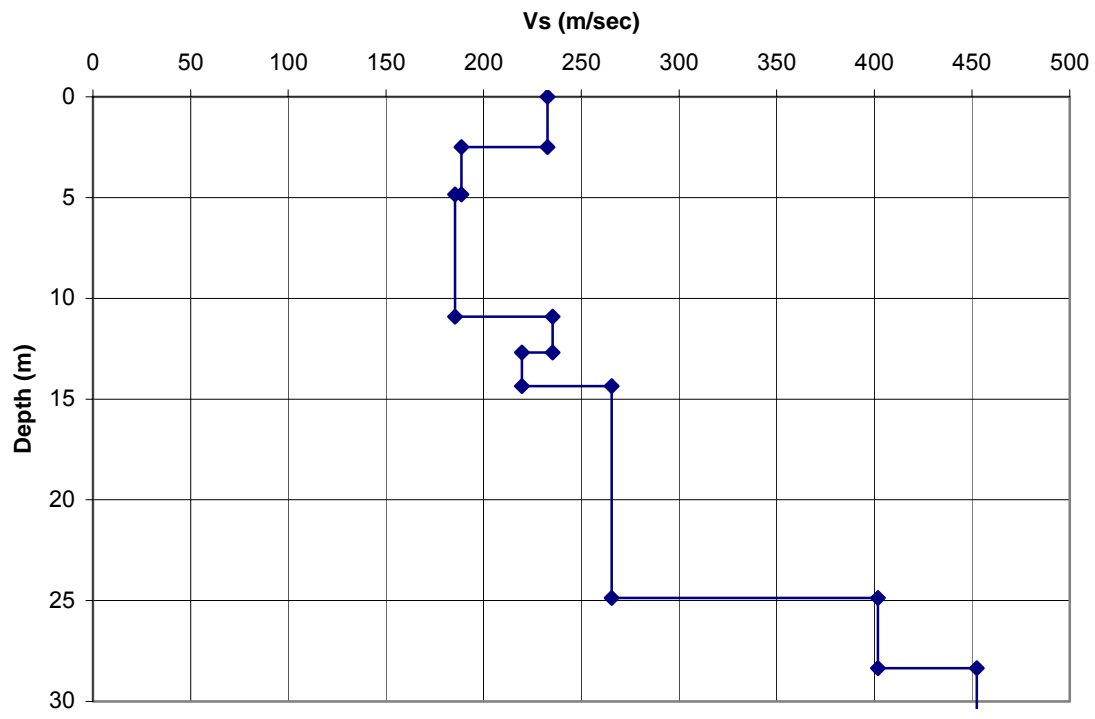


Figure 3.17: Shear wave velocity profile for the Ramírez de Arellano site.

Table 3.8: Layers thicknesses and shear wave velocities for the Ramírez de Arellano site.

Velocity Profile	
H [m]	Vs [m/sec]
2.50	232.68
2.33	188.71
6.07	185.33
1.78	235.31
1.65	219.52
10.51	265.49
3.48	401.88
∞	452.37

Sultanita Site

The Sultanita site is located in a baseball park of the Sultanita sector to the west of Mayagüez in the Sábalos neighborhood. As shown in Figure 3.18, a high shear wave velocity (1097 m/sec) was found beginning at 21 meters below the surface. It is likely that this high velocity layer underneath 21 m is composed of rock. Table 3.9 lists the layers thicknesses and velocity values for the Sultanita site. This site was classified as soil profile type Sd because the calculated average shear wave velocity up to 30 meters is 272.4 m/sec.

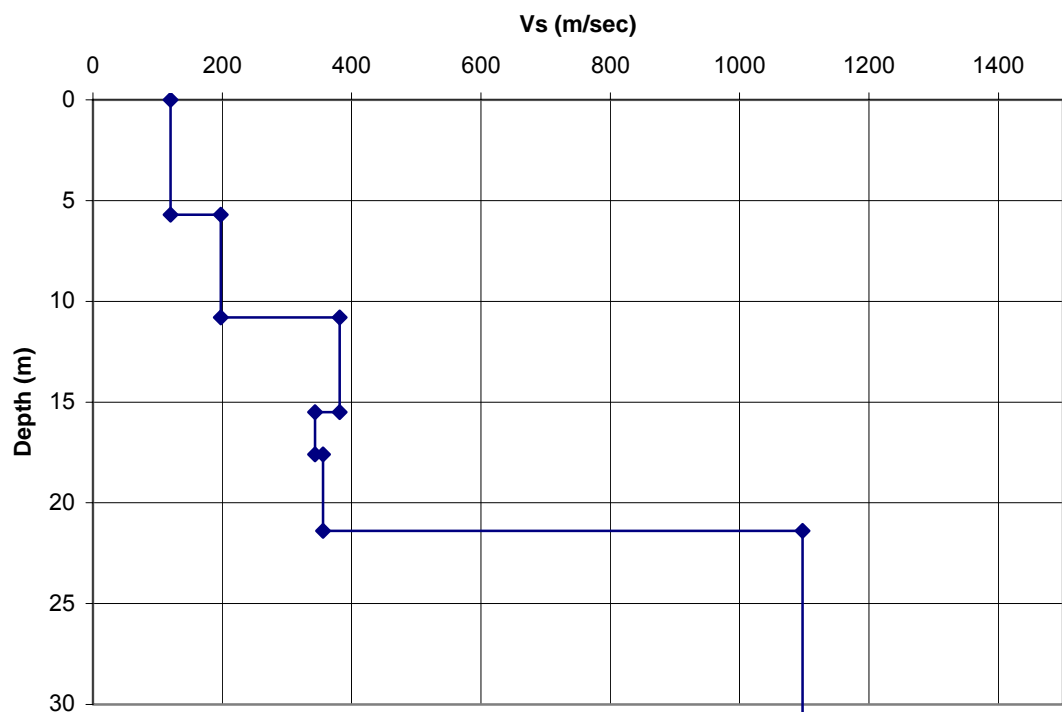


Figure 3.18: Shear wave velocity profile for the Sultanita site.

Table 3.9: Layers thicknesses and shear wave velocities for the Sultanita site.

Velocity Profile	
H [m]	Vs [m/sec]
5.70	120.00
5.20	197.70
4.70	381.70
2.10	343.30
3.90	355.70
9.50	1097.40
∞	3564.5

Civil site

The last site in Mayagüez where the SASW test was conducted was located next to the building of the Civil Engineering Department of the University of Puerto Rico at Mayagüez. For the sake of brevity, the site is simply identified as "Civil". As shown in Figure 3.19, this site has a shear wave velocity profile that increases with depth. A low shear wave velocity was found near the surface, but then quickly increases reaching a value of 935 m/sec below a depth of 14 meters. This site was classified as soil profile type Sc with an average shear wave velocity of 451 m/sec. up to 30 meters depth. Table 3.10 lists the thickness of each layer and its corresponding shear wave velocity.

Table 3.10: Layers thicknesses and shear wave velocities for the Civil site.

Velocity Profile	
H [m]	Vs [m/sec]
2.00	83.50
4.10	388.70
8.10	620.20
9.60	839.40
14.10	935.50

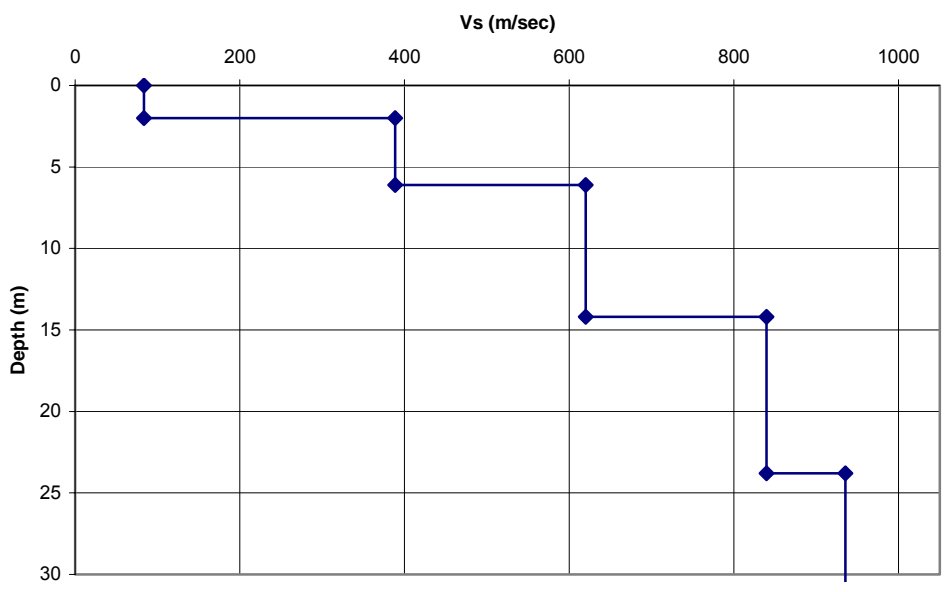


Figure 3.19: Shear wave velocity profile for the Civil site.

In Figures 3.18 through 3.20, the shear wave velocity (V_s) profiles are grouped in four areas in Mayagüez. Figure 3.18 shows the V_s profile for the sites near the coast. The sites located in the Añasco Valley are shown in Figure 3.19. The V_s profile for the sites located in the mountainous area, Sultanita and Civil site, are shown in figure 3.20. Table 3.11 lists the average shear wave velocity, UBC-97 soil profile classification, and the maximum depth reached.

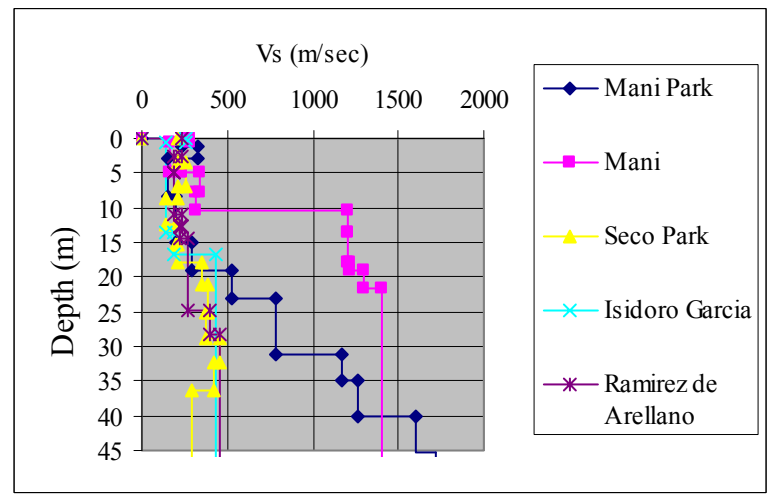


Figure 3.20: Shear wave velocity profile for the sites near the Mayagüez coast.

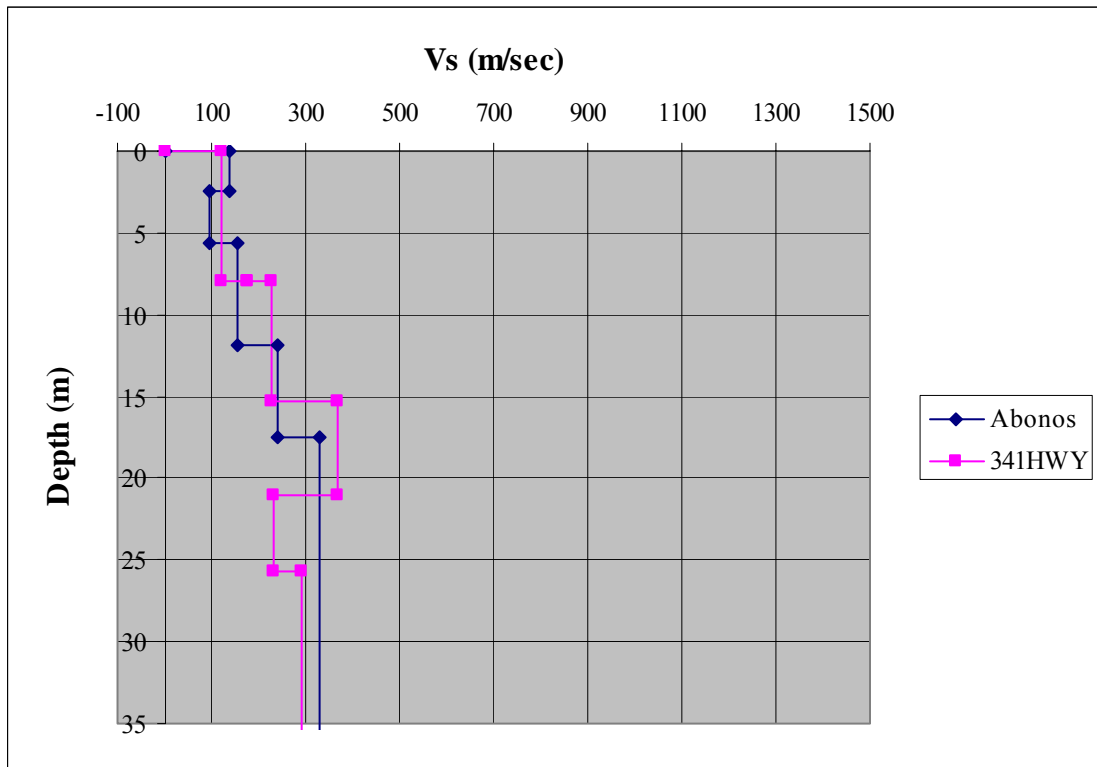


Figure 3.21: Shear wave velocity profile for the sites in the Añasco Valley.

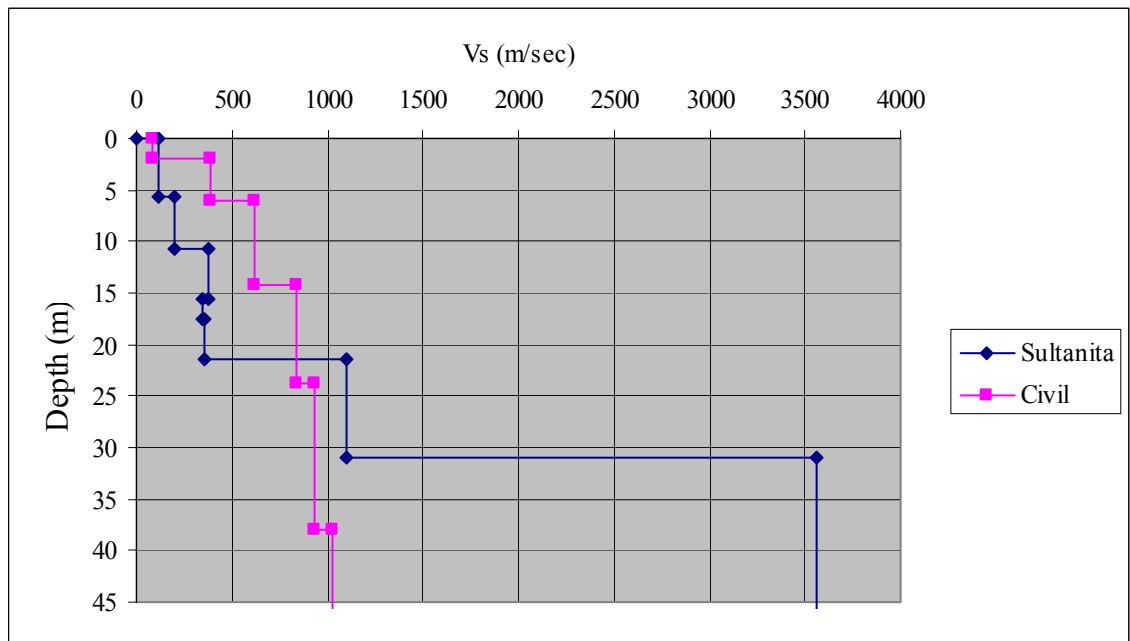


Figure 3.22: Shear wave velocity profile for the sites in the Mayagüez west area.

Table 3.11: Summary of results from the SASW tests.

Site	Vs30	UBC-97	Depth
	m/sec.	Soil Type	(m)
Abonos	196.90	S _D	30
341HWY	203.10	S _D	45
Civil	451.00	S _C	30
Isidoro García	211.50	S _D	30
Maní	503.43	S _C	30
Maní Park	274.74	S _D	30
Ramírez de Arrellano	244.00	S _D	30
Seco Park	243.72	S _D	30
Sultanita	272.40	S _D	30

CHAPTER 4

Simplified Vs30 Estimation Method with SASW Data

4.1 Introduction

A quantity very important for seismic risk studies, seismic hazard zonation, and characterization for seismic instrumentation is the average shear wave velocity in the upper 30 meters (100 ft) of the deposit. This quantity is known as Vs30. More importantly, the Vs30 is used in the NEHRP Provisions and in many codes such as the UBC-97 and the IBC-2003 for the seismic site classifications. The basic assumption is that sites with same soil profile type will respond in a similar manner during an earthquake, i.e, they will amplify in a similar way the seismic waves arriving at the bottom of the deposit.

Different field methods exist to determine the shear wave velocity profile of a site. Some of these methods are the Downhole, Crosshole, and the suspension logging methods. In these invasive seismic methods, geophones or accelerometers are placed inside borings and the wave velocity is calculated by measuring the travel time between two sensors. To obtain the shear wave velocity profile for Mayagüez sites, this thesis used the non-destructive method SASW test. The results from the SASW field tests performed at different locations within Mayagüez were presented in Chapter 3. From the shear wave velocity profile, i.e, a graph or table of the layers thickness and their corresponding shear wave velocity, one can obtain an average shear wave velocity. In most codes such as the UBC-97 and the IBC-2003, the average shear wave velocity is the Vs30 value calculated as

$$V_{s30} = \frac{\sum_{i=1}^n d_i}{\sum_{i=1}^n \frac{d_i}{v_{si}}} \quad (4.1)$$

In equation 4.1 n is the number of layers up to a depth of 30 meters (100 ft), d_i is the thickness of layer i , and v_{si} is the corresponding shear wave velocity.

A simplified method for estimating the average shear wave velocity up to 30 meters (100 ft) depth was proposed by Brown et al. (2000). This thesis examines this approach to validate and investigate its applicability in the soils deposits in Mayagüez. The method is based on the

correlation of the Vs30 value with the Rayleigh wave velocity. Based on their parametric study, Brown et al. developed a predictive equation to calculate an approximate Vs30 using the Rayleigh wave velocity at certain depth. The attractive feature of this method is that it makes use of only one SASW measurement. Therefore it is very convenient when Vs30 estimates in many sites are needed in a short period of time.

The following sections describe the background behind the Vs30 simplified method followed by the results of applying this approach to the SASW tests conducted in Mayagüez. A comparison with the results obtained with the traditional method found in the UBC-97 is also presented.

4.2 The Vs30 Simplify Method

In order to develop a simplify procedure to estimate the shear wave velocity up to 30 meters depth, Brown et al. (2000) correlated the Vs30 value with the Rayleigh wave velocity from SASW tests. They chose the SASW test because of the advantages of this method over other seismic methods. Some of these advantages cited by the authors are that the SASW test is a non-destructive method, the drilling costs and associated time are eliminated, the testing is performed on the ground surface, and the results correspond to a larger volume of the subsurface.

Brown et al. used a database comprised of 103 shear wave velocity profiles obtained from seismic methods. From these 103 profiles, 15 were randomly removed for the validation of the method. The depths of the profiles were 80 meters or more. The Vs30 was calculated for each profile by using the traditional equation such as the one prescribed in the UBC-97. A plot of Vs30 and Rayleigh wave velocities at different wavelength was prepared. A linear regression analysis was performed with values in the plot and they found that there is a high correlation between the Vs30 and the Rayleigh wave velocity at a wavelength of 40 meters. This value of the Rayleigh wave velocity is denoted Vr40. Figure 4.1 shows the plot of Vs30 versus Vr40 prepared by Brown et al. The correlation coefficient was 0.98 with a standard error of 14.5 m/sec. Based on this analysis, a predictive equation was developed. The equation proposed by Brown et al. is

$$V_{s30} = 1.045 * V_{r40} \quad (4.2)$$

To use equation 4.2, only the Vr40 value is needed from the dispersion curve obtained by the SASW field test. Because of this, only a single source-receiver spacing is needed.

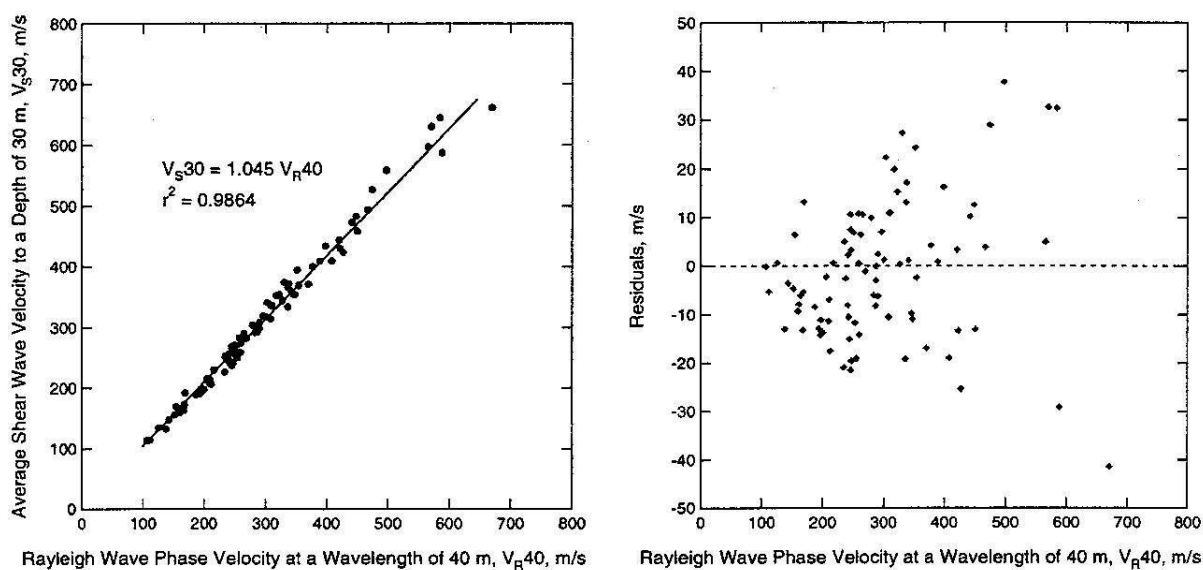


Figure 4.1: Linear regression of Vs30 versus Vr40 (after Brown et al. 2000).

4.3 Vs30 for Mayagüez sites based on the Brown et al. procedure

The method proposed by Brown et al. was used to determine the average shear wave velocity at a depth 30 meters with the data obtained from the SASW tests conducted in the Mayagüez area. The maximum spacing between sensors and source used in the field tests in Mayagüez was 45 meters. This meets the Brown's recommendation of using a spacing equal to 40 meters or more.

As an example of the procedure, the experimental dispersion curve in the wavelength domain for the Abonos site is shown in Figure 4.2. The dispersion curve is obtained after editing the phase spectrum of the cross power spectrum and performing the moving average process as explained in Chapter 3. From the graph, one obtains that for a wavelength of 40 meters, the corresponding Rayleigh wave velocity Vr40 is 192 m/sec. Introducing this value in equation 4.2 leads to an average shear wave velocity at 30 meters depth Vs30 equals to 200.64 m/sec. This value should be compared with the Vs30 obtained Vs30 = 196m/sec which is the value obtained with equation 4.1 of UBC-97. The difference is 4.64 m/sec which is equivalent to an error of 2.0%. Clearly the correlation is excellent for this case.

Table 4.1 lists the Vs30 values obtained with the two approaches for all the sites where the SASW tests were carried out. The UBC-97 soil profile types table is reproduced in Table 4.2 where the soil profile is classified according to the average shear wave velocity Vs30.

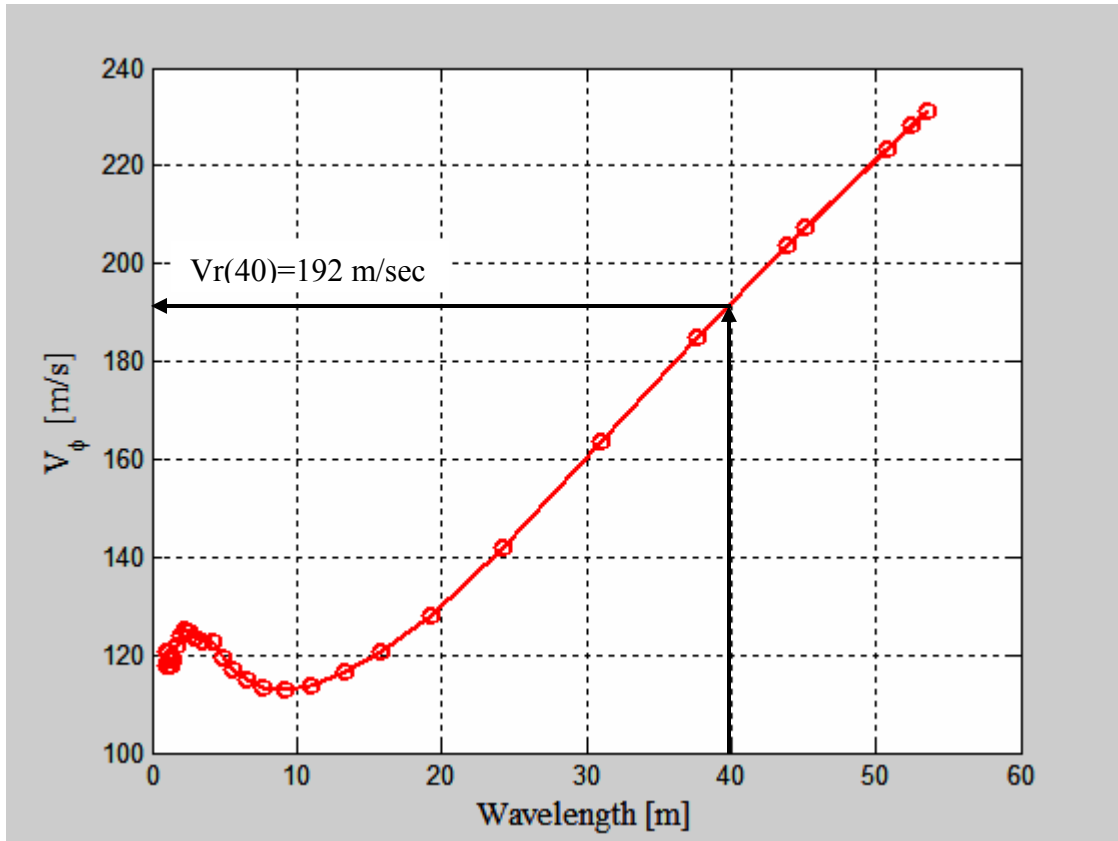


Figure 4.2: Dispersion curve in the wavelength domain for the Abonos site.

Table 4.1: Average shear wave velocity V_{s30} from the UBC-97 formula and the Simplified Procedure.

Site	UBC-97		Simplified V_{s30}			Error
	V_{s30}	Soil	V_{r40}	V_{s30}	Soil	
	m/sec	Type	m/sec	m/sec	Type	%
Abonos	196	S_D	192	200.64	S_D	2.37
341HWY	203.1	S_D	199	207.96	S_D	2.39
Civil	625.00	S_C	400	418.00	S_C	7.35
Isidoro García	211.2	S_D	175	182.88	S_D	13.41
Maní	503.4	S_C	426	445.17	S_C	11.57
Maní Park	274.7	S_D	227	237.22	S_D	13.65
Ramírez de rrellano	243.9	S_D	225.8	235.96	S_D	3.26
Seco Park	243.7	S_D	200	209.00	S_D	14.24
Sultanita	272.4	S_D	260.5	272.22	S_D	0.07

Table 4.2: UBC-97 soil profile types.

Soil Profile Type	Soil Profile Description	Shear wave velocity Vs30 ft/sec. (m/sec)
S _A	Hard Rock	> 5,000 (1,500)
S _B	Rock	2,500 to 5,000 (760 to 1,500)
S _C	Very Dense Soil and Soft Rock	1,200 to 2,500 (360 to 760)
S _D	Stiff Soil Profile	600 to 1,200 (180 to 360)
S _E	Soft Soil Profile	< 600 (180)
S _F	Soil required site specific evaluation	

Table 4.1 shows that the soil type classifications based on the average shear wave velocity in the upper 30 meters depth defined according to the UBC-97 and the simplified procedure coincide for all the sites. The smallest error was obtained for the Sultanita site, only 0.07%. The largest error occurred for the Seco Park site and is equal to 14.24%. Brown et al. reported that the average error obtained in their studies was 10%. The average error found for the nine sites in the Mayagüez area is 7.6%.

From the results listed in Table 4.1 one concludes that the application of the simplified Vs30 method for the Mayagüez sites results in average shear wave velocities with errors in the range stated by Brown et al. The method is recommended for a soil classification program in which many sites will be tested with SASW method in a short time because it permits a relatively quick estimation of the Vs30 values. Note that the velocity ranges used to classify the soil profiles is much larger than the average error (10%) obtained with the simplified method to calculate Vs30. For instance the bracket of the average shear wave velocity to define a soil profile type Sc is between 360 m/sec to 760 m/sec. Thus, if the value predicted by the simplified method falls anywhere within 324 m/sec to 684 m/sec it is most likely that the soil classification done with the approximate Vs30 is correct. If the approximate Vs30 is near the boundaries between two soil profile types, then the classification loses accuracy.

CHAPTER 5

One Dimensional Ground Response Analysis

5.1 Introduction

Chapter 3 presented the results obtained from the SASW tests in nine sites in the Mayagüez area. Using the information gathered, linear and equivalent non-linear one-dimensional ground response analyses were performed for these sites to study the seismic amplification at the surface considering in-situ soil properties. In addition, five more sites were selected and analyzed with information obtained from the Standard Penetration Tests. This chapter shows how the data obtained from the SASW tests and from the standard penetration tests was used in the ground response analysis. Also, the resulting ground response spectra at the surface for each site are presented.

5.2 One-dimensional ground response analysis

A ground response analysis consists of studying the behavior of a soil deposit subjected to an acceleration time history applied to a layer of the profile. When dealing with earthquake ground motions, the acceleration time history is usually specified at the bedrock. Examples of response quantities that can be obtained are the acceleration, velocity, displacement, stress, and strain time histories at any layer. Some of the applications of these analyses are in liquefaction assessment and for seismic risk and hazard studies.

Different methods of ground response analysis have been developed including one dimensional, two dimensional, and three dimensional analyses. Various modeling techniques like the finite element method were implemented for linear and non-linear analysis. The reader is referred to Kramer (1996) for information on these analyses. In this research project, an equivalent linear one-dimensional analysis as implemented in the computer program SHAKE2000 (Ordóñez, 2003) was used. The following is a brief explanation of the method used. The reader interested in detailed information on this topic can find it in Kramer (1996) and SHAKE (2003).

The term one-dimensional refers to the assumption that the soil profile extends to infinity in all the horizontal directions and the bottom layer is considered a half space. In this type of analysis, only the vertical propagation of seismic waves can be considered, usually shear waves. The equivalent linear one-dimensional analysis is an approximate linear method of analysis. The

non linear behavior of the soil is accounted by means of an iterative process in which the soil damping ratio and shear modulus are changed so that they are consistent with a certain level of strain calculated with linear procedures. The soil nonlinearities are not implicitly considered as in fully non linear methods; rather at each iteration cycle the equations of motion solved are those of an equivalent linear model. The process for the equivalent linear method is summarized below.

Figure 5.1 shows a simplified flowchart of the steps performed in an equivalent linear analysis in the frequency domain. The input data necessary are the time history of an earthquake, the soil profile, and the dynamic soil properties. The earthquake time history can be a corrected accelerogram recorded by seismic station or a synthetic or artificial ground motion. The soil profile consists of the layers and their corresponding thicknesses, initial damping ratio, unit weights, and shear moduli or shear wave velocities. The dynamic soil properties are defined by means of a damping ratio and shear modulus degradation curves. These are curves of the variation of the equivalent damping ratio and secant shear modulus with strain.

First, the Fourier transform of the acceleration time history is determined by using the Discrete Fourier Transform (DFT). Second, the Transfer Functions for the different layers are determined using the current properties of the soil profile. The transfer functions give the amplification factor in terms of frequency for a given profile. In the third step, the Fourier spectrum is multiplied by the soil profile transfer function to obtain an amplification spectrum transferred to the specified layer. Then, the acceleration time history is determined for that layer by the Inverse Fourier Transformation in step four. With the peak acceleration from the acceleration time history obtained and with the properties of the soil layer, the shear stress and strain time histories are determined in step five. In step six, new values of soil damping and shear modulus are obtained from the damping ratio and shear modulus degradation curves corresponding to the effective strain from the strain time history. With these new soil properties, new transfer functions are obtained and the process is repeated until the difference between the old and new properties fit in a specified range.

This method of analysis had proved to give good approximations of the response of a soil deposit subjected to an earthquake and it had been successfully compared with finite element method and fully non-linear analysis. A recent comparison made with the finite elements non-linear codes was performed in a seismic amplification study in Lotung, Taiwan (Borja, et.al., 2002) reporting good results.

5.3 Dynamic soil properties

In the equivalent linear one dimensional analysis implemented in the computer program SHAKE 2000, the dynamic soil properties are defined by the damping ratio and shear modulus degradation curves. Researchers had developed this type of curves for different soil materials. Example of this curves for sand and clay are those proposed by Seed and Idriss (1970) and Seed and Sun (1989), for gravel the ones proposed by Seed et al. (1986), and the damping ratio and shear modulus degradation curves for rock proposed by Shnabel (1973). These curves were the used in this thesis and are shown below.

Figure 5.2 shows the shear modulus degradation curves for sand proposed by Seed and Idriss (1970). Seed and Idriss presented three curves for a lower bound, upper bound, and average values. The damping curves for sand with the same range of shear strain are shown in Figure 5.3. Note that lower bound sand refers to less stiff sand with less damping ratio compared with the upper bound sand at a same shear strain.

Figure 5.4 shows the shear modulus degradation curve for clay proposed by Seed and Sun (1989) and Figure 5.5 the damping ratio degradation curves proposed by Seed and Idriss (1970). It must be mentioned that one can find in the literature these curves for different levels of plastic index for clay and for different confined pressure for sand. The SASW method does not provide this information directly and it was not a standard practice to report them in the boring logs done near the sites investigated. For this reason, general curves like those presented here were adopted for this study.

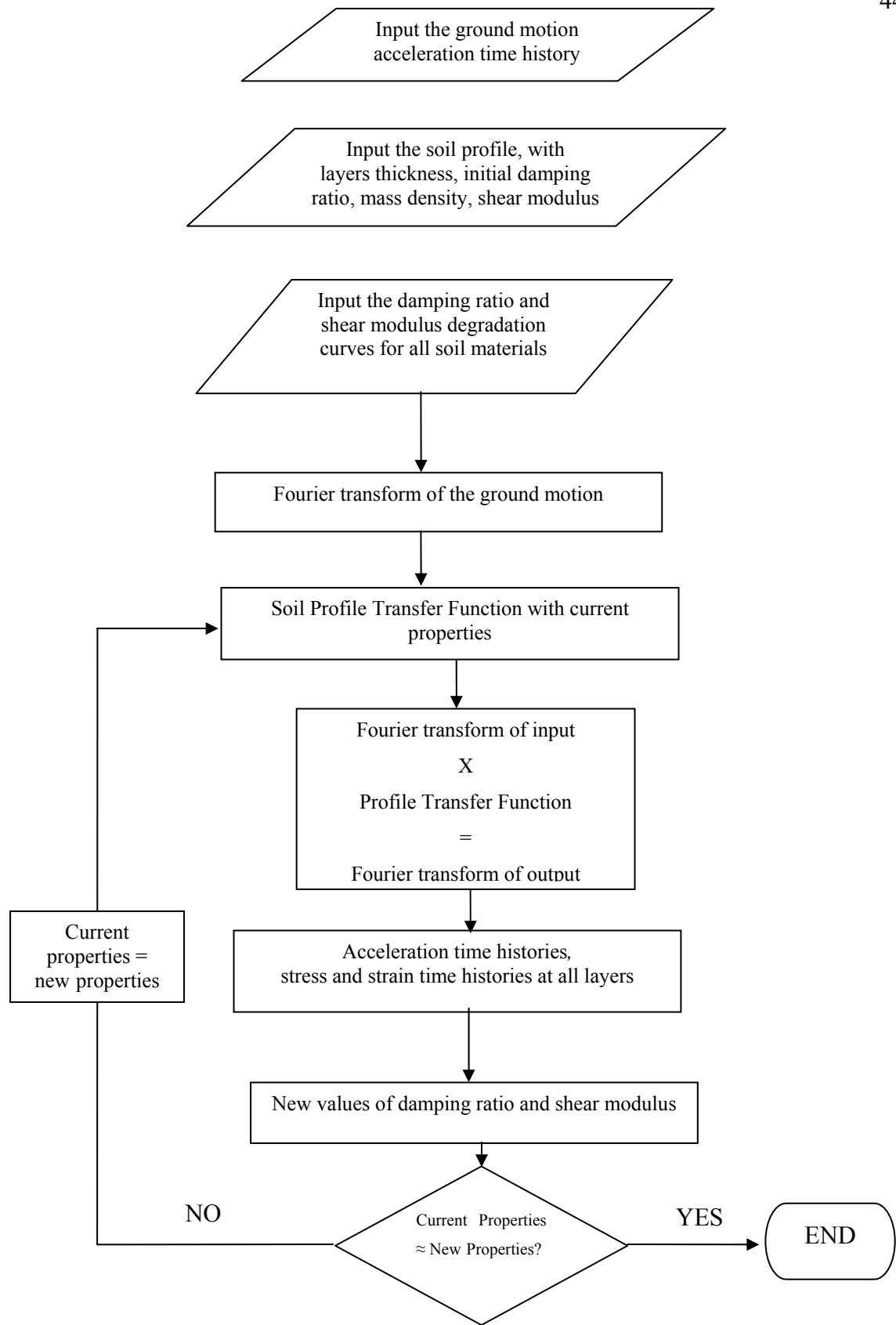


Figure 5.1: Flowchart for the equivalent linear ground response analysis.

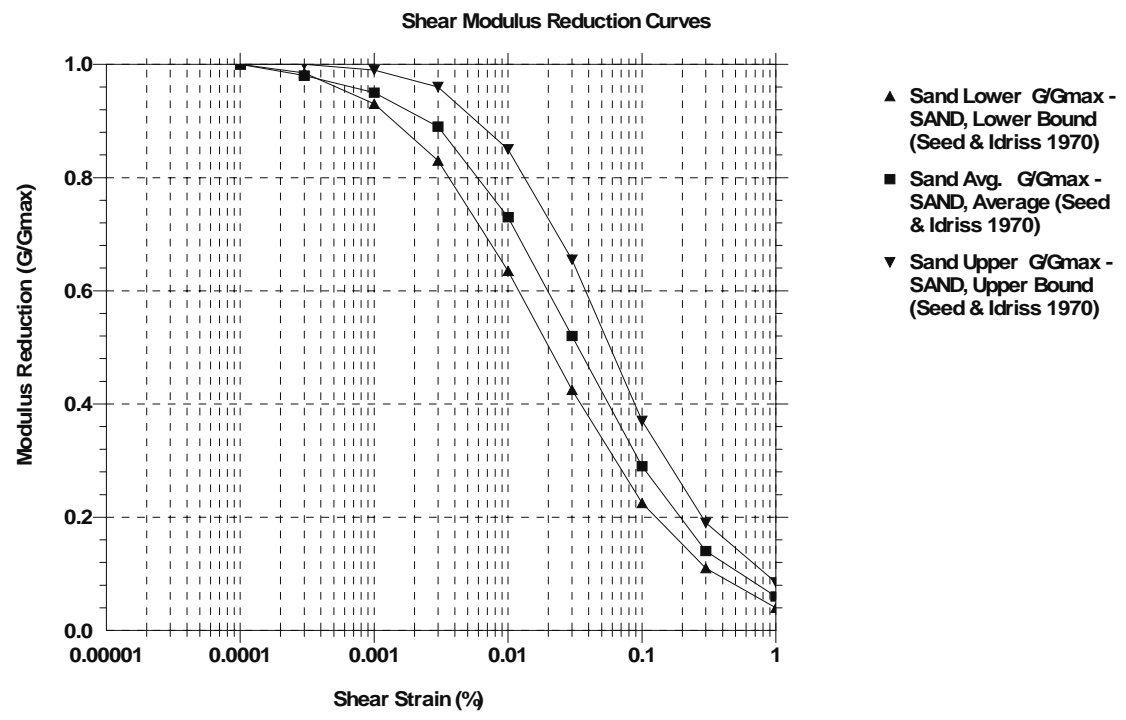


Figure 5.2: Shear modulus reduction curves for sand proposed by Seed and Idriss (1970).

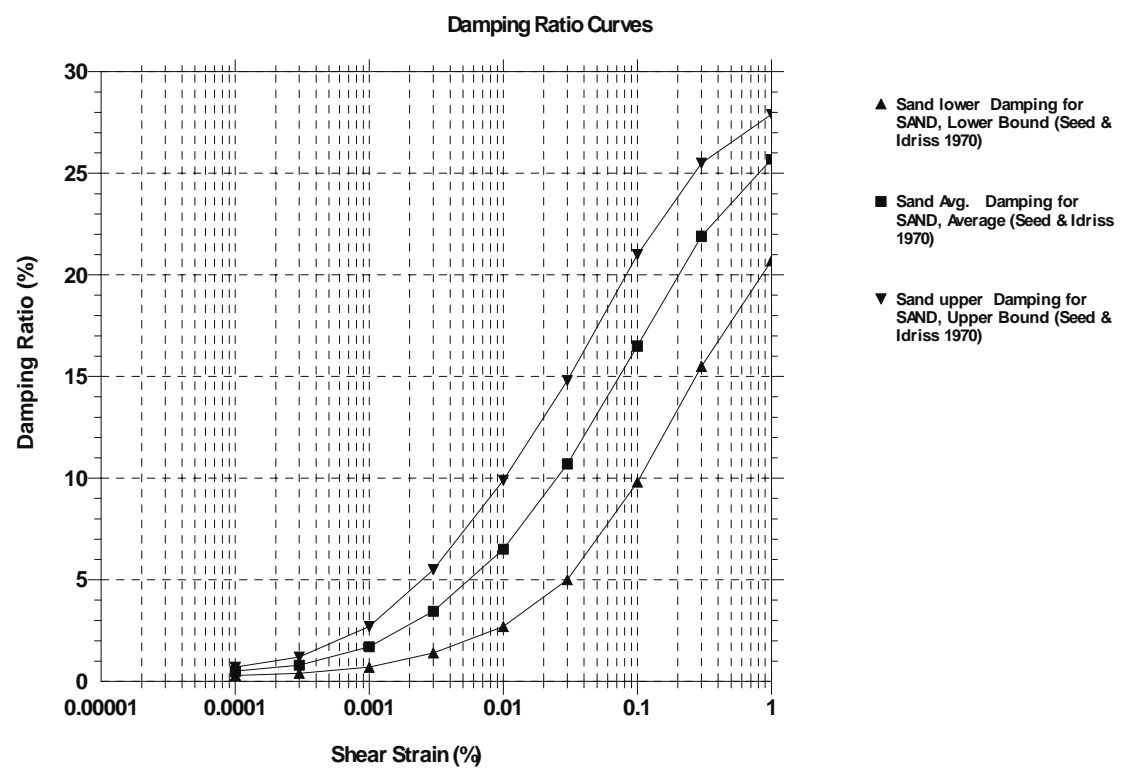


Figure 5.3: Damping ratio reduction curves for sand proposed by Seed and Idriss (1970).

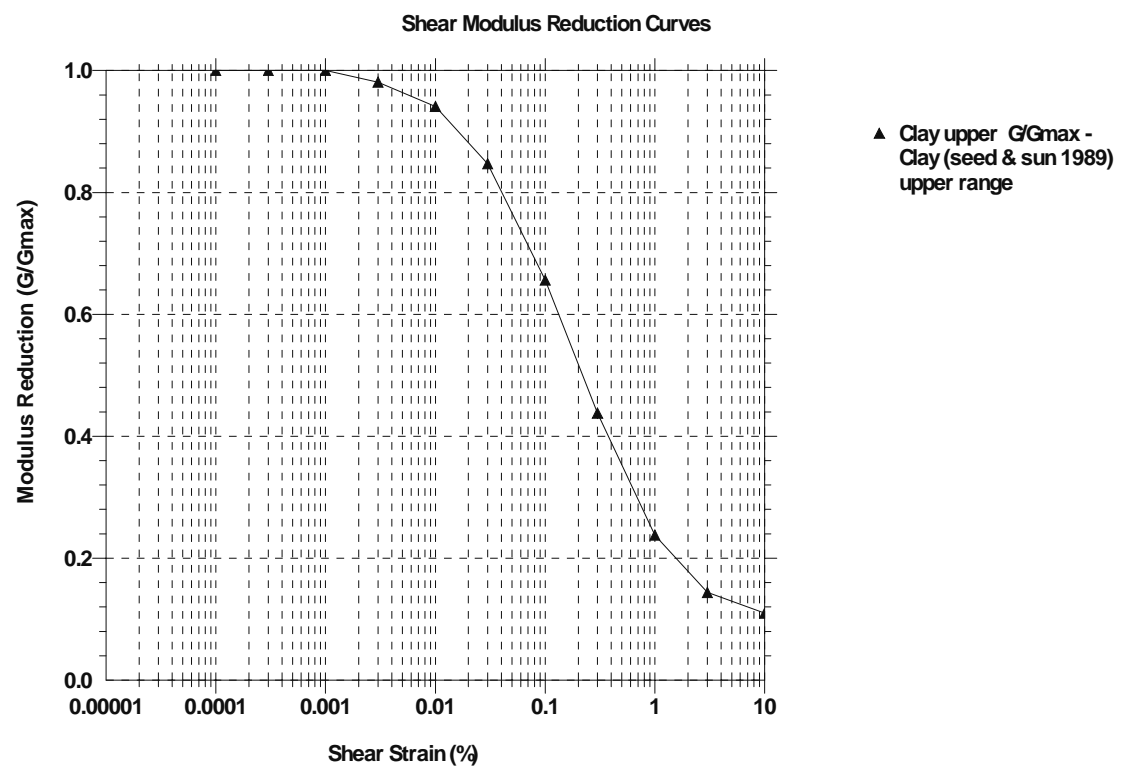


Figure 5.4: Shear modulus reduction curve for clay proposed by Seed and Sun (1989).

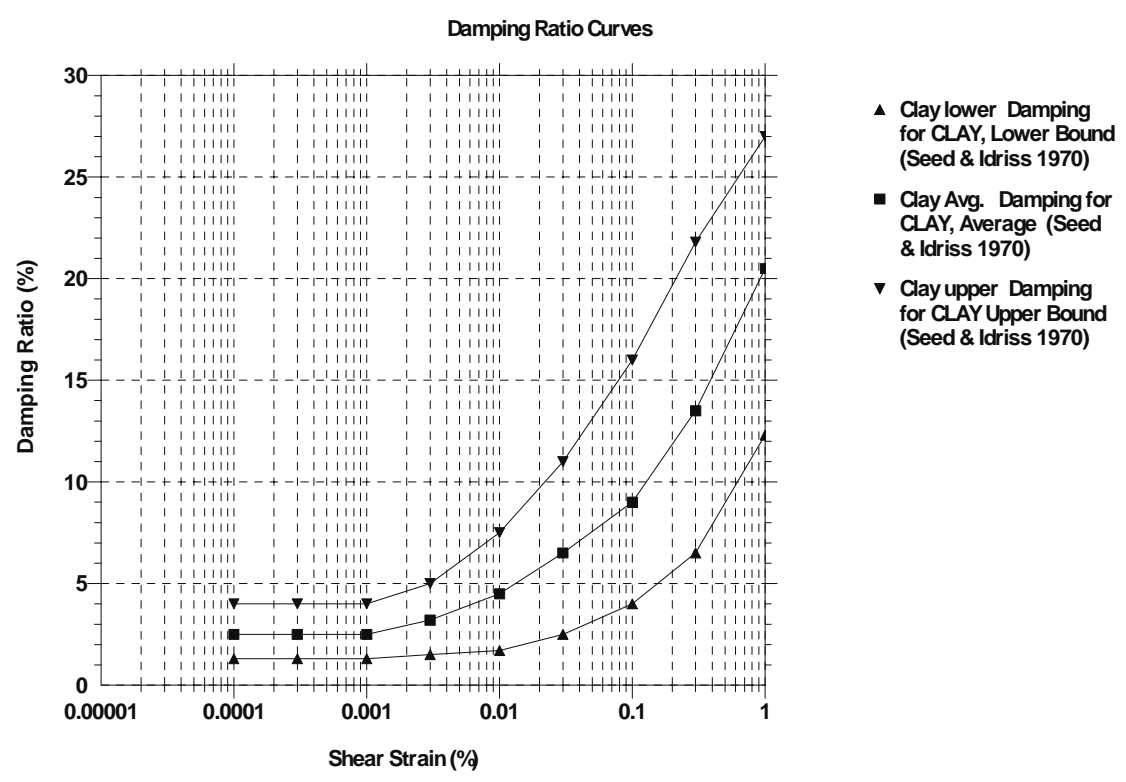


Figure 5.5: Damping ratio reduction curves for clay proposed by Seed and Idriss (1970).

The degradation curves for gravel and rock used in this project were those proposed by Seed et al. (1986) and Shnabel (1973), respectively. These are shown in Figures 5.6 and 5.7.

In order to identify the materials in the soil profile of each site and assign the most appropriate reduction curve for the analysis, a review of geotechnical boring logs was done by using a geotechnical exploration database for Mayagüez. The sites investigated were classified in three groups according to the site information available. Table 5.1 summarizes the groups created in this study with their description and the sites assigned to each group. The Viaducto, El Castillo, El Bosque, India, and Marina were the new sites included because there is information available in the geotechnical exploration database of the Civil Engineering Department of UPR-Mayagüez. Figure 5.8 shows the six additional sites located in the Mayagüez map. Those sites where shear wave velocity profile in combination with geotechnical boring logs near the sites was available were assigned to group A. For these sites where geotechnical information was not available, tables of correlations between soil materials and shear wave velocity prepared by ASTM and the U.S. Army Corps of Engineers (USACE 1995) were used. These sites were assigned to group B. The USACE table is reproduced in Table 5.2. From the geotechnical exploration database three sites were found in Mayagüez where the total depth reaches 100 ft. These sites, for which only geotechnical information was available, were assigned to group C. The relations between the N values from standard penetration tests with shear wave velocity proposed by Imai and Yoshimura (1970) and Imai and Tonouchi (1982) were used as recommended in the NAVFAC (1997). The curve that correlates the shear wave velocity and the N values is reproduced in Figure 5.9.

Tables 5.3, 5.4, and 5.5 shows a summary of the damping ratio and shear modulus reduction curves used for each of the sites analyzed in this thesis.

Table 5.1: Groups created and sites designation for the ground response analysis.

Group	Description	Sites
A	Sites with shear wave velocity profile and geotechnical boring logs near the site.	Abonos, Maní, Biología, Civil, Viaducto
B	Sites with shear wave velocity profile only.	341HWY, Maní Park, Seco Park, Ramírez de Arrellano, Isidoro García, Sultanita
C	Sites with geotechnical boring logs only.	<i>El Castillo, El Bosque, India, Marina</i>

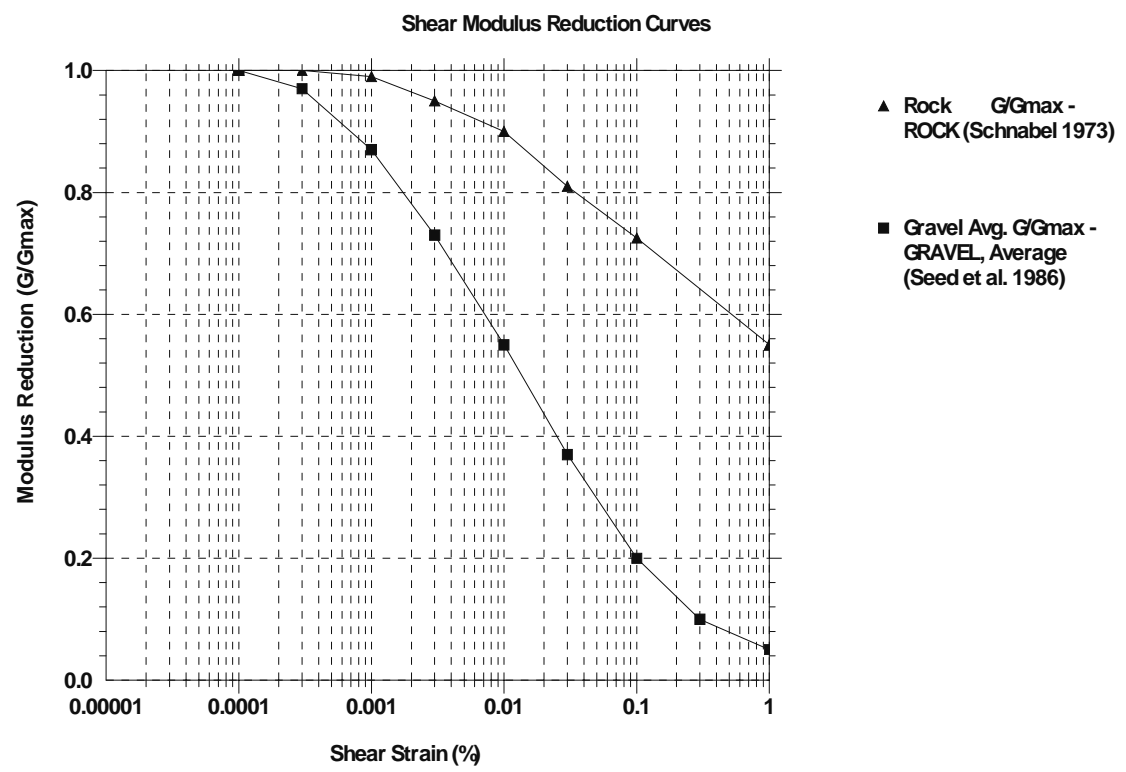


Figure 5.6: Shear modulus reduction curves for gravel and rock.

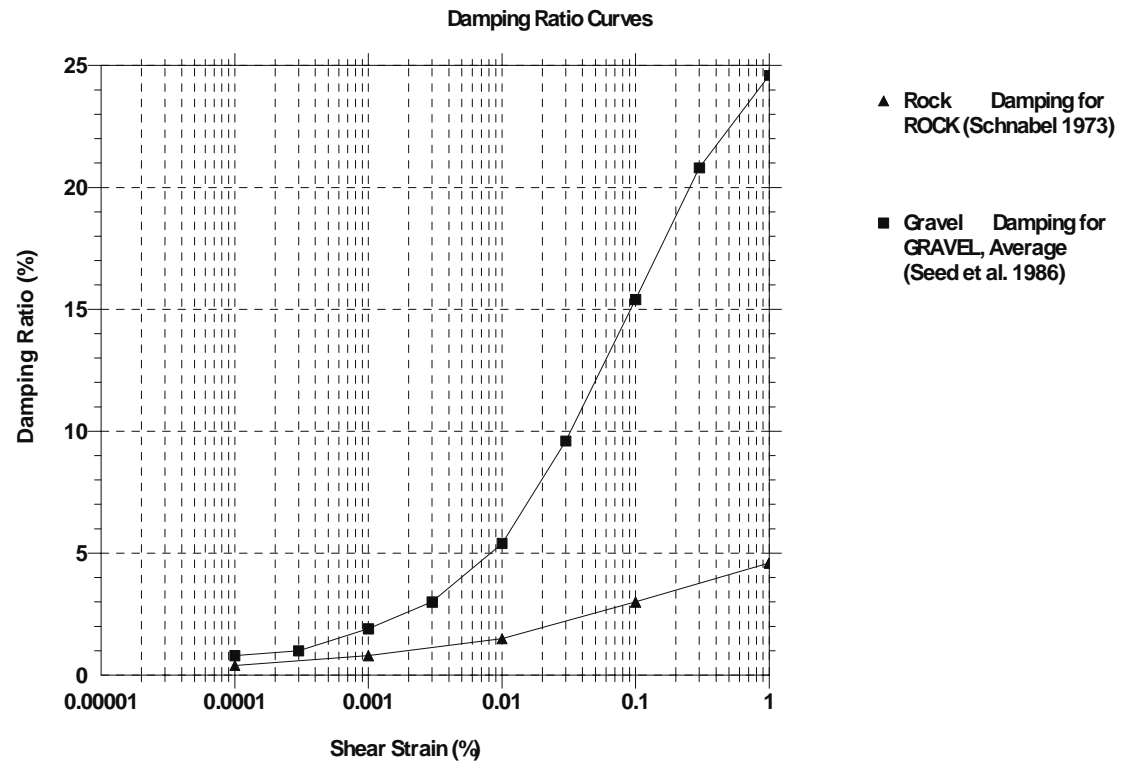


Figure 5.7: Damping ratio reduction curves for gravel and rock.



Figure 5.8: The six additional sites location in Mayagüez.

Table 5.2: Typical ranges of compression velocity, density, and Poisson ratio characteristics for different soil materials (from USACE, 1995).

Material	V_p (m/sec)	ρ_{dry} (mg/m ³)	ν
Dry Sand	450 - 900	1.6 – 2.0	0.30 – 0.35
Clay	900 – 1,800	1.3 – 1.8	0.50
Saturated, loose sand	1,500	-	-
Weathered Igneous Rock	450 – 3,700	-	-
Weathered Sedimentary Rock	600 – 3,000	-	-
Sandstone	2,200 – 4,000	1.9 – 2.7	-

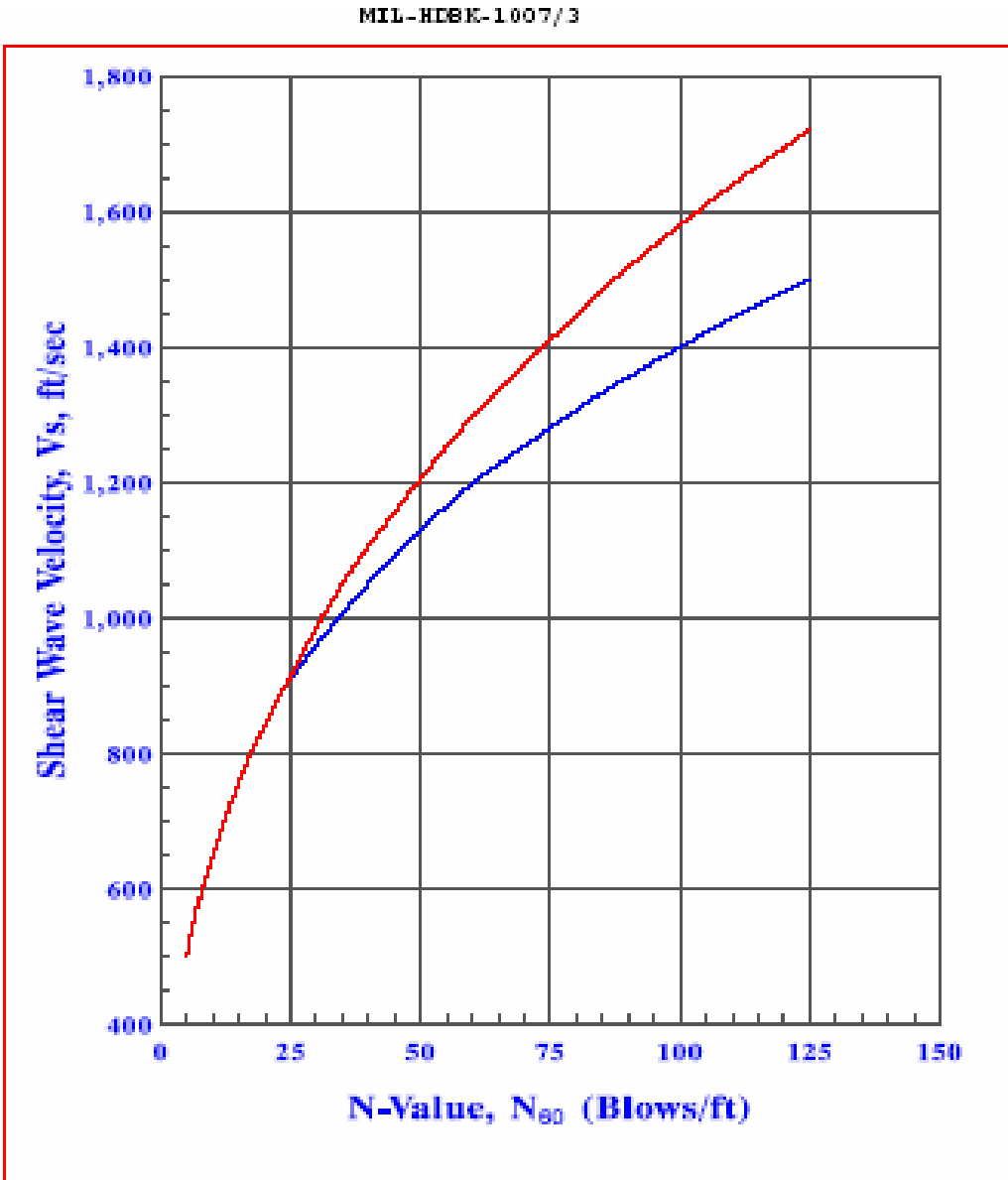


Figure 5.9: Correlation between N values from SPT with shear wave velocity proposed by Imai and Yoshimura (1970) (reproduced from NAVFAC, 1997).

Table 5.3: Dynamic soil properties assigned to group A.

Dynamic Soil Properties-Abonos site			
Soil ID	Soil Type	Damping ratio reduction	Shear modulus reduction
1	Clayey Silt	Damping for Clay, Average (Seed & Idris 1970)	G/Gmax Clay (Seed & Sun 1989) upper
2	Rock	Damping for Rock (Shnabel 1973)	Rock (Shnabel 1973)

Dynamic Soil Properties-Maní site			
Soil ID	Soil Type	Damping ratio reduction	Shear modulus reduction
1	Sand	Sand Avg. (Seed & Idris 1970)	Sand Avg. (Seed & Idris 1970)
2	Weath. Rock	Gravel Avg. (Seed 1986)	Gravel Avg (Seed 1986)
3	ROCK	Damping for Rock (Shnabel 1973)	Rock (Shnabel 1973)

Dynamic Soil Properties-Biología site			
Soil ID	Soil Type	Damping ratio reduction	Shear modulus reduction
1	Silty Clay	Damping for Clay, Lower bound (Seed & Idris 1970)	G/Gmax Clay (seed and sun 1989) upper bound
2	Silty Sand	Damping for Sand, Upper Bound (Seed & Idris 1970)	G/Gmax Sand, Upper Bound (Seed & Idris 1970)
3	Weath. Rock	Gravel Avg. (Seed 1986)	Gravel Avg (Seed 1986)
4	Rock	Damping for Rock (Shnabel 1973)	Rock (Shnabel 1973)

Dynamic Soil Properties-Viaducto site			
Soil ID	Soil Type	Damping ratio reduction	Shear modulus reduction
1	Clay	Damping for Clay, Average (Seed & Idris 1970)	G/Gmax Clay (Seed & Sun 1989) upper
2	Limstone	Damping for Gravelly soils (Seed et al 1988)	G/Gmax Gravel Average (Seed et al 1986)
3	Rock	Damping for Rock (Shnabel 1973)	Rock (Shnabel 1973)

Dynamic Soil Properties-Civil site			
Soil ID	Soil Type	Damping ratio reduction	Shear modulus reduction
1	Silty Clay	Damping for Clay, Lower bound (Seed & Idris 1970)	G/Gmax Clay (seed and sun 1989) upper bound
2	Silty Sand	Damping for Sand, Upper Bound (Seed & Idris 1970)	G/Gmax Sand, Upper Bound (Seed & Idris 1970)
3	Weath. Rock	Gravel Avg. (Seed 1986)	Gravel Avg (Seed 1986)
4	Rock	Damping for Rock (Shnabel 1973)	Rock (Shnabel 1973)

Table 5.4: Dynamic soil properties assigned to group B.

Dynamic Soil Properties-341HWY site			
Soil ID	Soil Type	Damping ratio reduction	Shear modulus reduction
1	Clayey Silt	Damping for Clay, Average (Seed & Idris 1970)	G/Gmax Clay (Seed & Sun 1989) upper
2	Rock	Damping for Rock (Shnabel 1973)	Rock (Shnabel 1973)

Dynamic Soil Properties-Maní Park site			
Soil ID	Soil Type	Damping ratio reduction	Shear modulus reduction
1	Sand	Sand Avg. (Seed & Idris 1970)	Sand Avg. (Seed & Idris 1970)
2	Rock	Damping for Rock (Shnabel 1973)	Rock (Shnabel 1973)

Dynamic Soil Properties-Seco Park site			
Soil ID	Soil Type	Damping ratio reduction	Shear modulus reduction
1	Sand	Sand Avg. (Seed & Idris 1970)	Sand Avg. (Seed & Idris 1970)
2	Weath. Rock	Gravel Avg. (Seed 1986)	Gravel Avg. (Seed 1986)

Dynamic Soil Properties-Isidoro García site			
Soil ID	Soil Type	Damping ratio reduction	Shear modulus reduction
1	Sand	Sand Avg. (Seed & Idris 1970)	Sand Avg. (Seed & Idris 1970)
3	Weath. Rock	Gravel Avg. (Seed 1986)	Gravel Avg. (Seed 1986)

Dynamic Soil Properties-Ramírez de Arrellano site			
Soil ID	Soil Type	Damping ratio reduction	Shear modulus reduction
1	Sand	Sand Avg. (Seed & Idris 1970)	Sand Avg. (Seed & Idris 1970)
3	Weath. Rock	Gravel Avg. (Seed 1986)	Gravel Avg. (Seed 1986)

Dynamic Soil Properties-Sultanita site			
Soil ID	Soil Type	Damping ratio reduction	Shear modulus reduction
1	Clay	Damping for Clay, Average (Seed & Idris 1970)	G/Gmax Clay (seed and sun 1989) upper bound
2	Weath. Rock	Gravel Avg. (Seed 1986)	Gravel Avg. (Seed 1986)
3	Rock	Damping for Rock (Shnabel 1973)	Rock (Shnabel 1973)

Table 5.5: Dynamic soil properties assigned to group C.

Dynamic Soil Properties-El Bosque site			
Soil ID	Soil Type	Damping ratio reduction	Shear modulus reduction
1	Silty Clay	Damping for Clay, Lower bound (Seed & Idris 1970)	G/Gmax Clay (seed and sun 1989) upper bound
2	Clayey Silt	Damping for Clay, Average (Seed & Idris 1970)	G/Gmax Clay (seed and sun 1989) upper bound
3	Weath. Sandstone	Gravel Avg. (Seed 1986)	Gravel Avg. (Seed 1986)
4	Rock	Damping for Rock (Shnabel 1973)	Rock (Shnabel 1973)

Dynamic Soil Properties-El Castillo site			
Soil ID	Soil Type	Damping ratio reduction	Shear modulus reduction
1	Clayey Silt	Damping for Clay, Average (Seed & Idris 1970)	G/Gmax Clay (seed and sun 1989) upper bound
2	Weath. Sandstone	Gravel Avg. (Seed 1986)	Gravel Avg. (Seed 1986)
3	Rock	Damping for Rock (Shnabel 1973)	Rock (Shnabel 1973)

Dynamic Soil Properties-India site			
Soil ID	Soil Type	Damping ratio reduction	Shear modulus reduction
1	Sandy Clay	Sand Avg. (Seed & Idris 1970)	Sand Avg. (Seed & Idris 1970)
2	Silty Clay	Damping for Clay, Lower bound (Seed & Idris 1970)	G/Gmax Clay (seed and sun 1989) upper bound
3	Silty Sand	Sand Avg. (Seed & Idris 1970)	Sand Avg. (Seed & Idris 1970)
4	Rock	Damping for Rock (Shnabel 1973)	Rock (Shnabel 1973)

Dynamic Soil Properties-Marina Site			
Soil ID	Soil Type	Damping Ratio	Modulus Reduction
1	Clayey silt	Damping for Clay, Average (Seed & Idris 1970)	G/Gmax Clay (seed and sun 1989) upper bound
2	Weathered Rock	Gravel Avg. (Seed 1986)	Gravel Avg. (Seed 1986)
3	Rock	Damping for Rock (Shnabel 1973)	Rock (Shnabel 1973)

5.4 Soil simplified profiles

Using the information obtained in the field from the SASW tests in combination with the geotechnical data available near the sites, soil profiles were constructed for the fourteen sites analyzed. As mentioned before, the sites were classified in three categories depending on the information available for the sites. Group A comprises the sites where there is shear wave velocity profile and geotechnical information near the site. The sites in which only shear wave velocity information is available were assigned to group B. In group C were assigned the sites where only geotechnical information is available. The additional information necessary to perform the ground response analysis was obtained by correlation studies obtained from the technical literature. This section presents the simplified soil profiles. Because the depth of the bedrock in Mayagüez is unknown for all the sites, it was assumed that the bedrock is located at a depth of 30 meters (100 ft) unless it is indicated otherwise in the geotechnical borings.

5.4.1 Group A soil profiles

Figures 5.10 to 5.14 show the simplified profiles for the sites in group A. The Abonos site profile is shown in Figure 5.10. The Abonos site, located in the Añasco Valley, presents a deep soil deposit of clayey silt with low shear wave velocity. Macari (1994) cited in his report that this site is comprised of loose alluvial deposits and it may extend more than 100 ft (30 m) deep. The next site is the Maní site located near the coast of Mayagüez. The information obtained for this site is presented in Figure 5.11. A geotechnical boring done near this site showed weathered rock beginning at a depth of 35 ft (10.66 m) with N values over 50. This coincides with the 4000 ft/sec (1,219.20 m/sec) shear wave velocity found from the SASW test at that depth. The third site in group A is the Biología site and the fourth is the Viaducto site. Macari reported that he performed SASW tests near the Viaducto site in the area around the Darlington Building reaching up to 30 ft (9.14 m) depth. In his study, Macari found that the shear wave velocity increases to 1500 ft/sec (457.2 m/sec) at 80 ft (24.38 m) depth where the geotechnical exploration shows weathered rock. The last site for group A is located in the Civil Engineering Department of the University of Puerto Rico at Mayagüez, referred to as the Civil site for brevity. For the Civil site, the soil stratigraphy of the Biología lot was adopted because of its nearness. Due to the low shear wave velocity up to 100 ft (30 m) depth found with the SASW test in the Civil site, it was assumed that the silty clay found in the borings done at the Biología site extends up to 100 ft (30 m) down. Figure 5.9 (c) to 5.13 (c) show the N_1 and N_{field} values, i.e. the N_{field} refers to the N

value obtained in the field with the STP test and the N1 value refers to the corrected Nfield by the Liao and Whitner (1986) procedure.

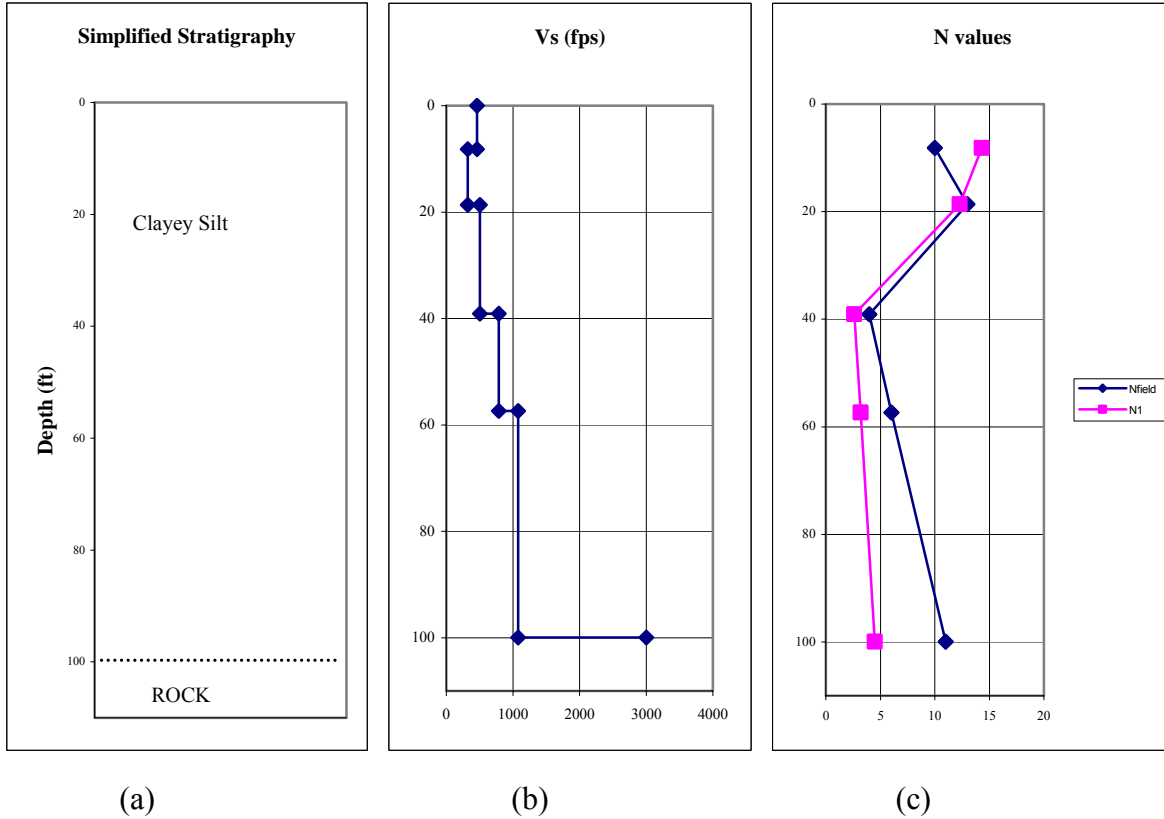


Figure 5.10: (a) Soil materials, (b) shear wave velocities, and (c) N values for the Abonos site.

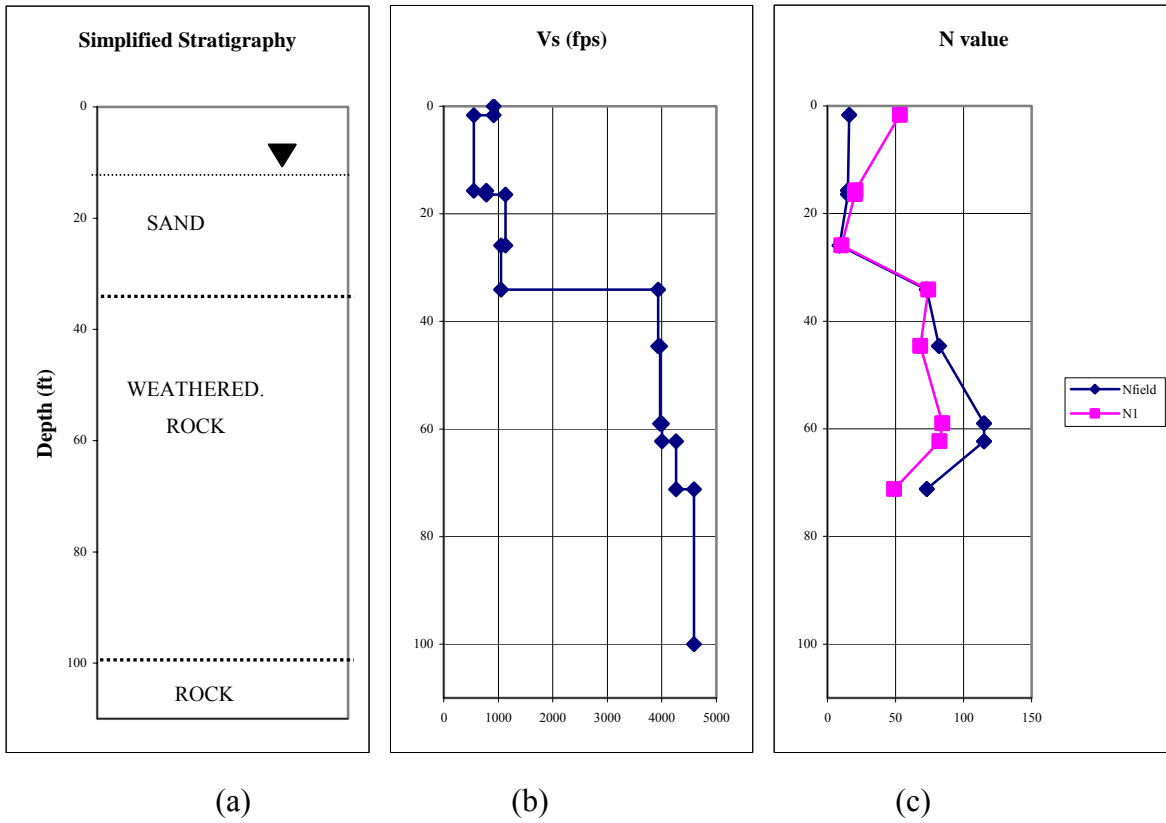


Figure 5.11: (a) Soil materials, (b) shear wave velocities, and (c) N values for the Maní site.

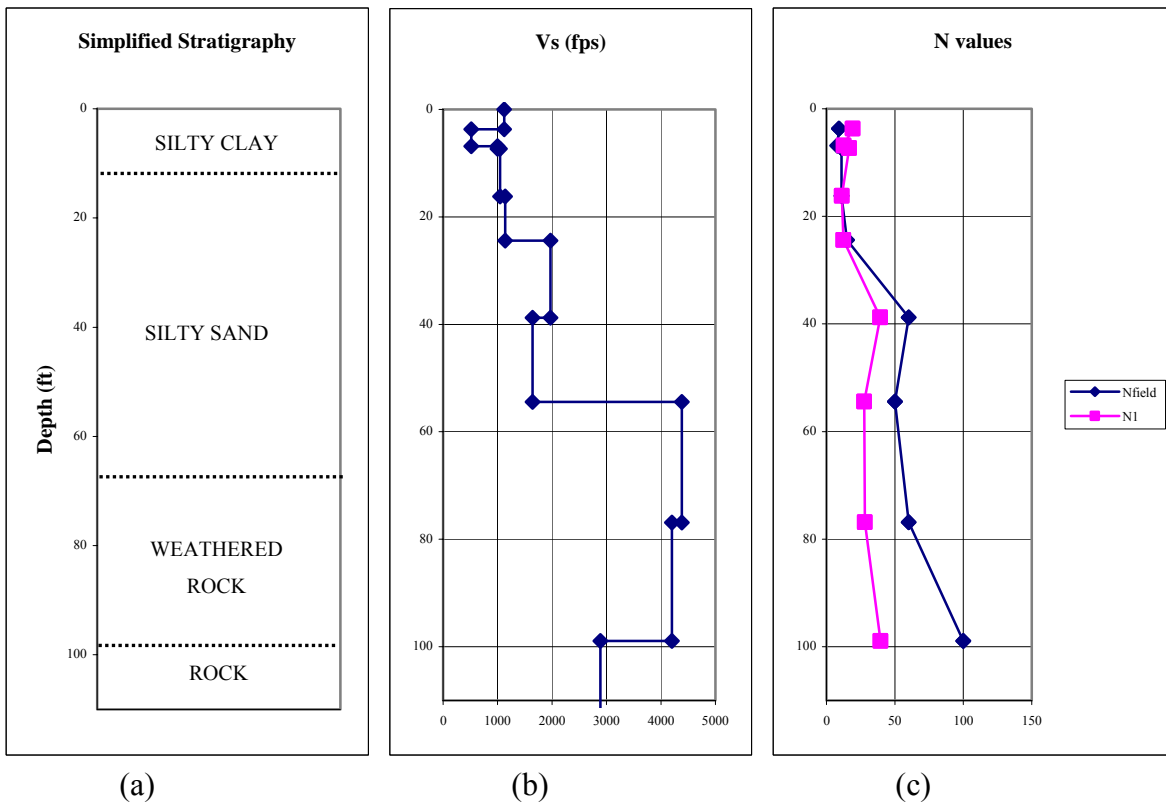


Figure 5.12: (a) Soil materials, (b) shear wave velocities, and (c) N values for the Biología site.

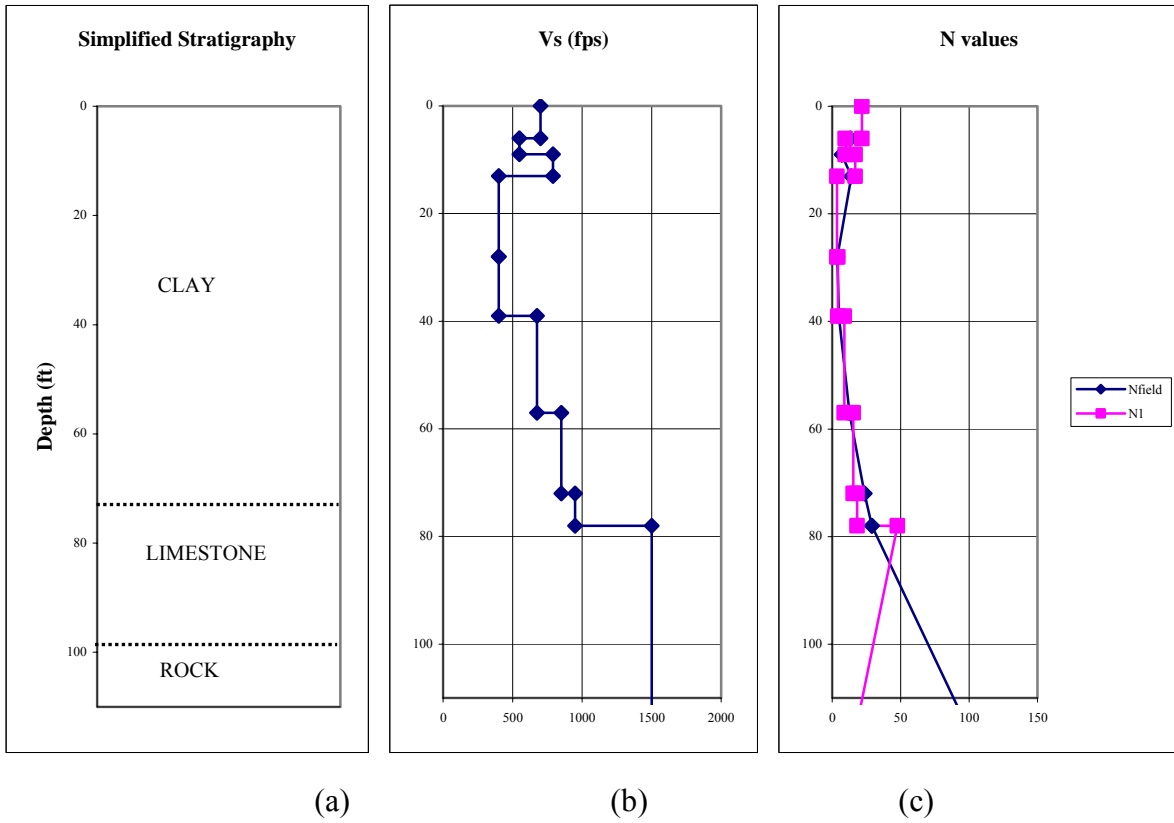


Figure 5.13: (a) Soil materials, (b) shear wave velocities, and (a) N values for the Viaducto site.

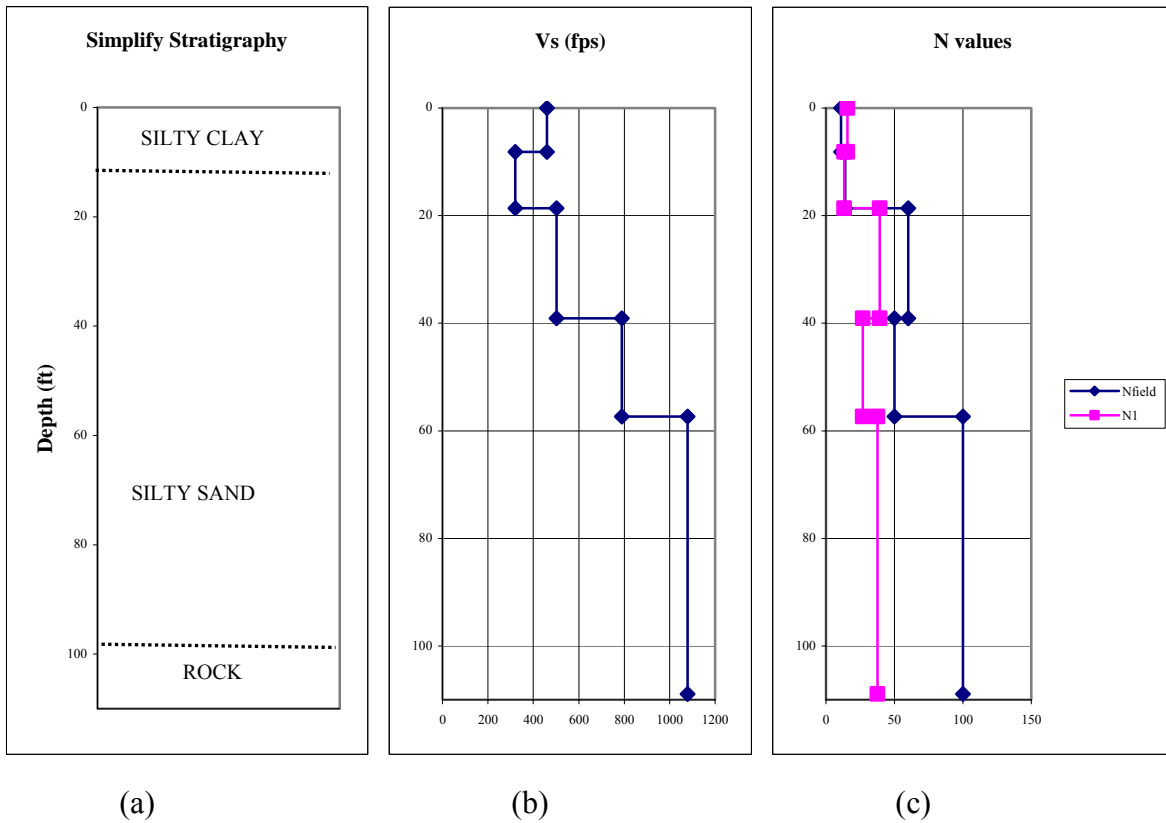


Figure 5.14: (a) Soil materials, (b) shear wave velocities, and (c) N values for the Civil site.

5.4.2 Group B soil profiles

In group B were assigned the sites for which a shear wave velocity profile was available and the soil materials for the profile were obtained from correlations with shear wave velocity. Figures 5.15 to 5.20 show the simplified material profile for each site. The first site in group B is the 341HWY site. This site is located in the Añasco Valley to the west of the Abonos site in group A. This site shows a very deep soil deposit as in the Abonos site. The second site in group B, the Maní Park, is a municipal baseball park near the coast of Mayagüez. The soil material at this site was modeled as sand because of its location in the coast and its shear wave velocity values which are in the range typical of sands. The simplified stratigraphy and S-wave velocity profile are shown in Figure 5.16. The third locality in group B is the Seco Park site. A similar shear wave velocity profile as Maní Park was found and sand was assumed throughout its depth. The information for this site is displayed in Figure 5.17. The fourth and fifth sites are the Isidoro García and Ramírez de Arellano sites. The same range of shear wave velocity between 900 ft/sec (274.2 m/sec) to 1500 ft/sec (457.2 m/sec) shear wave velocity obtained in previous sites in the coast was also found here. Figures 5.18 and 5.19 display the soil materials selected and the velocity profiles for these two sites. The sixth and last site in group B is the Sultanita lot located in the east part of the city of Mayagüez near the mountains. From the shear wave velocity profile obtained from the SASW tests, a clay soil was assigned up to 100 ft (30 m) depth. As in the previous group, the bedrock was assumed to be located at 100 ft (30 m) depth for the six sites.

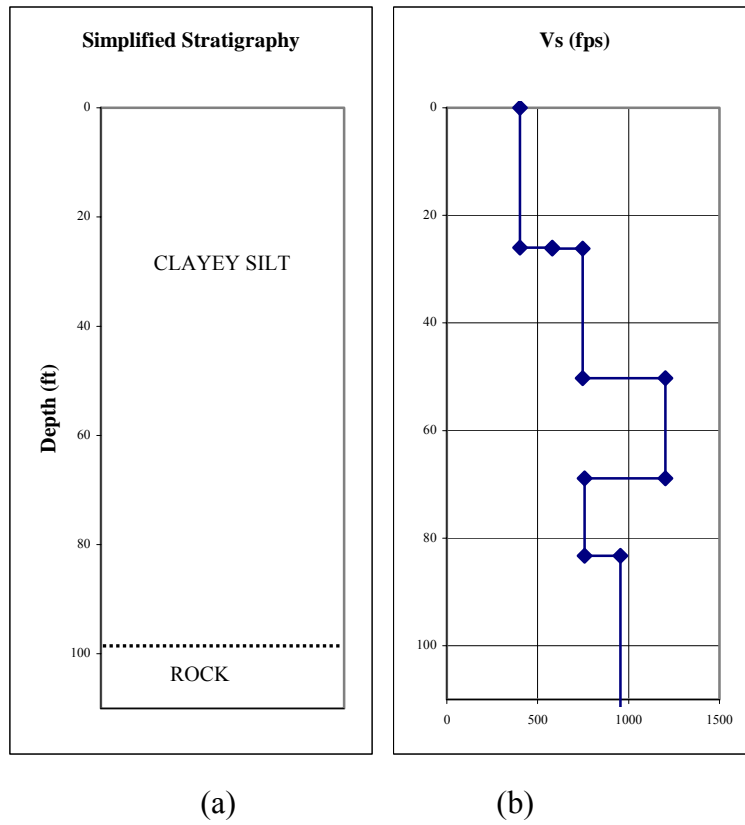


Figure 5.15: (a) Soil materials and (b) shear wave velocity profile for the 341HWY site.

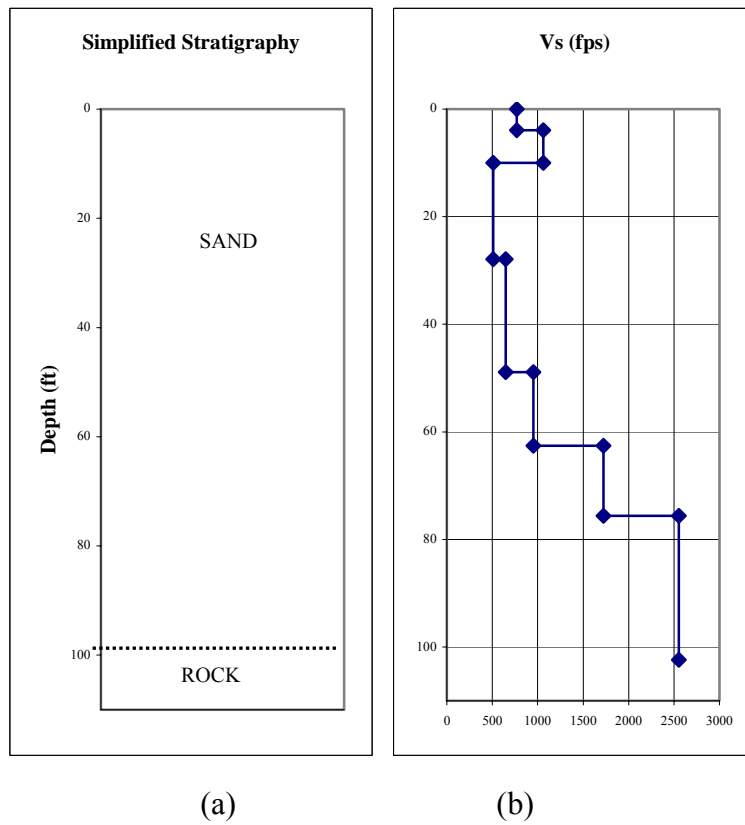


Figure 5.16: (a) Soil materials and (b) shear wave velocity profile for the Maní Park site.

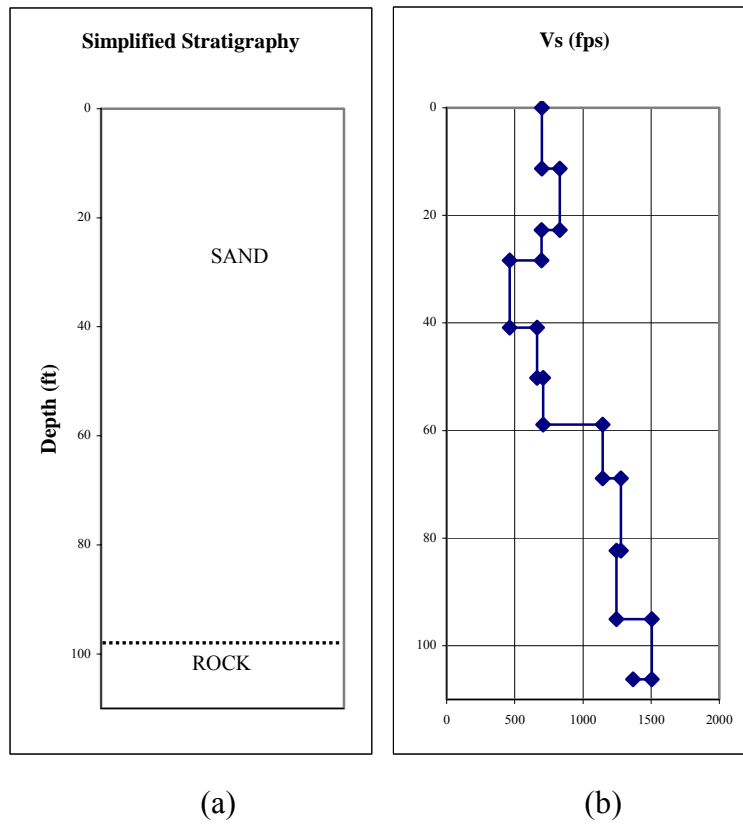


Figure 5.17: (a) Soil materials and (b) shear wave velocity profile for the Seco Park site.

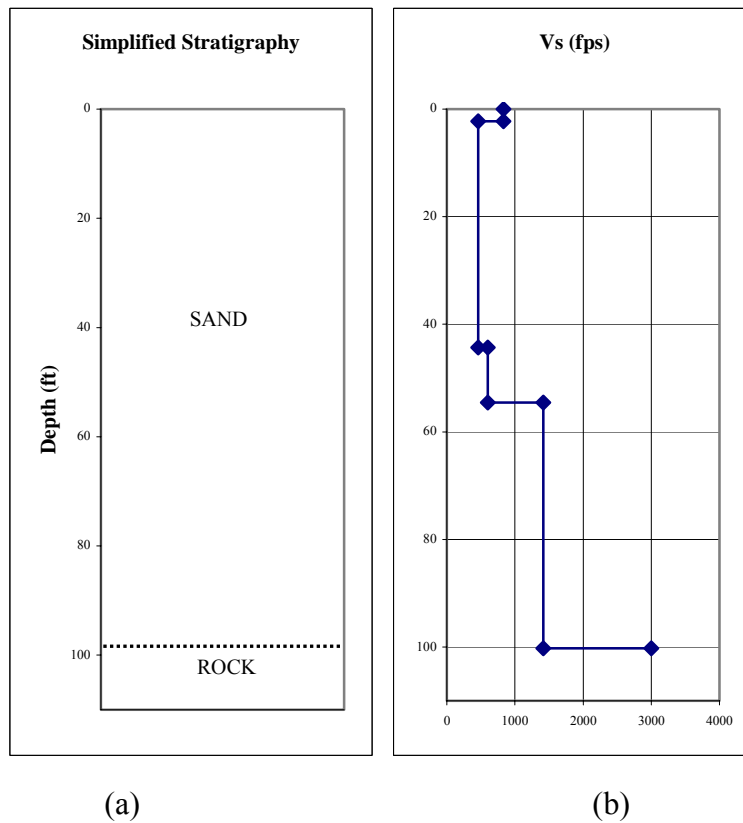


Figure 5.18: (a) Soil materials and (b) shear wave velocity profile for Isidoro García site.

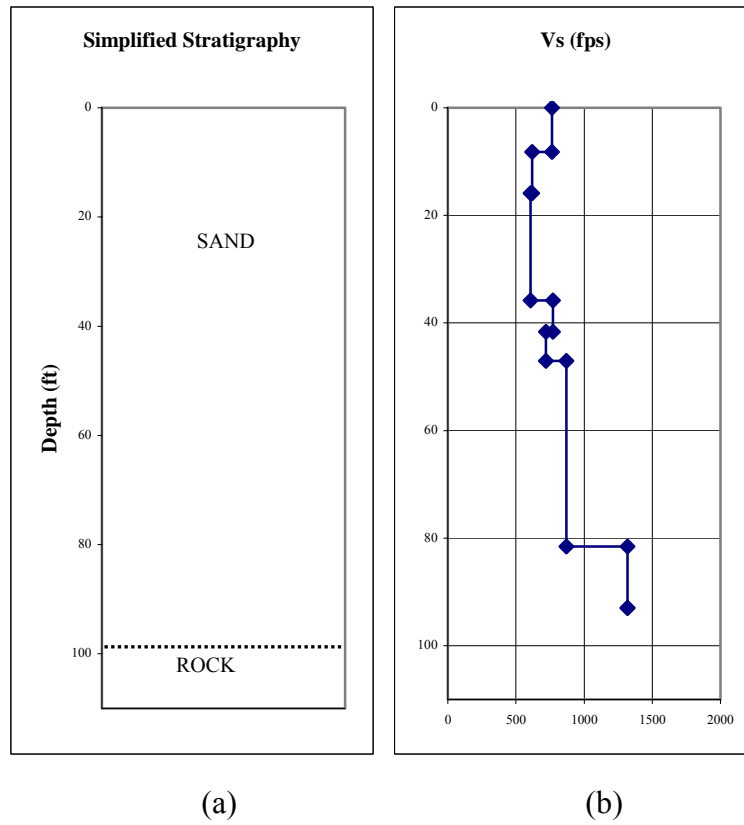


Figure 5.19: (a) Soil materials and (b) shear wave velocity profile for the Ramirez de Arellano site.

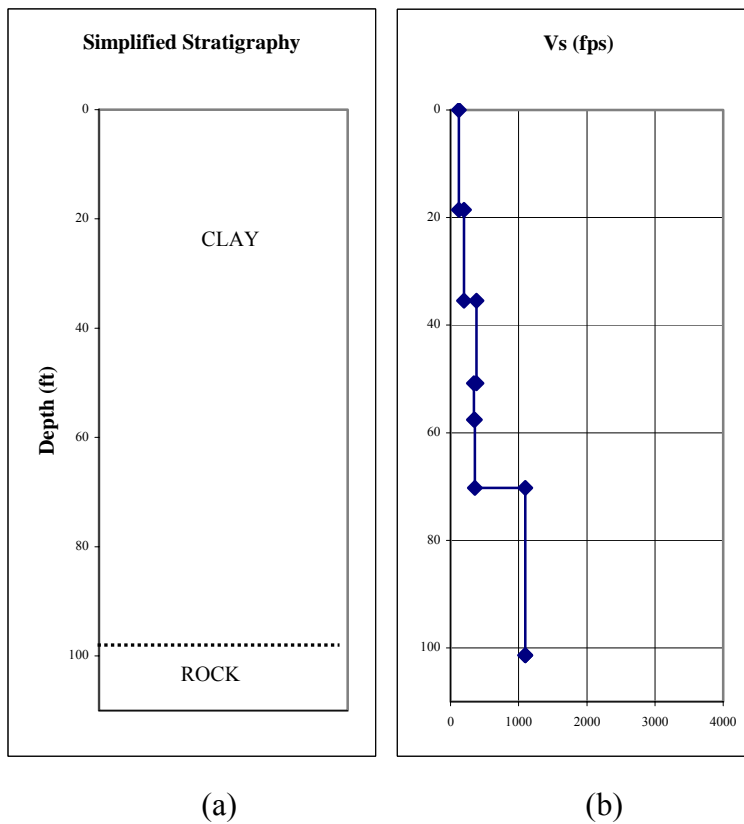


Figure 5.20: (a) Soil materials and (b) shear wave velocity profile for the Sultanita site.

5.4.3 Group C soil profiles

Three sites were assigned to group C: They are the El Bosque, El Castillo, India, and Marina. For these sites only geotechnical boring logs were available. For these sites the shear wave velocities were obtained by correlating them with the N values reported. The El Bosque site consisted of clayey silt and silty clay. Sandstone was found at 80 ft (24.38 m) depth. For the El Castillo site a layer of clayey silt was found followed by weathered rock at a depth of 25 ft (7.62 m). The India site is located in a deep soil deposit of sandy and silty clay. For all the sites the bedrock was assumed to begin at 100 ft (30 m). Figures 5.21 through 5.24 show the simplified soil profile for these sites. Figure 5.21 (c) to 5.25 (c) show the N1 and Nfield values, i.e. the Nfield refers to the N value obtained in the field with the STP test and the N1 value refers to the corrected Nfield by the Liao and Whitner (1986) procedure.

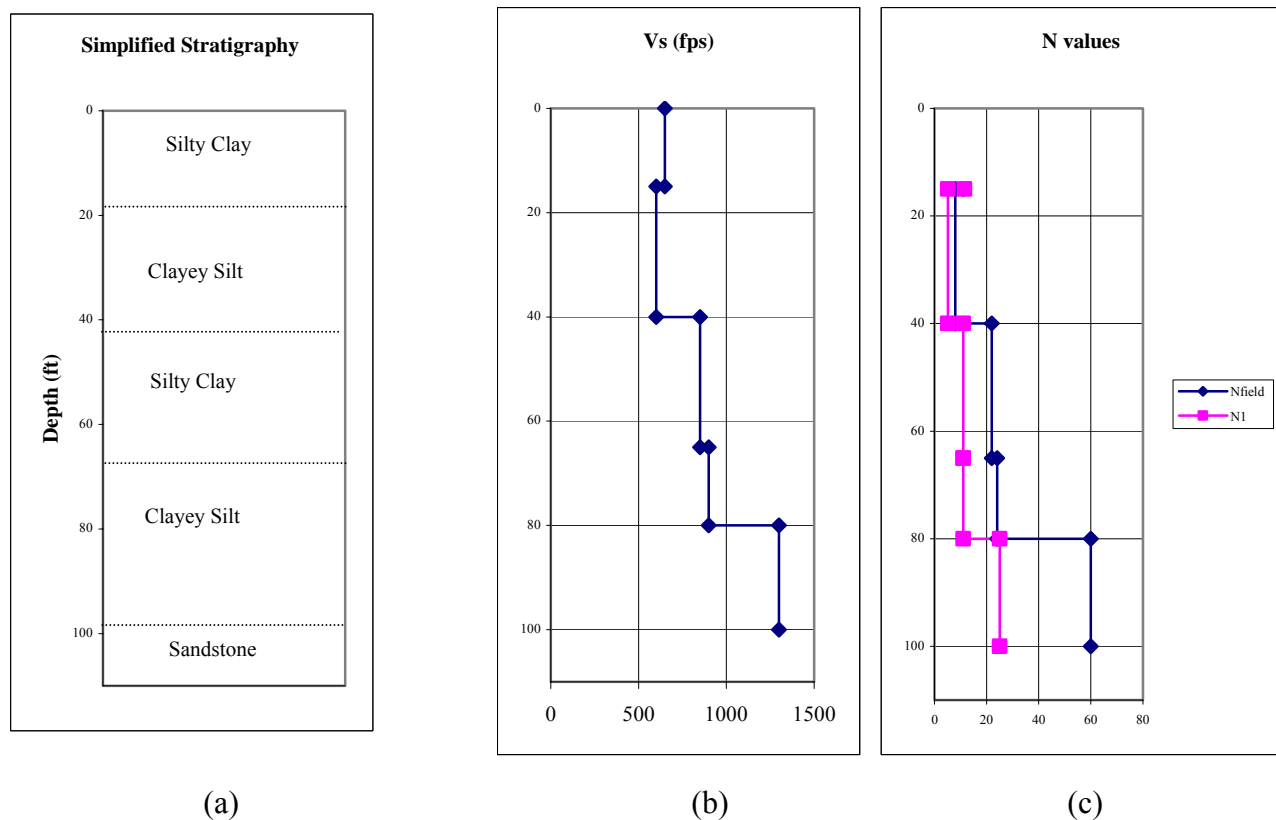


Figure 5.21: (a) Soil materials, (b) shear wave velocities, and (c) N values for the El Bosque site.

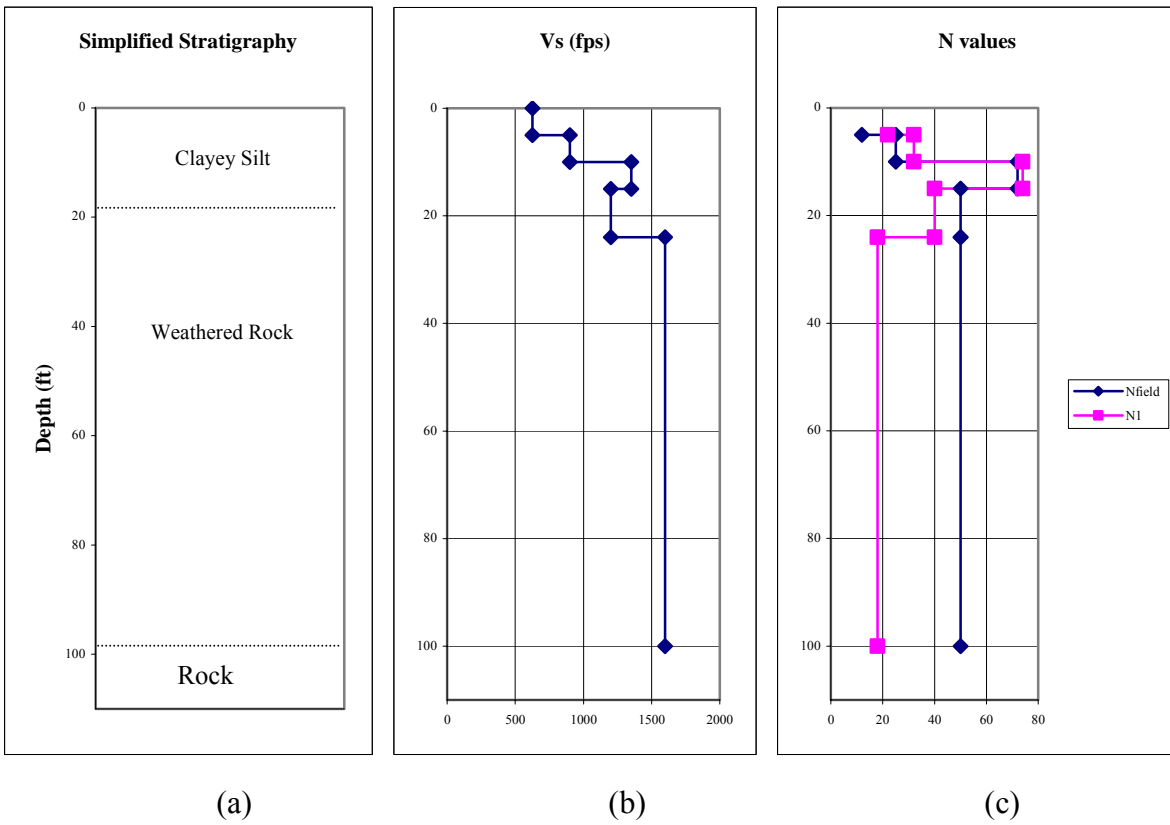


Figure 5.22: (a) Soil materials, (b) shear wave velocity, and (c) N values for the El Castillo site profile.

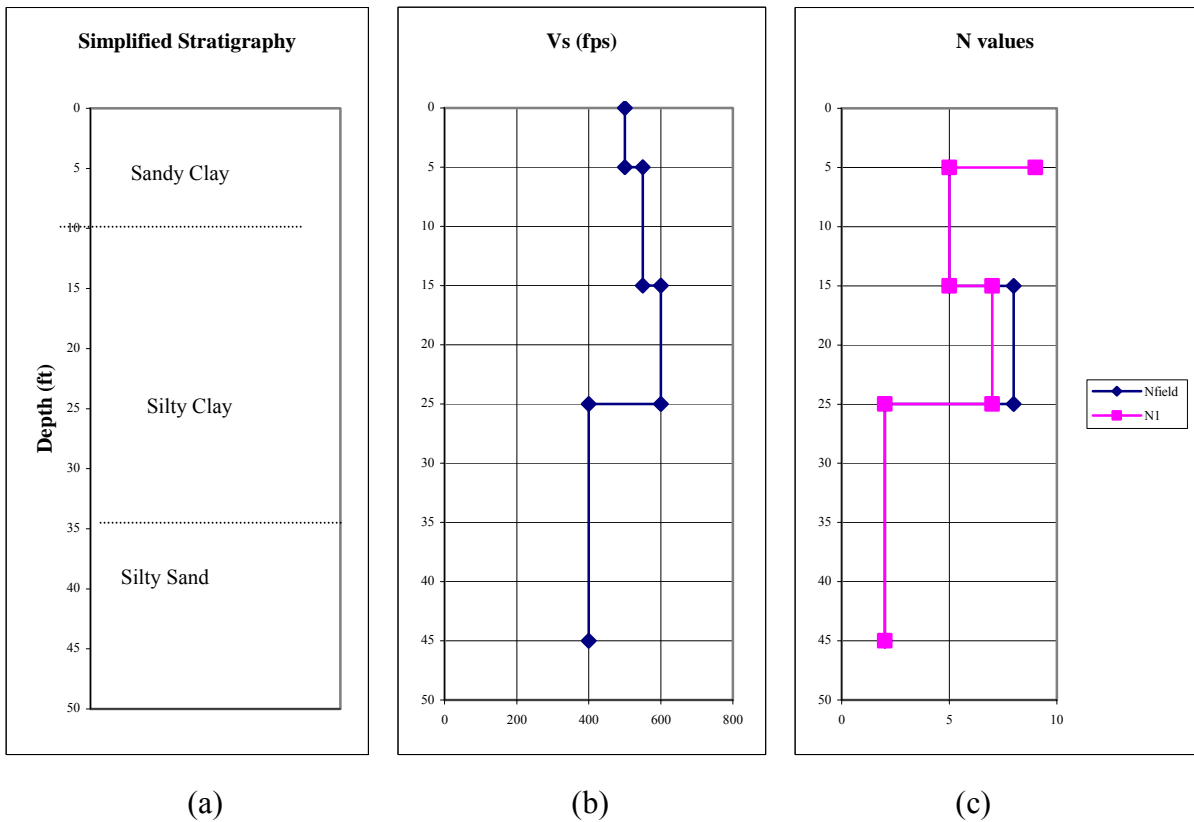


Figure 5.23: (a) Soil materials, (b) shear wave velocity, and (c) N values for the India site.

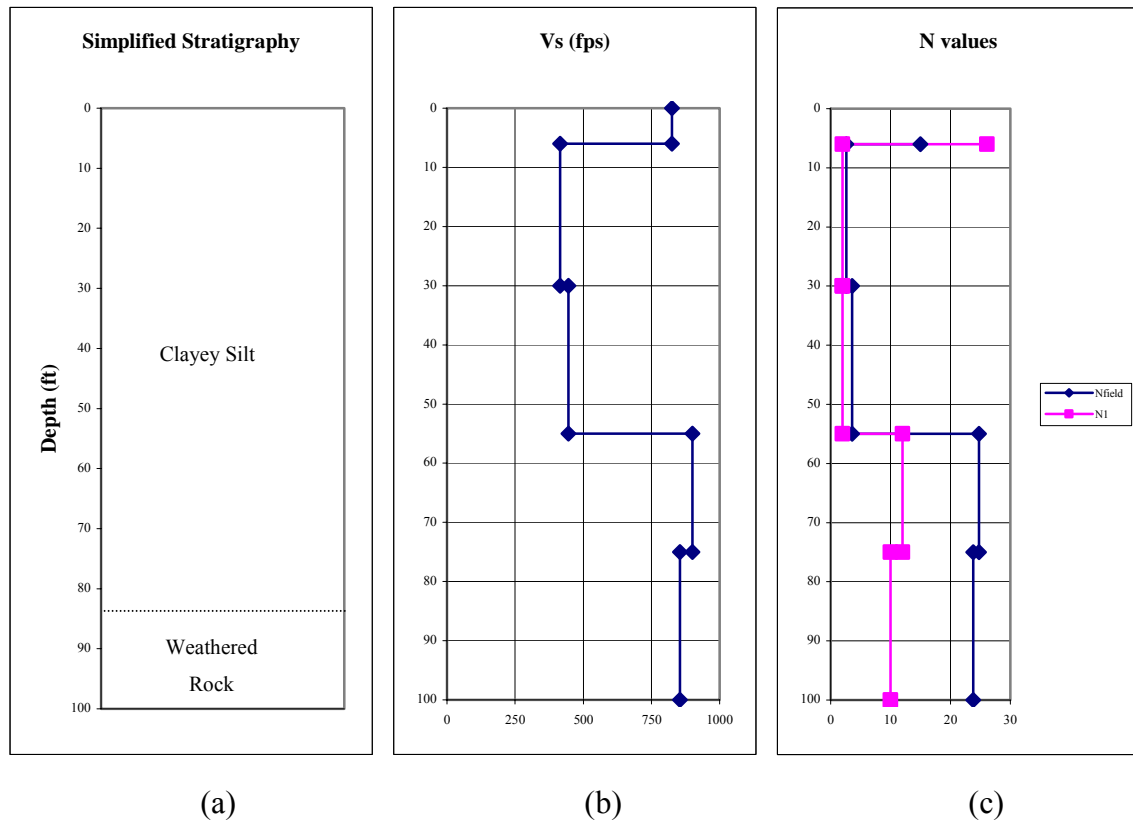


Figure 5.24: (a) Soil materials, (b) shear wave velocity, and (c) N values for the Marina site.

5.5 Ground Motions

Four artificial ground motions time histories and one earthquake record were used for the ground response analyses. The artificial ground motions were obtained using the methodology proposed by Montejo (2004) based on the wavelet transform. The real earthquake accelerogram used corresponds to the El Salvador earthquake of October 10, 1986 obtained from the Geotechnical Investigation Center instrument at the north-west direction. The following sections describe the characteristics of the time histories used and how they were applied for the analyses.

5.5.1 Artificial ground motions

The methodology proposed by Montejo (2004) was applied for the development of four ground motion time histories to be used in the ground response analyses. Montejo developed a computer program written in Matlab for the generation of ground motion time histories compatible with a design response spectrum by using the wavelet transform. The UBC-97 design response spectrum for seismic zone 3 in rock (soil profile type Sb) and 5 % damping was used as the target spectrum. Figure 5.25

shows the UBC-97 design spectrum for seismic zone 3 in rock and the response spectra for the four artificial ground motions developed. The characteristics of these ground motions are listed in Table 5.6. The dominant period of these time histories range from 0.36 seconds for the ground motion 4 to 0.61 seconds for the ground motion 3. The peak ground acceleration varies from 0.34g for ground motion 4 to 0.39g for ground motion 2. The table also lists the bracketed duration, defined as the time interval between the first and last peak acceleration greater than 0.05g. Figure 5.26 through 5.29 show the acceleration time history and the Fourier amplitude spectrum for each of the four artificial ground motions. The Fourier spectra are plotted as a function of period instead of frequency as it is usually done.

5.5.2 El Salvador earthquake

Martínez, Irizarry, and Portela (2001) developed elastic design spectra for the principal cities of Puerto Rico by using a database of world wide ground motions. They found that for the city of Mayagüez the El Salvador earthquake of October 10, 1986 was dominant among the earthquakes analyzed for the western part of Puerto Rico. The El Salvador earthquake satisfied the parameters explained in Chapter 2 in this thesis specified by the authors. From their study, Martínez et al. found that, for the city of Mayagüez the design spectrum prescribed in the UBC-97 for zone 3 underestimates the seismic demand expected for this area. They recommended to use the UBC-97 design spectrum for zone 4, for which the El Salvador earthquake is more compatible, as shown in Figure 5.30. Table 5.7 lists the characteristics of the acceleration time history of the El Salvador earthquake. Figure 5.31 shows the acceleration time history and its Fourier Amplitude spectrum. The dominant period for this earthquake record is 0.69 seconds and it has a peak ground acceleration of 0.42g.

Table 5.6: Characteristics of the artificial ground motions.

Ground motion ID	Peak Acc. (g)	Peak Vel. (in/sec)	Freq. (Hz)	Period (sec)	Bracketed Duration (sec)	Modified From	Station of Original Earthquake
1	0.37	10.39	1.94	0.52	9.4	Coalinga, CA 09/05/1983 Ms(4.7)	1608 Oil Field Fire St.
2	0.39	11.45	2.22	0.45	21.5	Loma Prieta, CA 18/10/1989 Ms(7.1)	58117 Treasure Island
3	0.37	10.80	1.64	0.61	10.9	Coyote Lake, CA 06/08/1979 Ms(5.6)	57217 C.L. Dam
4	0.34	13.45	2.77	0.36	6.6	Friuli, Italy 15/09/1976 Ms(5.7)	8014 Forgia C.

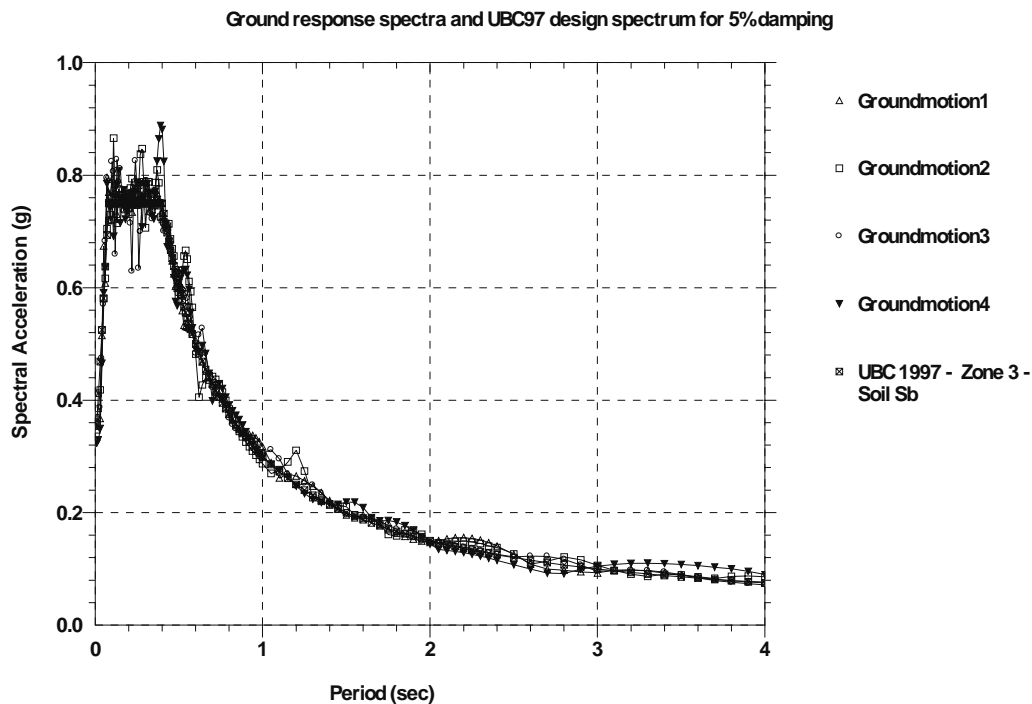
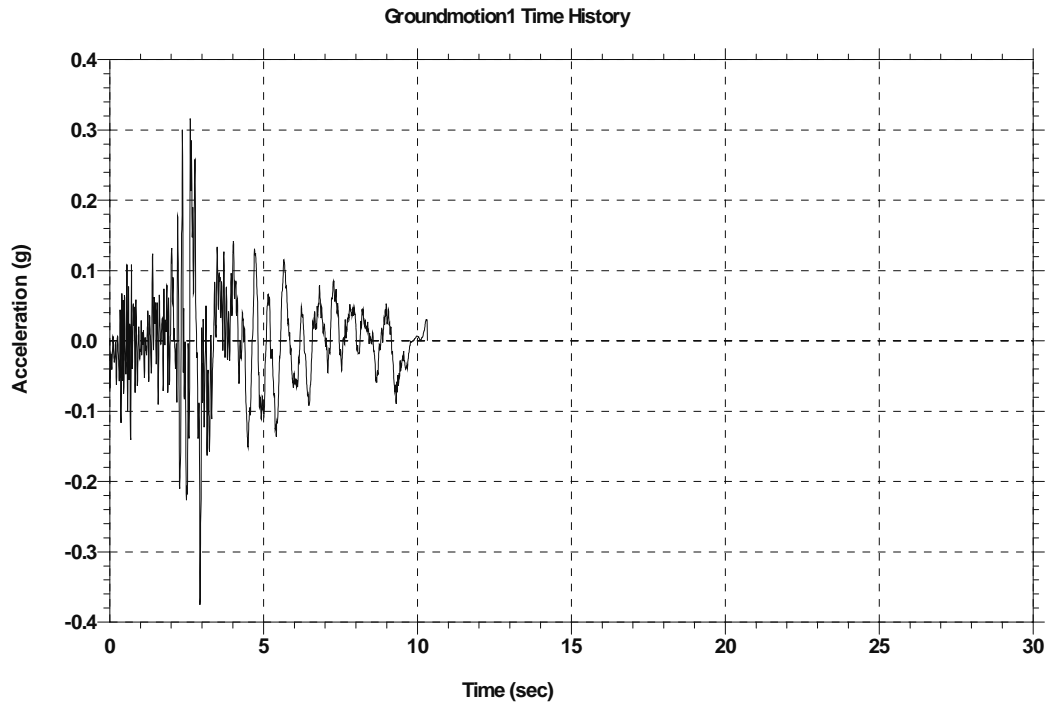
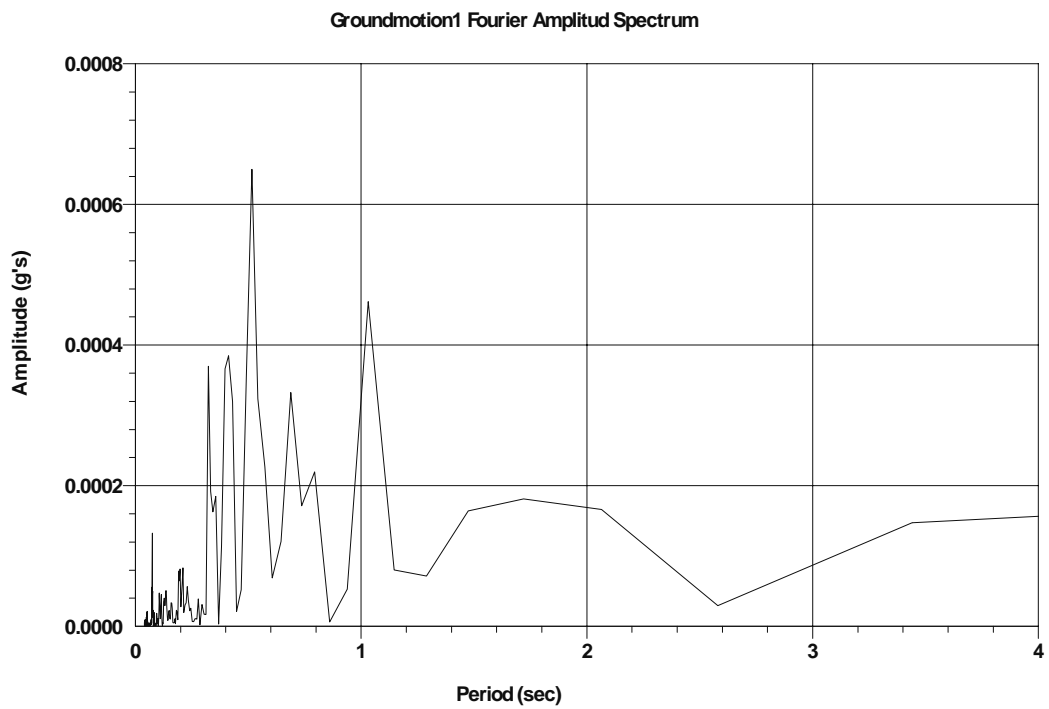


Figure 5.25: Response spectra of artificial accelerograms and UBC 97 design spectrum for rock in zone 3.



(a)



(b)

Figure 5.26: (a) Time history and (b) Fourier amplitude spectrum for ground motion 1.

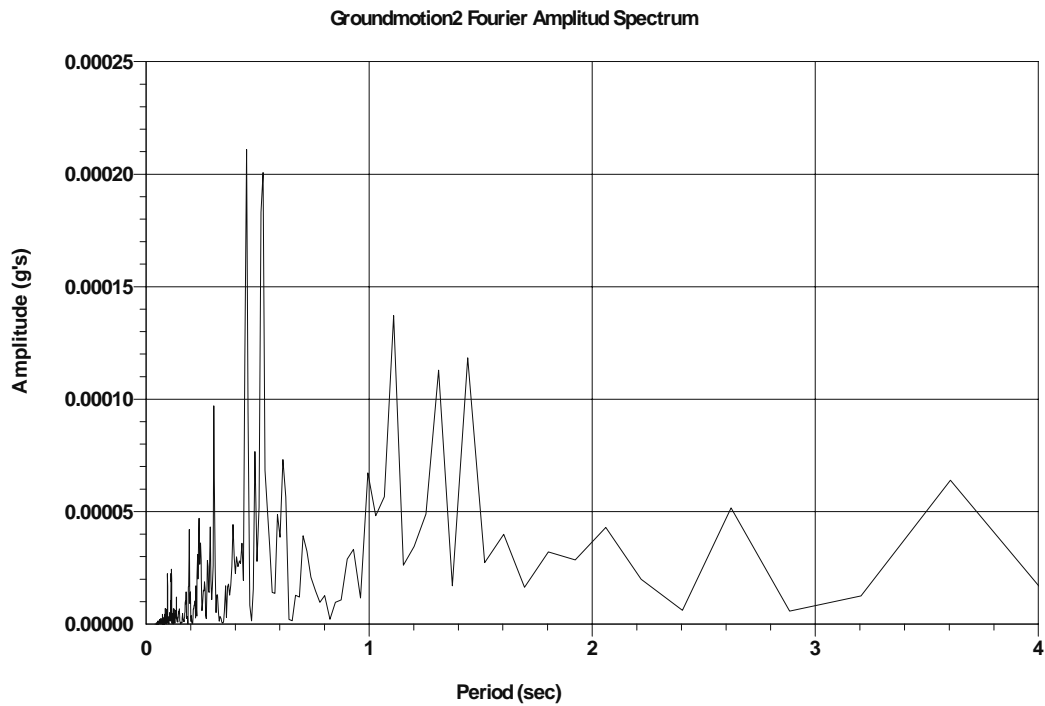
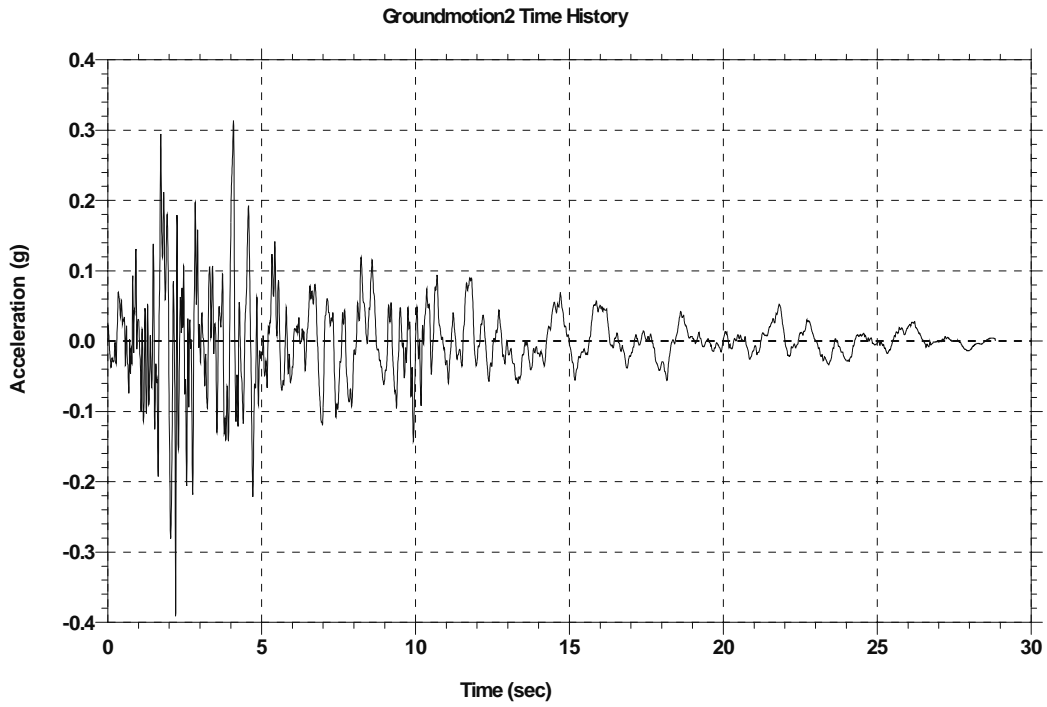


Figure 5.27: (a) Time history and (b) Fourier amplitude spectrum for ground motion 2.

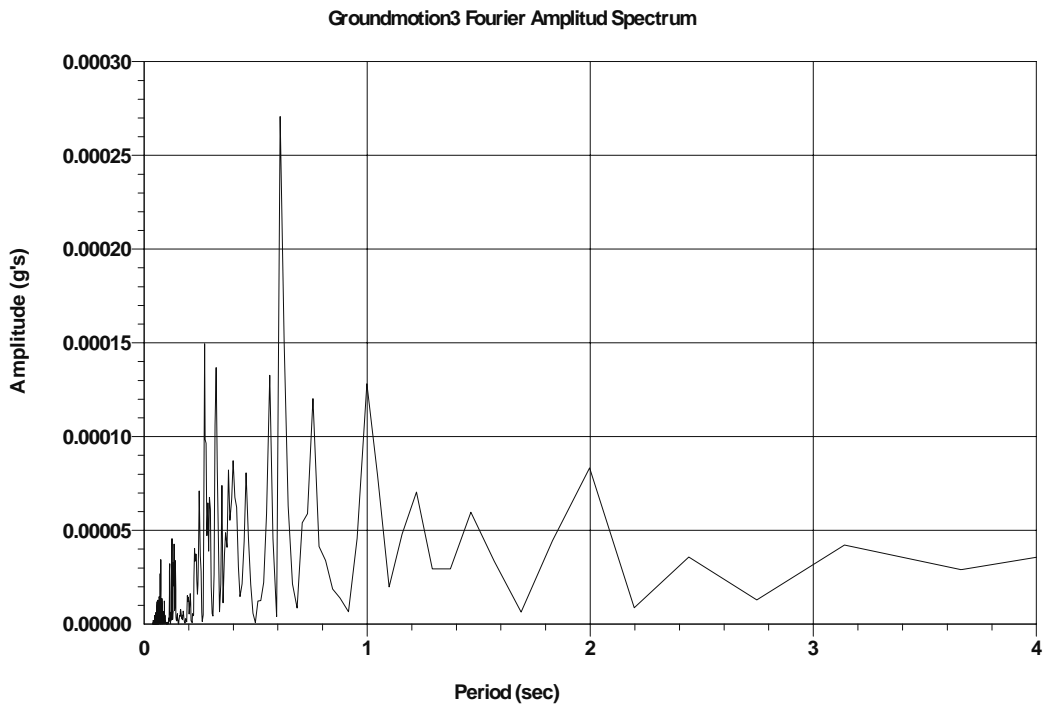
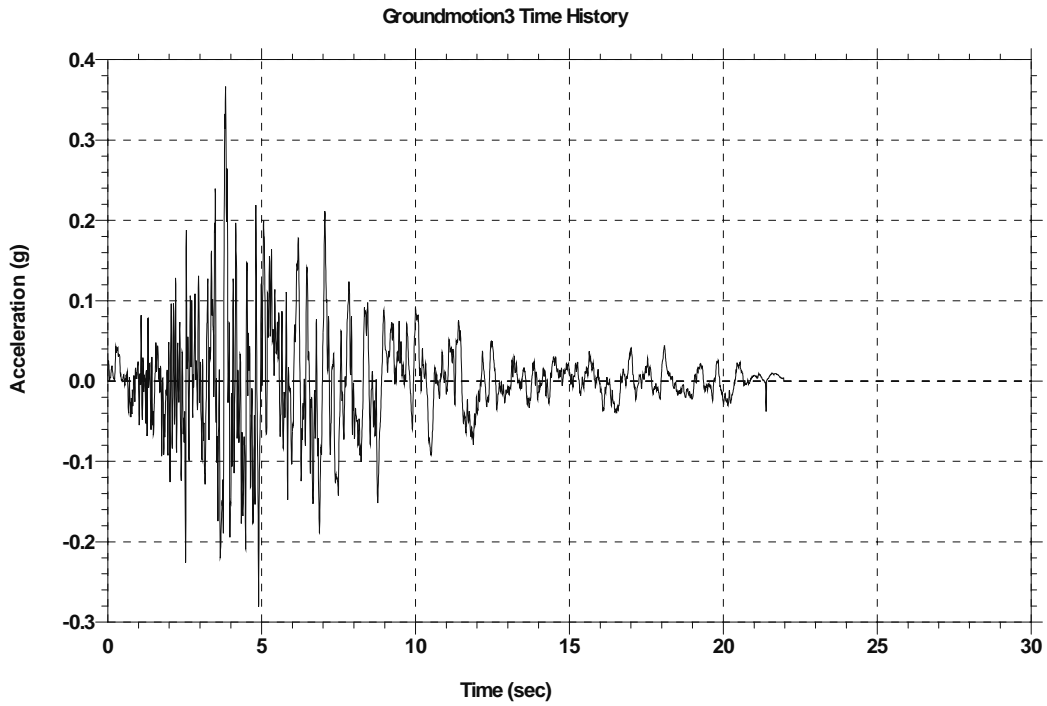
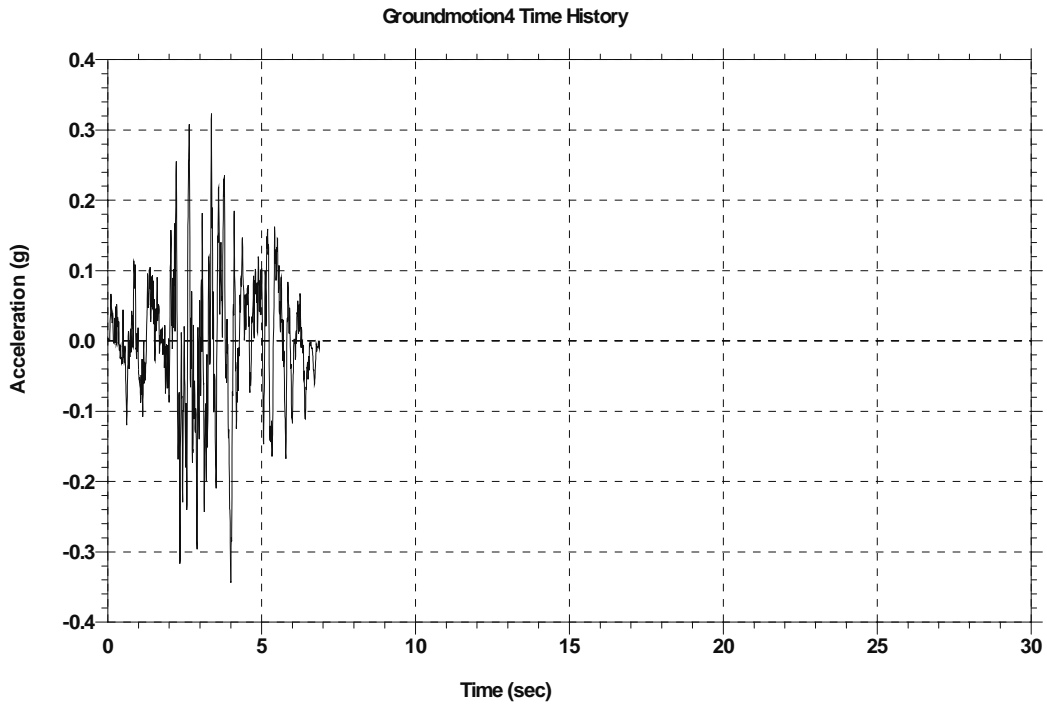
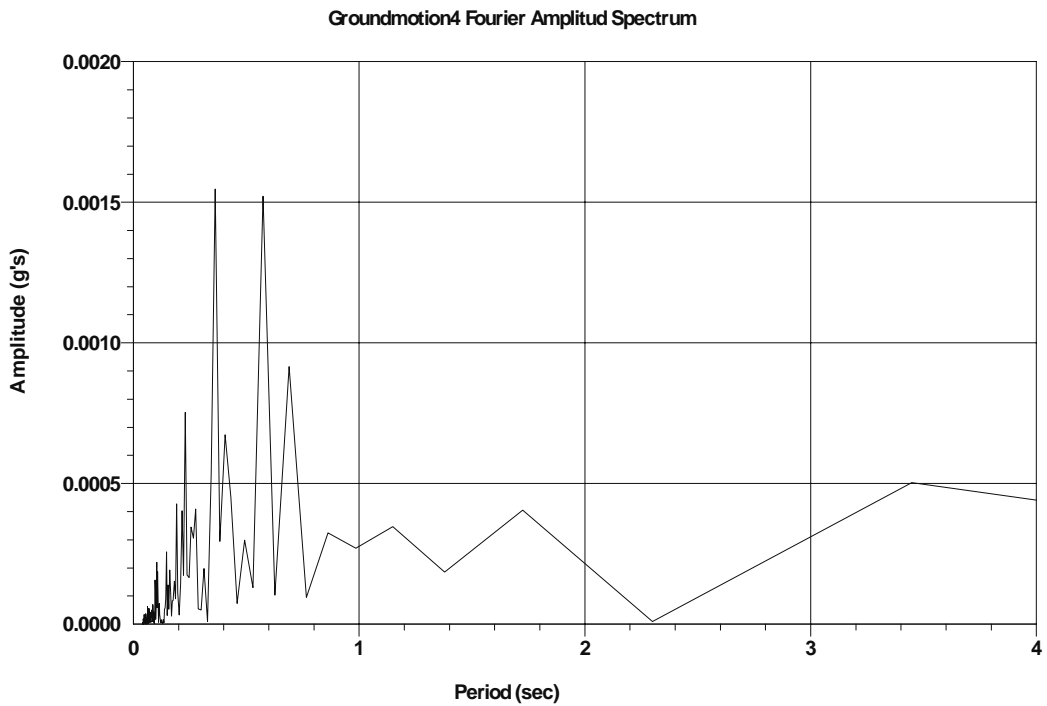


Figure 5.28: (a) Time history and (b) Fourier amplitude spectrum for ground motion 3.



(a)



(b)

Figure 5.29: (a) Time history and (b) Fourier amplitude spectrum for ground motion 4.

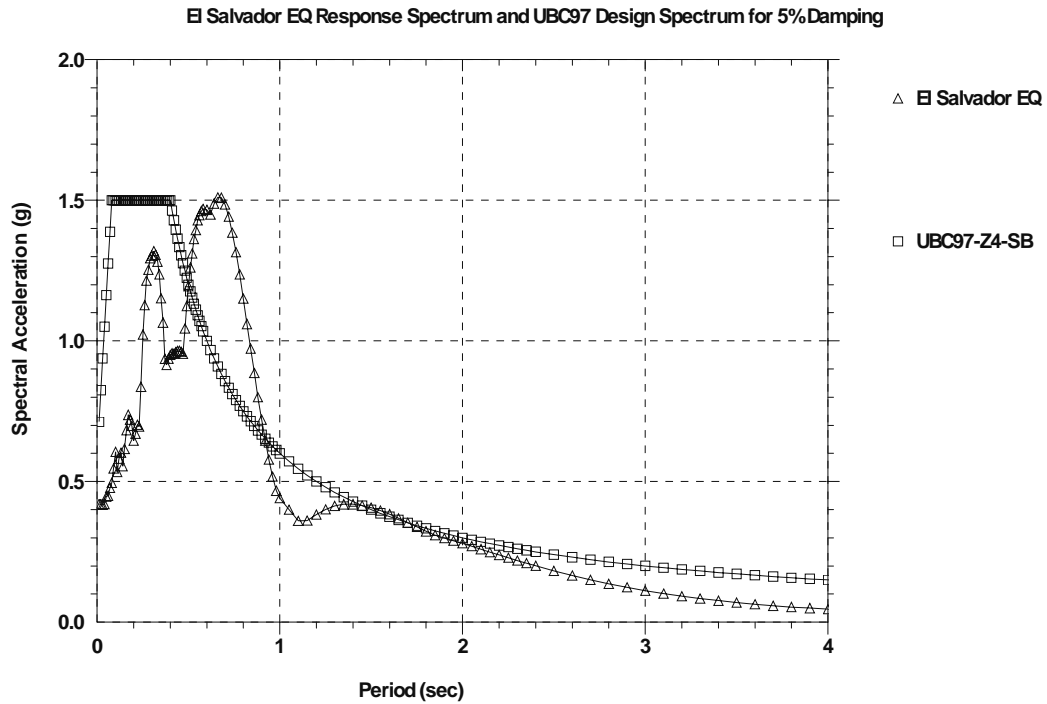
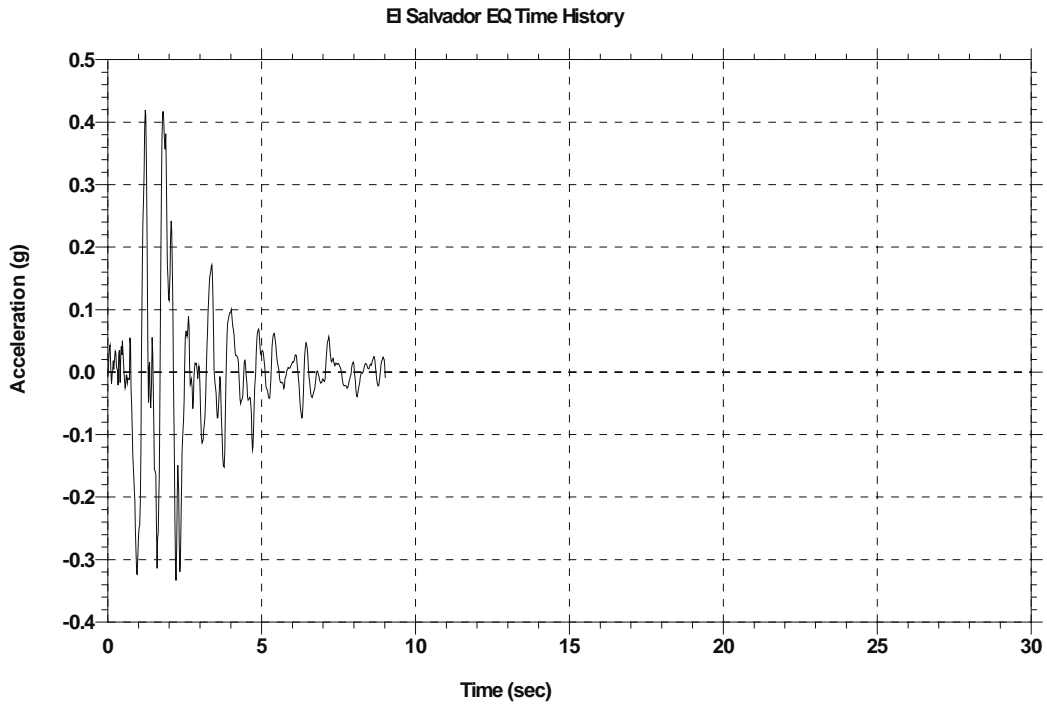


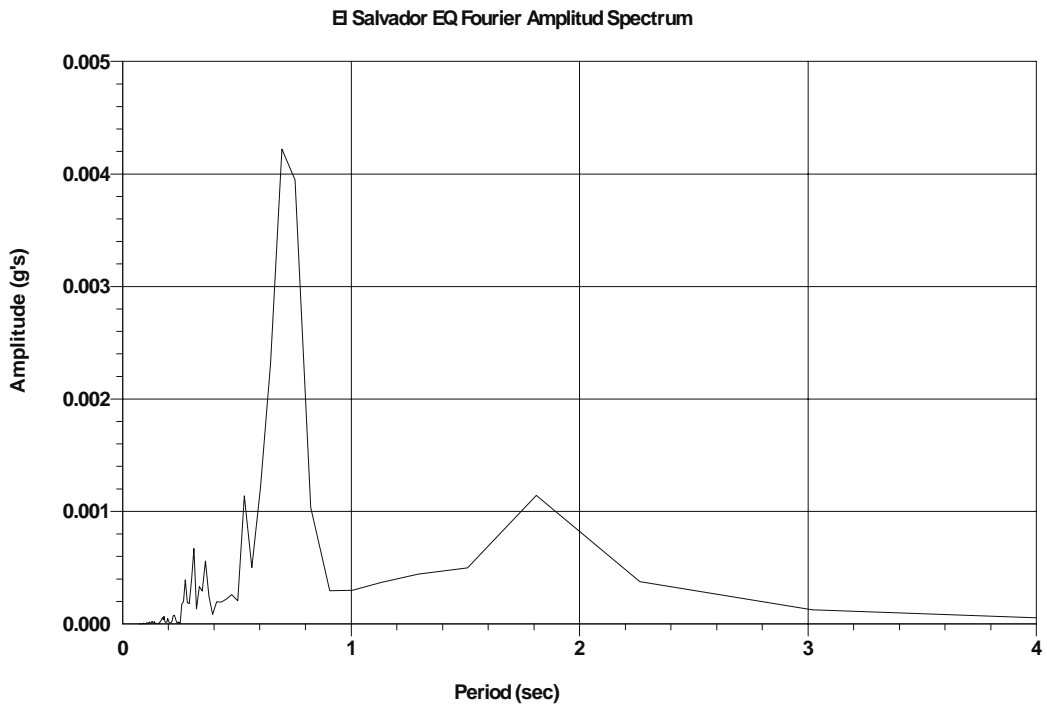
Figure 5.30: El Salvador earthquake response spectrum and the UBC 97 design spectrum for rock in zone 4.

Table 5.7: Characteristics of the El Salvador earthquake

Ground Motion ID	El Salvador
Peak Acceleration	0.42g
Peak Velocity	23.62 in/sec
Dominant Frequency	1.45 Hz
Dominant Period	0.69 sec.
Bracketed Duration	6.4 sec.



(a)



(b)

Figure 5.31: (a) Time history and (b) Fourier amplitude spectrum for El Salvador Earthquake.

5.6 Ground response analysis results

This section presents the results obtained from the equivalent linear one dimensional ground response analyses. The detailed results for the linear analyses are summarized in Appendix C. As mentioned before, all the sites were assigned to one of three groups depending of the information available for the analysis.

5.6.1 Group A

The first set of results corresponds to the sites in group A. It is recalled that the sites in group A have available the shear wave velocity profile from field tests as well as geotechnical information gathered near the sites. The analyses were performed by using as input the four artificial ground motions compatible with the UBC-97 design spectrum for rock in zone 3 and the El Salvador earthquake record. As discussed in a previous section, this record has a response spectrum comparable to the UBC-97 spectrum for rock in zone 4. For each site the following quantities were calculated: the soil deposit fundamental period, the peak acceleration at the surface, and the ground response spectrum at the surface for a 5% damping ratio. The results from the four artificial ground motions were arithmetically averaged and they are presented in Table 5.8. The results for each artificial ground motions are summarized in Appendix B. Table 5.9 list similar results but obtained with the El Salvador earthquake accelerogram as input.

The results show that the UBC-97 spectrum under predicts in some cases the seismic acceleration at the surface. Relatively high acceleration values were obtained because the initial (linear) period of the soil deposit is close to the dominant periods of the earthquakes. The Maní and Biología site which have the stiffest profile have the smaller increase in period (or degradation) after the iterations, and this result in the higher responses. The same trend was obtained with the El Salvador earthquake as shown in Table 5.9.

Using the acceleration time histories obtained at the surface, ground response spectra for a 5% damping ratio were developed and they are shown in Figures 5.32 through 5.36. The part (a) of the figures present the average curve for the artificial ground motions along with the UBC-97 design spectrum for zone 3 for the corresponding soil profile classification. Parts (b) of Figures 5.32 to 5.36 display the response spectrum of the 1986 El Salvador earthquake accelerogram and in the same plots the UBC-97 design spectrum for seismic zone 4 for the corresponding soil profile type.

Table 5.8: Summary of average results for Group A sites subjected to artificial ground motions.

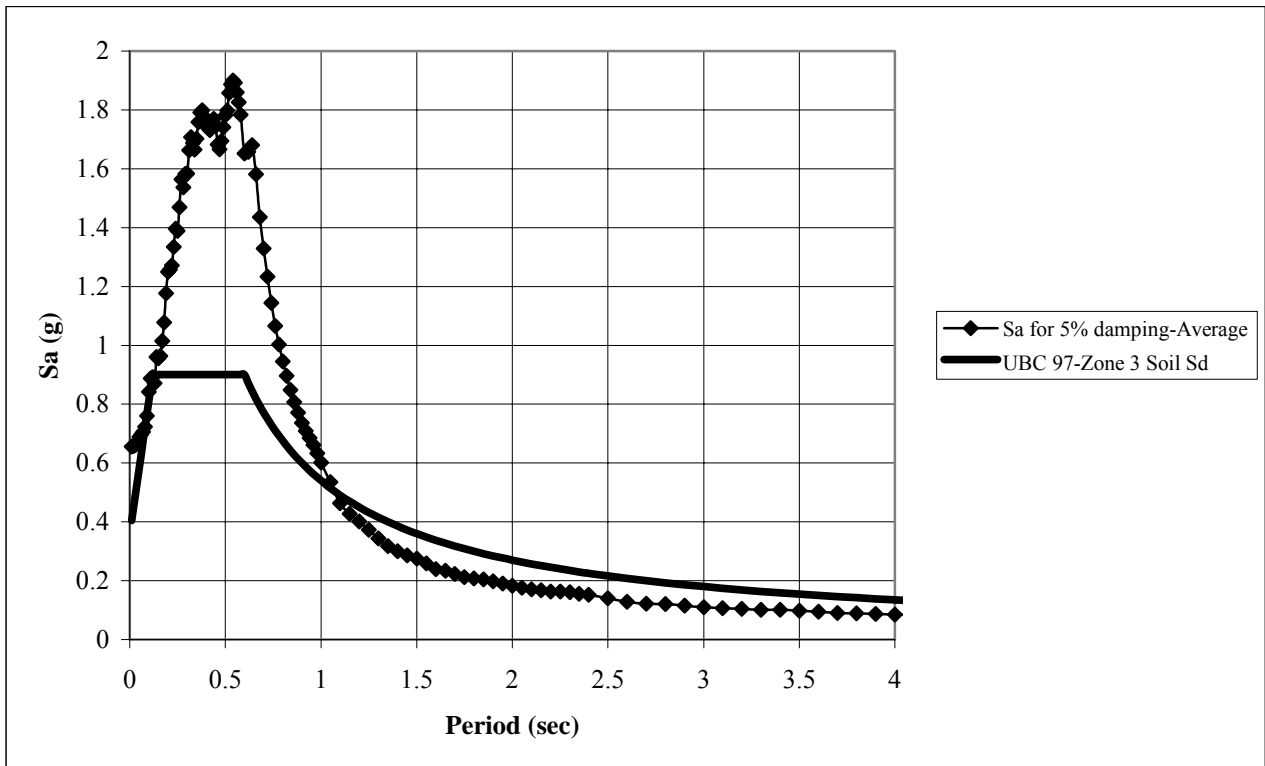
Site ID	\bar{V}_s^a ft/sec	UBC-97 Classification	T_s^b (linear) sec	T_s^b (non linear) sec	UBC-97 ^c Acc. g	Max. Acc. ^d (linear) g	Max. Acc. ^d (non linear) g
Abonos	646	Sd	0.51	0.59	0.36	0.92	0.65
Maní	1651	Sc	0.38	0.62	0.33	0.42	0.32
Biología	1875	Sc	0.17	0.22	0.33	0.88	0.77
Viaducto	710	Sd	0.50	0.74	0.36	0.85	0.46
Civil	1479	Sc	0.54	0.75	0.33	0.89	0.33

- a. Represents an average wave velocity in upper 30m (100ft) as defined in UBC-97.
- b. Soil periods (T_s) are average values for the four artificial ground motions.
- c. UBC-97 ground acceleration for seismic zone 3 (seismic coefficient C_a).
- d. The maximum accelerations (Max. Acc.) reported are the average values at the surface of the soil deposit.

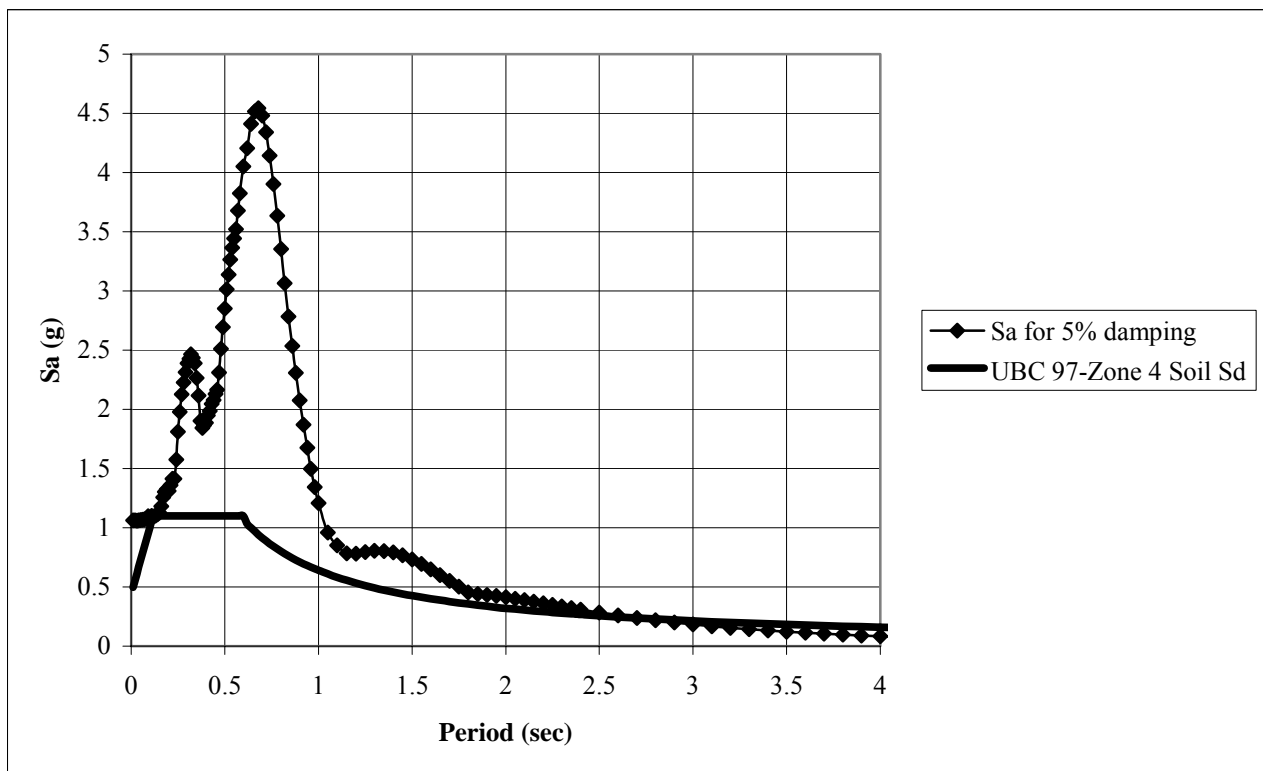
Table 5.9: Summary of results for Group A sites subjected to the El Salvador earthquake record.

Site ID	\bar{V}_s^a ft/sec	UBC-97 Classification	T_s^b (linear) sec	T_s^b (non linear) sec	UBC-97 ^c Acc. g	Max. Acc. (linear) g	Max. Acc. (non linear) g
Abonos	646	Sd	0.51	0.67	0.44	1.12	1.06
Maní	1651	Sc	0.38	0.77	0.40	0.53	0.34
Biología	1875	Sc	0.17	0.24	0.40	0.79	0.97
Viaducto	710	Sd	0.50	0.88	0.44	1.35	0.67
Civil	1479	Sc	0.54	0.98	0.40	1.18	0.51

- a. Represents an average wave velocity in upper 30m (100ft) as defined in UBC-97.
- b. Soil periods (T_s) are average values for the four artificial ground motions.
- c. UBC-97 ground acceleration for seismic zone 4 and near source factor $N_a = 1.0$ (seismic coefficient C_a).

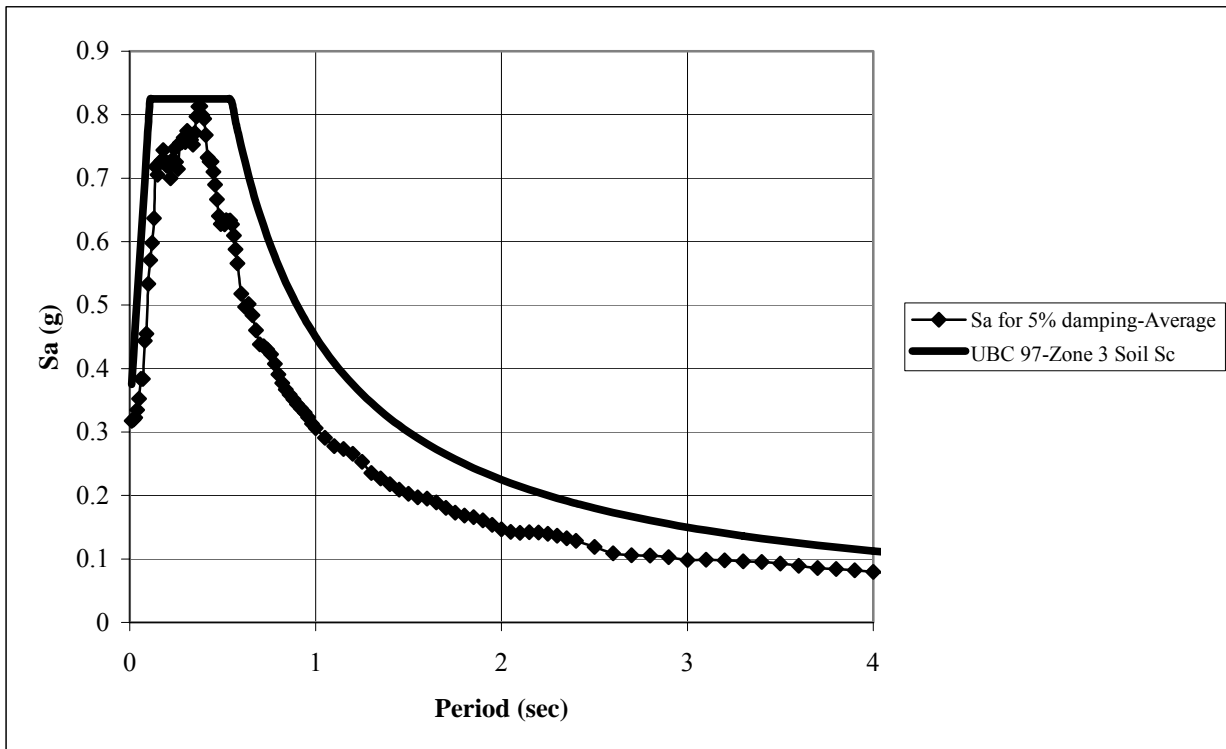


(a) Artificial ground motions

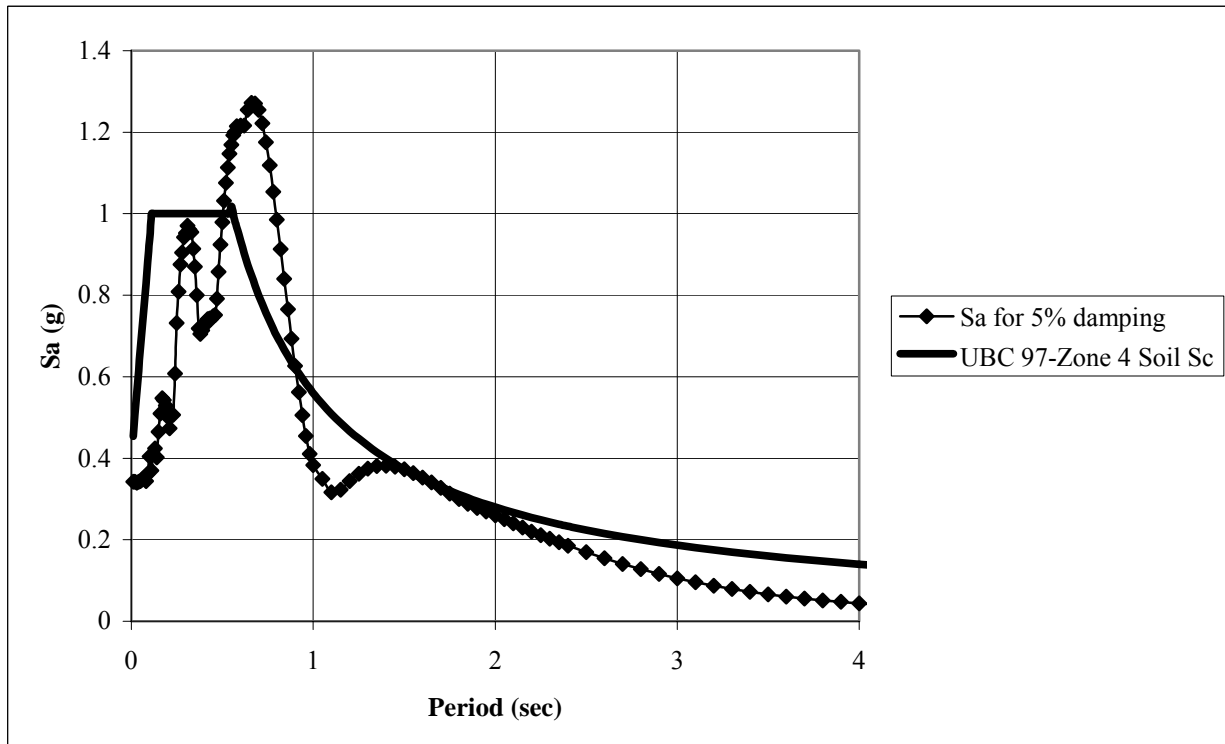


(b) El Salvador earthquake

Figure 5.32: Response spectrum at surface of the Abonos site from non linear analysis and UBC 97 design spectrum.

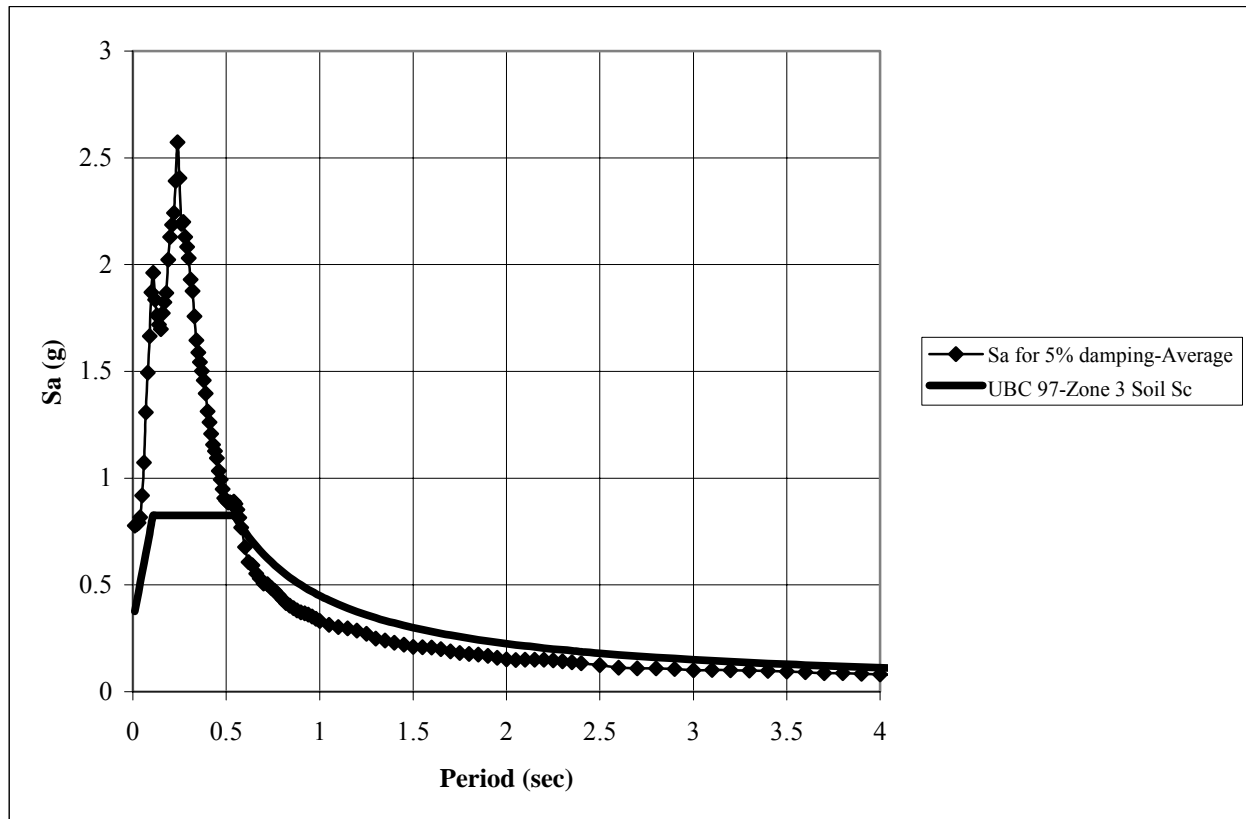


(a) Artificial ground motions

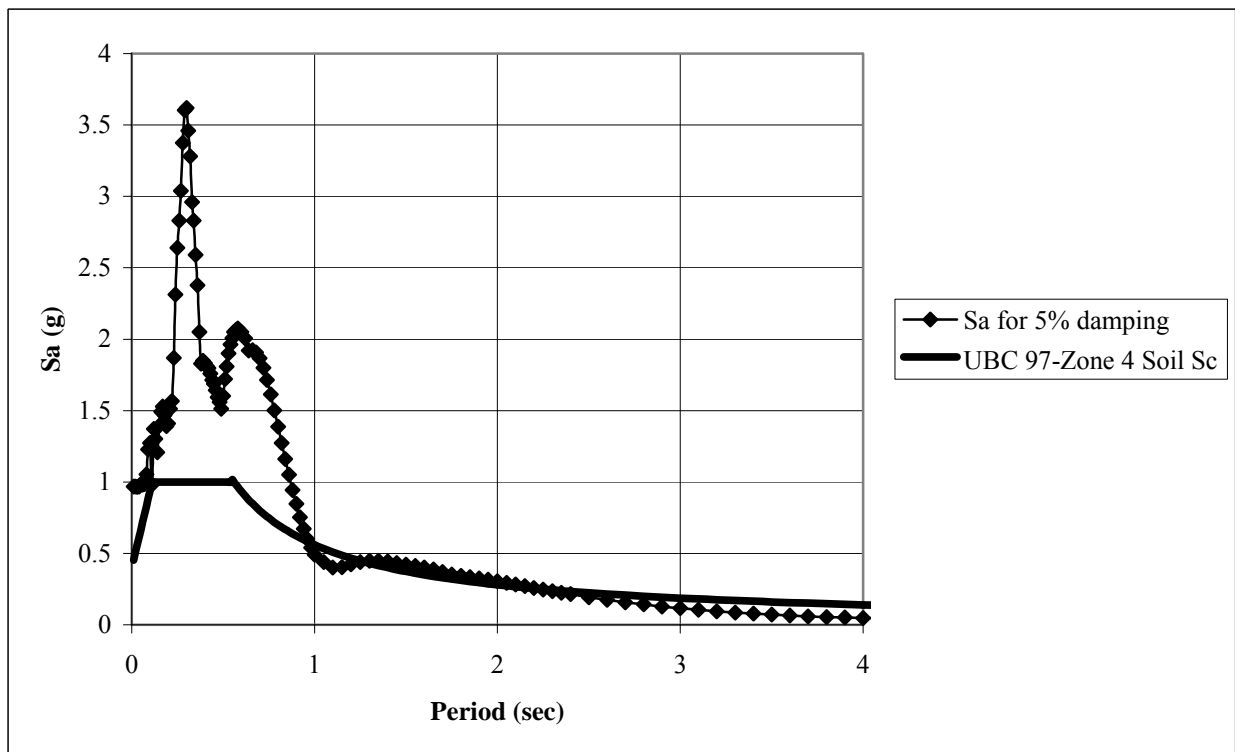


(b) El Salvador earthquake

Figure 5.33: Response spectrum at surface of the Maní site from non linear analysis and UBC 97 design spectrum.

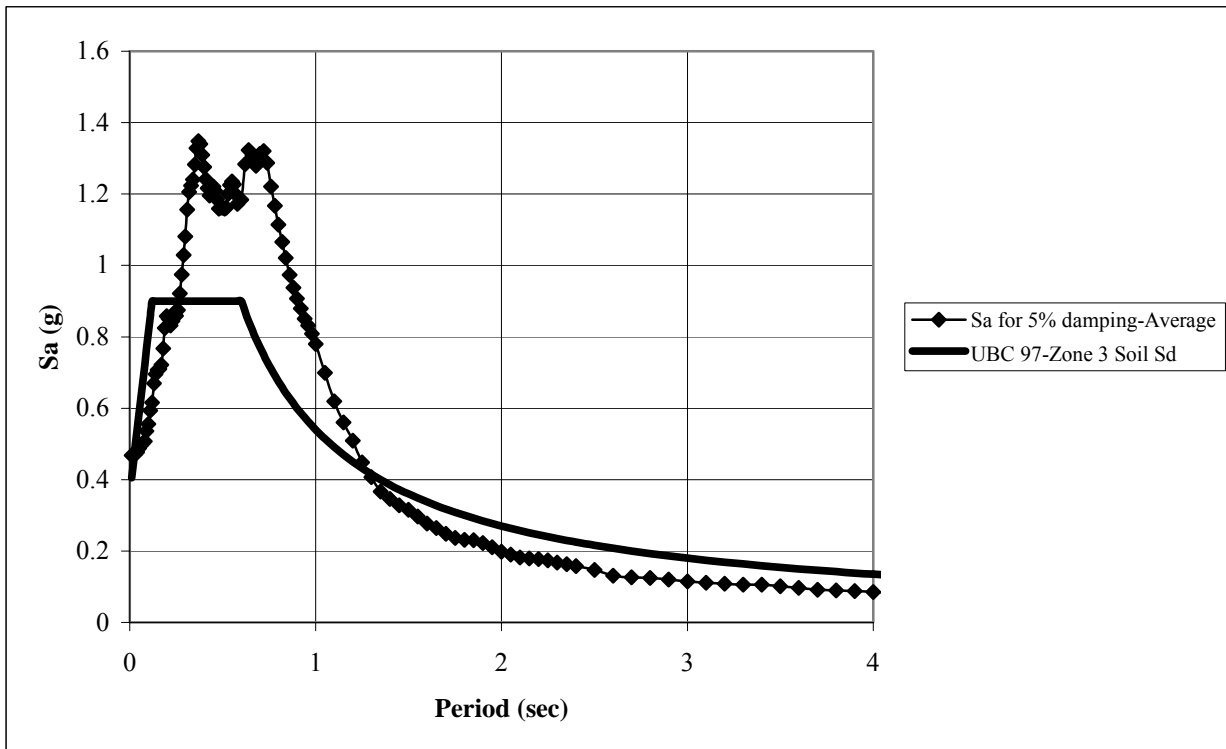


(a) Artificial ground motions

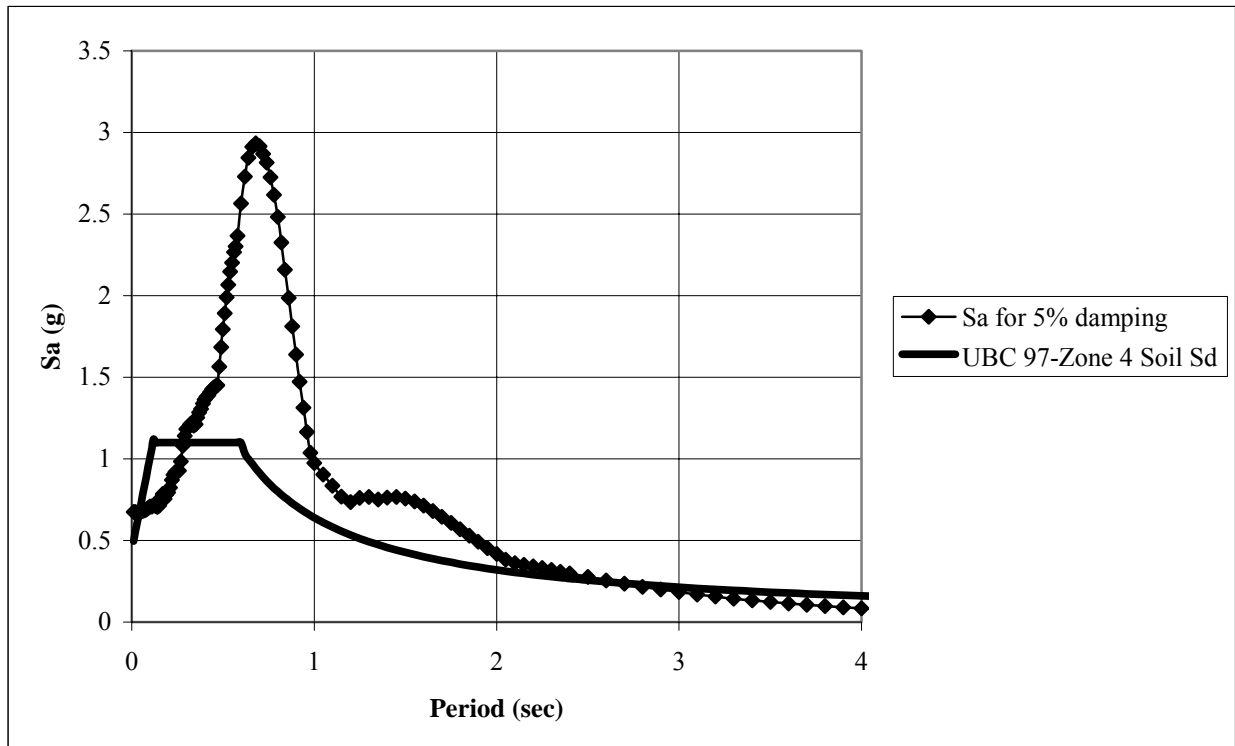


(b) El Salvador earthquake

Figure 5.34: Ground response spectrum at surface of the Biología site from non linear analysis and UBC 97 design spectrum.

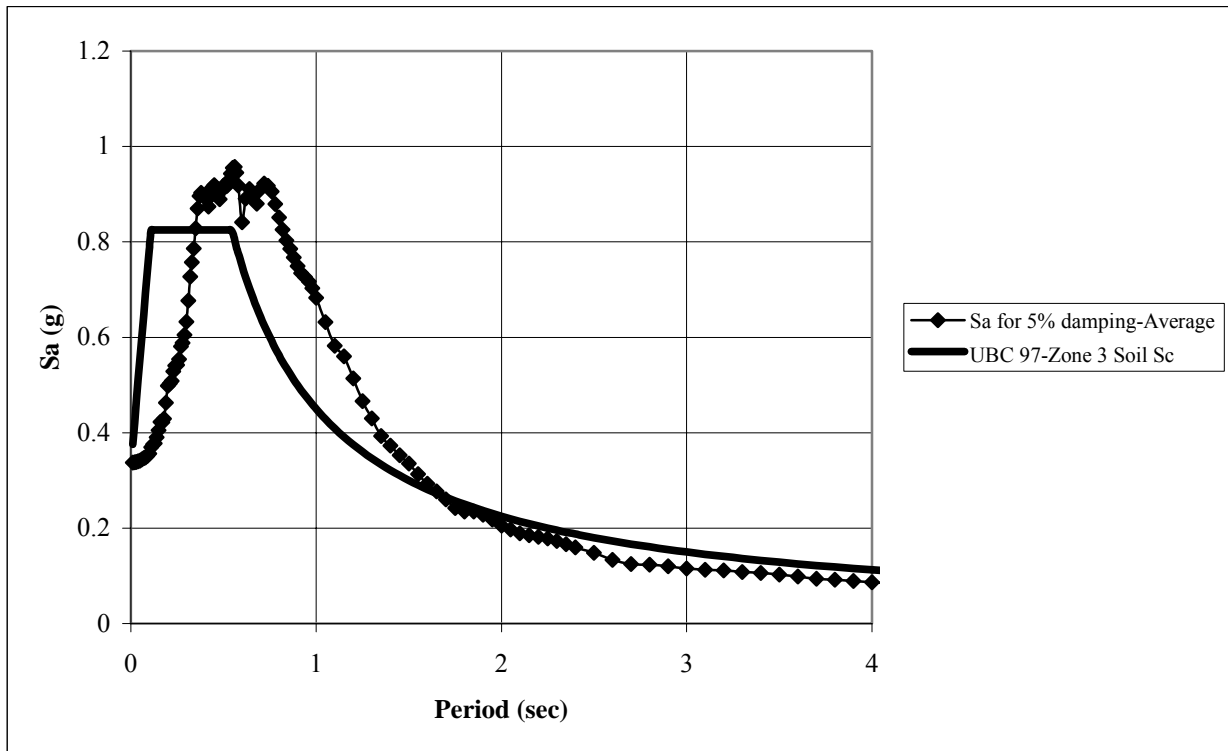


(a) Artificial ground motions

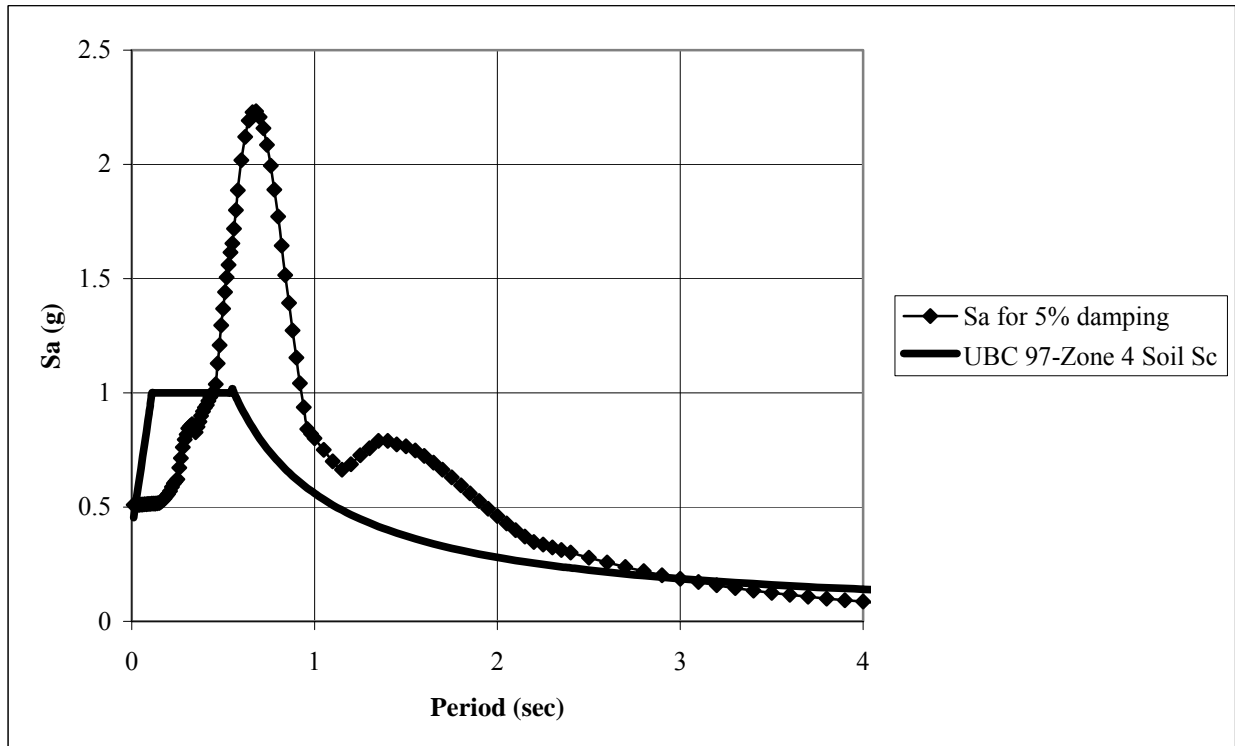


(b) El Salvador earthquake

Figure 5.35: Response spectrum at surface and of the Viaducto site from non linear analysis and UBC 97 design spectrum.



(a) Artificial ground motions



(b) El Salvador earthquake

Figure 5.36: Response spectrum at surface and of the Civil site from non linear analysis UBC 97 design spectrum.

5.6.2 Group B

The results for the sites in group B are presented in this section. The sites in this group have a shear wave velocity profile but there is no geotechnical boring logs. For each site, linear and equivalent non linear analyses were performed. Table 5.10 shows the fundamental period of the soil deposit and the peak acceleration at the surface for the linear and non linear cases obtained with the artificial ground motions. The quantities listed in Table 5.10 are the arithmetic average of the four individual results for the artificial ground motions. For the details of the analyses for each ground motion refer to Appendix B. The results obtained from the El Salvador earthquake for group B are listed in Table 5.11.

It can be observed from the table that for this group there are only small differences between the seismic accelerations prescribed at the surface by the UBC-97 and those obtained by the site specific analyses, except for the 341HWY site. As mentioned in the discussion of the soil profiles in this chapter and as explained in Chapter 3 when the SASW tests results were examined, the 341HWY site is located in the Añasco Valley near the Abonos site. Greater amplifications were expected for this site because of the low shear wave velocities in the layers and in fact that it is a very deep soil deposit. The same pattern of results was obtained with the El Salvador earthquake, as shown in Table 5.11.

Figures 5.37 through 5.42 show the ground response spectrum for a 5% damping ratio at the surface of each site obtained with the acceleration time history computed at the surface. This section presents the results from the equivalent non linear analyses and Appendix B those for the linear cases. The average ground response spectrum curves for the artificial ground motions are presented and compared with the UBC-97 design spectrum for seismic zone 3 for the corresponding soil profile classification in Figures 5.37(a) to 5.42(a). Figures 5.37(b) to 5.42(b) display similar results but for the 1986 El Salvador earthquake. In this case the UBC-97 design spectrum for zone 4 was used for comparison.

Table 5.10: Summary of average results for Group B subjected to artificial ground motions.

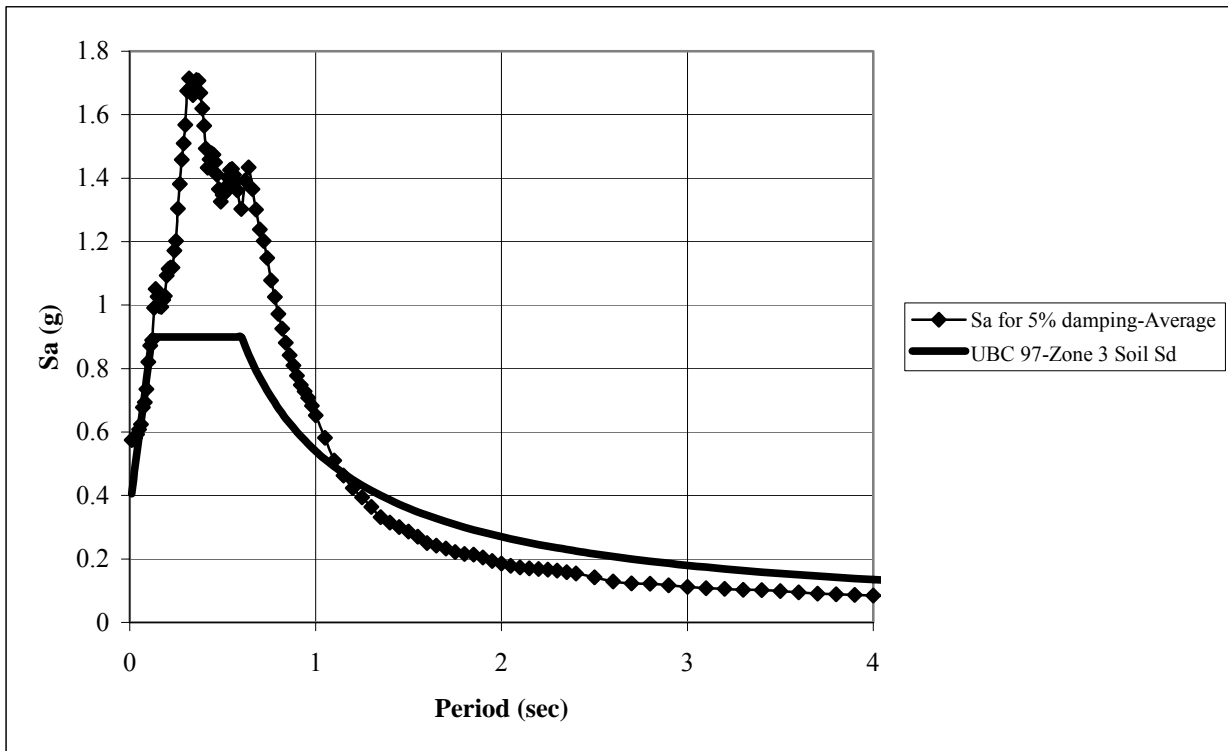
Site ID	\bar{V}_s^a ft/sec	UBC-97	T_s^b (linear) sec	T_s^b (non linear) sec	UBC-97 ^c Acc. g	Max. Acc. ^d (linear) g	Max. Acc. ^d (non linear) g
341HWY	666	Sd	0.62	0.72	0.36	0.72	0.57
Maní Park	901	Sd	0.31	0.39	0.36	0.82	0.32
Seco Park	799	Sd	0.44	0.66	0.36	0.79	0.27
Isidoro García	692	Sd	0.44	0.63	0.36	0.81	0.28
Ramírez de Arrellano	800	Sd	0.36	0.52	0.36	0.54	0.36
Sultanita	893	Sd	0.78	1.34	0.36	0.88	0.28

- a. Represents an average wave velocity in upper 30m (100ft) as defined in UBC-97.
- b. Soil periods (T_s) are average values for the four artificial ground motions.
- c. UBC-97 ground acceleration for seismic zone 3 (seismic coefficient C_a).
- d. The maximum accelerations (Max. Acc.) reported are the average values at the surface of the soil deposit.

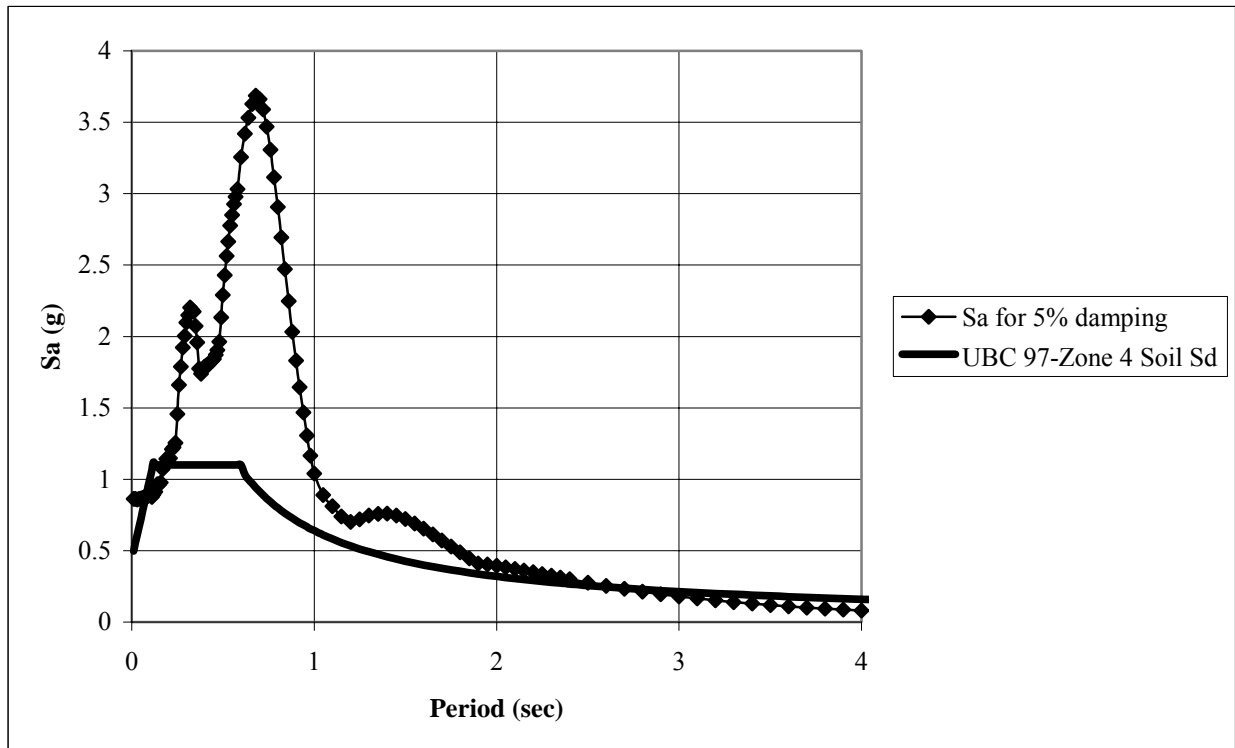
Table 5.11: Summary of results for Group B sites subjected to the El Salvador earthquake record.

Site ID	\bar{V}_s^a ft/sec	UBC-97	T_s^b (linear) sec.	T_s^b (non linear) sec.	UBC-97 ^c Acc. g	Max. Acc. (linear) g	Max. Acc. (non linear) g
341HWY	666	Sd	0.62	0.86	0.44	1.22	0.62
Maní Park	901	Sd	0.31	0.43	0.44	0.90	0.44
Seco Park	799	Sd	0.44	0.77	0.44	0.97	0.34
Isidoro García	692	Sd	0.44	0.76	0.44	1.00	0.40
Ramírez de Arrellano	800	Sd	0.36	0.63	0.44	0.97	0.34
Sultanita	893	Sd	0.78	1.91	0.44	1.44	0.45

- Represents an average wave velocity in upper 30m (100ft) as defined in UBC-97.
- Soil periods (T_s) are average values for the four artificial ground motions.
- UBC-97 ground acceleration for seismic zone 4 and near source factor $N_a = 1.0$ (seismic coefficient C_a).

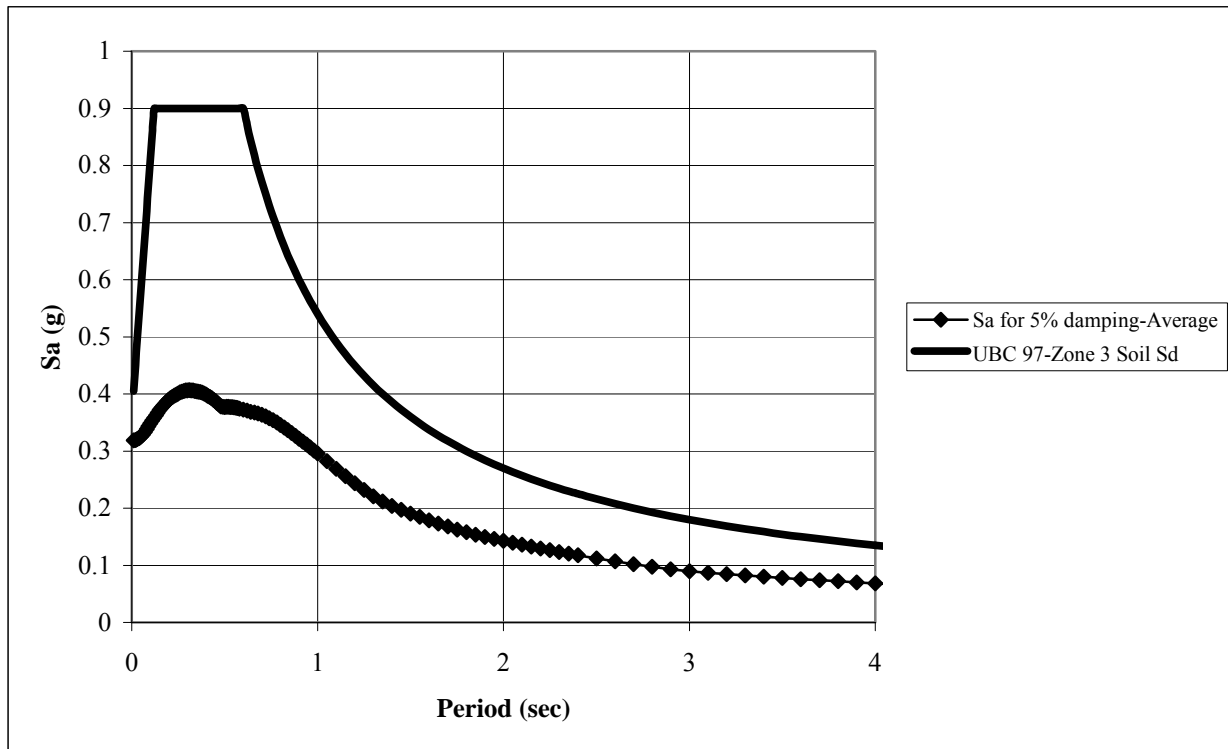


(a) Artificial ground motions

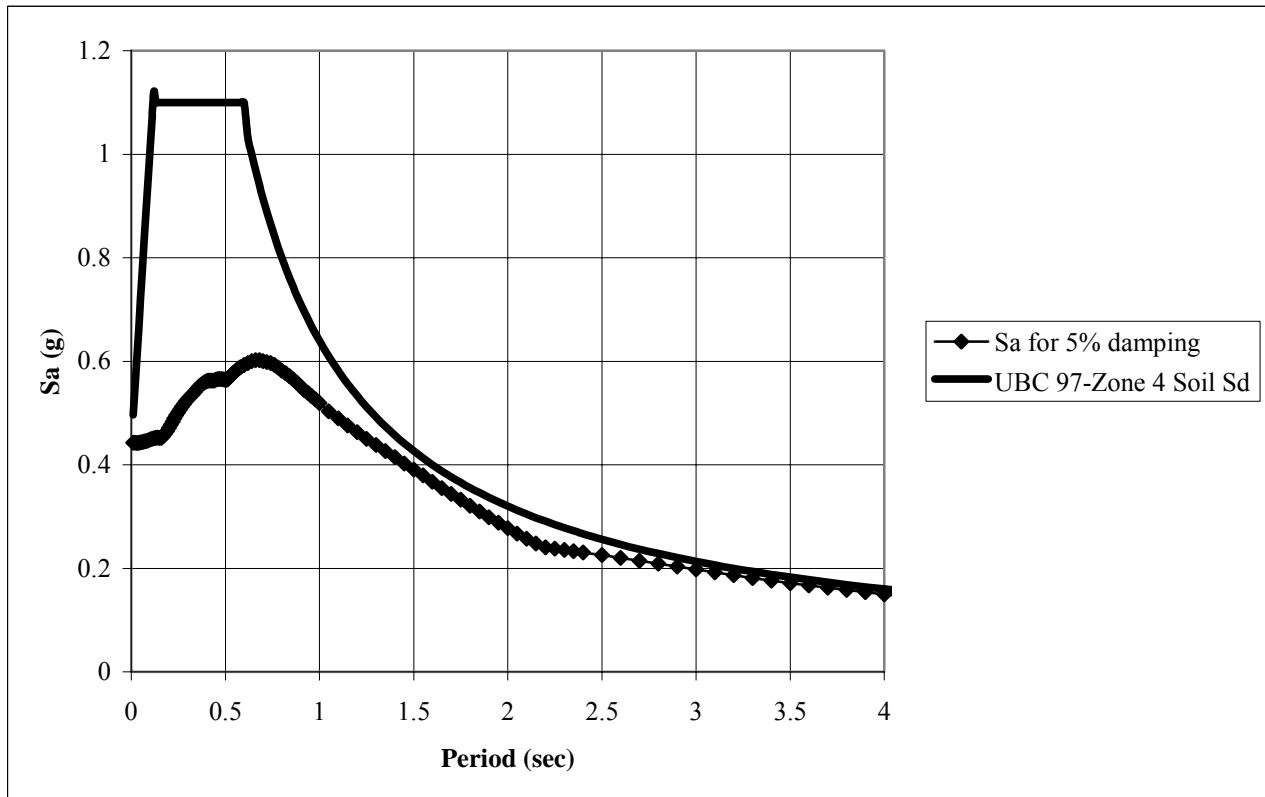


(b) El Salvador earthquake

Figure 5.37: Response spectrum at surface of the 341HWY site from non linear analysis and UBC 97 design spectrum.

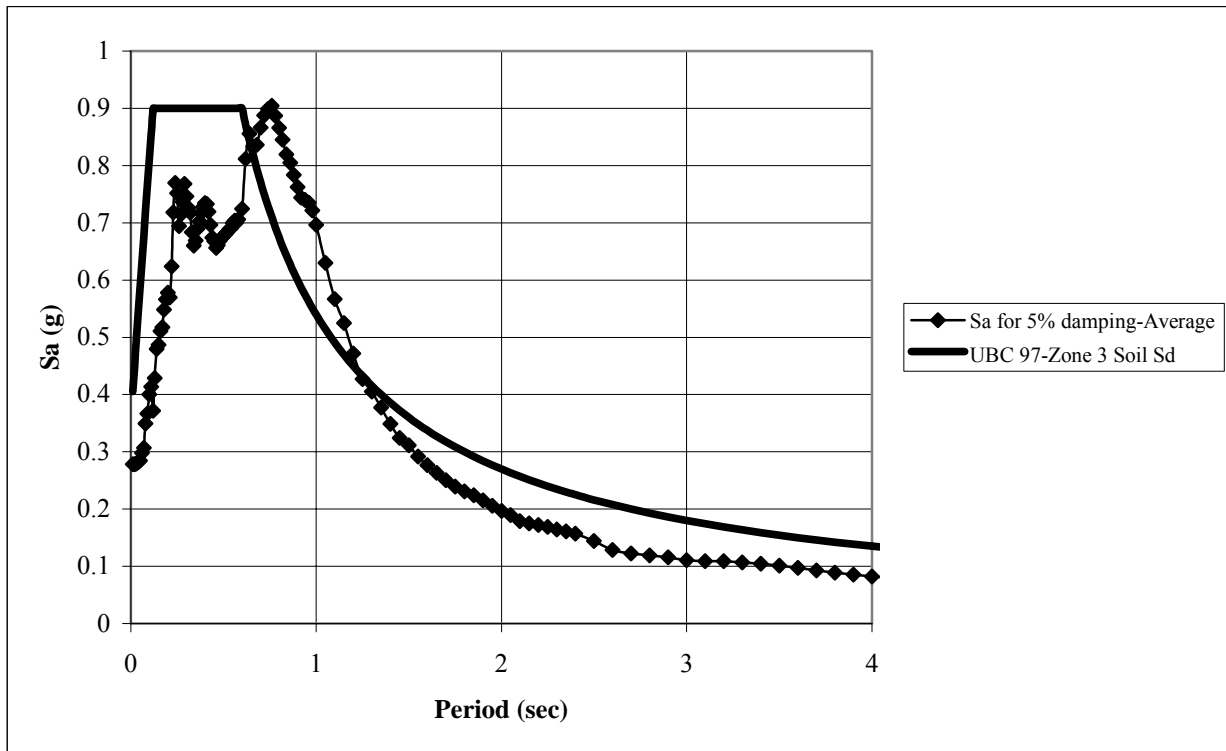


(a) Artificial ground motions

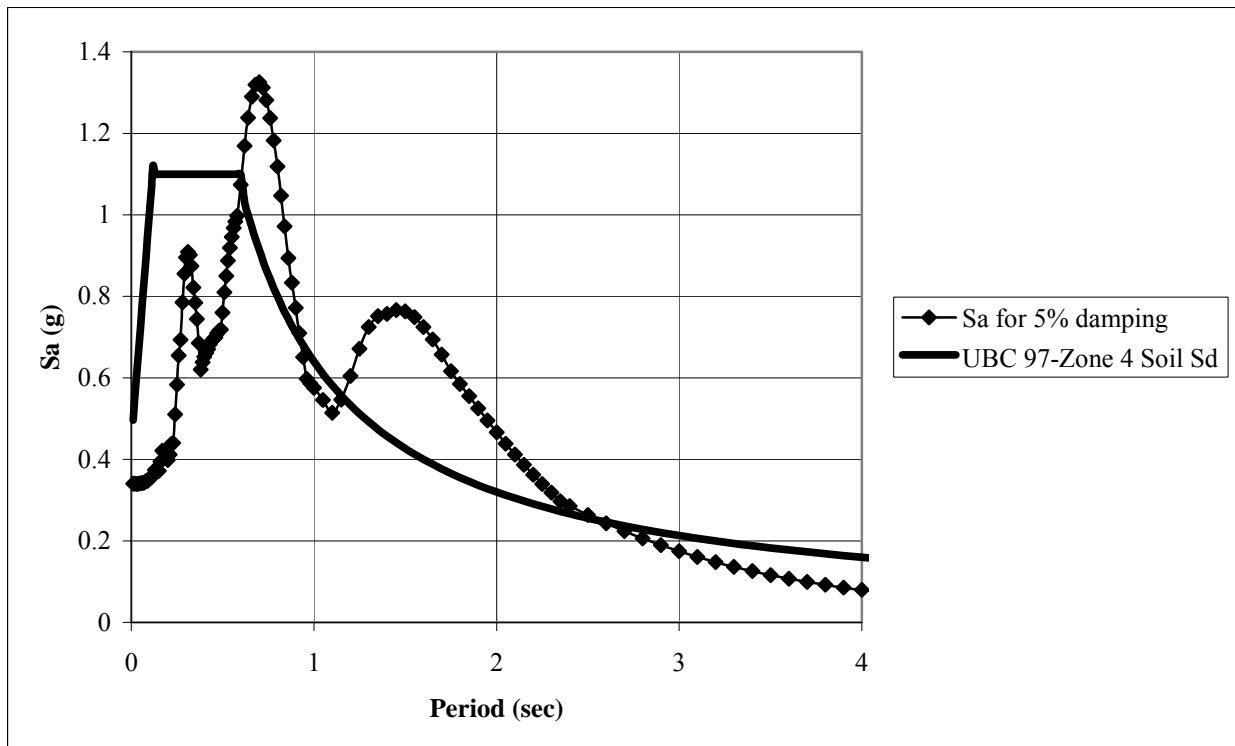


(b) El Salvador earthquake

Figure 5.38: Response spectrum at surface of the Maní Park site from non linear analysis and UBC 97 design spectrum.

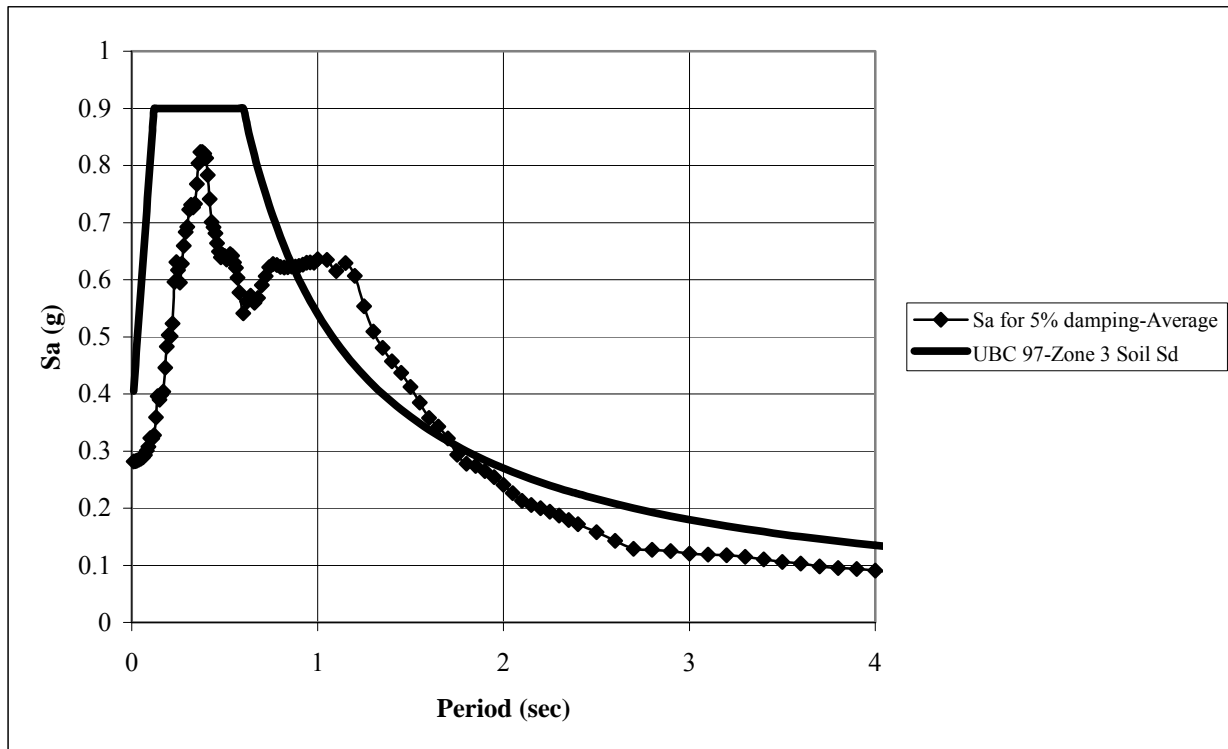


(a) Artificial ground motions

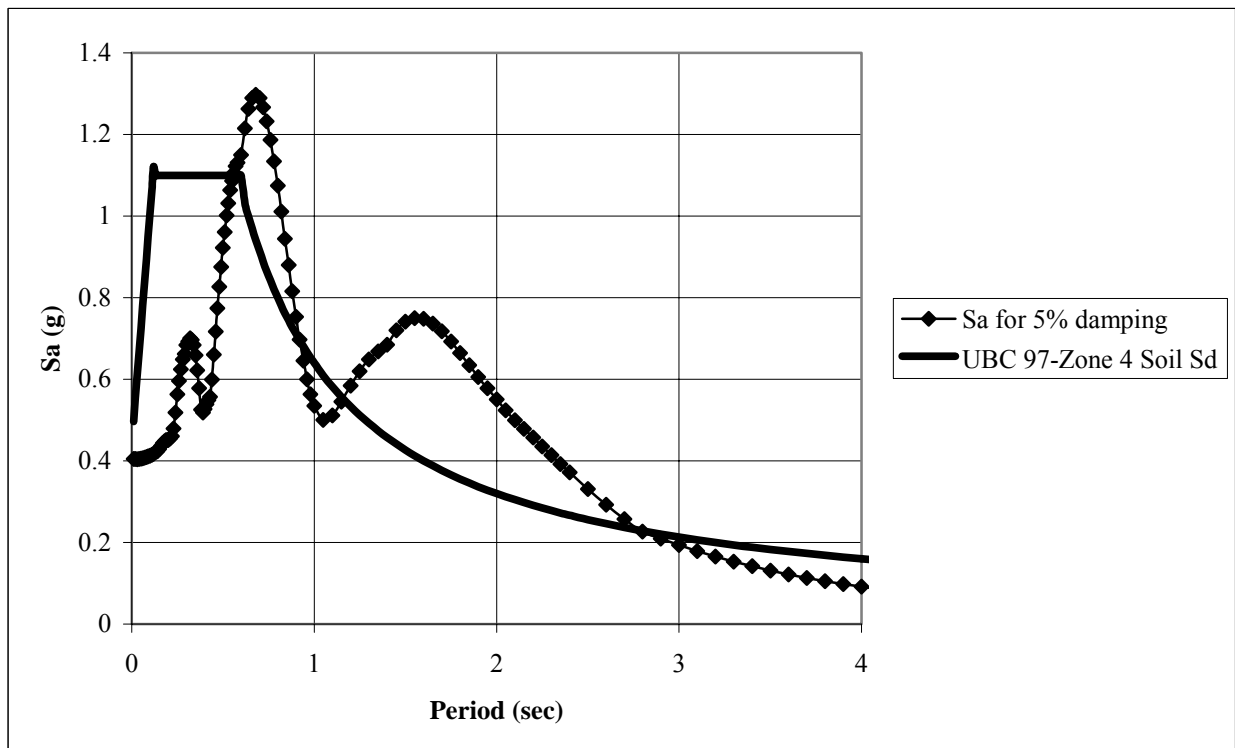


(b) El Salvador earthquake

Figure 5.39: Response spectrum at surface of the Seco Park site from non linear analysis and UBC 97 design spectrum.

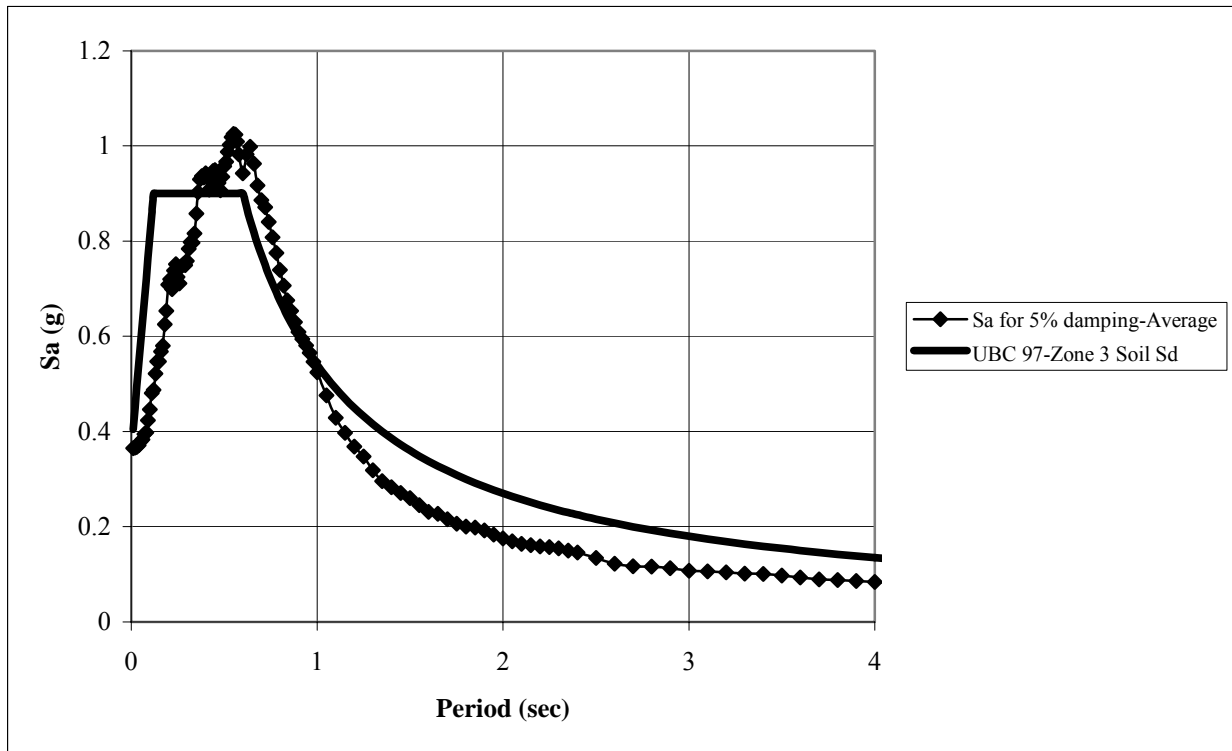


(a) Artificial ground motions

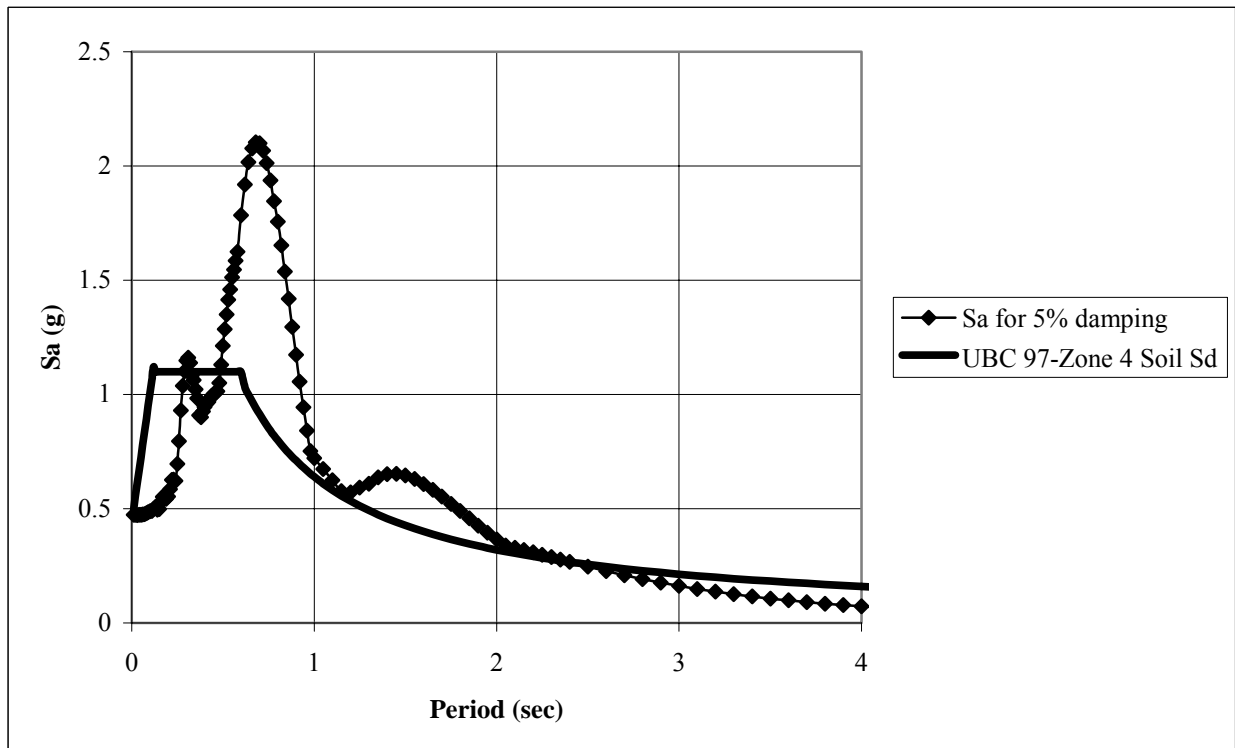


(b) El Salvador earthquake

Figure 5.40: Response spectrum at surface of the Isidoro García site from non linear analysis and UBC 97 design spectrum.

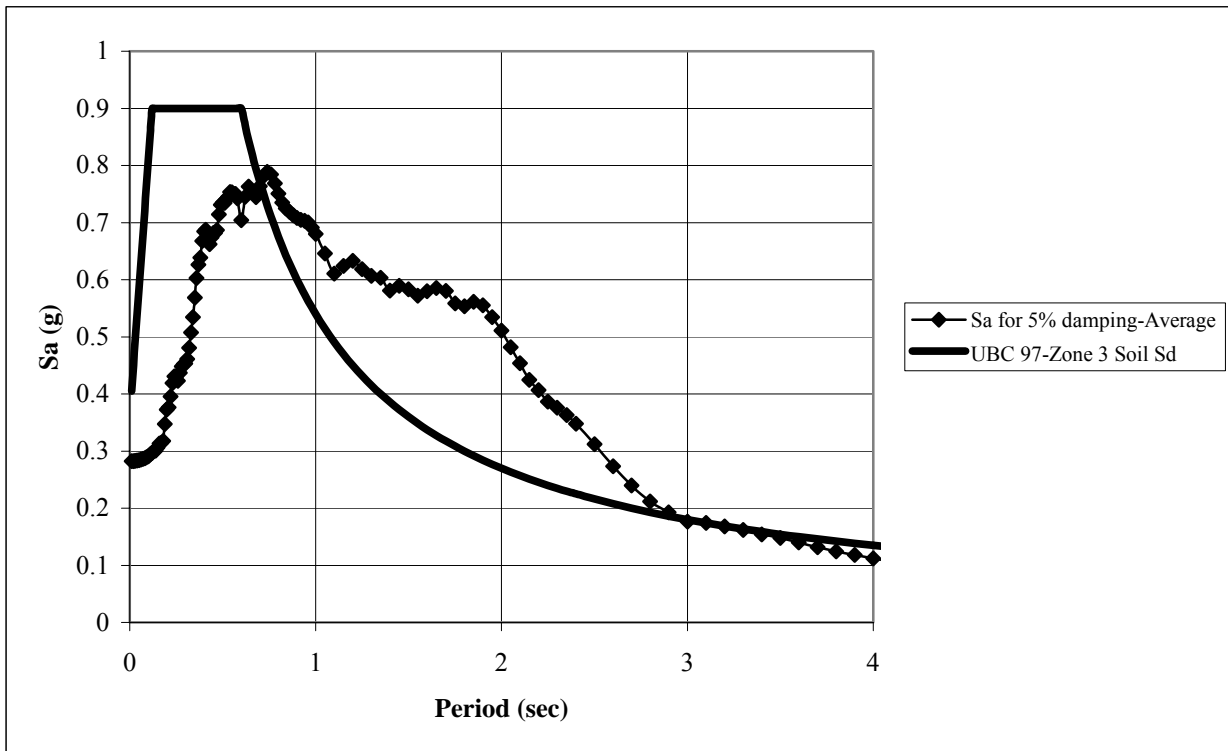


(a) Artificial ground motions

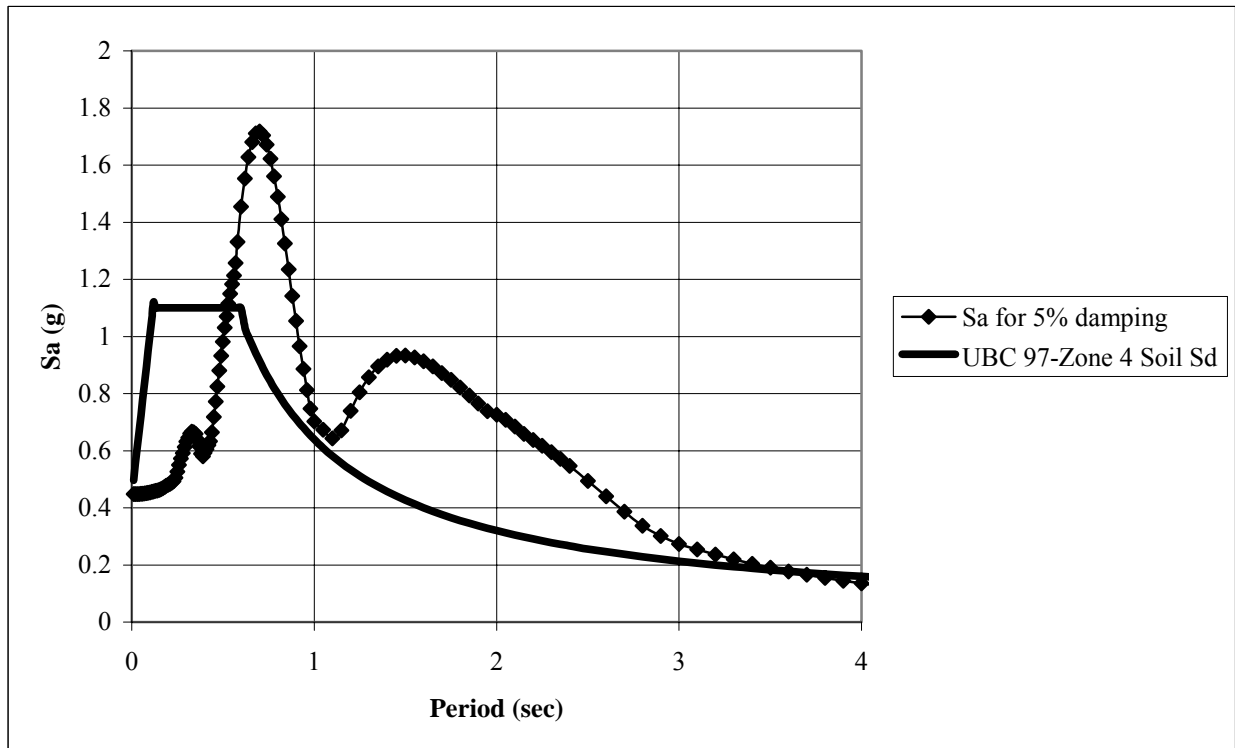


(b) El Salvador earthquake

Figure 5.41: Response spectrum at surface of the Ramírez de Arellano site from non linear analysis and UBC 97 design spectrum.



(a) Artificial ground motions



(b) El Salvador earthquake

Figure 5.42: Response spectrum at surface of the Sultanita site from non linear analysis and UBC 97 design spectrum.

5.6.3 Group C

This section presents the results for the sites assigned in group C. Group C correspond to the sites where only geotechnical information from boring logs was available and the shear wave velocity profile was correlated with the N value from the SPT. Tables 5.12 and 5.13 list the soil fundamental periods and peak accelerations at the surface obtained with the artificial ground motions and from El Salvador earthquake, respectively. Low shear wave velocities were calculated and very deep soil deposits were found for these sites. As expected from the previous group, high acceleration values at the surface were obtained.

Figures 5.43 through 5.46 show the ground response spectra at the surface for the artificial ground motions and for the 1986 El Salvador earthquake record. The response spectra were computed with the acceleration time histories from the equivalent linear analyses performed. Appendix B contains the curves for the linear analyses. The ground response spectra for the artificial ground motions presented in Figures 5.43(a) to 5.46(a) were averaged.

Table 5.12: Summary of average results for Group C sites subjected to artificial ground motions.

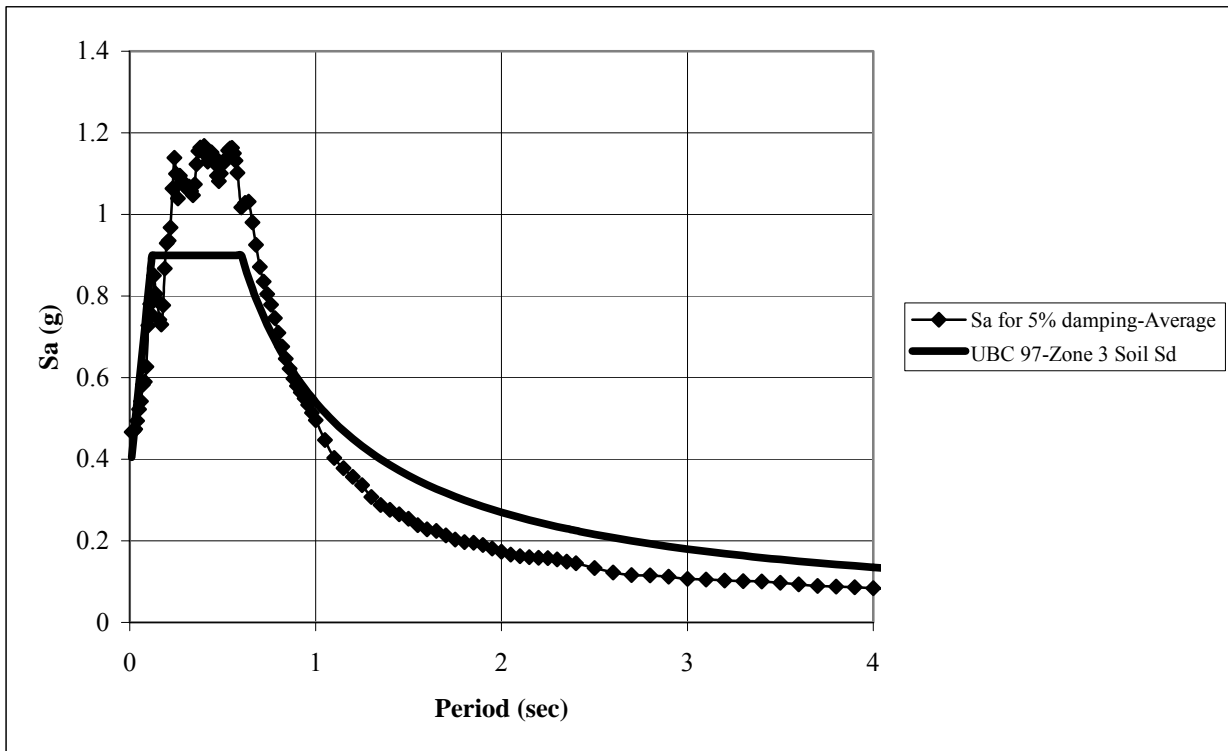
Site ID	\bar{V}_s^a ft/sec	UBC-97	T_s^b (linear) sec	T_s^b (non linear) sec	UBC-97 ^c Acc. g	Max. Acc. ^d (linear) g	Max. Acc. ^d (non linear) g
El Bosque	793	Sd	0.47	0.63	0.36	0.61	0.46
El Castillo	1388	Sc	0.27	0.45	0.33	0.44	0.42
India	475	Se	0.39	0.59	0.36	0.43	0.35
Marina	567	Se	0.53	0.76	0.36	0.83	0.31

- Represents an average wave velocity in upper 30m (100ft) as defined in UBC-97.
- Soil periods (T_s) are average values for the four artificial ground motions.
- UBC-97 ground acceleration for seismic zone 3 (seismic coefficient C_a).
- The maximum accelerations (Max. Acc.) reported are the average values at the surface of the soil deposit.

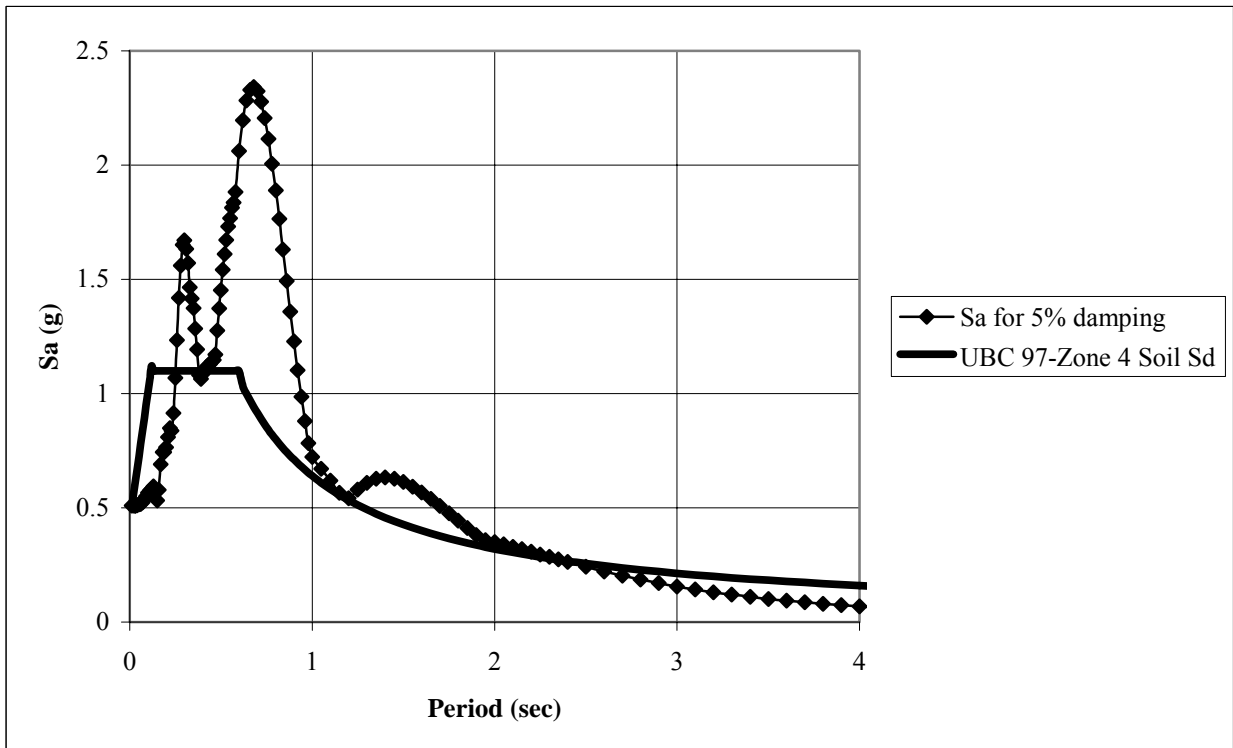
Table 5.13: Summary of results for Group C sites subjected to the El Salvador earthquake record.

Site ID	\bar{V}_s^a ft/sec	UBC-97	T_s^b (linear) sec.	T_s^b (non linear) sec.	UBC-97 ^c Acc. g	Max. Acc. (linear) g	Max. Acc. (non linear) g
El Bosque	793	Sd	0.47	0.72	0.44	0.78	0.51
El Castillo	1388	Sc	0.27	0.58	0.40	0.47	0.58
India	475	Se	0.39	0.76	0.36	0.57	0.39
Marina	567	Se	0.53	0.83	0.36	1.26	0.37

- Represents an average wave velocity in upper 30m (100ft) as defined in UBC-97.
- Soil periods (T_s) are average values for the four artificial ground motions.
- UBC-97 ground acceleration for seismic zone 4 and near source factor $N_a = 1.0$ (seismic coefficient C_a).

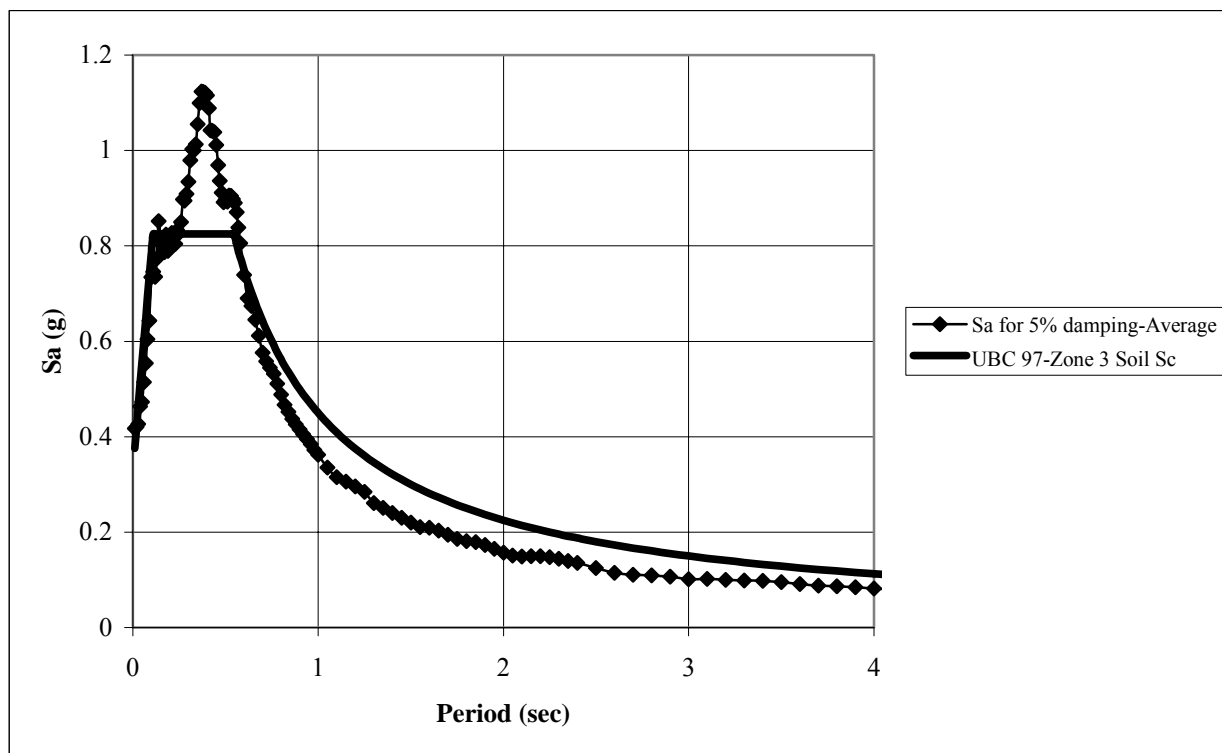


(a) Artificial ground motions

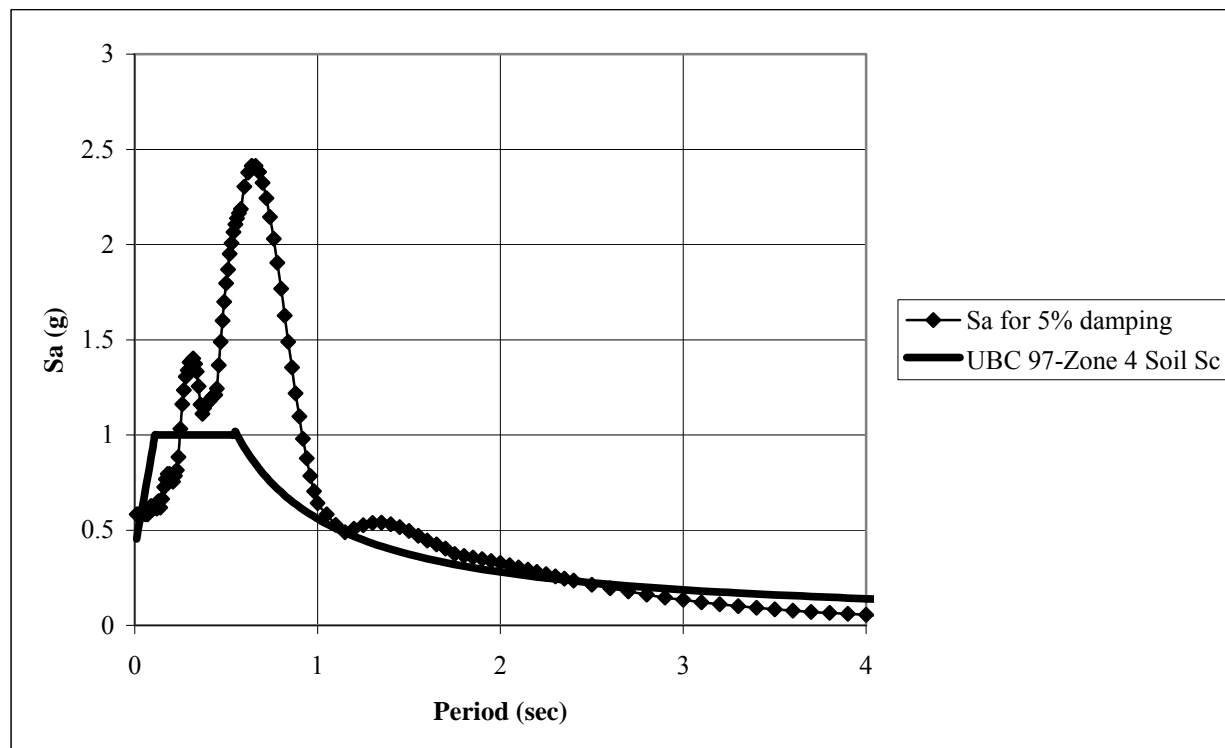


(b) El Salvador earthquake

Figure 5.43: Response spectrum at surface of the El Bosque site from non linear analysis and UBC 97 design spectrum.

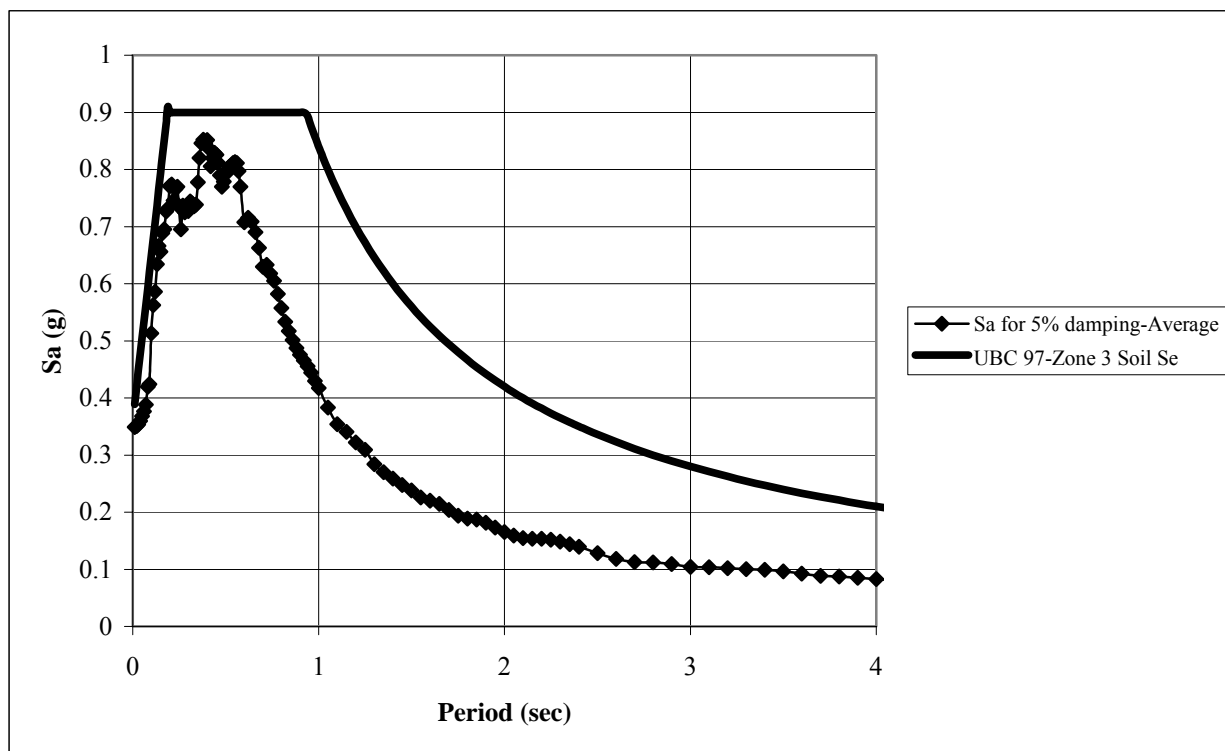


(a) Artificial ground motions

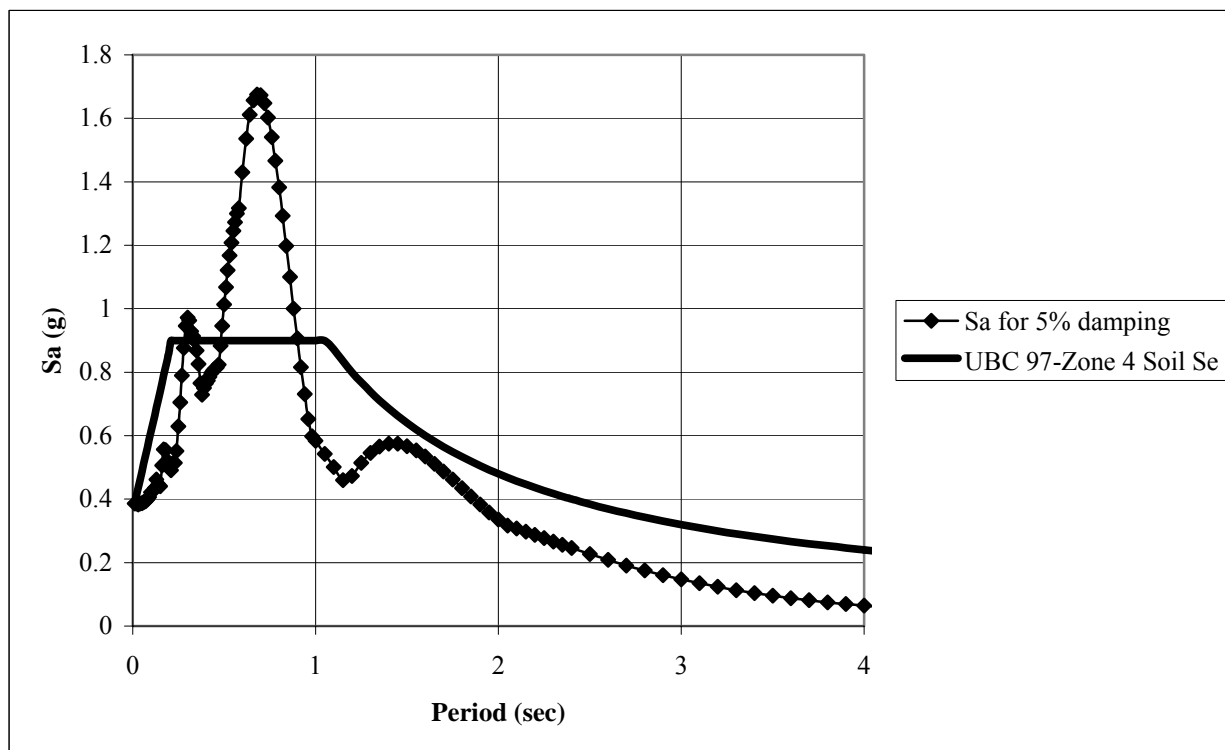


(b) El Salvador earthquake

Figure 5.44: Response spectrum at surface for the El Castillo site from non linear analysis and UBC 97 design spectrum.

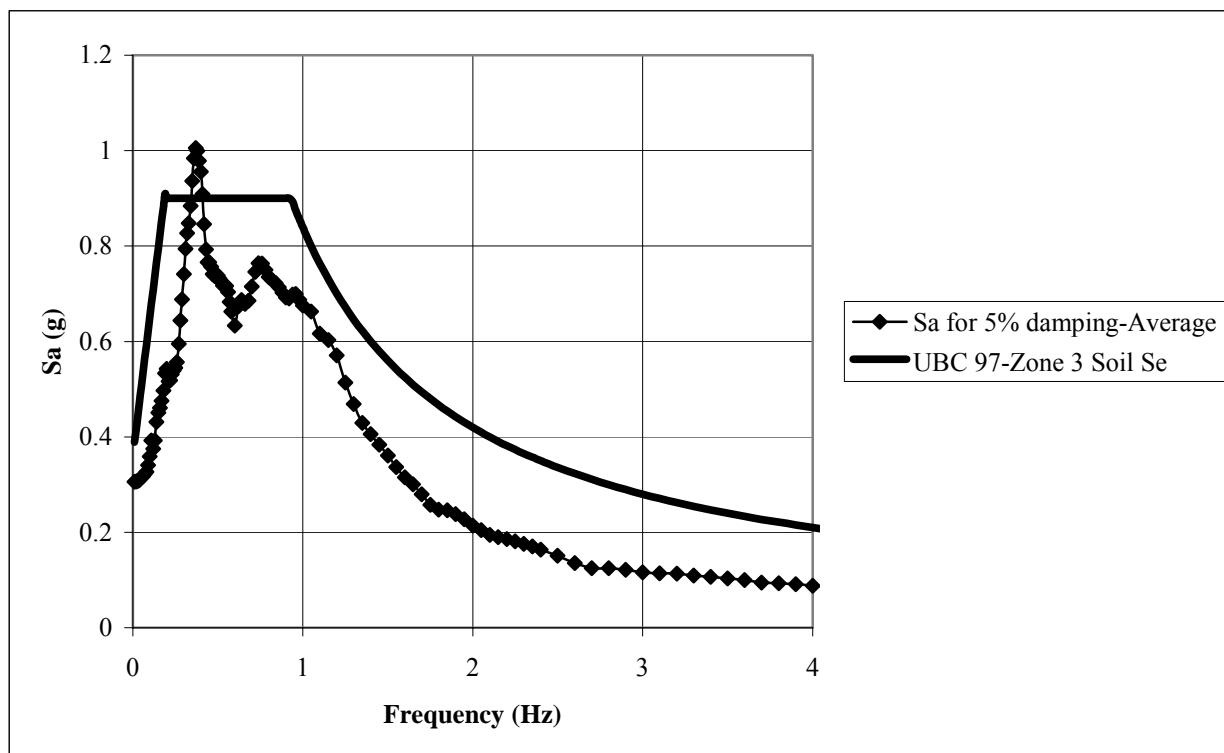


(a) Artificial ground motions

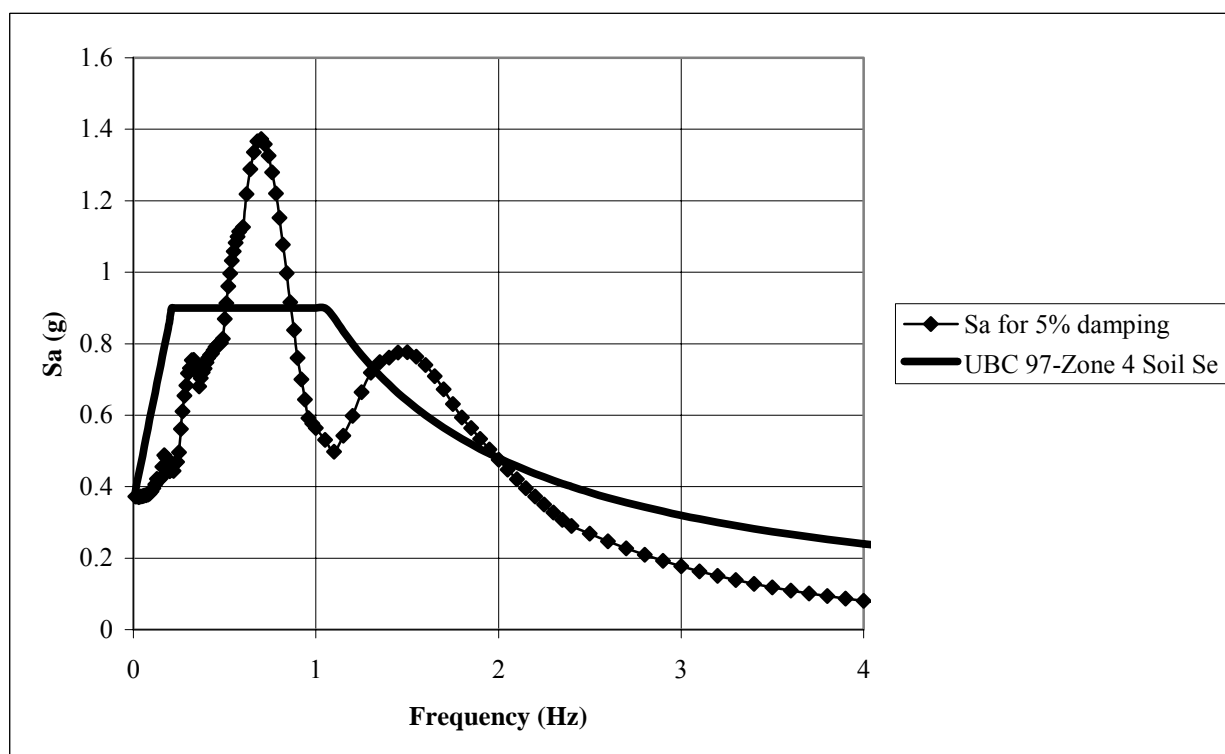


(b) El Salvador earthquake

Figure 5.45: Response spectrum at surface of the India site from non linear analysis and UBC 97 design spectrum.



(a) Artificial ground motions



(b) El Salvador earthquake

Figure 5.46: Response spectrum at surface of the Marina site from non linear analysis and UBC 97 design spectrum.

CHAPTER 6

Conclusions and recommendations

6.1 Introduction

The previous chapters described the procedure and the results obtained from a ground response analyses that considered in-situ dynamic soil properties obtained from the Spectral Analysis of Surface Waves (SASW). Chapter 2 described the findings of recent studies in Mayagüez. These projects were essential to identify the subsoil, seismic faults, and expected ground motions characteristics, to identify the areas in Mayagüez more susceptible to seismic amplifications, and to measure soil dynamic properties by the SASW method. The SASW field work to obtain the shear wave velocity profile at nine sites in Mayagüez was described in Chapter 3 along with the results obtained. Also in this chapter the sites analyzed were classified according to the UBC-97 soil profile types by using the average shear wave velocity in the upper 30 meters. A simplified procedure for the estimation of the average shear wave velocity at 30 meters by using the Rayleigh wave velocity obtained from the SASW method was investigated in Chapter 4. The predictive equation developed by Brown et al. (2000) was applied in the Mayagüez sites. The accuracy of the results was examined and it was found that the errors are in the range reported by Brown et al. In general, the simplified method yielded satisfactory results for the Mayagüez sites and thus it is recommended to be used for future SASW tests program. With the data obtained from the SASW tests, a series of ground response analyses was performed using the computer program SHAKE2000. The procedure and the results were presented in Chapter 5. In this chapter, the sites fundamental periods, peak acceleration at the surface, the amplification factors, and response spectrum at the surface were obtained for fourteen sites including the nine sites tested with SASW. The results were compared with the design response spectrum of the UBC-97 code for the corresponding NEHRP soil profile classification.

In the following sections the main findings of this research project are reported. Also, recommendations for future research and some limitations of the results obtained in this project are provided.

6.2 Soil Dynamic Properties at Various Sites in Mayagüez

In this section, the soil dynamic properties at the sites analyzed are summarized. The dynamic properties include the average shear wave velocity and fundamental periods for each site. These soil properties are commonly used in engineering analysis and design for the estimation of earthquake forces in structures via a design spectrum and liquefaction hazard assessments between others. The values presented can be used as a guide and for the initial evaluation of a proposed project near the sites tested in this study considering the limitations presented in this chapter.

Table 6.1 presents the average shear wave velocity in the upper 30 meters obtained with the UBC-97 equation and from SASW field data. Also, the UBC-97 soil profile classification for each site is listed. These values were previously presented in Chapter 5 with a description of their development.

The fundamental period for each site is presented in Table 6.1 from the linear analysis results. It is assumed that this period represents the initial condition of the site. During an earthquake, the soil deposit will respond depending on their soil non-linear properties and on the earthquake characteristics. It is expected that during a strong earthquake the soil deposit will start to degrade becoming more flexible and thus increasing its period of vibration. The same reduction occurs with the average shear wave velocity because of the degradation of the shear modulus during an earthquake. Depending on the earthquake characteristics, this change may decrease or increase the response of the soil.

For a homogeneous single layer under laid by a rigid bottom, the fundamental period is proportional to the depth of the soil deposit and inversely proportional to the shear wave velocity. For a soil deposit with multiple layers, the fundamental period follows a similar pattern, but the exact form of the relationship is unknown. Even though for all the sites the bedrock was assumed to be at a depth of 100 ft, there were some sites that a high shear wave velocity was found before 100 ft, with a shear modulus greater than 7,800 ksf. SHAKE2000 considers as competent rock a material with shear modulus greater than 7,800 ksf. Example of this situation occurs in the Maní, Biología, and for El Castillo sites.

Table 6.1: Summary of average shear wave velocities and soil periods for the sites in Mayagüez.

Sites	Vs30 (ft/sec)	UBC-97 Classification	Linear Period (seconds)
Abonos	646	S _D	0.51
341HWY	666	S _D	0.62
Maní Park	901	S _D	0.31
Maní	1652	S _C	0.38
Seco Park	799	S _D	0.44
Isidoro García	693	S _D	0.44
Ramírez de Arellano	800	S _D	0.36
Sultanita	894	S _D	0.78
Civil	1480	S _C	0.54
Biología	1875	S _C	0.17
Viaducto	710	S _D	0.50
El Castillo	1388	S _C	0.27
El Bosque	793	S _D	0.47
India	475	S _E	0.39
Marina	567	S _E	0.53

6.3 Ground Response Spectra for Mayagüez sites

Another set of results obtained for each site were the peak ground acceleration and the ground response spectra at the surface of the soil studied. The frequency content of the ground motion, the soil profile properties, and the soil materials dynamic characteristics are examples of parameters that control the results obtained. As explained in Chapter 5, the soil profiles for the sites in group A and B were obtained from the SASW field tests. Even though the soil materials for group A were obtained from geotechnical explorations conducted near the sites found in a database developed for Mayagüez, there is no guarantee that the soils profile will be the same at the site tested and thus differences are expected.

From the fourteen sites analyzed, nine sites were classified as SD, four sites were classified as soil profile type SC, and one site was classified as SE. As mentioned in Chapter 5, the artificial

ground motions were obtained from the design response spectrum for rock (Soil SB) prescribed in the UBC-97. Due to the way that for the artificial accelerograms are generated their peak accelerations was slightly higher than the 0.3g recommended by UBC-97 for rock in seismic zone 3. Also, as evidenced by the various peaks at different frequencies in the Fourier amplitude spectra the ground motions have various dominant frequencies. The presence of various dominant frequencies increases the likelihood that the soil deposits investigated can shift toward a resonant condition with the earthquake ground motions. Those sites with soil properties that are more susceptible to experience degradation had more chances of moving away from the earthquake dominant frequencies thus resulting in a lower response. Moreover, in these soils the damping ratios increases significantly thus contributing to the response reduction.

Figure 6.1 shows the average ground response spectra at the surface of the sites in group A for the artificial ground motions. Figure 6.2 and 6.3 show similar results for the sites in group B and C, respectively. The ground response spectra at the surface obtained by using El Salvador earthquake record are summarized in Figures 6.4 through 6.6 for groups A, B, and C. The results for each of the individual artificial ground motions are summarized in Appendix B.

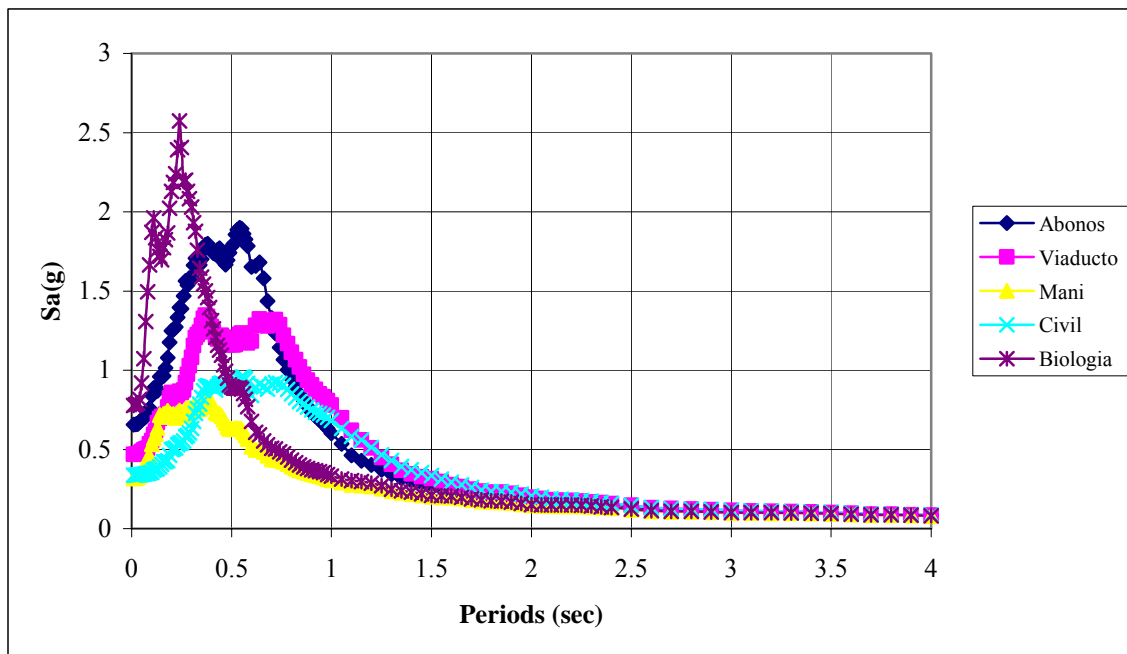


Figure 6.1: Average ground response spectra for the artificial ground motions for the sites in group A and 5% damping ratio.

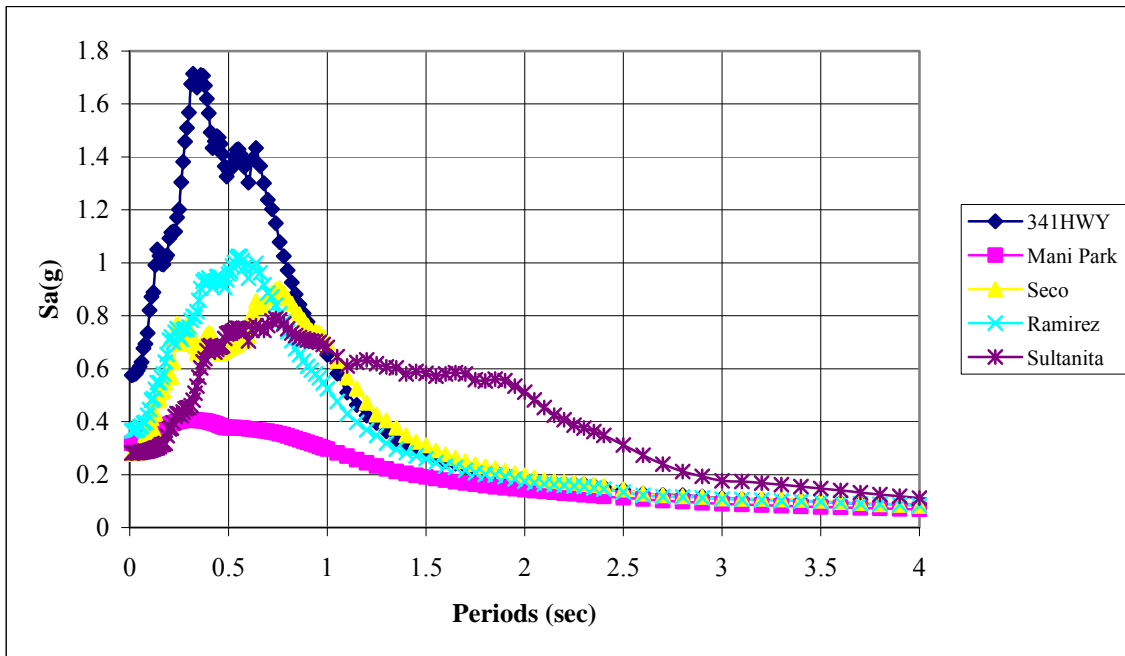


Figure 6.2: Average ground response spectra for the artificial ground motions for the sites in group B and 5% damping ratio.

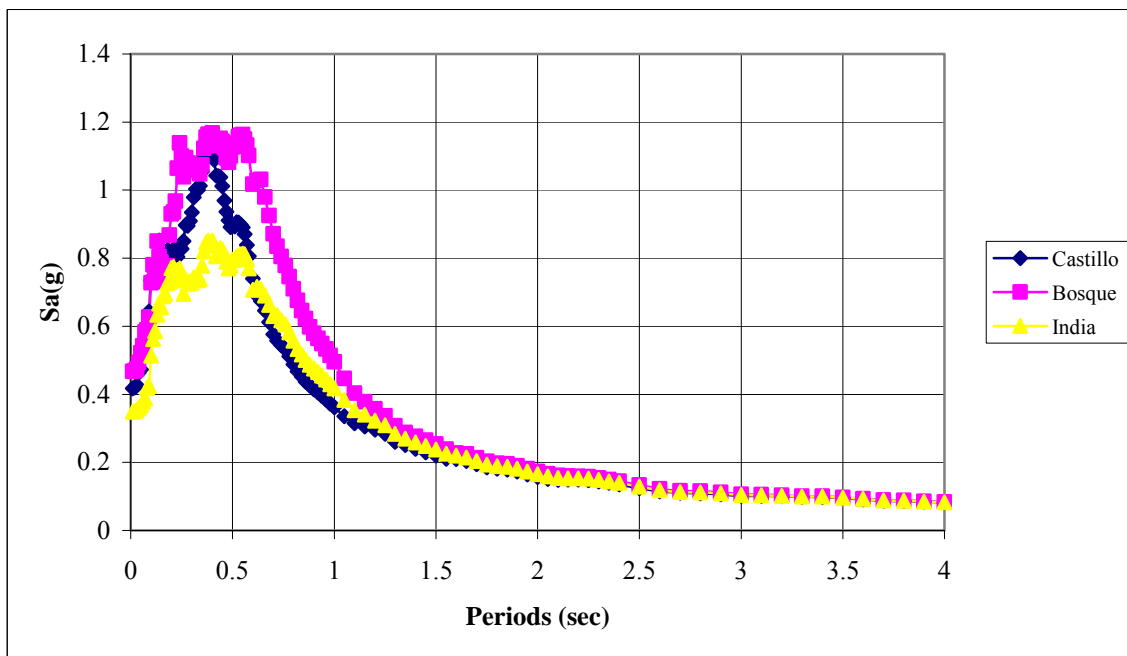


Figure 6.3: Average ground response spectra for the artificial ground motions for the sites in group C and 5% damping ratio.

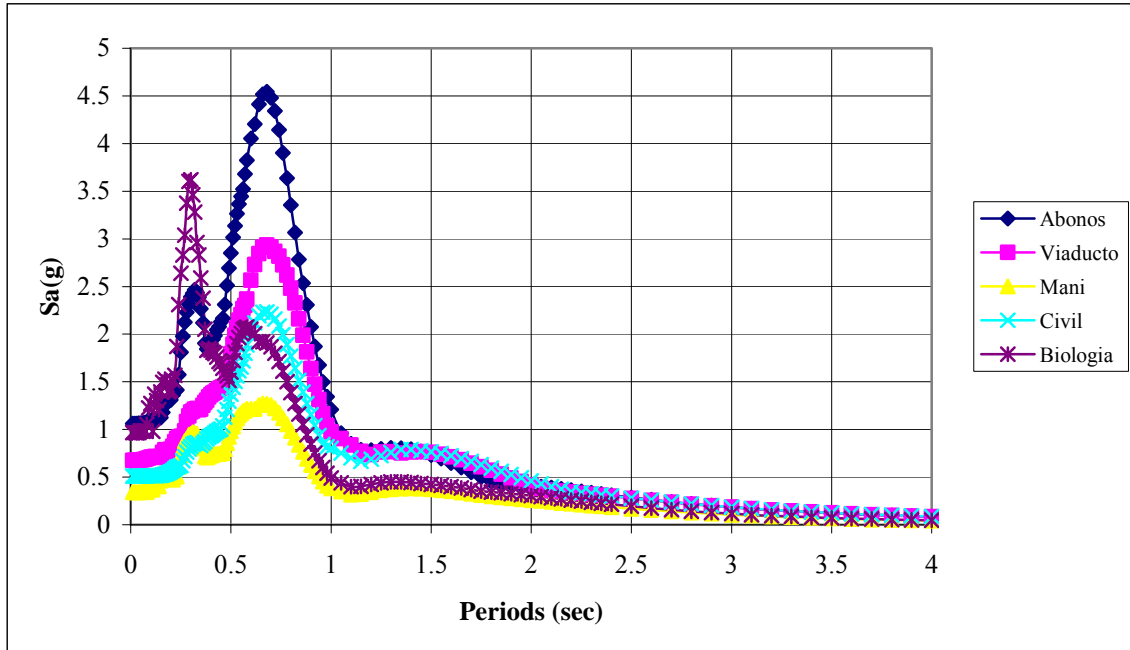


Figure 6.4: Ground response spectra for the El Salvador earthquake record for the sites in group A and 5% damping ratio.

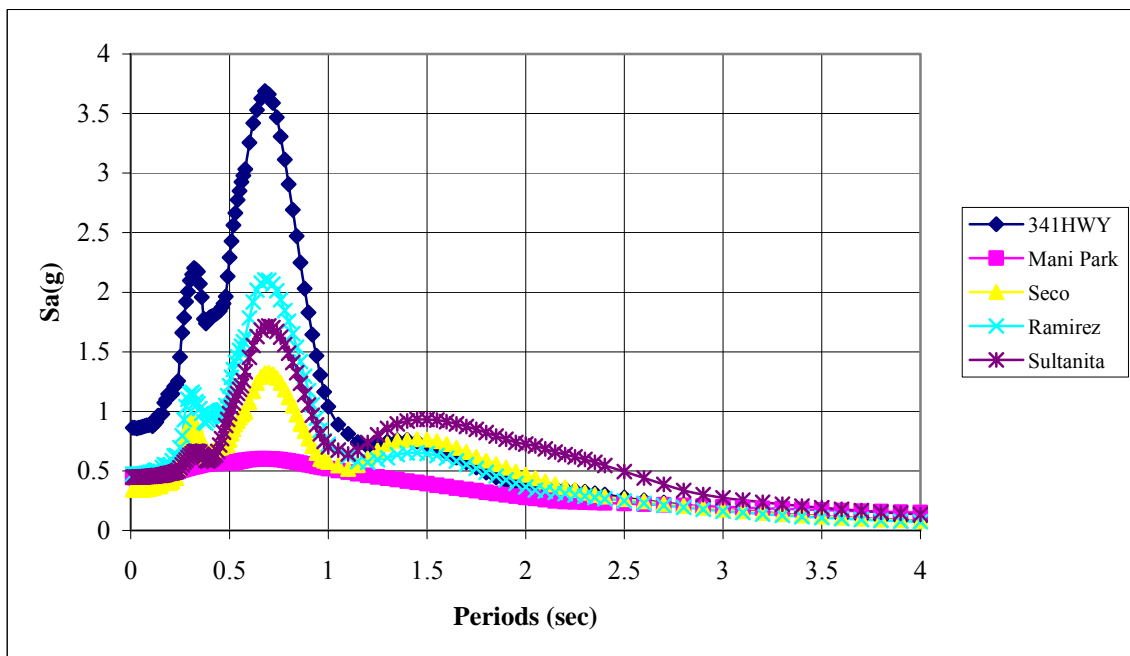


Figure 6.5: Ground response spectra for the El Salvador earthquake record for the sites in group B and 5% damping ratio.

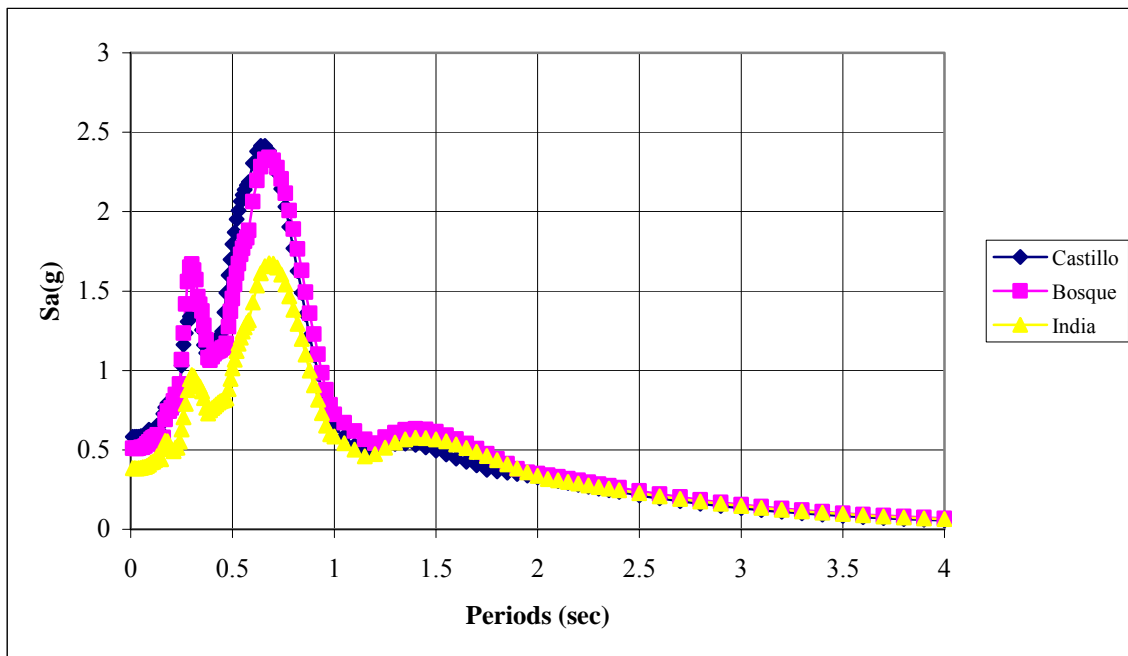


Figure 6.6: Ground response spectra for the El Salvador earthquake record for the sites in group C and 5% damping ratio.

Figure 6.7 shows the ground response spectra for the sites classified as soil profile type SC with the corresponding design response spectra prescribed in the UBC-97 for seismic zone 3. Figures 6.8 and 6.9 display the same for the sites classified as soil profile types SD and SE, respectively. One can observe from the figures that the design response spectra prescribed in the UBC 97 are in the average of the spectra obtained in this project for most of the cases. More attention shall be given to the sites classified as soil profile type SD where spectral accelerations for the Abonos, 341HWY, Viaducto, and El Bosque sites resulted in higher values. A same set of figures are shown in Figures 6.10 to 6.12 for the soil profile types SC, SD, and SE, respectively. The resulting ground response spectra are compared in this time with the corresponding design response spectra prescribed in the UBC 97 for seismic zone 4.

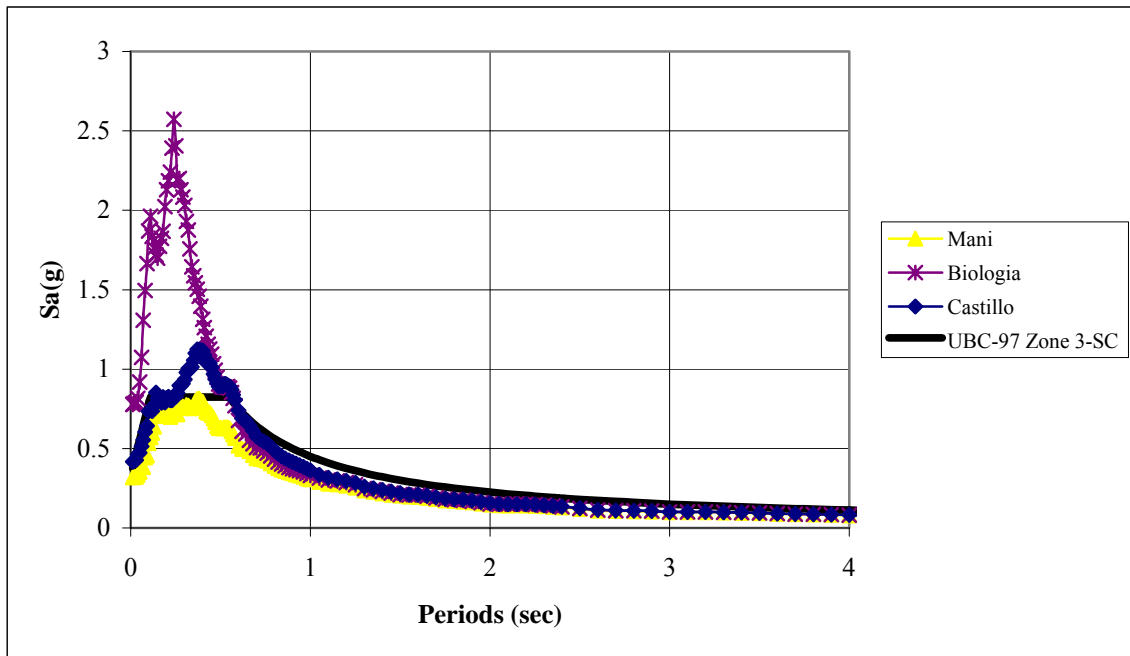


Figure 6.7: Average ground response spectra for the sites classified as soil profile type S_C and the UBC design response spectrum for seismic zone 3.

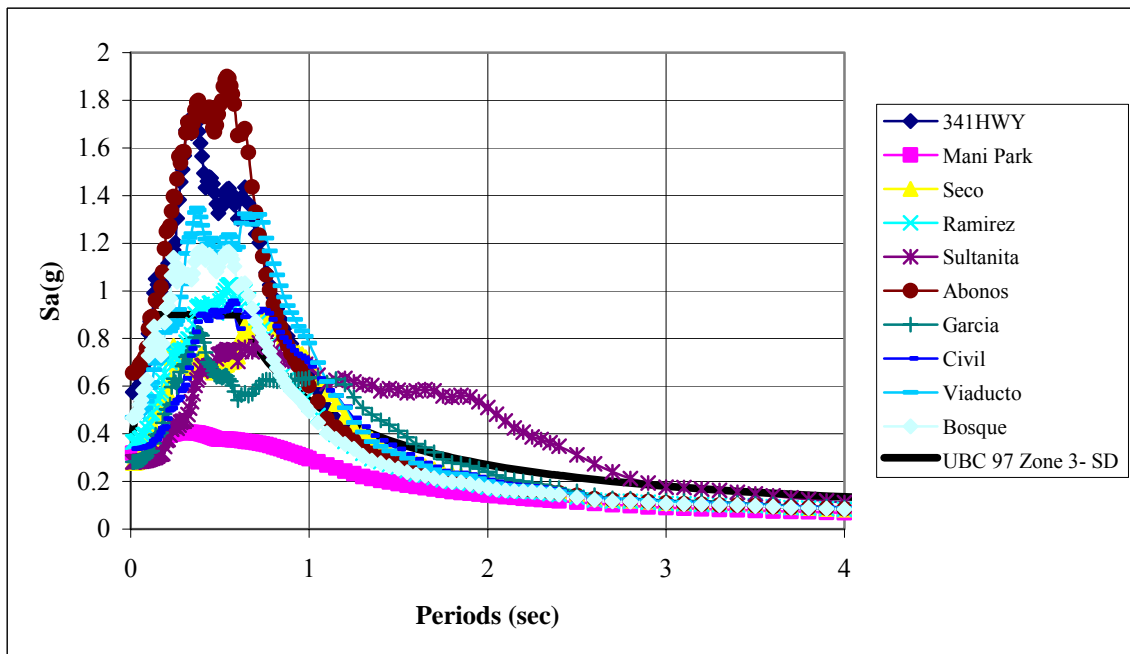


Figure 6.8: Average ground response spectra for the sites classified as soil profile type S_D and the UBC design response spectrum for seismic zone 3.

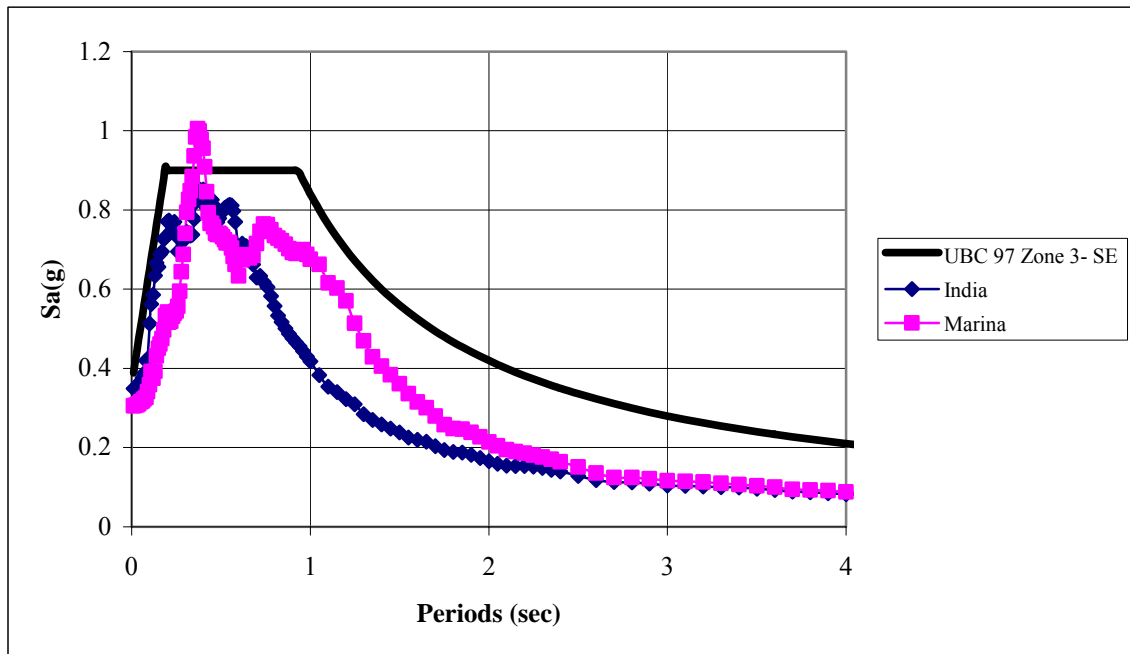


Figure 6.9: Average ground response spectra for the site classified as soil profile type S_E and the UBC design response spectrum for seismic zone 3.

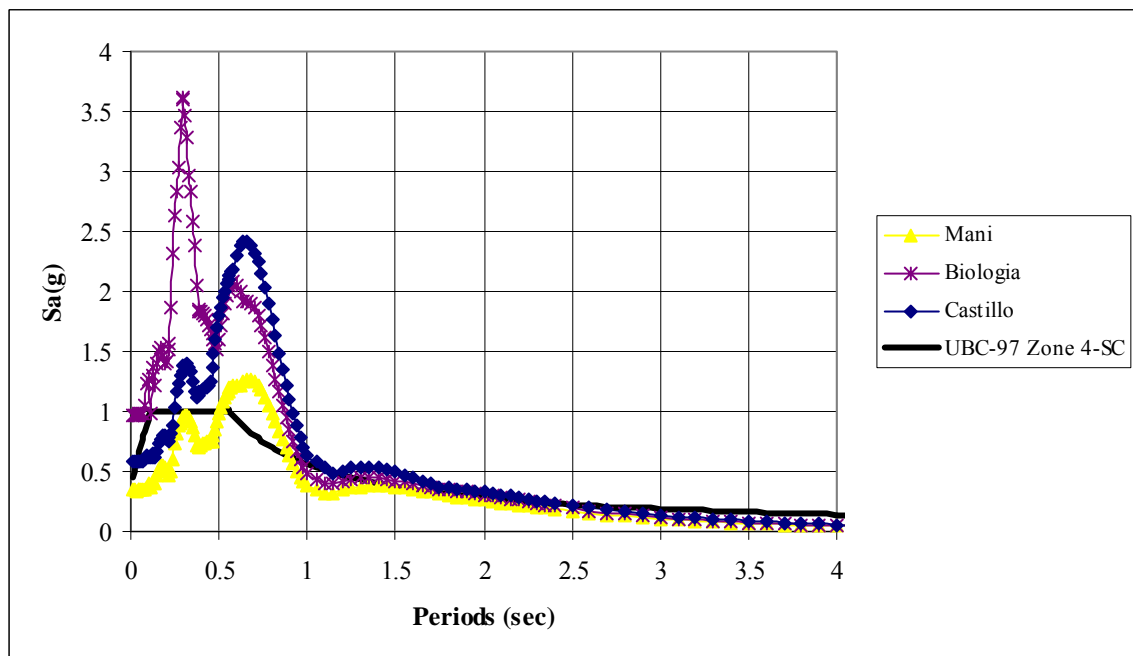


Figure 6.10: Average ground response spectra for the sites classified as soil profile type S_C and the UBC design response spectrum for seismic zone 4.

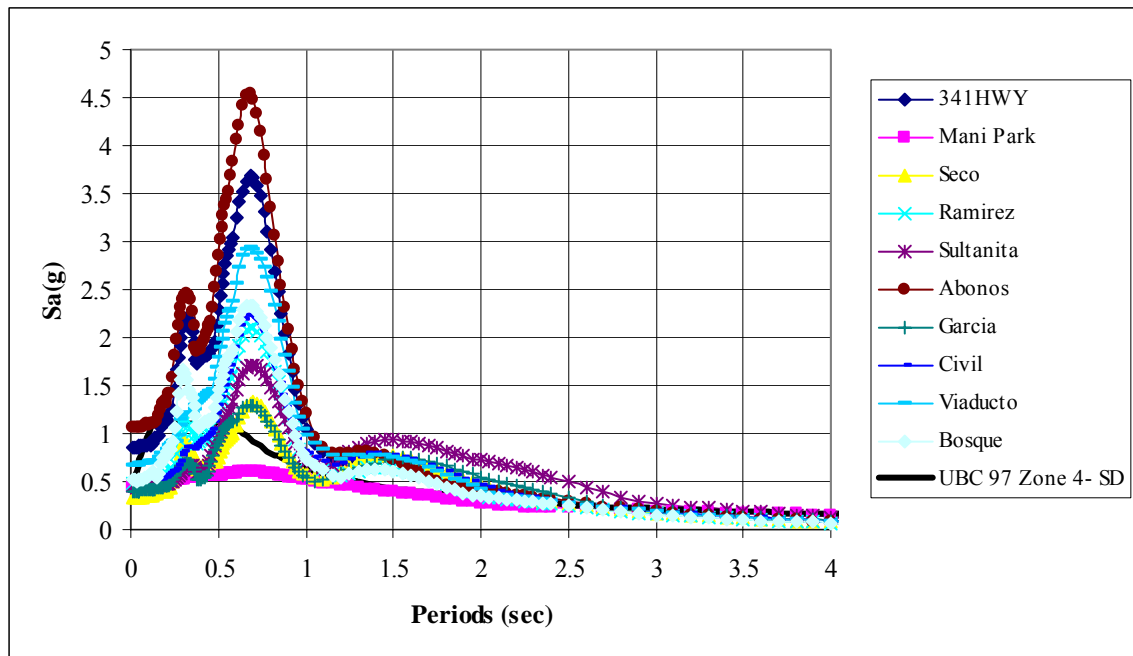


Figure 6.11: Average ground response spectra for the sites classified as soil profile type S_D and the UBC design response spectrum for seismic zone 4.

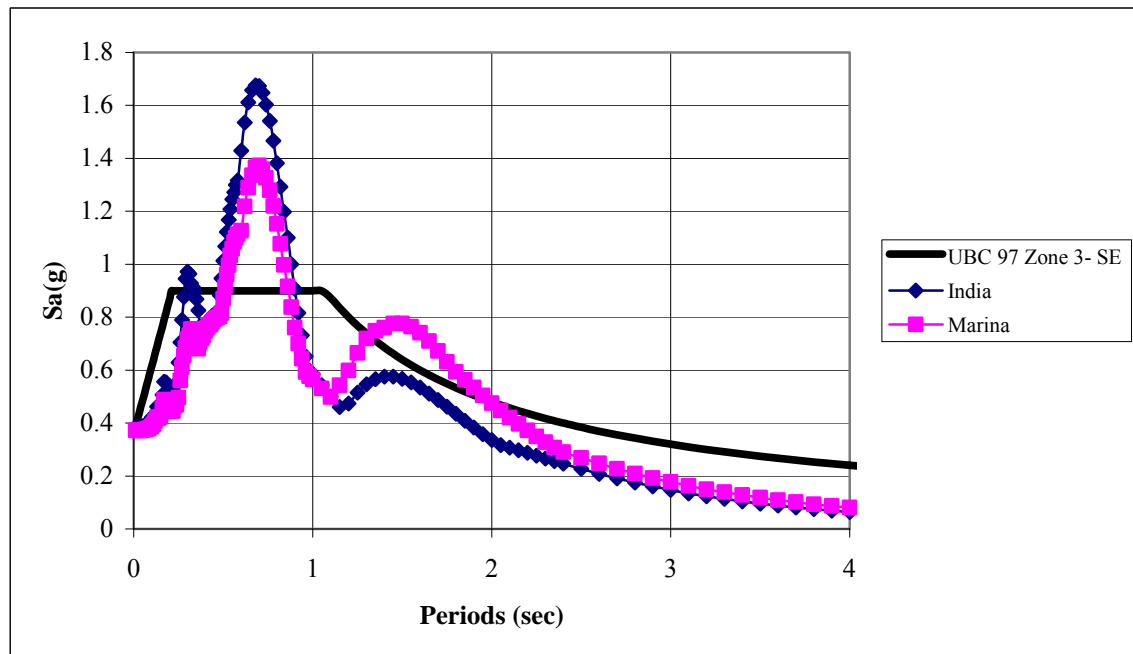


Figure 6.12: Average ground response spectra for the site classified as soil profile type S_E and the UBC design response spectrum for seismic zone 4.

6.4 Suggestions for Future Works

One should bear in mind that the results obtained in this research project have restraints due to the limitations and assumptions of each of the methods used. Also, the background information of the sites, as well as the physical resources available to perform the investigation has its own limitations. Because of this, several issues that need to be addressed in future studies, either to improve the results or to extend their scopes, are presented in this section.

One limitation of the SASW field tests was the source of excitation used for the test. It is useful to investigate new impact sources to expedite the tests, especially when many sites need to be tested in a short time. The use of explosive shot-guns could be an alternative to look for if it is not needed to reach deep below the surface. Also to reach the bottom layers in deep soils deposits, the source needs to generate low frequency waves with enough energy. Moreover, sources that are appropriate to be used in terrains with difficult topography are needed.

For the ground response analyses, the major assumption was the location of bedrock in many sites. It is recommended to conduct a research program to locate the bedrock in the Mayagüez area. Also, the soil materials were identified from geotechnical explorations done near the sites. Because in Puerto Rico in general the soil properties can change in short distances, it is recommended to drill geotechnical boring logs to identify better the soil material in the sites studied. Laboratory tests can be performed on these soil samples to obtain their dynamic properties like the damping ratio and shear modulus degradation curves. Another area of research recommended for future projects is the evaluation of existing methods or the development of new ones if necessary, for the in-situ determination of soil damping.

REFERENCES

- Borja, R. I., Chao, H. Y., Montáns, F.J., and Lin C.H. (1999). "Nonlinear Ground Response At Lotung LSST Site", *Journal of Geotechnical and Geoenvironmental Engineering*, ASCE, Vol. 125 No. 3, pp. 187-197.
- Brown, L.T., Diehl, J.G., and Nigbor, R.L. (2000). "A Simplify Method to Measure Average Shear-Wave Velocity in the Top 30 M (V_{s30})", *Proceedings of the Sixth International Conference in Seismic Zonation, Managing Earthquake Risk for the 21st Century*, Palm Springs, November 12-15. Earthquake Engineering Research Institute, Oakland Ca.
- Dames and Moore (1999). "Probabilistic Seismic Hazard Analysis of Puerto Rico and Recommended Revisions to the Seismic Coefficients of the ANSI/ASCE 7-95 Standard." Puerto Rico Earthquake Commission, 47 pp.
- Imai, T. and Yoshimura, Y. (1970). "Elastic Wave Velocity and Dynamics Characteristics of the Soft Ground". *Soils and Foundation*, Vol. 18, No. 1, pp. 17-22.
- Imai, T. and Tonouchi, K. (1982). "Correlation of N Values with S-wave Velocity". *Proc. of 2nd European Symposium on Penetration Testing*, pp. 67-72.
- Joh, S. H. (1996). "Advances in the Data Interpretation Technique for Spectral Analysis of Surface Waves (SASW) Measurements." Ph. D. Dissertation, The University of Texas at Austin, Austin, Texas, 240 pp.
- Kramer, S. L. (1996). *Geotechnical Earthquake Engineering*, Prentice Hall, Upper Saddle River, New Jersey.
- Llavona, A. (2004). "Clasificación de Suelos (UBC-97) del Municipio de Mayagüez", Master of Science thesis, University of Puerto Rico, Mayagüez Campus, Mayagüez.
- Macari, E. J. (1994). "A Field Study in Support of the Assessment for Liquefaction and Soil Amplification in Western Puerto Rico". Presented to the Puerto Rico Earthquake Safety Commission, Georgia Institute of Technology, Atlanta, Georgia.
- Martínez, J. A., Irizarry, J., and Portela, G. (2001). "Espectros de diseño para las ciudades principales de Puerto Rico basado en registros de aceleracion mundiales", *Revista de Desastres Naturales, Accidentes e Infraestructura Civil*, UPR-Mayaguez, Vol. 1 No. 1, pp. 21-31.
- Military Handbook (MIL HDBK) 1007_3 (1997). *Soil Dynamics and Special Design Aspects*, Naval Facility Engineering Command, Washington, DC.
- Montejo, L. A. (2004). "Generation and Analysis of Spectrum-Compatible Earthquakes Time-Histories using Wavelet", Master of Science thesis, University of Puerto Rico, Mayagüez Campus, Mayagüez, 203 pp.
- Muract, J. (2004). "El Método de Análisis Espectral de Ondas Superficiales y su Automatización Mediante Redes Neuronales", Master of Science thesis, University of Puerto Rico, Mayagüez Campus, Mayagüez, Mayagüez, 145 pp.
- Nazarian, S., (1984). "In Situ Determination of Elastic Moduli of Soil Deposits and Pavement System by Spectral-Analysis-of-Surface-Wave Method," Ph. D. Dissertation, The University of Texas at Austin, Austin, Texas, 458 pp.

Nazarian, S. and Desai, M. R. (1993). "Automated Surface Wave Method: Inversion Technique," *Journal of Geotechnical Engineering*, ASCE, Vol. 119, No. 7, pp. 1112-1126.

Ordóñez G.A. (2003). SHAKE2000: A computer Program for the 1-D Analysis of Geotechnical Earthquake Engineering Problem.

Reid, H.F., Taber, S., (1919). "The Porto Rico Earthquakes of October-November, 1918," *The Bulletin of the Seismological Society of America*, Vol. 9, No. 4, pp. 94-127.

Richart, F. E., Jr., Hall, J. R. Jr., and Woods, R. D. (1970), *Vibrations of Soil and Foundations*, Prentice Hall, Englewood Cliffs, New Jersey.

Rix, G. J., Lai, C. G., and Spang, A. W. Jr., (2000). "In Situ Measurement of Damping Ratio Using Surface Waves," *Journal of Geotechnical and Geoenvironmental Engineering*, ASCE, Vol. 126, No. 5, pp. 472-480.

Seed, H. B., Idriss, I. M. (1970). "Soil Moduli and Damping Factors for Dynamic Response Analyses." *Earthquake Engineering Research Center, Report No. EERC 70-10*, University of California, Berkeley, California.

Seed, H. B. and Idriss, I. M. (1971). "Simplified Procedure for Evaluating Soil Liquefaction Potential." *Journal of Geotechnical Engineering Division.*, ASCE, 97(9), 1249-1273.

Seed, H. B. and Sun, J. H. (1989). "Implication of Site Effects in the Mexico City Earthquake of September 19, 1985 for Earthquake-Resistance-Design Criteria in the San Francisco Bay Area of California." *Report No. UCB/EERC-89/03*, University of California, Berkeley, California.

Stokoe, K. H., Rix, G. J., and Nazarian, S. (1989). "In Situ Testing with Surface Waves," *Proceedings of the 12th International Conference on Soil Mechanics and Foundation Engineering*, Rio de Janeiro, Brazil, pp. 331-334.

Shnabel, P. B. (1973). "Effects of Local Geology and Distance from Source on Earthquake Ground Motions". Ph.D. Thesis, University of California, Berkeley, California.

Stokoe, K. H., Wright, S. G., Bay, J. A., and Roesset, J. M. (1994). "Characterization of Geotechnical Sites by SASW Method," *Technical Report: Geophysical Characterization of Sites*, Volume prepared by ISSMFE Technical Committee #10 for the XIII ICSSMFE (International Conference on Soil Mechanics and Foundation Engineering), New Delhi, India, International Science Publisher, New York, NY, pp. 15-25.

USACE (1995) "Geophysical Exploration for Engineering and Environmental Investigation". *Engineering Manual EM 1110-1-1802*, Washington, DC.

Youd, T. L., Idriss, I. M., Andrus, R. D. (2001). "Liquefaction Resistance of Soils: Summary Report from the 1996 NCEER and 1998 NCEER/NSF Workshops on Evaluation of Liquefaction Resistance of Soils", *Journal of Geotechnical and Geoenvironmental Engineering*, ASCE, Vol. 127, No. 10, pp. 817-833.

Zomorodian, A., (1995). "Shear Wave Velocity of Soil by the Spectral Analysis of Surface Waves (SASW) Method", Ph. D. Dissertation, The University of Ottawa, Ottawa, Ontario, 252 pp.

APPENDIX A

EXPERIMENTAL VERSUS THEORETICAL DISPERSION CURVES FROM SASW TESTS IN MAYAGÜEZ

This appendix presents the experimental versus the theoretical dispersion curves obtained from the SASW tests in Mayagüez. The matching process was performed by inverse modeling with the Matlab code written by Muract (2004). This procedure uses the neural network technique in combination with the down-hill simplex method to optimize the matching of the two curves. The shear wave velocity profiles for each site were presented in Chapter 3. The sites tested in Mayagüez are: (1) Abonos, (2) 341HWY, (3) Maní, (4) Maní Park, (5) Seco Park, (6) Isidoro García, (7) Ramírez de Arellano, (8) Sultanita, and (9) Civil.

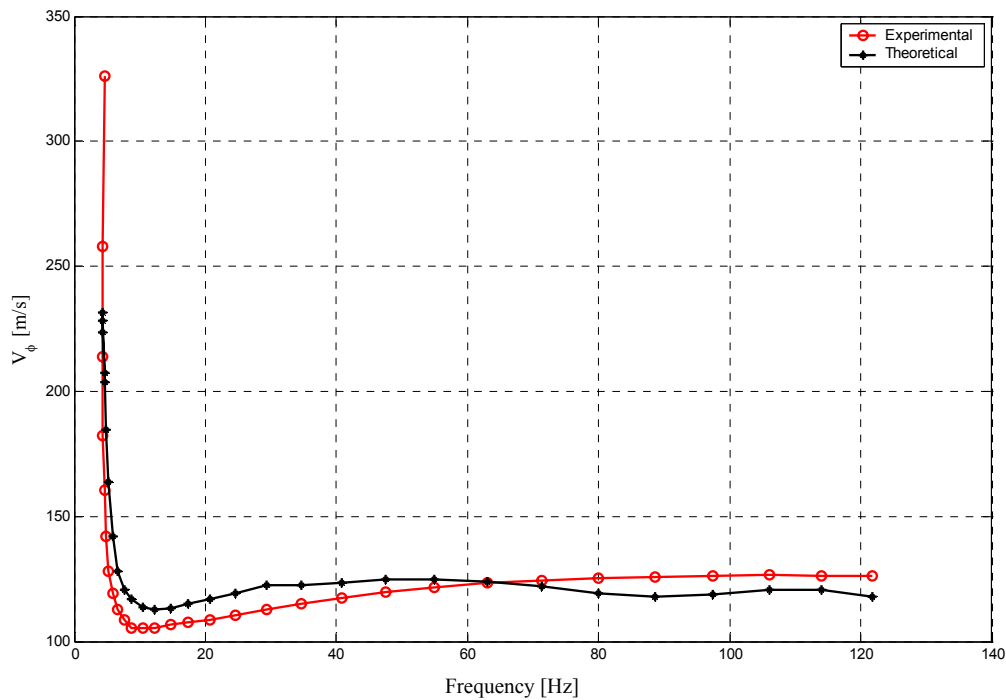


Figure A.1: Experimental versus theoretical dispersion curves for the Abonos site.

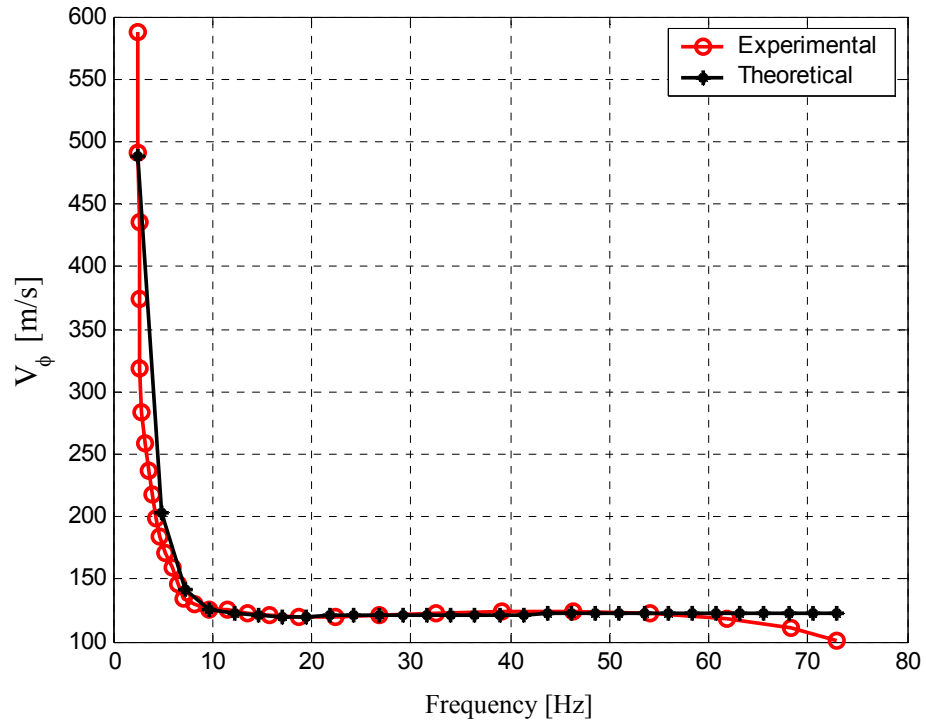


Figure A.2: Experimental versus theoretical dispersion curves for the 341HWY site.

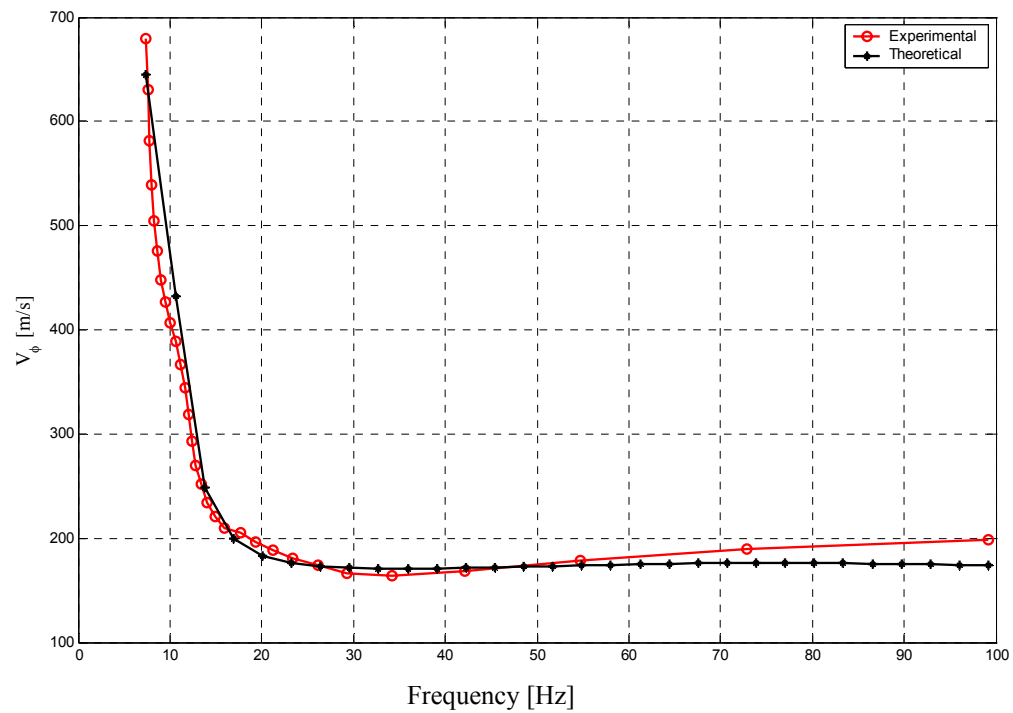


Figure A.3: Experimental versus theoretical dispersion curves for the Maní site.

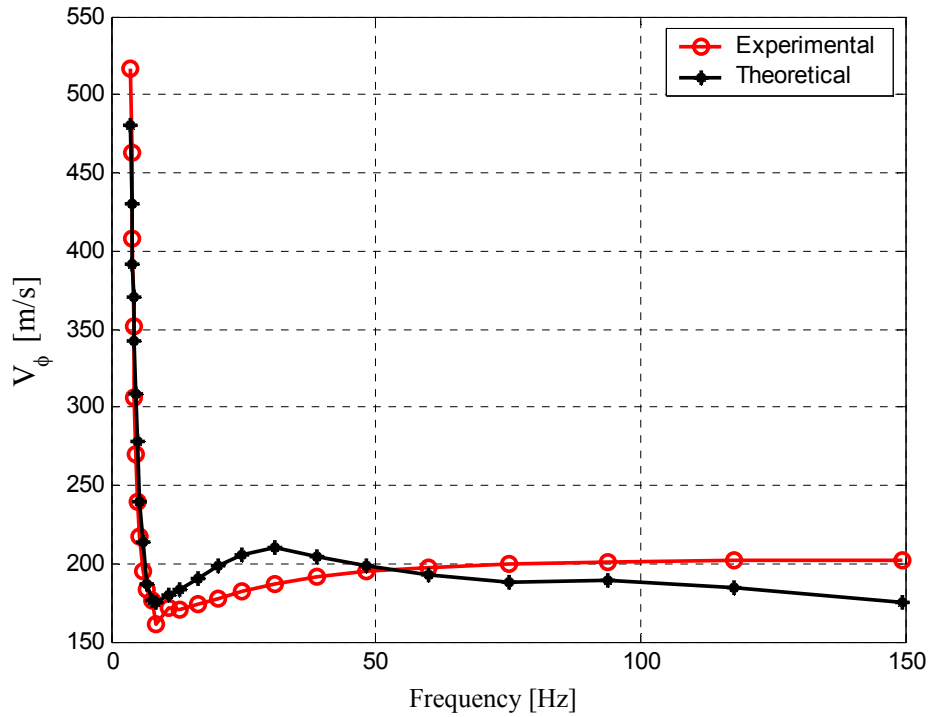


Figure A.4: Experimental versus theoretical dispersion curves for the the Maní Park site.

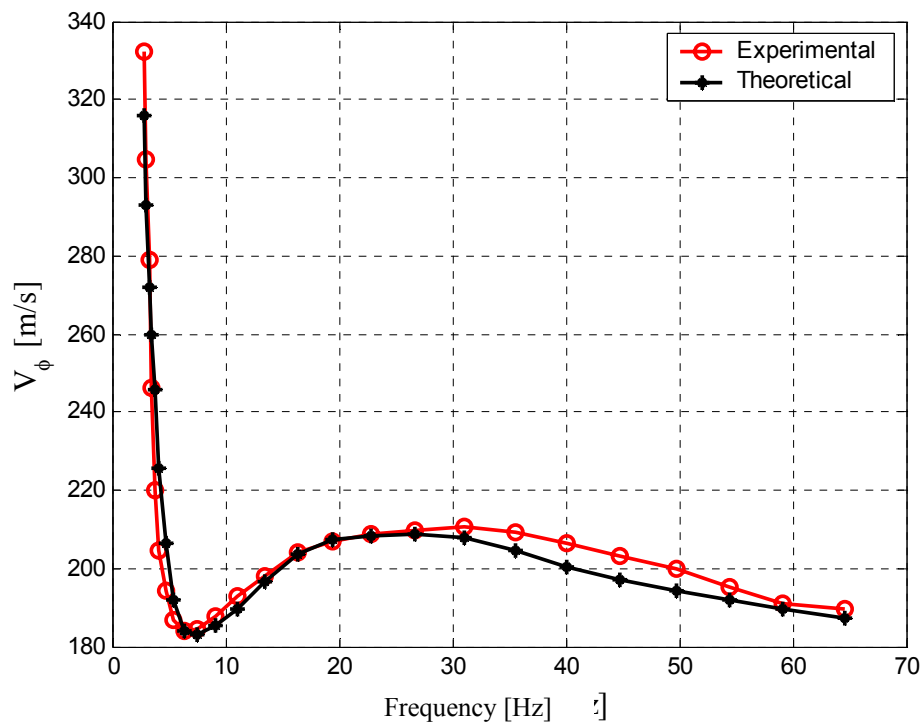


Figure A.5: Experimental versus theoretical dispersion curves for the Seco Park site.

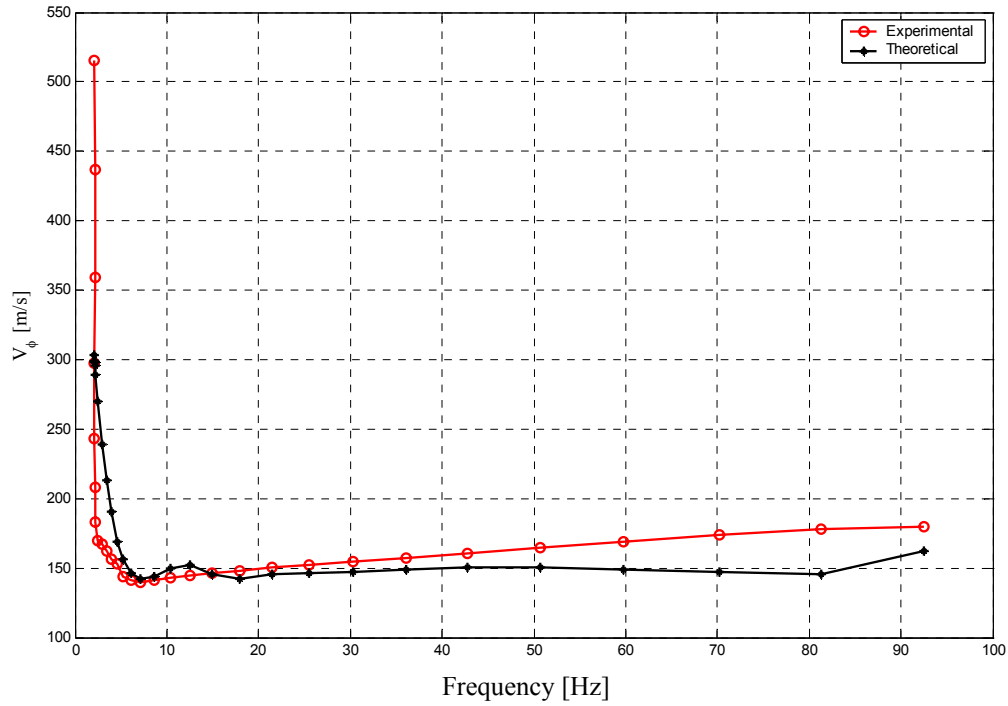


Figure A.6: Experimental versus theoretical dispersion curves for the Isidoro García site.

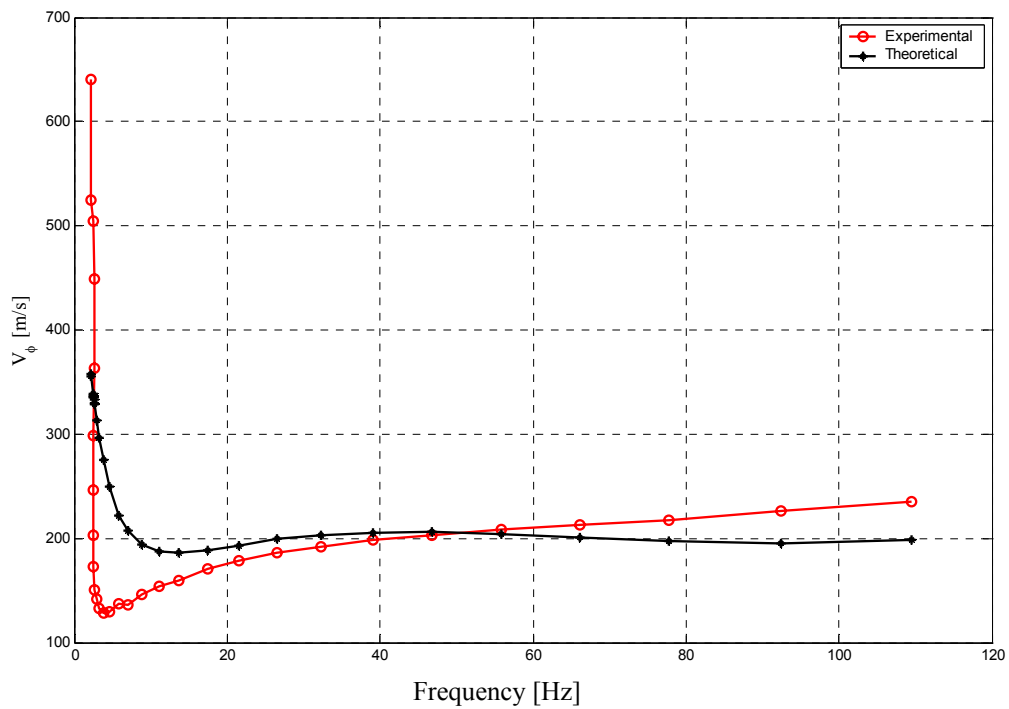


Figure A.7: Experimental versus theoretical dispersion curves for the Ramírez de Arellano site.

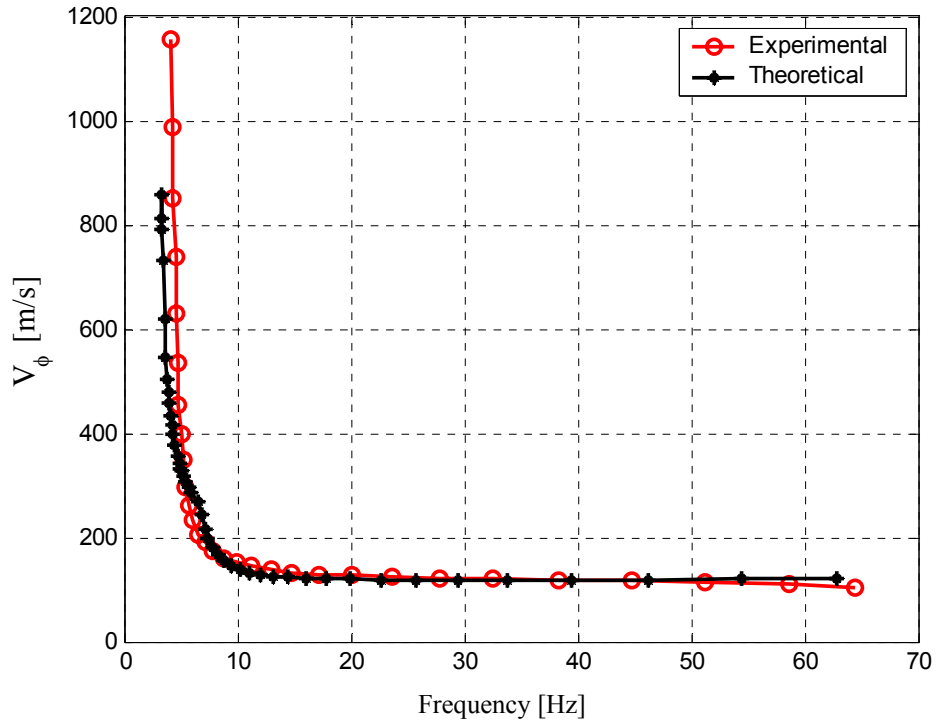


Figure A.8: Experimental versus theoretical dispersion curves for the Sultanita site.

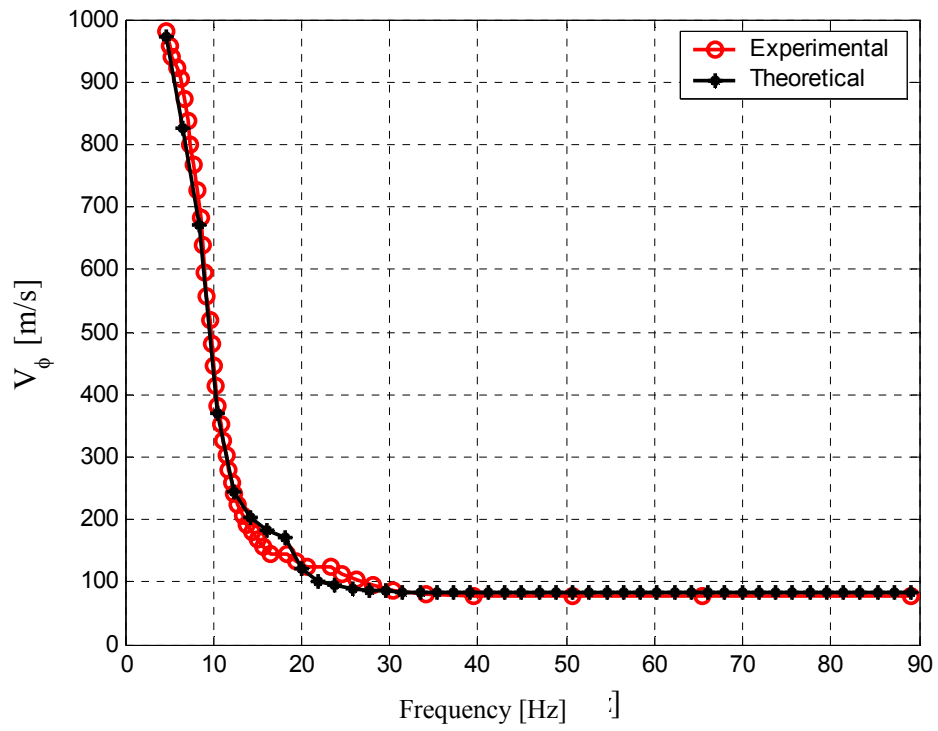


Figure A.9: Experimental versus theoretical dispersion curves for the Civil site.

APPENDIX B

DETAILED RESULTS OF ONE-DIMENSIONAL GROUND RESPONSE ANALYSES FROM THE ARTIFICIAL GROUND MOTIONS

The results of the one dimensional ground response analyses performed with the computer program SHAKE2000 were presented in Chapter 5 for the fourteen sites studied in this thesis. The four artificial ground motions developed for the analyses were compatible with the UBC-97 design response spectrum for seismic zone 3 in rock. The results presented in Chapter 5 are the average values of those obtained with the four ground motion records. As shown in this appendix, there were no significant differences on the results among the four ground motions. The following tables show the fundamental site periods and peak acceleration at the surface for each artificial ground motion at all sites.

Table B.1: Artificial ground motions results for Group A.

Site ID	Ground Motion ID	Period Linear (sec)	Period Non Linear (sec)	Acceleration Linear (g)	Acceleration Non Linear (g)
Abonos	1	0.51	0.59	0.92	0.66
	2	0.51	0.60	0.93	0.65
	3	0.51	0.59	0.98	0.71
	4	0.51	0.60	0.88	0.60
Maní	1	0.38	0.62	0.41	0.29
	2	0.38	0.64	0.46	0.28
	3	0.38	0.62	0.52	0.39
	4	0.38	0.63	0.43	0.32
Biología	1	0.17	0.22	0.82	0.80
	2	0.17	0.22	1.09	0.70
	3	0.17	0.22	1.07	0.85
	4	0.17	0.21	0.81	0.76
Viaducto	1	0.5	0.77	0.92	0.45
	2	0.5	0.74	0.80	0.49
	3	0.5	0.72	0.88	0.42
	4	0.5	0.74	0.80	0.51
Civil	1	0.54	0.75	0.86	0.34
	2	0.54	0.77	0.90	0.32
	3	0.54	0.72	0.98	0.32
	4	0.54	0.78	0.82	0.36

Note: All accelerations in this table are reported at the surface of the soil deposit.

Table B.2: Artificial ground motions results for Group B.

Site ID	Ground Motion ID	Period Linear (sec)	Period Non Linear (sec)	Acceleration Linear (g)	Acceleration Non Linear (g)
341HWY	1	0.62	0.73	0.70	0.57
	2	0.62	0.73	0.72	0.58
	3	0.62	0.72	0.76	0.62
	4	0.62	0.72	0.73	0.53
Mani Park	1	0.31	0.40	0.80	0.29
	2	0.31	0.40	0.76	0.28
	3	0.31	0.38	0.87	0.32
	4	0.31	0.40	0.85	0.39
Seco Park	1	0.44	0.68	1.09	0.27
	2	0.44	0.68	1.26	0.29
	3	0.44	0.67	1.23	0.30
	4	0.44	0.70	1.20	0.32
Isidoro García	1	0.44	0.67	0.84	0.24
	2	0.44	0.67	0.71	0.27
	3	0.44	0.64	0.89	0.27
	4	0.44	0.67	0.74	0.33
Ramírez de Arellano	1	0.36	0.52	0.54	0.37
	2	0.36	0.54	0.50	0.37
	3	0.36	0.51	0.66	0.34
	4	0.36	0.51	0.49	0.37
Sultanita	1	0.78	1.29	0.81	0.28
	2	0.78	1.39	0.91	0.28
	3	0.78	1.34	0.92	0.24
	4	0.78	1.34	0.89	0.32

Note: All accelerations in this table are reported at the surface of the soil deposit.

Table B.3: Artificial ground motions results for Group C.

Site ID	Ground Motion ID	Period Linear (sec)	Period Non Linear (sec)	Acceleration Linear (g)	Acceleration Non Linear (g)
El Bosque	1	0.47	0.63	0.63	0.49
	2	0.47	0.64	0.56	0.42
	3	0.47	0.62	0.69	0.48
	4	0.47	0.64	0.56	0.48
El Castillo	1	0.27	0.44	0.45	0.43
	2	0.27	0.45	0.44	0.38
	3	0.27	0.46	0.46	0.45
	4	0.27	0.46	0.38	0.41
India	1	0.39	0.59	0.43	0.34
	2	0.39	0.61	0.39	0.32
	3	0.39	0.58	0.49	0.38
	4	0.39	0.61	0.42	0.36
Marina	1	0.53	0.76	0.83	0.26
	2	0.53	0.77	0.82	0.31
	3	0.53	0.74	0.85	0.30
	4	0.53	0.77	0.81	0.35

Note: All accelerations in this table are reported at the surface of the soil deposit.

APPENDIX C

RESPONSE SPECTRA AT SURFACE IN MAYAGUEZ SITES FROM LINEAR ANALYSIS

This appendix contains the results from the linear ground response analysis. The ground response spectra at the surface obtained with the equivalent linear analyses were presented in Chapter 5. In the equivalent linear analysis the non-linear behavior of the soil is considered by using reduction curves for the damping ratio and shear modulus. In this thesis by the linear results it is meant those results obtained without considering the degradation of the soil material during the earthquake. In the computer program SHAKE2000 a linear analysis can be performed by specifying a constant damping and shear modulus reduction curve. These linear response is useful to help the interpretation of the results obtained with the equivalent linear analysis, for instance to follow the degradation of the soil deposit during the earthquake. The following figures show the ground response spectrum at the surface for each site. The response spectra from the artificial earthquakes were averaged as explained in Appendix B. The sites considered are those discussed in Chapter 5.

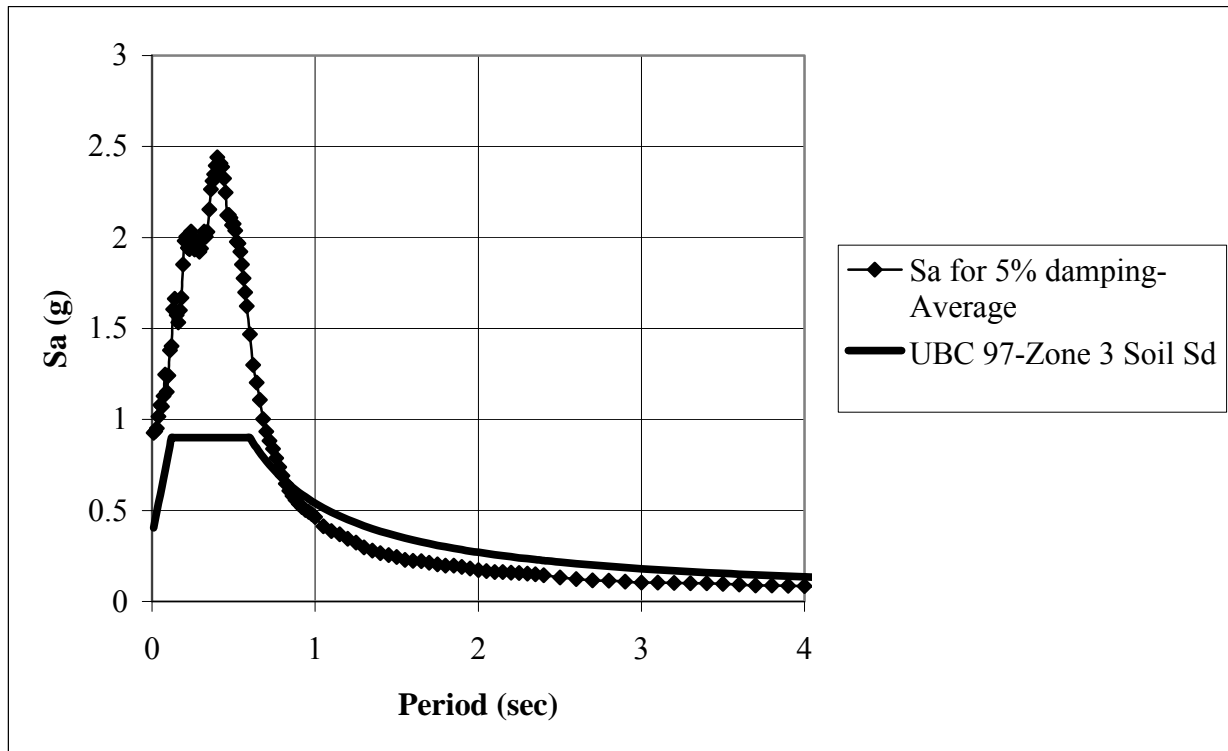


Figure C.1: Average ground response spectrum at surface from linear analysis for the Abonos Site and UBC 97 design spectrum.

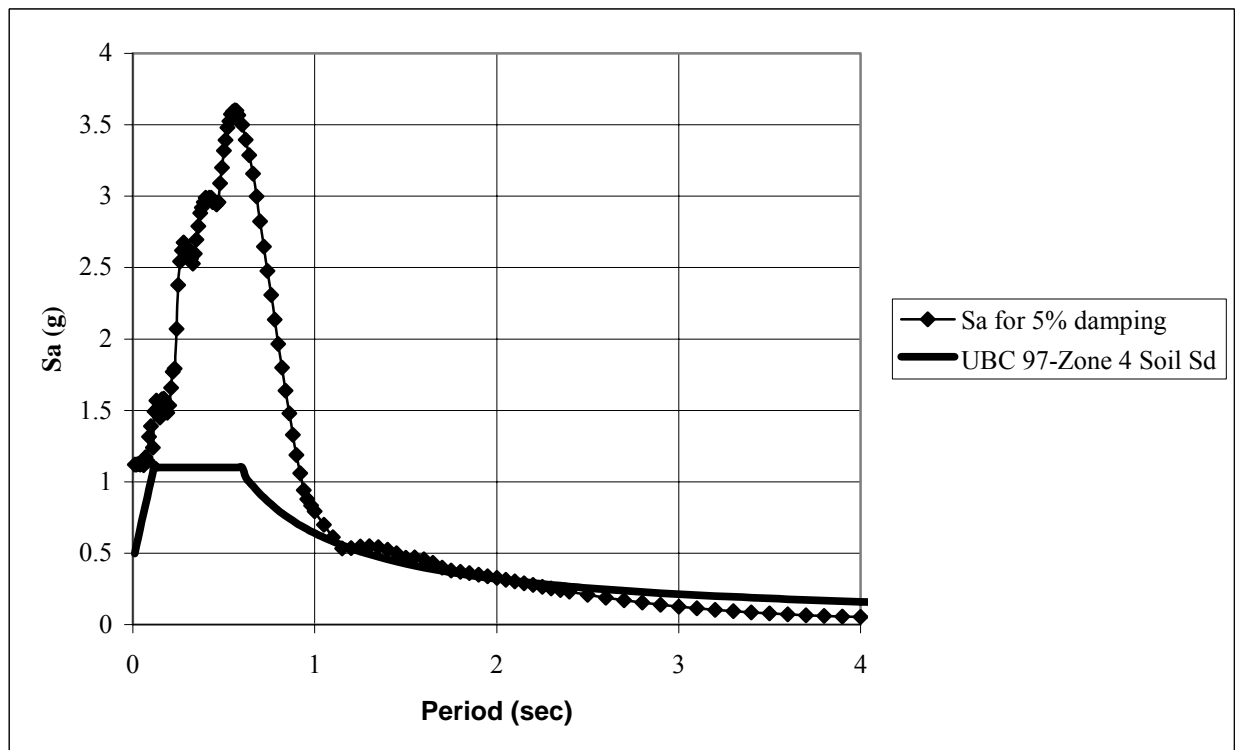


Figure C.2: Ground response spectrum at surface from linear analysis for the El Salvador earthquake for the Abonos site and UBC 97 design spectrum.

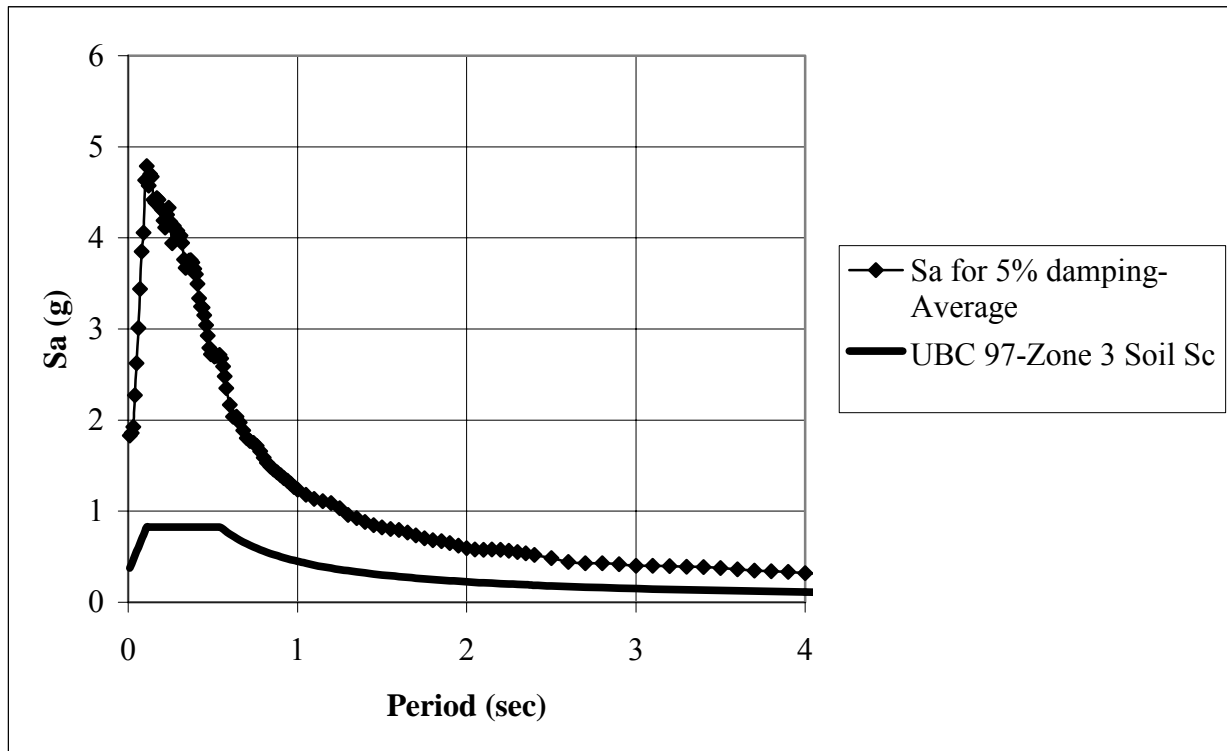


Figure C.3: Average ground response spectrum at surface from linear analysis for the Maní site and UBC 97 design spectrum.

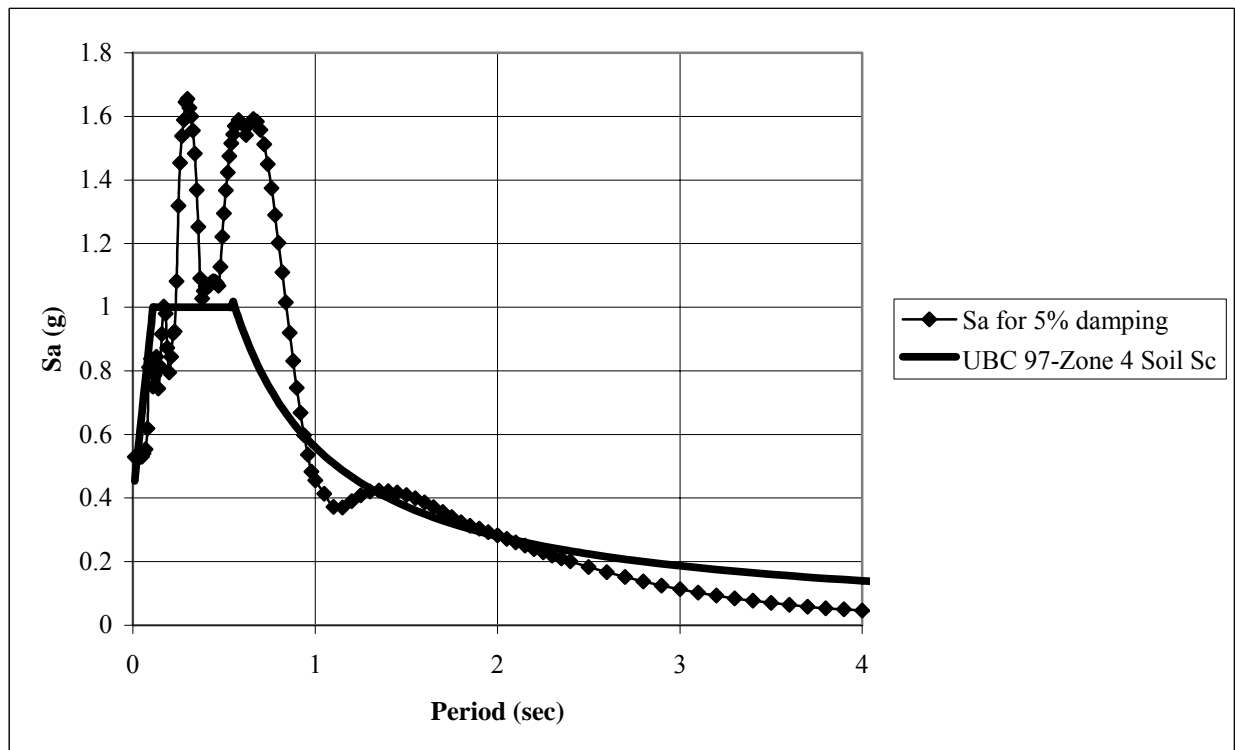


Figure C.4: Ground response spectrum at surface from linear analysis for the El Salvador earthquake for the Maní site and UBC 97 design spectrum.

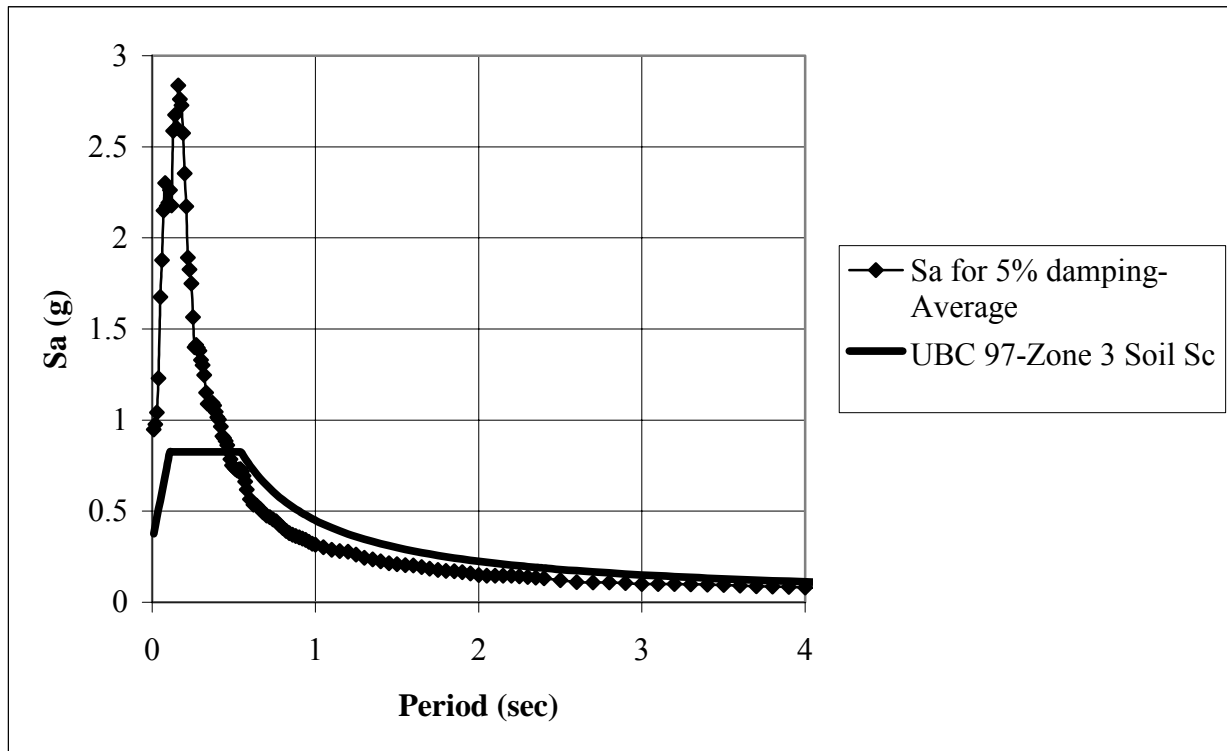


Figure C.5: Average ground response spectrum at surface from linear analysis for the Biología site and UBC 97 design spectrum.

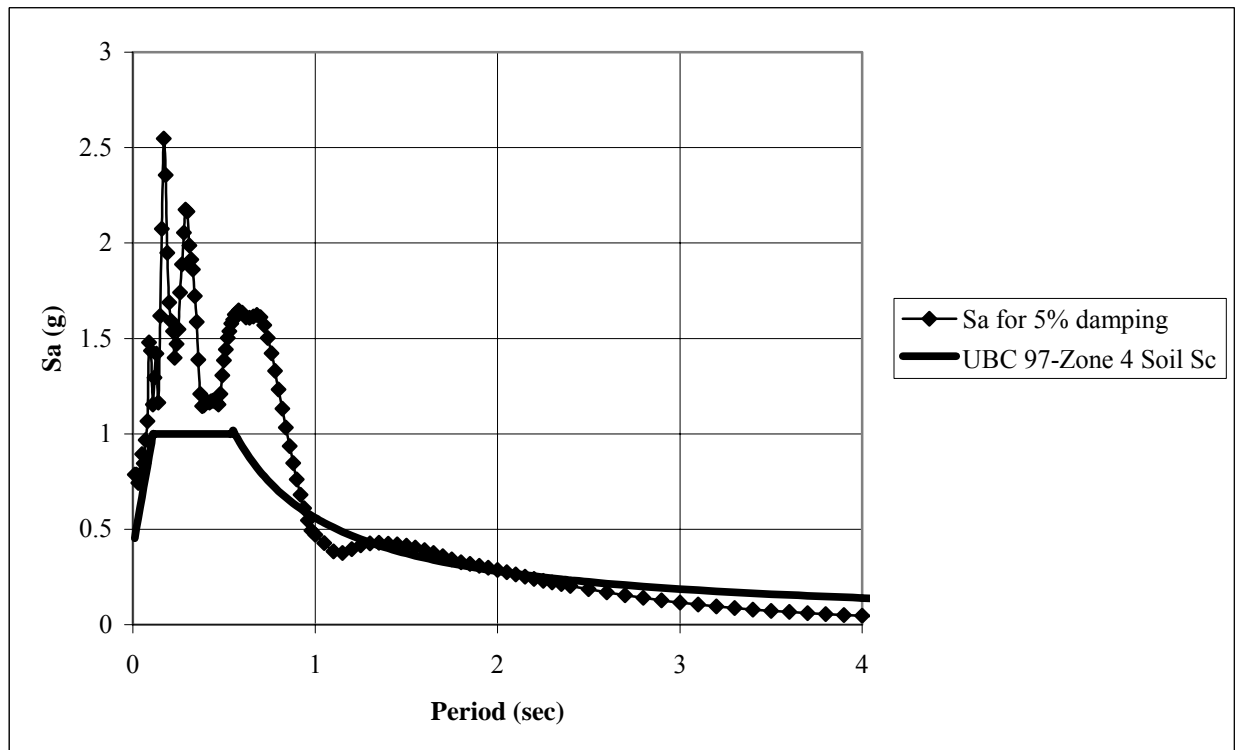


Figure C.6: Ground response spectrum at surface from linear analysis for the El Salvador earthquake for the Biología site and UBC 97 design spectrum.

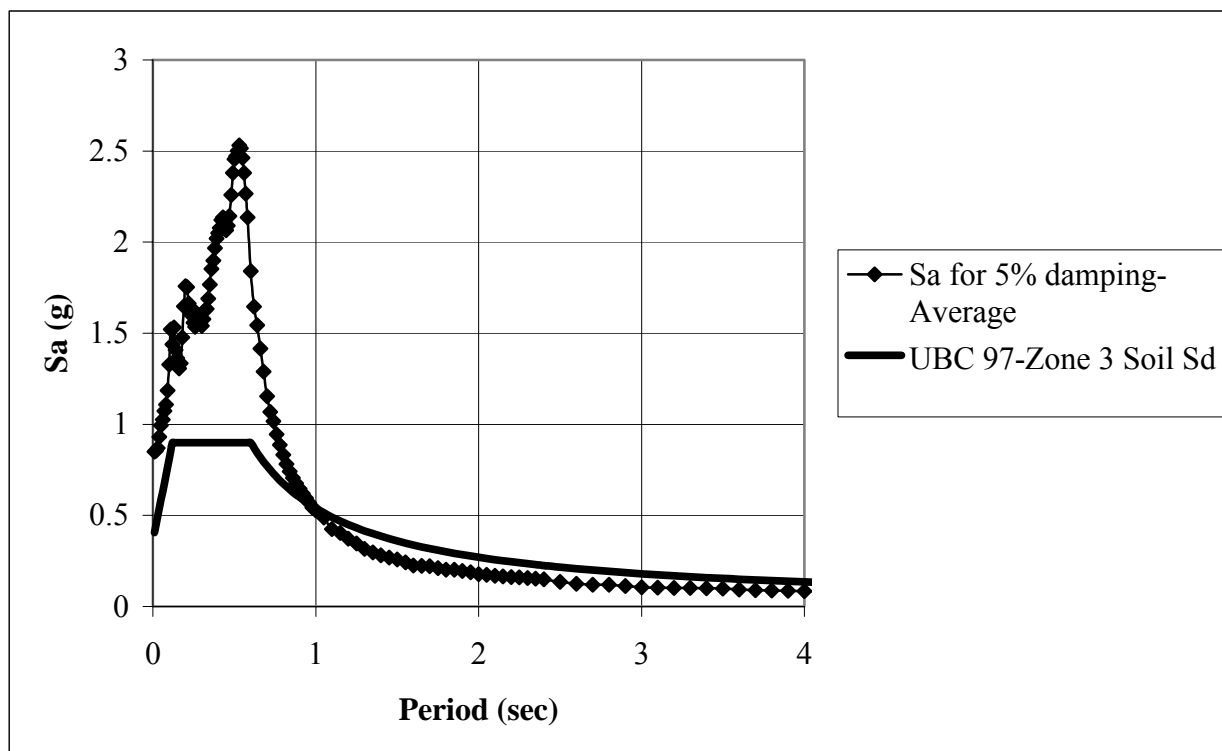


Figure C.7: Average ground response spectrum at surface from linear analysis for the Viaducto site and UBC 97 design spectrum.

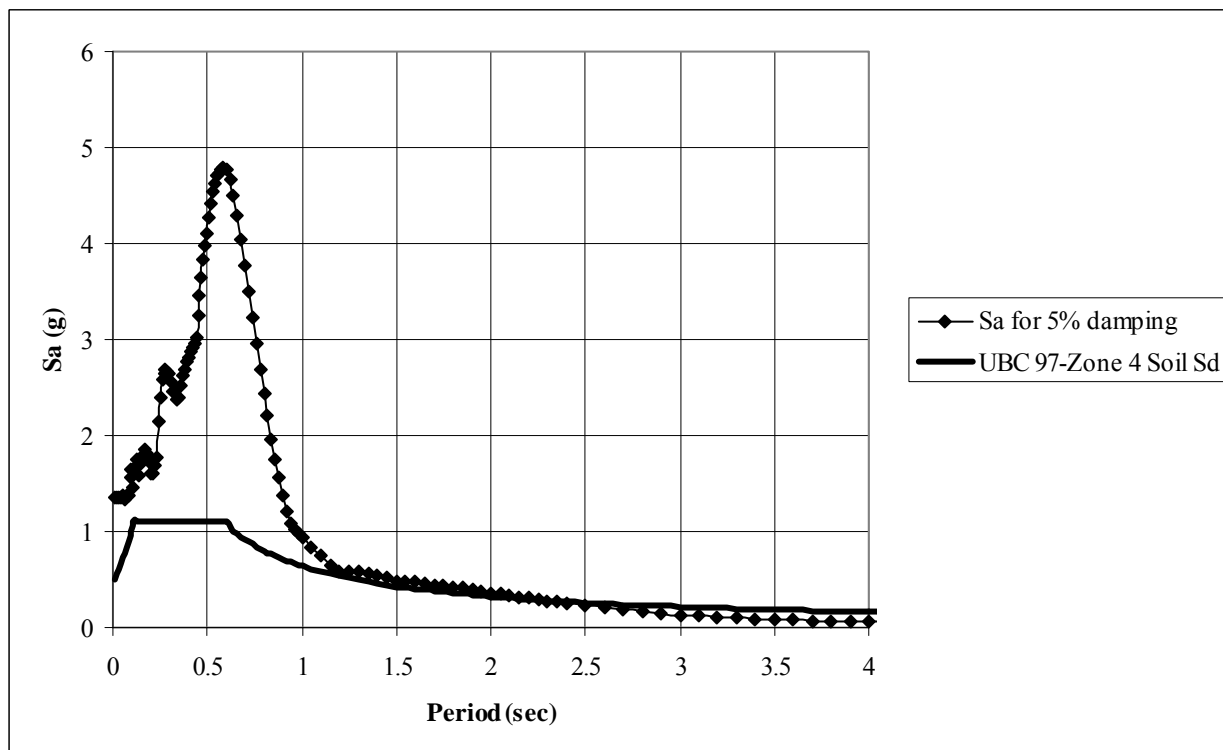


Figure C.8: Ground response spectrum at surface from linear analysis for the El Salvador earthquake for the Viaducto site and UBC 97 design spectrum.

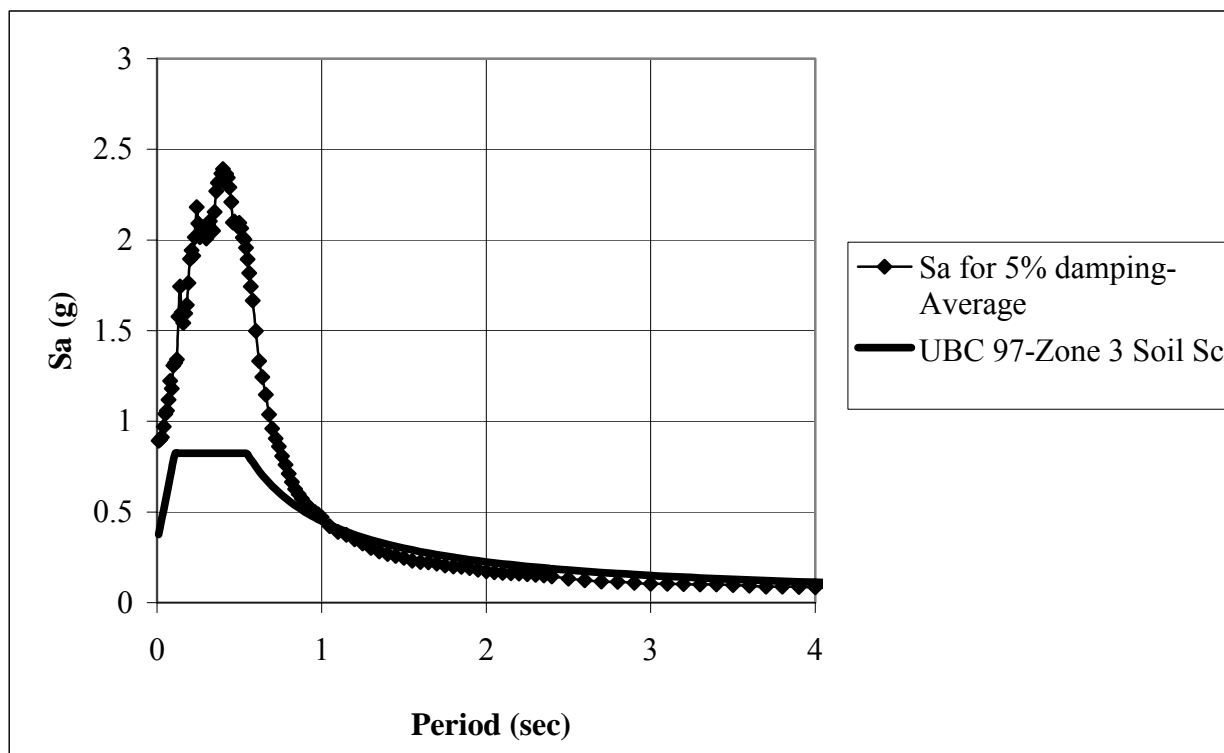


Figure C.9: Average ground response spectrum at surface from linear analysis for the Civil site and UBC 97 design spectrum.

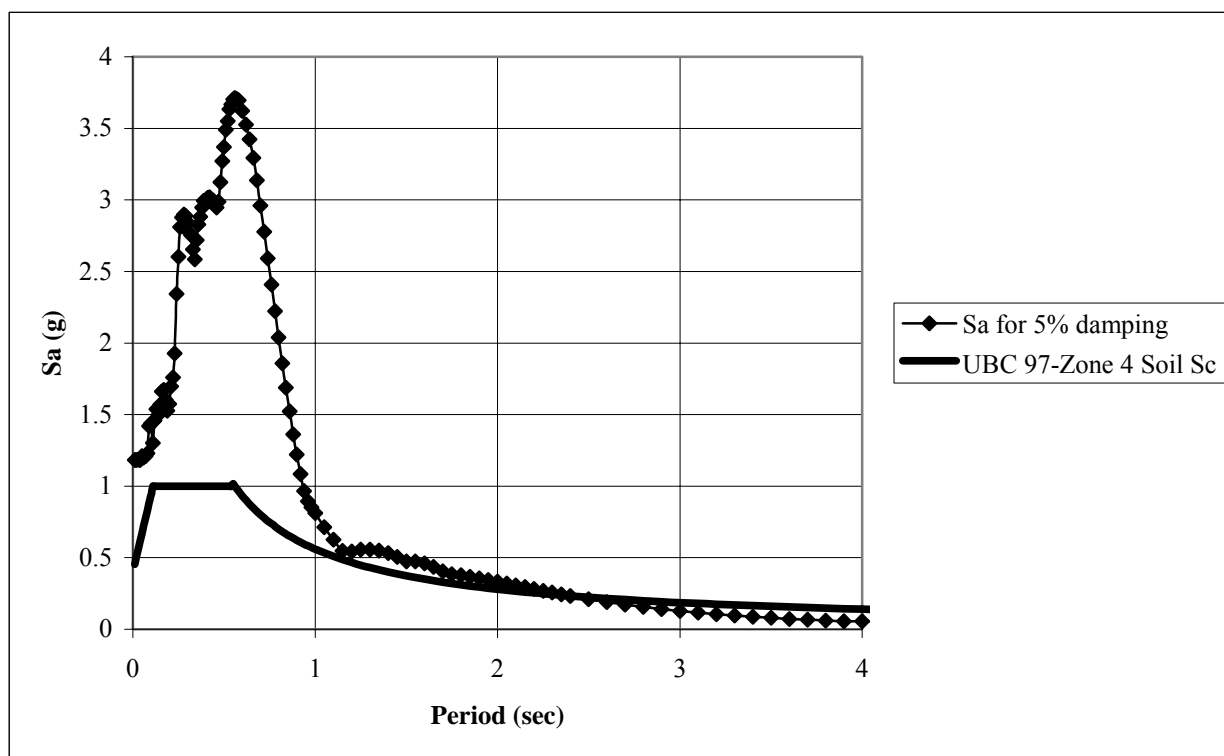


Figure C.10: Ground response spectrum at surface from linear analysis for the El Salvador earthquake for the Civil site and UBC 97 design spectrum.

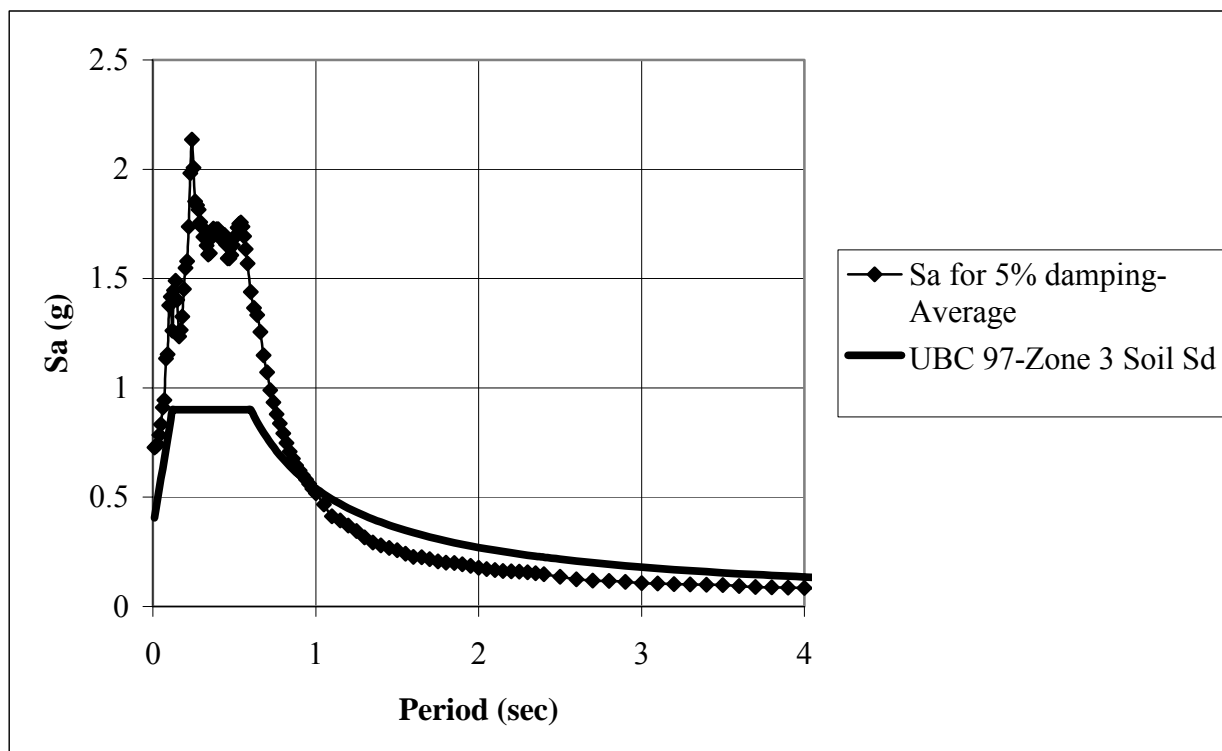


Figure C.11: Average ground response spectrum at surface site from linear analysis for the 341HWY and UBC 97 design spectrum.

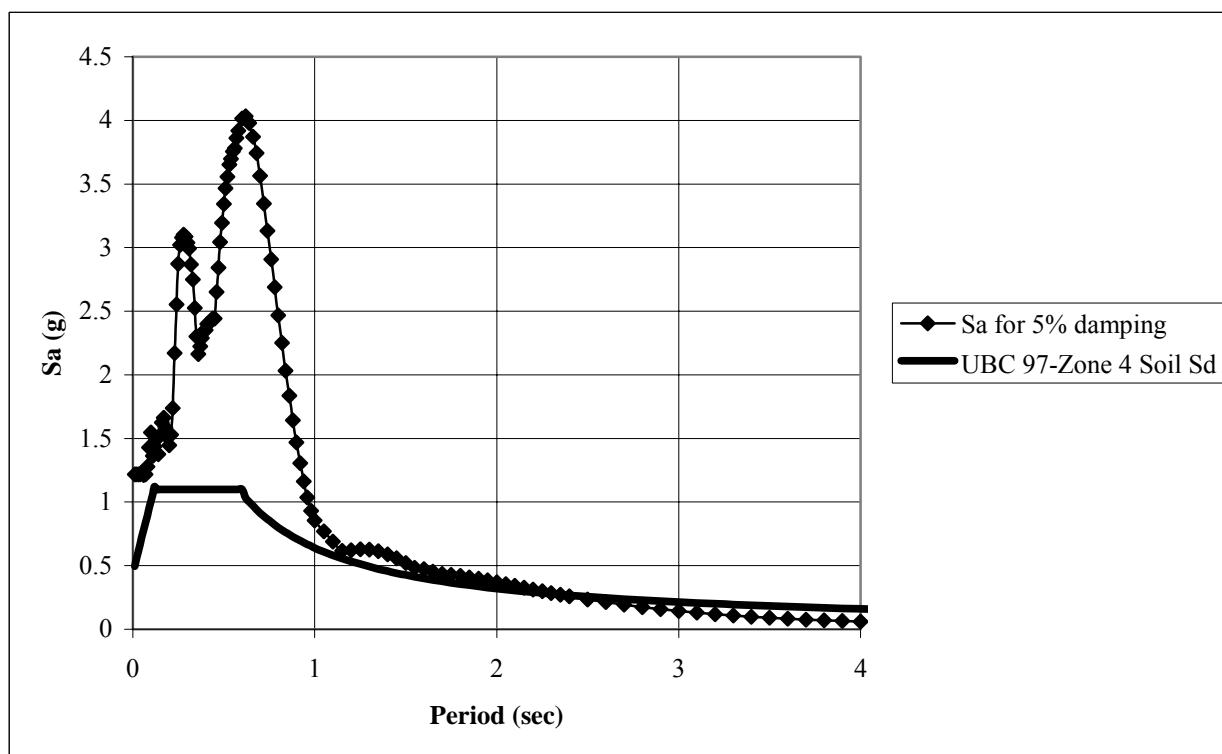


Figure C.12: Ground response spectrum at surface from linear analysis for the El Salvador earthquake for the 341HWY site and UBC 97 design spectrum.

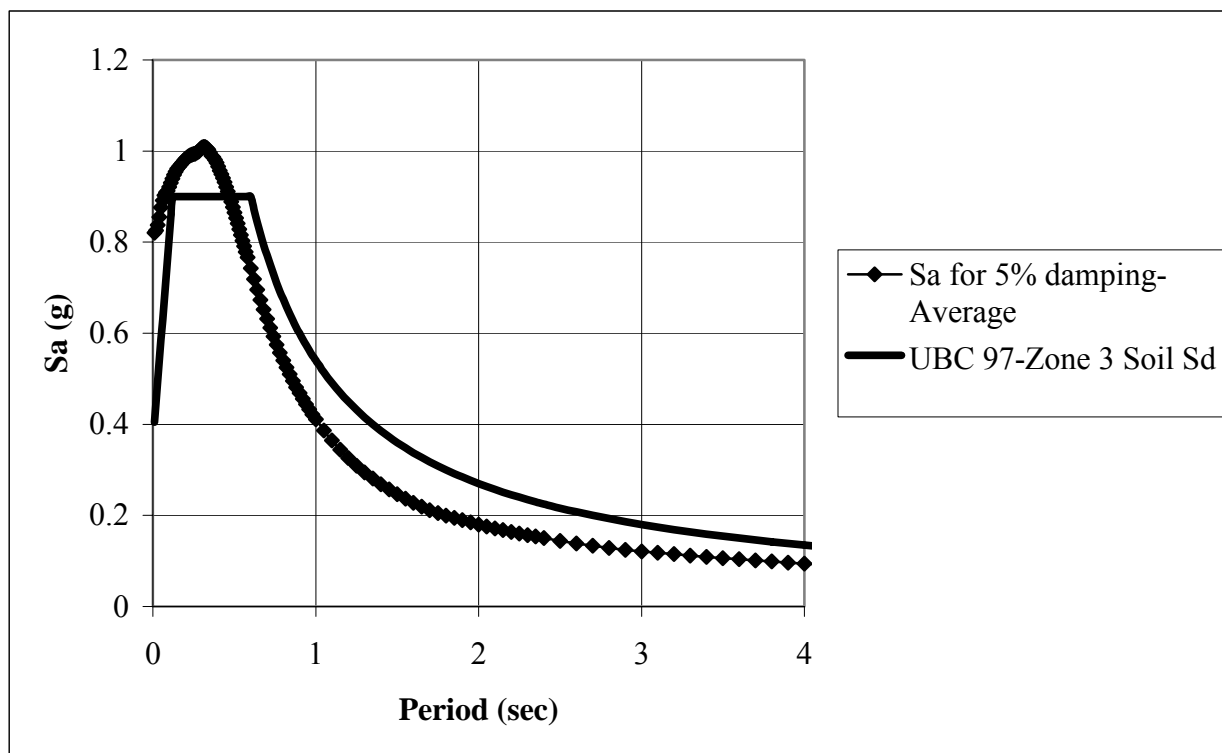


Figure C.13: Average ground response spectrum at surface from linear analysis for the Maní Park site and UBC 97 design spectrum.

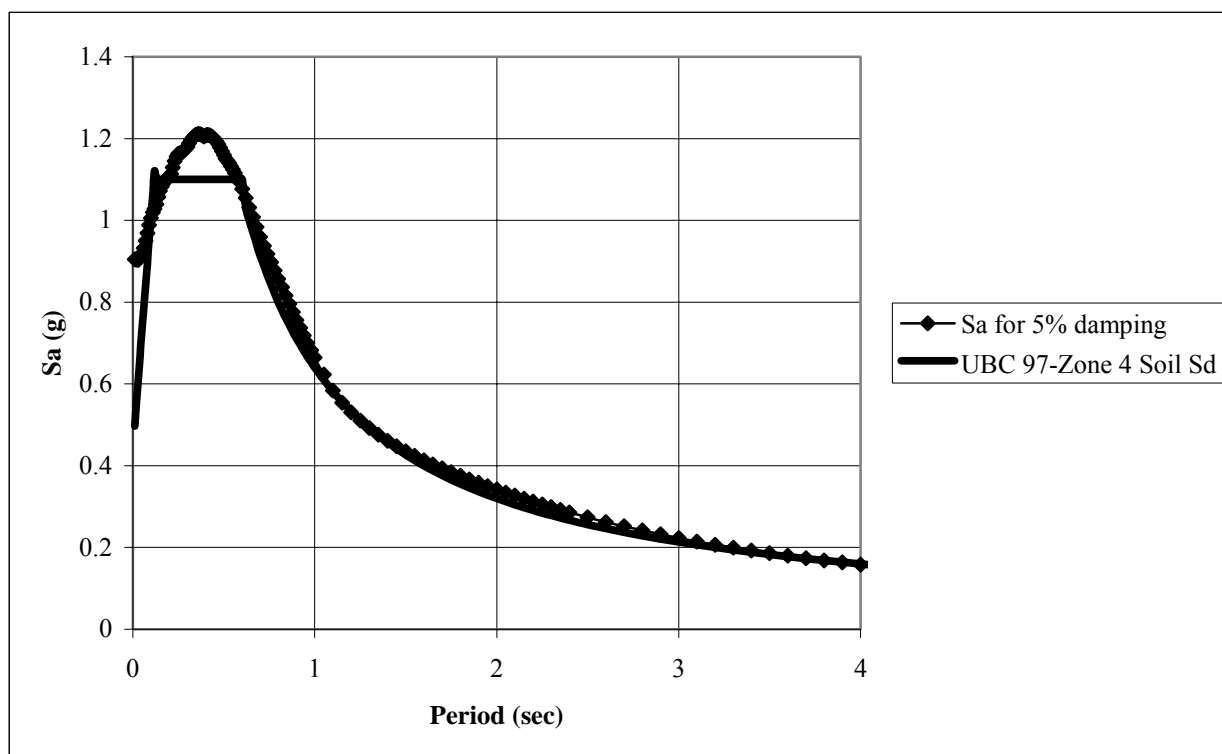


Figure C.14: Ground response spectrum at surface from linear analysis for the El Salvador earthquake for the Maní Park site and UBC 97 design spectrum.

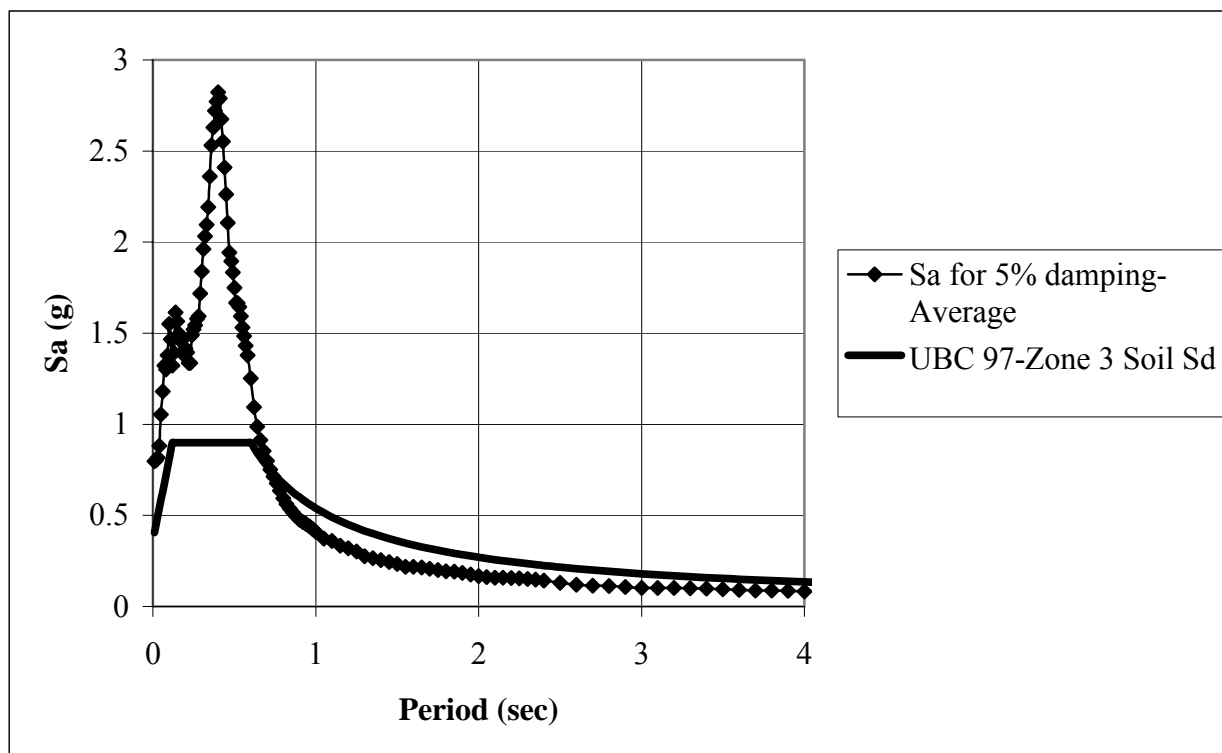


Figure C.15: Average ground response spectrum at surface from linear analysis for the Seco Park site and UBC 97 design spectrum.

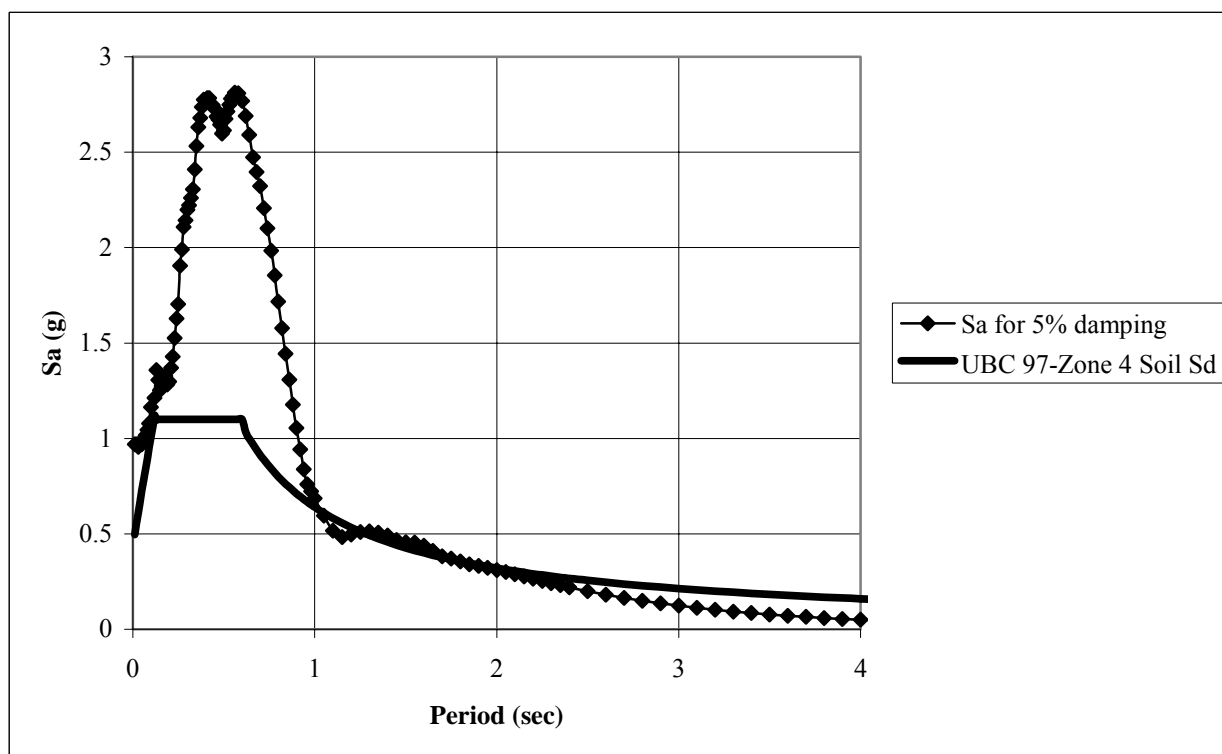


Figure C.16: Ground response spectrum at surface from linear analysis for the El Salvador earthquake for the Seco Park site and UBC 97 design spectrum.

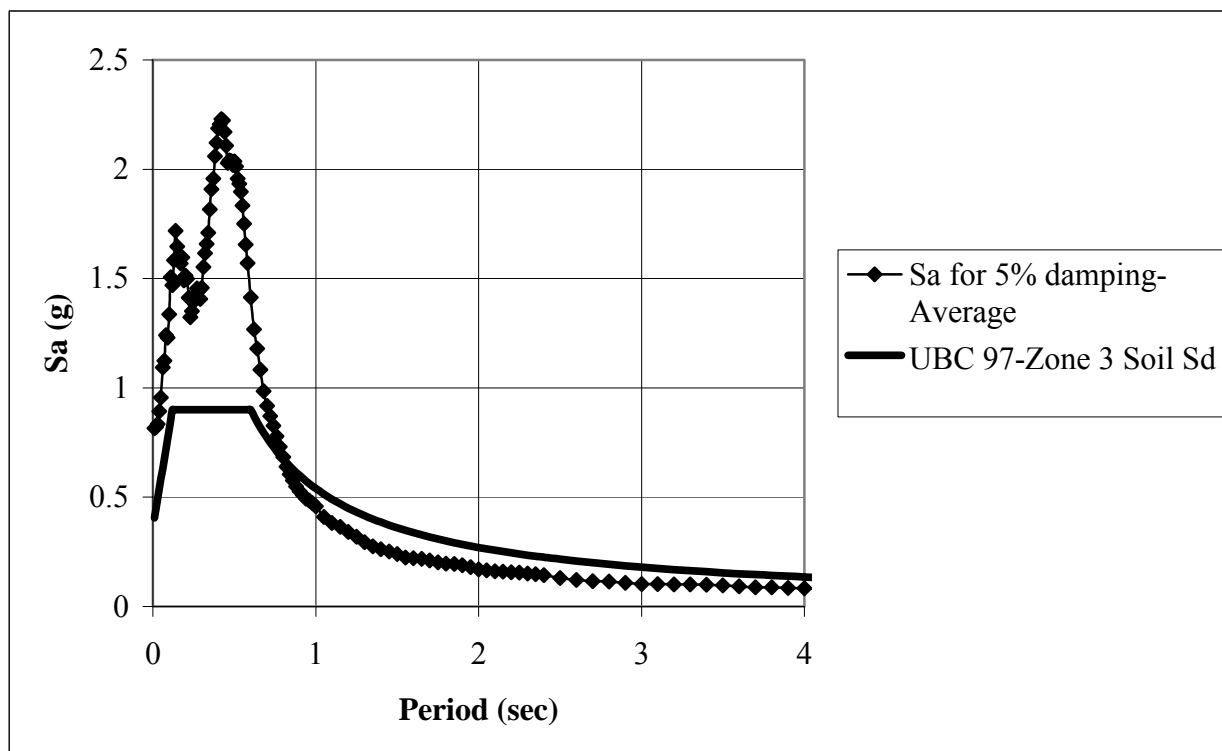


Figure C.17: Average ground response spectrum at surface from linear analysis for the Isidoro García site and UBC 97 design spectrum.

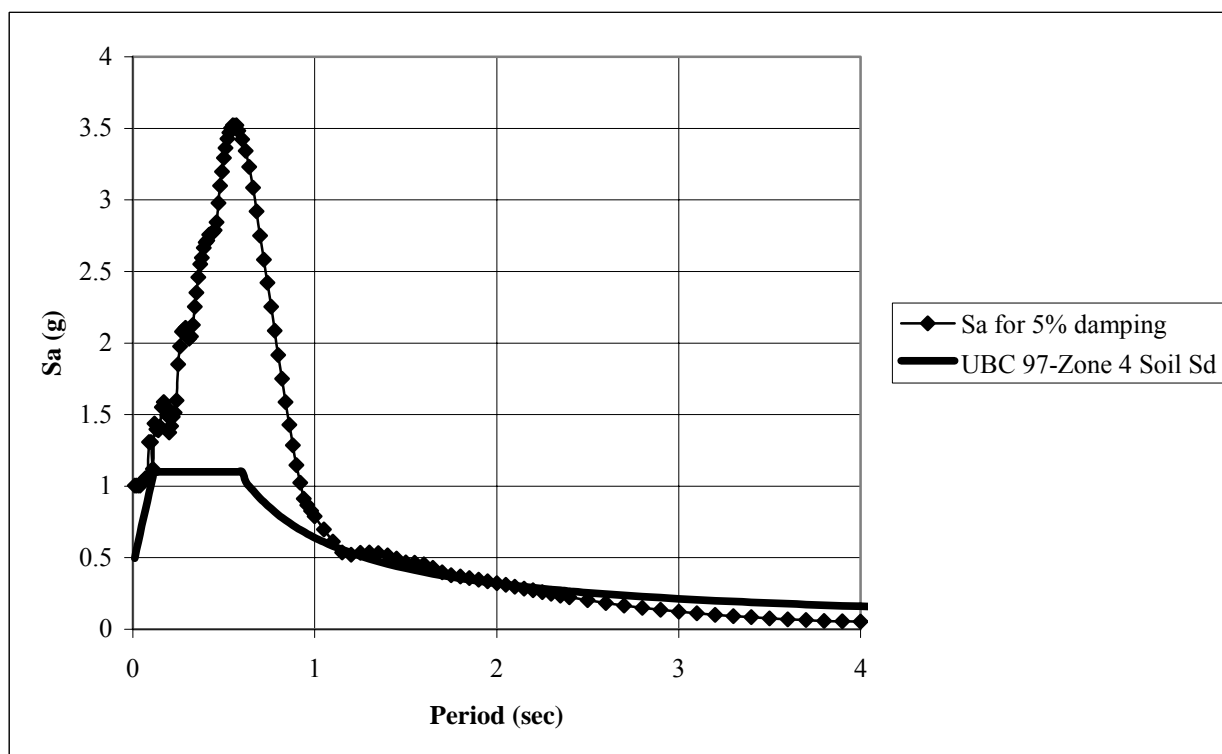


Figure C.18: Ground response spectrum at surface from linear analysis for the El Salvador earthquake for the Isidoro García site and UBC 97 design spectrum.

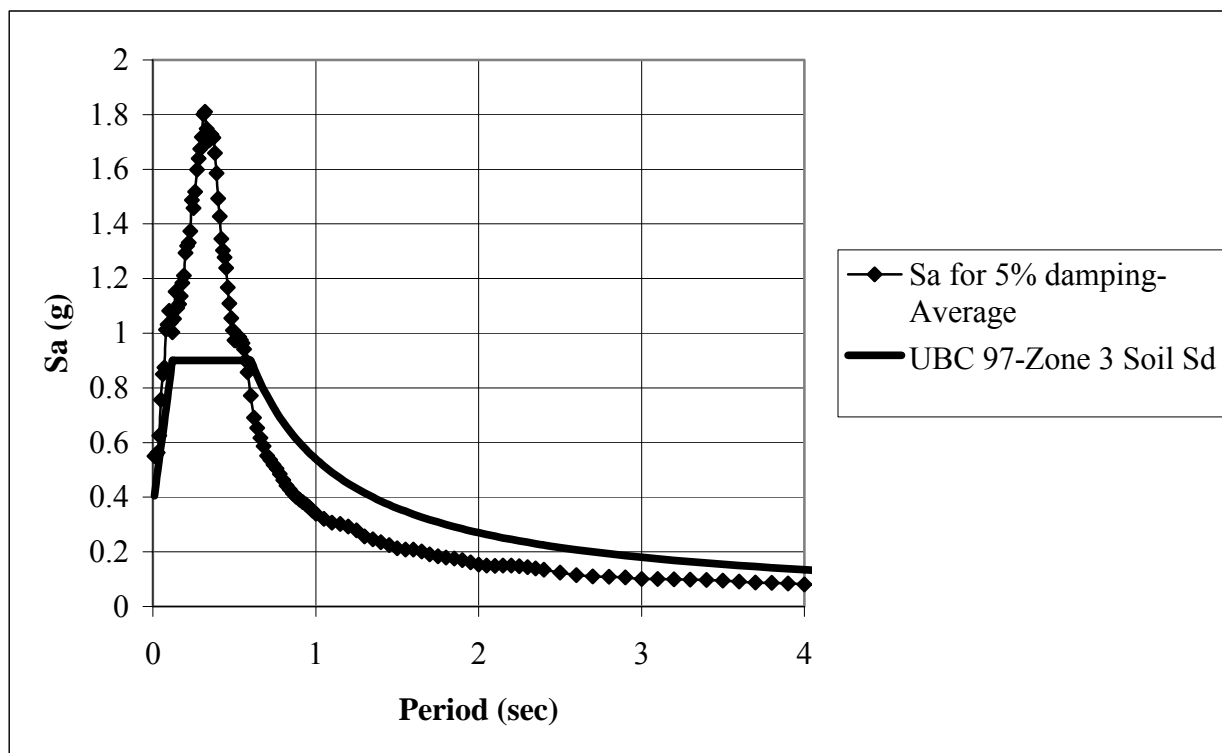


Figure C.19: Average ground response spectrum at surface from linear analysis for the Ramírez de Arellano site and UBC 97 design spectrum.

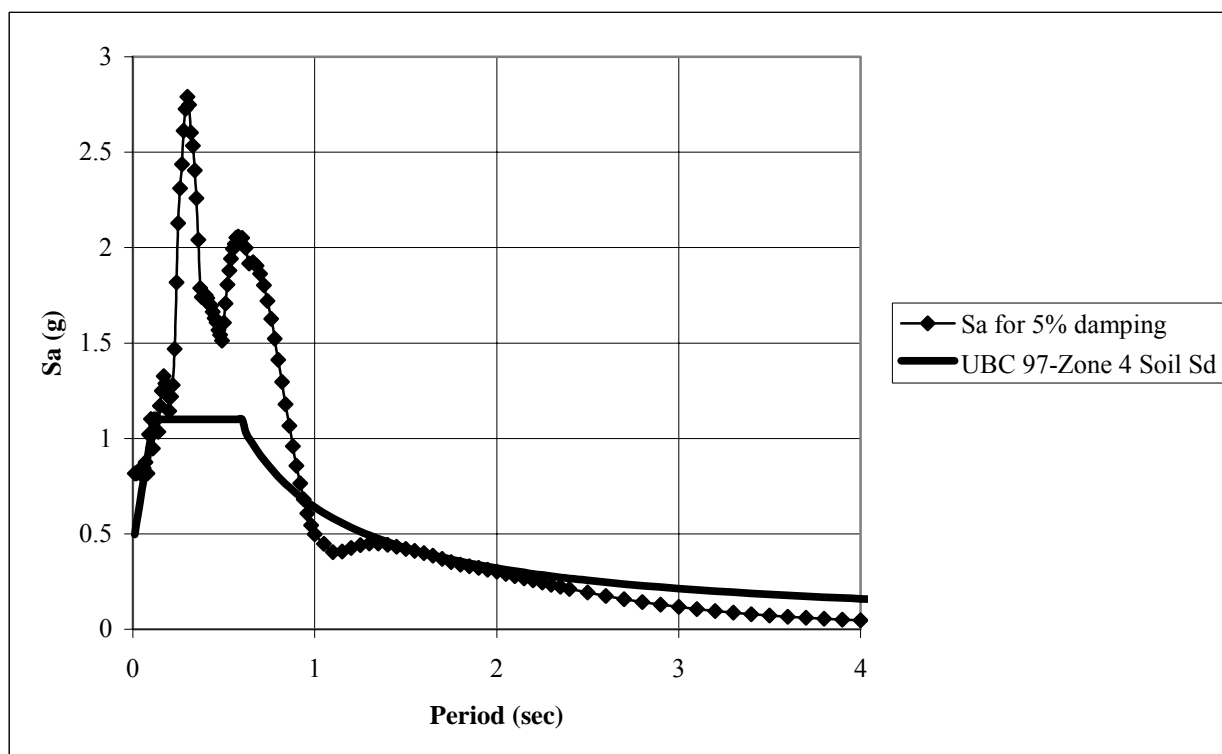


Figure C.20: Ground response spectrum at surface from linear analysis for the El Salvador earthquake for the Ramírez de Arellano site and UBC 97 design spectrum.

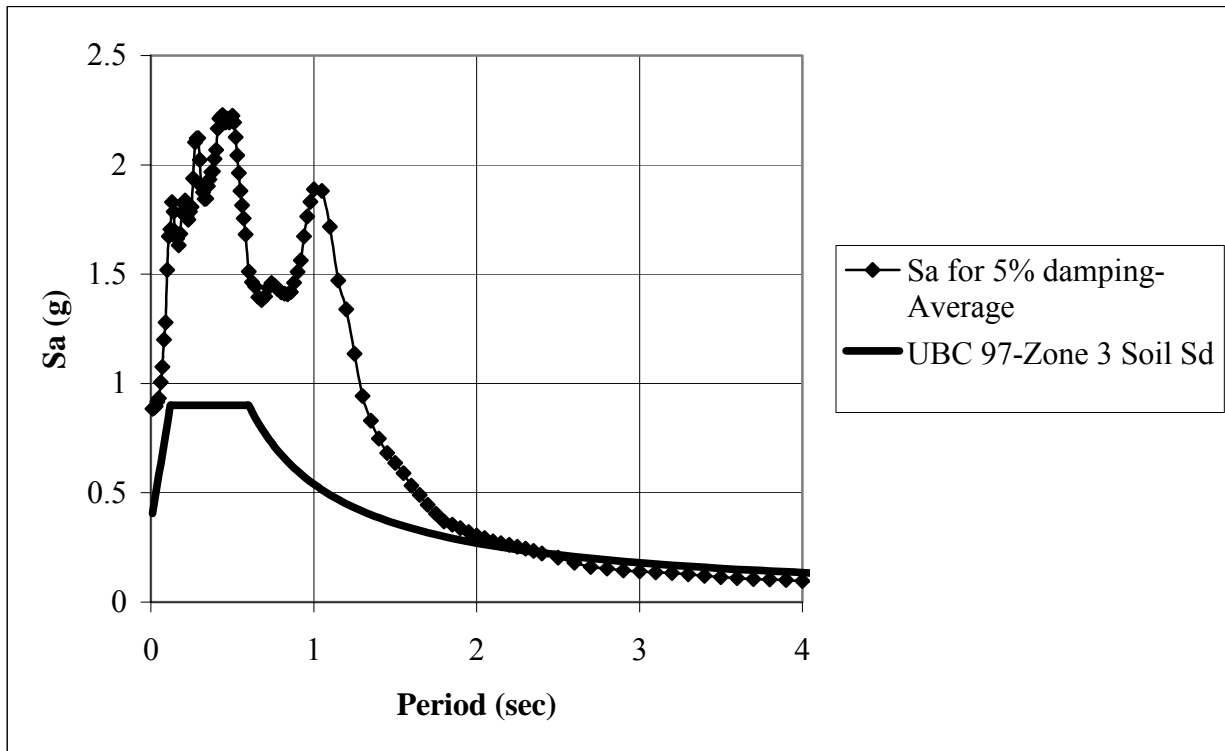


Figure C.21: Average ground response spectrum at surface from linear analysis for the Sultanita site and UBC 97 design spectrum.

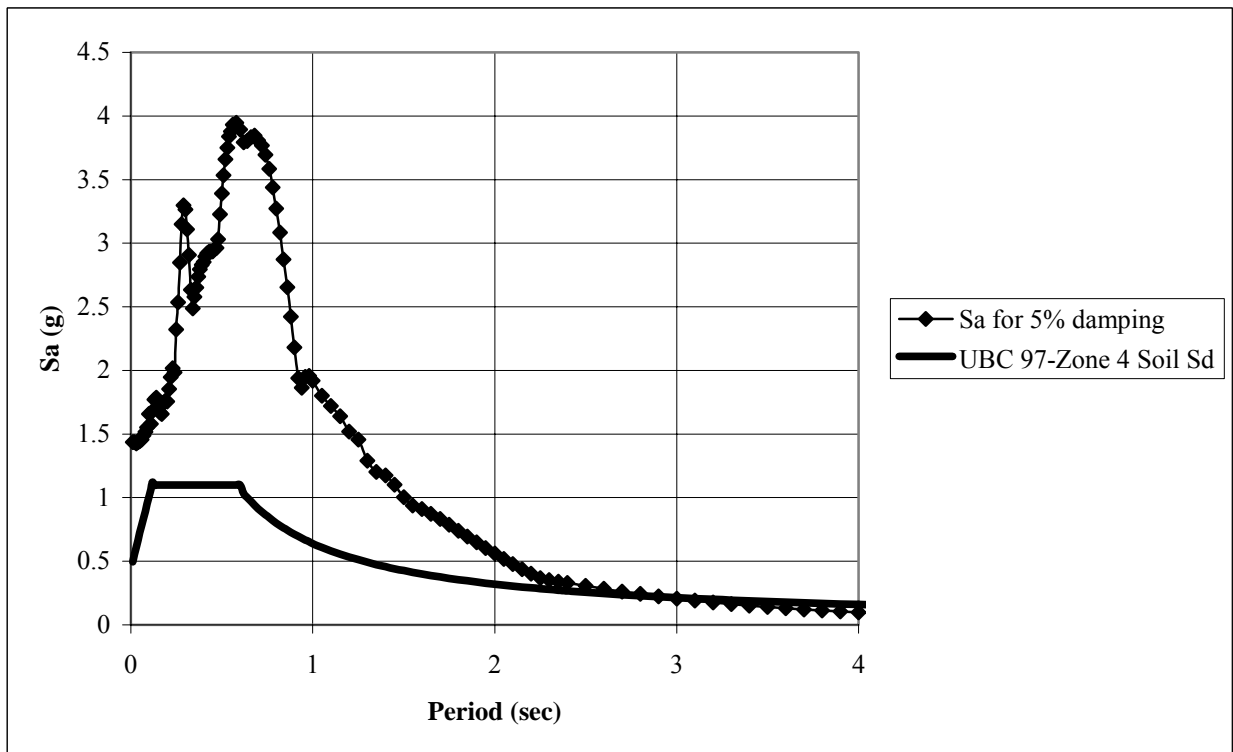


Figure C.22: Ground response spectrum at surface from linear analysis for the El Salvador earthquake for the Sultanita site and UBC 97 design spectrum.

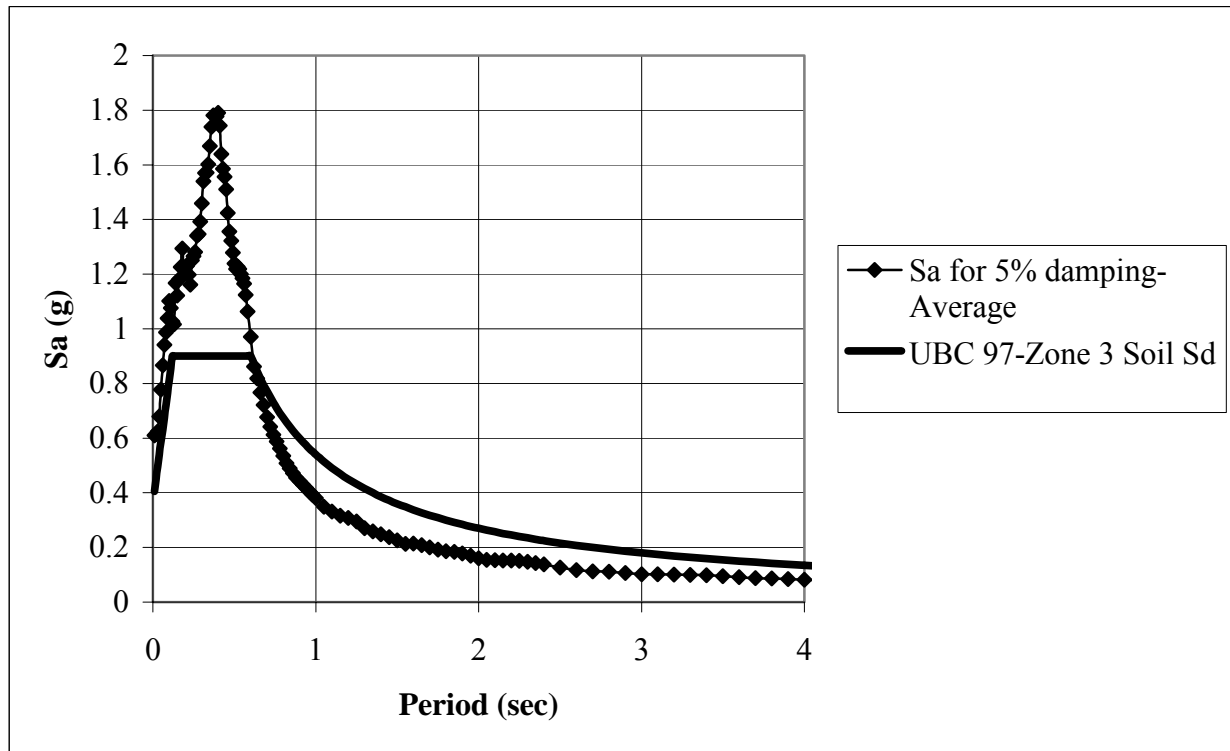


Figure C.23: Average ground response spectrum at surface from linear analysis for the El Bosque site and UBC 97 design spectrum.

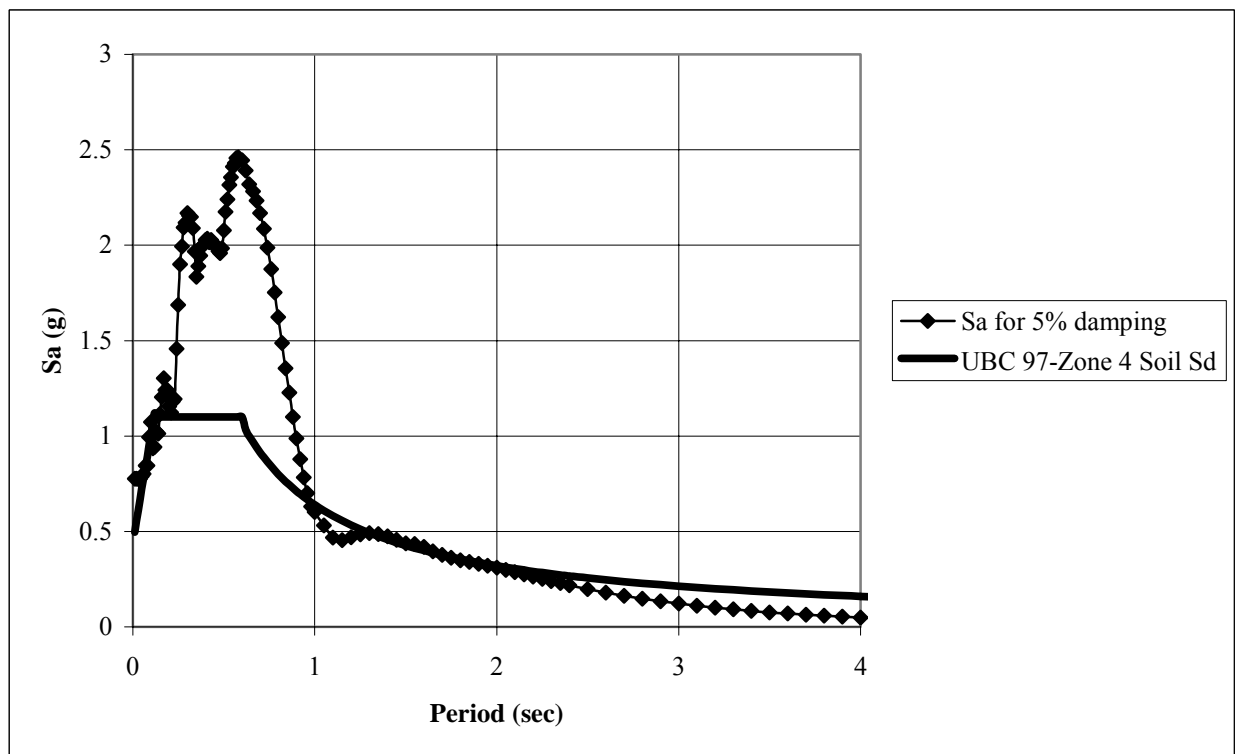


Figure C.24: Ground response spectrum at surface from linear analysis for the El Salvador earthquake for the El Bosque site and UBC 97 design spectrum.

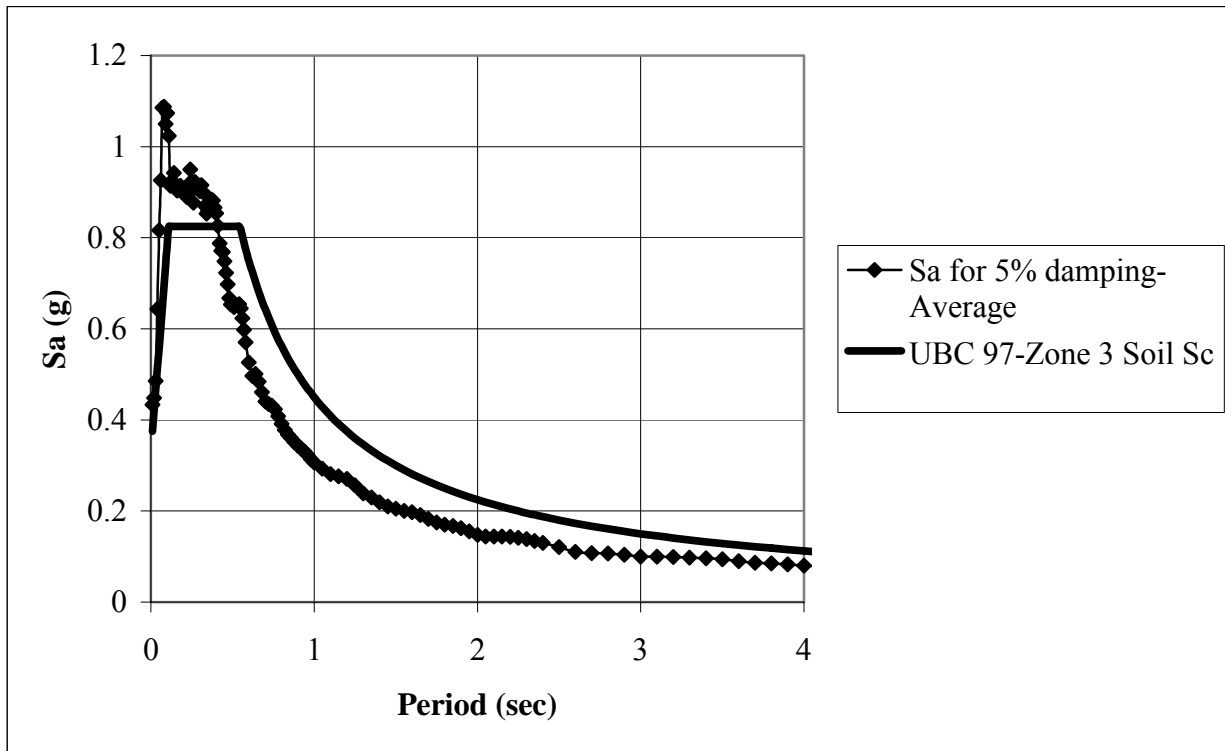


Figure C.25: Average ground response spectrum at surface and UBC 97 design spectrum for El Castillo Site from linear analysis.

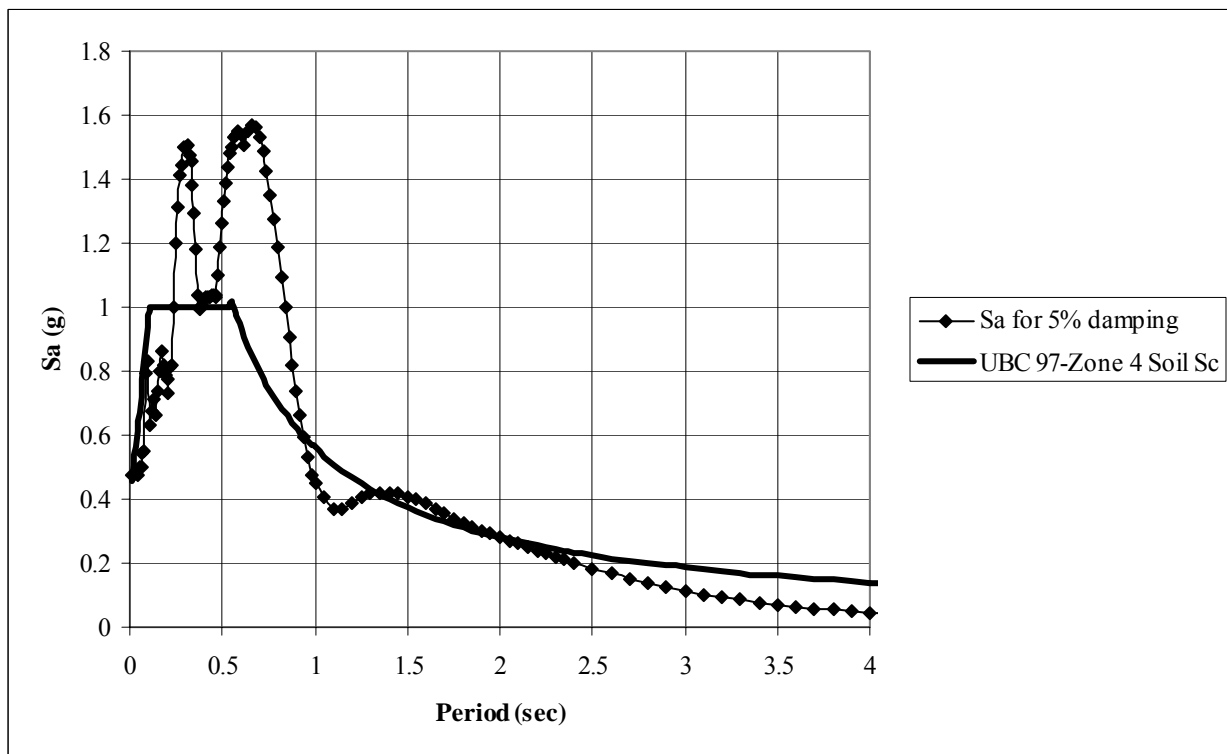


Figure C.26: Ground response spectrum at surface from linear analysis for the El Salvador earthquake for the El Castillo site and UBC 97 design spectrum.

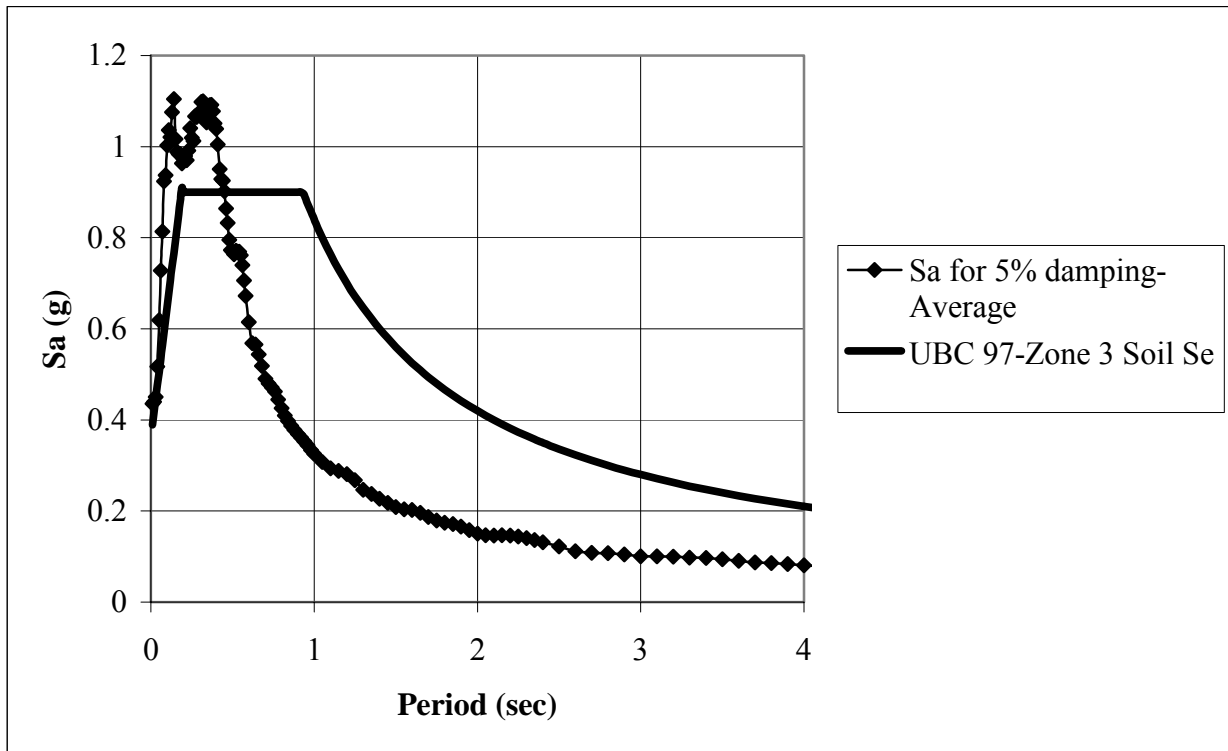


Figure C.27: Average ground response spectrum at surface from linear analysis for the India Site and UBC 97 design spectrum.

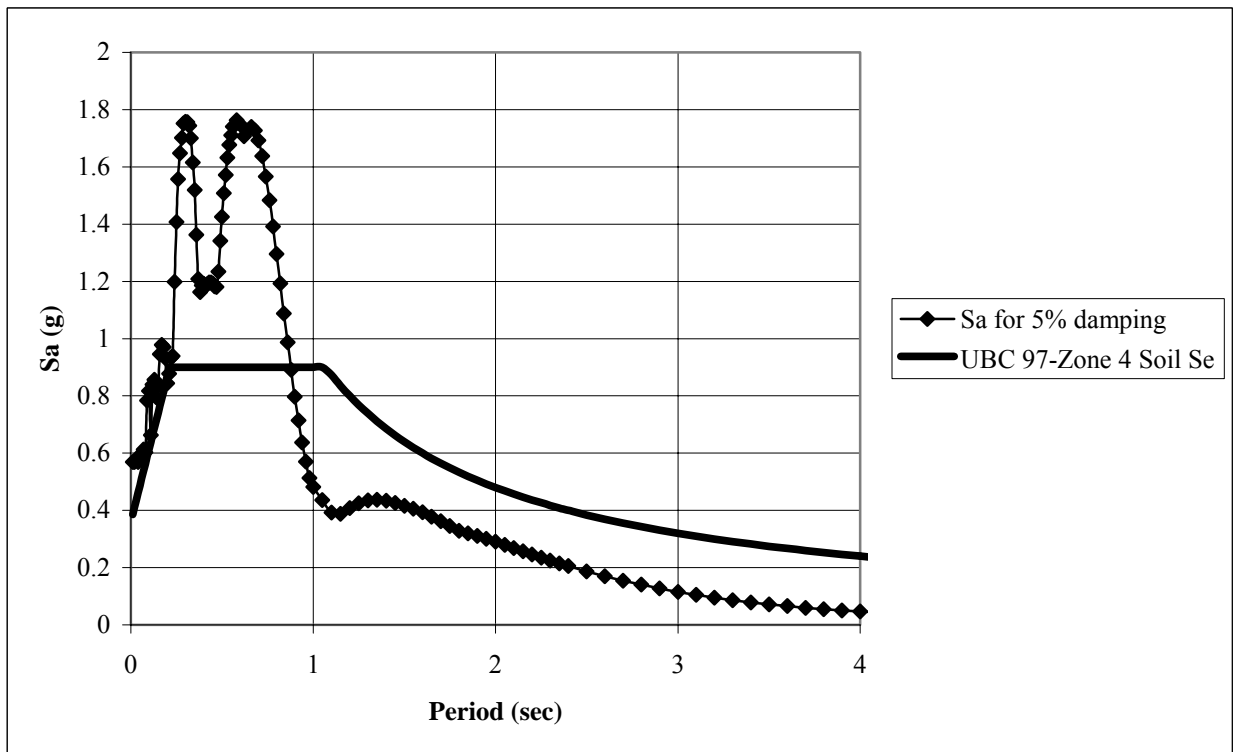


Figure C.28: Ground response spectrum at surface from linear analysis for the El Salvador earthquake for the India site and UBC 97 design spectrum.

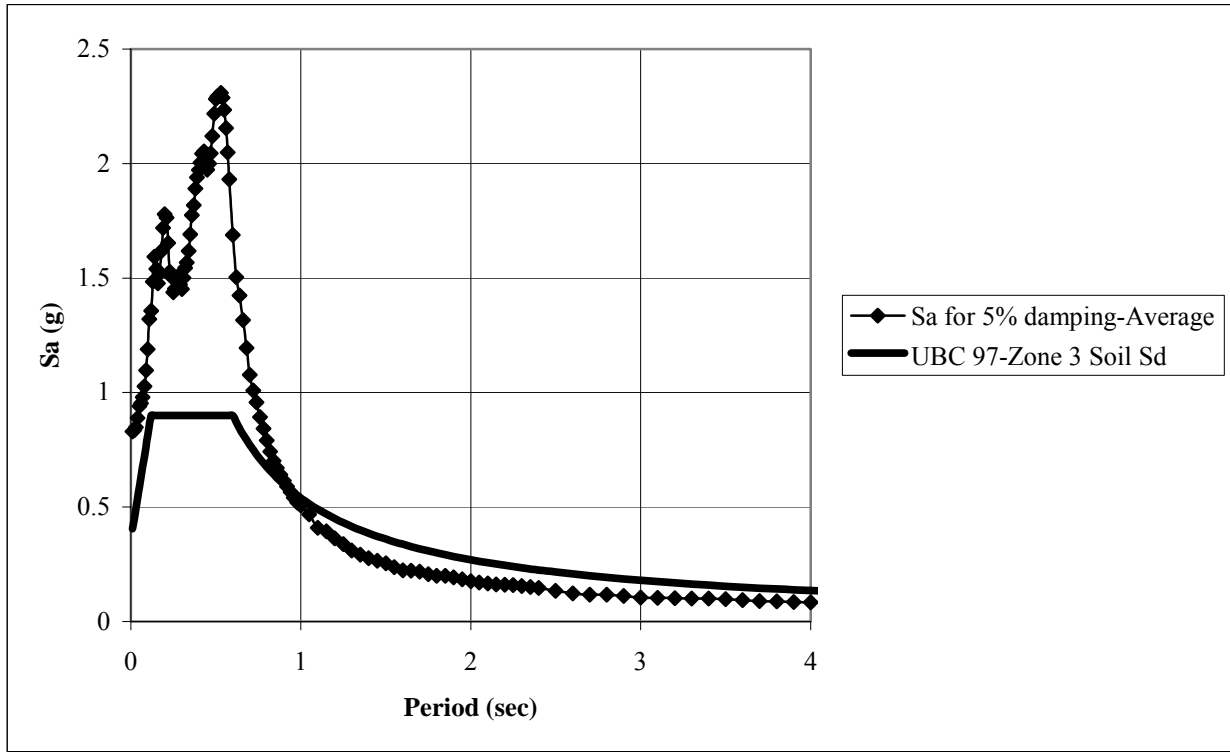


Figure C.29: Average ground response spectrum at surface from linear analysis for the Marina Site and UBC 97 design spectrum.

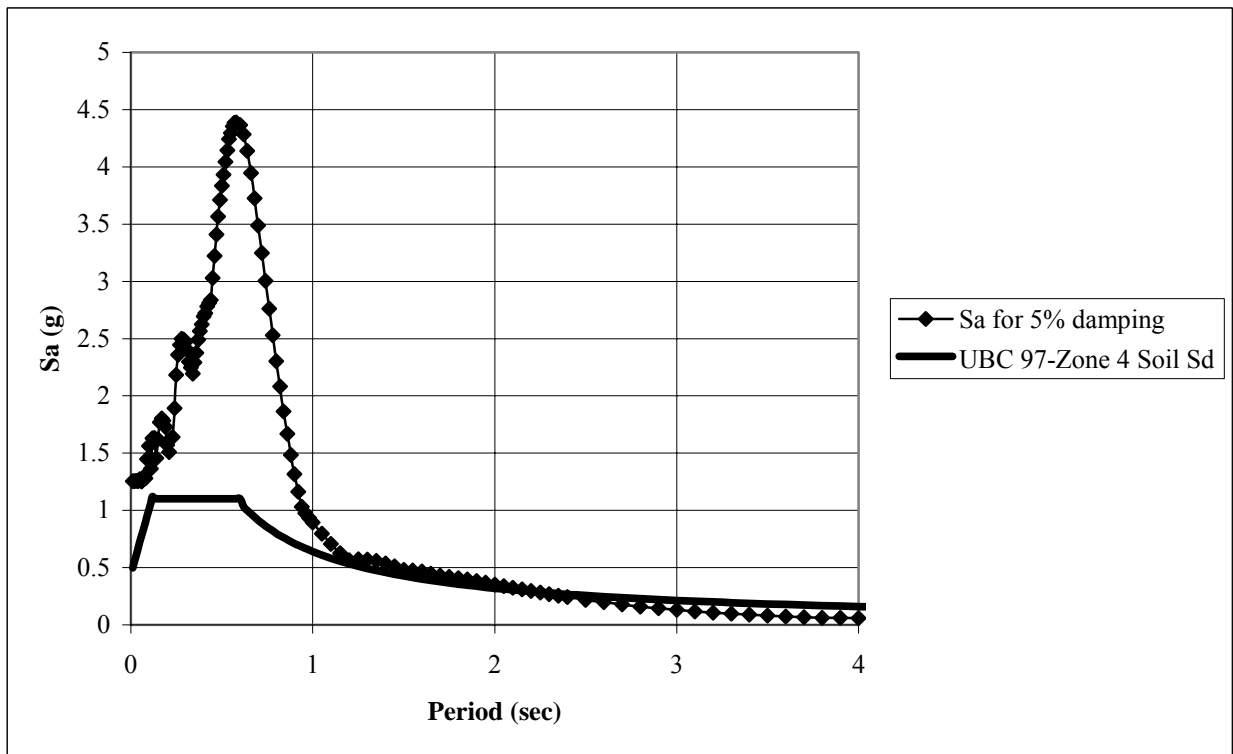


Figure C.30: Ground response spectrum at surface from linear analysis for the El Salvador earthquake for the India site and UBC 97 design spectrum.